Faculty of Sciences
Department of Computer Science

Sara Hebal

Energy Routing Problem

A thesis submitted to the Sétif 1 University Ferhat Abbas
in partial fulfillment of the requirements for the degree of
Doctor of Philosophy

Committee:

Semcheddine	Fouzi	Prof. Sétif 1 University Ferhat Abbas	President
Saad	Harous	Prof. Sharjah University	Supervisor
Djamila	Mechta	MCA. Sétif 1 University Ferhat Abbas	Co-Supervisor
Chirihene	Gherbi	MCA. Sétif 1 University Ferhat Abbas	Examiner
Samir	Akrouf	Prof. University Mohamed Boudiaf M'Sila	Examiner
Farouq	Zitouni	MCA. Kasdi Merbah University Ouargla	Examiner

2024

Statement of Originality

I hereby certify that the work embodied in this thesis is the result of original research, is free of plagiarised materials, and has not been submitted for a higher degree to any other University or Institution.

May. 2024

. . . .

Date

Signature

. . . .

Acknowledgment

In the name of ALLAH, the most Gracious and the most Merciful. I thank ALLAH for the Strength and Blessing, He has Given me to achieve this work.

I would like to express my heartfelt thanks to my supervisor, Prof. Saad Harous, and my co-supervisor, Dr. Djamila Mechta, for their unfailing support, insightful counsel, and patience during my PhD journey. Their competence and effort have been critical in completing my thesis.

My most sincere gratitude goes to Dr. Lemia Louail for her invaluable advice, helpful suggestions, and unwavering professional and personal support.

I would like to thank Dr. Farouq Zitouni for the meetings and research discussions which have significantly enriched my research.

I extend my warmest thanks to all members of the Department of Computer Science, and all my teachers, for their direct and indirect contributions to the success of my studies.

I wish to thank the members of my dissertation committee for their generous sharing of expertise, guidance, and valuable time throughout the review of this document.

I thank the College of Computing and Informatics of Sharjah University for hosting my internships.

On a personal note, I would like to express my heartfelt appreciation to my source of inspiration, my parents Abderrezak and Abla, and my sisters Nour ElHouda, Chaima, Ghozlene, and Katre Nadda, for their unwavering love and support. Without your encouragement and sacrifices, this achievement would not have been possible.

A heartfelt thanks to my dear friends Mohammed and Zahra, who have been constant companions in my daily life and unwavering supporters throughout.

Sara Hebal, May 2024

To Maroua my friend, my sister, to the pure soul who is no longer with us but will forever remain in our hearts

Abstract

The Energy Internet (EI) is a new concept mainly related to peer-to-peer energy trading (P2PET) in a smart grid power network. It allows energy trading pairs to route energy between each other directly. Energy routing algorithms and routing devices are the core components of the energy internet. The effective transmission of power between trading pairs in P2PET over the complicated EI is significantly dependent on the deployment of an efficient energy routing algorithm. There are three main problems surrounding energy routing algorithms: subscriber matching, finding efficient energy path and transmission scheduling. The fundamental objective of this thesis is to focus on designing and building a realistic and efficient energy-routing approach that handles subscriber matching, energy-efficient paths, and transmission scheduling. Initially, we start by performing a comprehensive literature review. Firstly, we combine matching prosumers and non-congestion energy efficient path selection by the same objective function and propose an energy routing algorithm that optimizes both energy prices and transmission losses. Then, we focus on minimizing energy transmission losses and propose the shift from single-path to multi-path-based energy routing. The energy routing problem is formulated as a non-convex non-linear optimization problem and a semi-decentralized multi-path energy routing approach is proposed. For more realistic energy routing, we integrate the P2P power market constraints into the multi-path-based energy routing and create a non-convex mixed integer non-linear optimization problem. To solve the problem we proposed a new semi-decentralized energy routing approach that solves effectively subscriber matching, energy-efficient path and transmission scheduling problems.

Key words: Energy Internet, peer-to-peer energy trading, energy routers, energy routing problem, subscriber matching, energy-efficient path, transmission scheduling, congestion management, optimization problem.

ملخص

إنترنت الطاقة هو مفهوم جديد يتعلق بشكل أساسي بتداول الطاقة من نظير إلى نظير في شبكة الطاقة الذكية. يسمح لأزواج تجارة الطاقة بتوجيه الطاقة بين بعضهم البعض مباشرة. خوارزميات توجيه الطاقة وأجهزة التوجيه هي المكونات الأساسية لإنترنت الطاقة. ويعتمد النقل الفعال للطاقة بين أزواج التداول في تداول الطاقة بين النظراء عبر شبكة إنترنت الطاقة المعقدة اعتمادًا كبيرًا على نشر خوارزمية توجيه الطاقة الفعالة. هناك ثلاث مشاكل رئيسية تحيط بخوارزميات توجيه الطاقة: مطابقة المشتركين، وإيجاد مسار طاقة فعال، وجدولة الإرسال. ويتمثل الهدف الأساسي لهذه الأطروحة في التركيز على تصميم وبناء نهج واقعي وفعال لتوجيه الطاقة يتعامل مع مطابقة المشتركين والمسارات الفعالة للطاقة وجدولة الإرسال. في البداية، نبدأ بإجراء مراجعة شاملة للأدبيات. أولاً، نقوم بين الجمع بين مطابقة الموفرين واختيار المسار الفعال للطاقة دون ازدحام من خلال نفس دالة الهدف، ونقترح خوارزمية توجيه الطاقة التي تعمل على تحسين كل من أسعار الطاقة وخسائر الإرسال. بعد ذلك، نركز على تقليل خسائر نقل الطاقة إلى الحد الأدنى ونقترح التحول من توجيه الطاقة أحادي المسار إلى توجيه الطاقة متعدد المسارات. تُصاغ مشكلة توجيه الطاقة كمشكلة تحسين غير خطية غير محدبة ويتم اقتراح نهج شبه لا مركزي متعدد المسارات لتوجيه الطاقة. من أجل توجيه الطاقة بشكل أكثر واقعية، قمنا بدمج قيود سوق الطاقة من نظير إلى نظير في توجيه الطاقة القائم على المسارات المتعددة وإنشاء مشكلة تحسين غير خطية غير محدبة متعددة الأعداد الصحيحة المختلطة. ولحل هذه المشكلة اقترحنا نهجًا جديدًا شبه لا مركزي لتوجيه الطاقة يحل بفعالية مشاكل مطابقة المشتركين والمسار الموفر للطاقة وجدولة الإرسال.

الكلمات المفتاحية: إنترنت الطاقة، تداول الطاقة من نظير إلى نظير، موجهات الطاقة، مشكلة توجيه الطاقة، مطابقة المشتركين، المسار الموفر للطاقة، جدولة الإرسال، إدارة الازدحام، مشكلة التحسين.

Contents

List of Figures

List of Tables

List of Algorithms

Acronyms

AC	Alternating Current
DC	Direct Current
DG	Distributed Generation
DR	Demand Response
DESs	Distributed Energy Sources
EI	Energy Internet
ER	Energy Router
ESSs	Energy Storage Systems
EV	Electric Vehicle
EVEI	Electric Vehicle Energy Internet
FiT	Feed-in-Tariff
HEMS	Home Energy Management System
HVAC	High-Voltage Alternating Current
IoT	Internet of Things
LVAC	Low-Voltage Alternating Current
LVDC	Low-Voltage Direct Current
MAS	Multi-Agent System
MPC-based ER	Multi-Port Converter-based Energy Router
MVDC	Medium-Voltage Direct Current
NSO	Network System Operator
OPF	Optimal Power Flow problem
P2PET	Peer-to-Peer Energy Trading
PLC-based ER	Power line Communication-based ER
RESs	Renewable Energy Sources
SA-based ER	Switch Array-based ER
SG	Smart Grid
SOS	Symbiotic Organisms Search
SQP	Sequential Quadratic Programming
SST	Solid State Transformer

SST-based ER	Solid State Transformer-based Energy Router
V2G	Vehicle-to-Grid technology

General Introduction

Rising energy demands in the twenty-first century, coupled with the threat of depleting fossil fuel supplies and growing environmental concerns about the fuel's role in pollution and carbon emissions, have resulted in a major focus on investment in, and development of clean renewable energy and low carbon technologies particularly photovoltaic and wind energy. The rapid penetration of these distributed renewable energy sources has marked a notable transition from a centralized traditional power grid to a decentralized power system. Nevertheless, despite their benefits, owing to their inherent distributed and intermittent nature the vast incorporation of distributed renewable generation poses critical issues for grid operators regarding policy, energy management, and operation, driving smart grid development.

To build an efficient, flexible and resilient energy system, the Energy Internet (EI) has emerged as an extension of the smart grid to promote peer-to-peer energy trading (P2PET) across the power system. Analogous to the information Internet, all distributed energy devices are interconnected through a mesh network of energy routers (ERs) with bidirectional power and communication flow, where energy flow is treated as a data packet and can be routed from a producer to a consumer. As the ability to effectively transmit energy is the most desired aspect of the EI, energy routing algorithms and routing devices constitute the core components of the EI. Recently the development of ERs and energy routing protocols have progressively become a prominent study issue in the EI which makes energy routing the next expected step of EI expansion. Therefore, addressing the EI's energy routing problem is a very promising and significant field of study.

The effective transmission of power between trading peers in P2PET over the complicated EI is significantly dependent on the deployment of an efficient energy routing algorithm. Given this context, designing an energy routing approach for P2PET within EI is a challenging task. The designed energy routing approach should incorporate an appropriate subscriber-matching mechanism that allows consumers to select the best producers to satisfy their demand, an efficient energy path selection algorithm to determine the energy transmission path with the least loss of energy,

and a transmission scheduling method to avoid network congestion issues for normal EI's operations.
Even though various algorithms have been proposed to address the energy routing problem, including its three distinct challenges (subscriber matching, energy-efficient path, and transmission scheduling), only a handful of existing solutions in the literature have addressed all three challenges (detailed in Chapter 2). Thus, the fundamental objective of this thesis is to bridge this gap by building a realistic and efficient energy-routing approach that handles subscriber matching, energy-efficient paths, and transmission scheduling. Because the energy routing procedure is much slower than power transmission across transmission lines, the routing protocol should be dynamic to adapt to the dynamic structure of EI and quick with low complexity.

In this thesis, first, a P2PET scheme is proposed. This scheme introduces a new energy routing protocol based on meta-heuristic algorithms called the hybrid energy routing protocol in Energy Internet. The proposed protocol addresses the three energy routing issues: subscriber matching, energy-efficient paths, and transmission scheduling. In which the best producers for each consumer with the non-congested minimum loss path are determined.

Subsequently, focusing on tackling energy-efficient path and transmission scheduling issues, a new formulation for the energy-efficient path issue is proposed as a non-convex, non-linear optimization problem based on multi-path energy routing. To solve this problem a new semi-decentralized energy routing algorithm that incorporates graph theory and non-convex nonlinear programming, is designed. The algorithm consistently produces an efficient multi-path solution for a particular energy trading pair, taking into account the power flow direction constraint and precisely computing power losses during transmission. For possible path conflict scenarios caused by simultaneous decentralized energy routing decisions, a centralized algorithm with a new ranking concept is proposed.

Finally, focusing on solving the energy routing problem, including subscriber matching, energy-efficient paths, and transmission scheduling. The energy routing problem is formulated as a non-convex mixed-integer non-linear optimization problem that minimizes the consumer's energy cost. A new semi-decentralized energy routing approach that incorporates graph theory and meta-heuristics is introduced to allow each consumer to select the best producers that minimize the energy cost, the amount of power to get from each one, and the least energy transmission cost paths between the energy trading pair while respecting the market and network physical constraints. The simulation results demonstrate the effectiveness of the proposed algorithms.

Outline of the Thesis

The substance of this thesis is structured as follows:

Chapter 1 introduces the evolution phases of power systems, following their history from traditional power systems to the EI. It presents the EI, its essential components, and technologies, with a categorization of current ERs. Following that, the chapter discusses the energy routing problems with an explanation of its three major challenges.

Chapter 2 provides an overview of research that has studied energy routing algorithms. It gives a detailed study of existing power routing algorithms as well as a novel classification of them that addresses their limitations, which can benefit a large audience with an interest in this field of study.

Chapter 3 provides the primary hypotheses that will drive our research. It describes the common aspects that underlie the approaches employed in Chapters 4, 5, and 6. These factors include the mathematical formulation of the energy routing problem, system components and parameters, and simulation tools used.

In Chapter 4, a hybrid energy routing protocol to address the three energy routing issues: subscriber matching, energy-efficient paths, and transmission scheduling is proposed. The proposed protocol combines the power losses and energy prices in the same objective function and selects the best producer for each mono-source or multi-source consumer with the free congestion energy efficient path. The efficiency of the proposed energy routing algorithm is evaluated by performing thorough simulations and comparing its performance to that of previously developed energy routing algorithms.

In Chapter 5, the mathematical energy routing model in Chapter 3 is expanded to include multi-path power transmission and Power Flow Direction constraint (PFD). Due to the non-convexity of the PFD constraint, the energy routing problem is transformed into a non-convex non-linear optimization problem. A semi-decentralized energy routing algorithm is proposed to determine an efficient free-congestion multi-path solution for a particular energy trading pair while respecting the network's physical constraints including the PFD and capacity constraints. For possible path conflict scenarios caused by simultaneous decentralized energy routing decisions, a path conflict management algorithm is employed by an NSO. The efficiency of the proposed energy routing algorithm is evaluated by performing thorough simulations and comparing its performance to that of previously developed energy routing algorithms.

Chapter 6 introduces a new P2P energy trading framework. It enhanced the mathematical energy routing model in Chapter 5 by integrating the trading market constraints to the multi-path energy routing, which makes the problem a constrained non-convex mixed-integer non-linear optimization problem to optimize the total energy cost. A novel semi-decentralized energy routing approach that uses graph theory and metaheuristic methods to match the prosumers and select the free-congestion least-cost paths. The energy transmission paths are determined based on their transmission costs rather than their energy losses. The simulation results demonstrate the effectiveness of the suggested semi-decentralized energy routing approach in solving the energy routing issues.

Chapter 6.5 concludes the thesis by reviewing the contributions and making suggestions for further research.

Part I

State of the art

Chapter 1

Evolution of Power Systems and the Energy Internet

The work in this chapter and Chapter 2 has been published in The Journal of Supercomputing since 2024 [4]: Sara Hebal, Djamila Mechta, Saad Harous, and Lemia Louail. A comparative study of energy routing algorithms to optimize energy transmission in energy internet. The Journal of Supercomputing, pages 1–57, 2024. internet. The Journal of Supercomputing, 2024.
This chapter provides an overview of power systems, focusing on the Energy Internet (EI). It investigates the issues of energy routing inside the EI, emphasizing the key needs for energy routers and efficient energy routing algorithms. The chapter emphasizes the significance of establishing sophisticated energy routing algorithms to enable smooth energy distribution in the EI.

1.1 Background on power system

For decades, traditional power systems have met the energy needs of consumers for their homes and businesses effectively. However, the over-reliance on fossil fuels (crude oil, coal, and natural gas) to fulfil the rising energy demand has led to several undesirable results, including natural resource depletion, increasing pollution, impending climate change, with an increase in the generation and service prices. To fulfil current and future energy demands, practically all nations have shifted their attention to renewable energy sources and low-carbon technology as one of the most promising solutions. The integration of renewable energy sources has led to a transition in the power system structure from centralized power systems to the advent of the energy internet, passing through distributed generation systems, smart grids, and peer-to-peer energy trading systems (Figure 1.1).

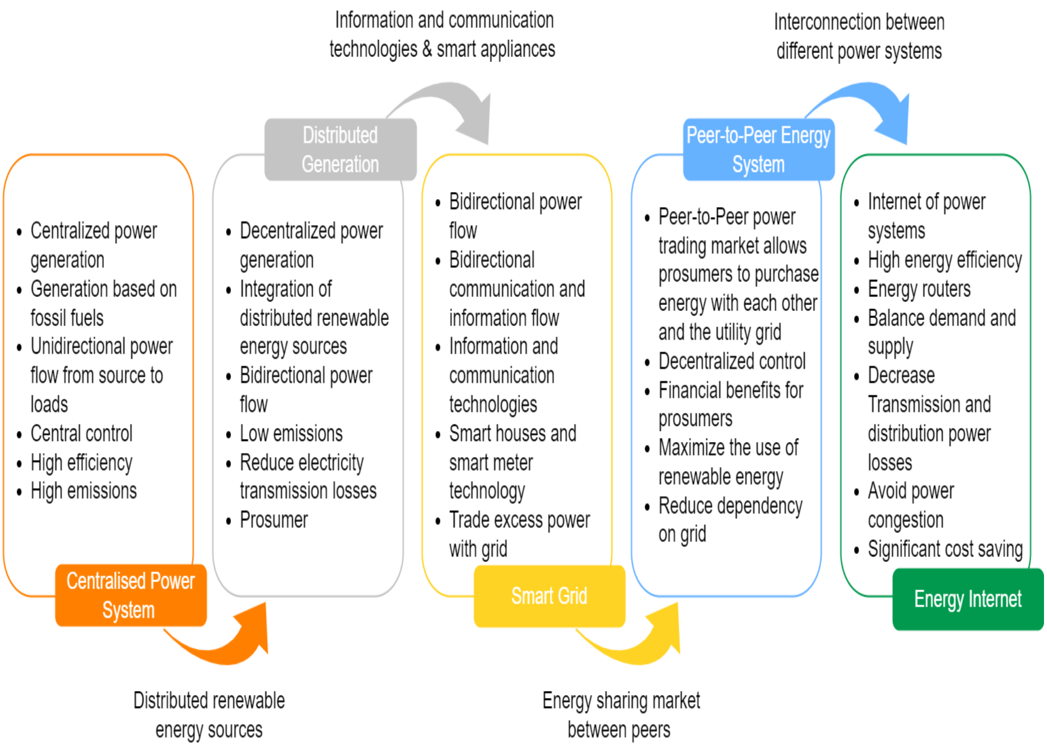

FIGURE 1.1: Development of power systems.

1.1.1 Conventional centralised power system

Most countries' conventional electric power systems have been designed in the manner depicted in Figure 1.2. Large-scale power plants, also known as generation stations, such as thermal, hydro, and nuclear power plants, generate electricity. The electricity flows in one direction from the power plant to the end consumers through transmission and distributed systems. In the transmission system transformers increase the voltage to high levels to reduce power losses, while substation transformers reduce the voltage level at the distribution system, where energy is provided to customers [5]. The electricity market is frequently arranged in a unidirectional manner. Generation companies often sell massive amounts of electricity to wholesale retailers. Then, these retailers sell smaller amounts of electricity to end consumers [6]. Consumers are charged according to the amount of power they use during a certain period (in kWh).

Despite the central energy system's effectiveness in satisfying customers' demands to this day, it has several shortcomings that must be addressed. A single component

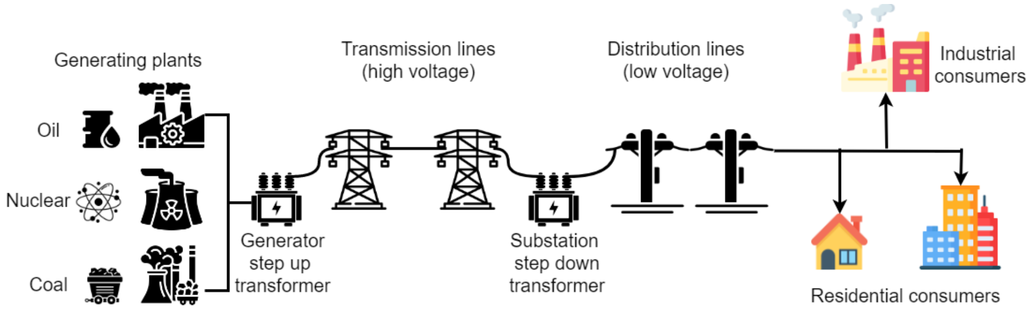

FIGURE 1.2: Conventional centralized power system.

failure in the power system can have a huge influence on the entire system, producing power generation issues, local power outages, and even widespread blackouts. Furthermore, absolute reliance on fossil fuels for energy generation has significantly contributed to environmental pollution and the developing issue of climate change, as burning fossil fuels for electricity generation is the main source of greenhouse gas emissions [7]. Besides, it is commonly acknowledged that fossil fuels will be depleted and will become extremely costly to use.

1.1.2 Distributed generation

In response to increased pollution caused by traditional centralized energy systems' use of fossil-fired power plants, growing energy demand, and rising energy costs, almost all countries have shifted their focus to replacing these sources with renewable and environmentally friendly energy sources. Renewable energy generators are generally significantly smaller than fossil-fuelled and nuclear-powered generators. With the exception of large-scale hydropower generators and big offshore and onshore wind farms, most renewable energy generators are far smaller than fossil fuel generators and nuclear power [8], and so produce significantly less energy. Because high-voltage transformers and switchgear are expensive, small renewable energy generators cannot be integrated into the transmission system. As a result, these generators must be linked to the distribution network. This type of generation is referred to as a distributed generation. In distributed power generation (DG) also called decentralized generation and embedded generation, electricity is generated at the distribution level using renewable energy sources (RESs) and low-carbon technologies such as solar panels, wind turbines, combined heat and power, and fuel cells [8]. These RESs are distributed across the grid to enable the production and transfer of energy from various locations to consumers, where consumers equipped with small-scale RESs such as photovoltaic systems and battery storage can also produce power and are known as prosumers. The increasing penetration of such RESs has shifted the grid's centralized structure to a distributed structure. Figure 1.3 illustrates a distributed generation power system.

DG systems [9] improve network efficiency, reduce CO_2 emissions and minimize energy costs and power losses throughout transmission and distribution networks compared to typical centralized power systems. However, due to the volatility and intermittency of RESs, these systems cannot ensure energy self-balancing [10].

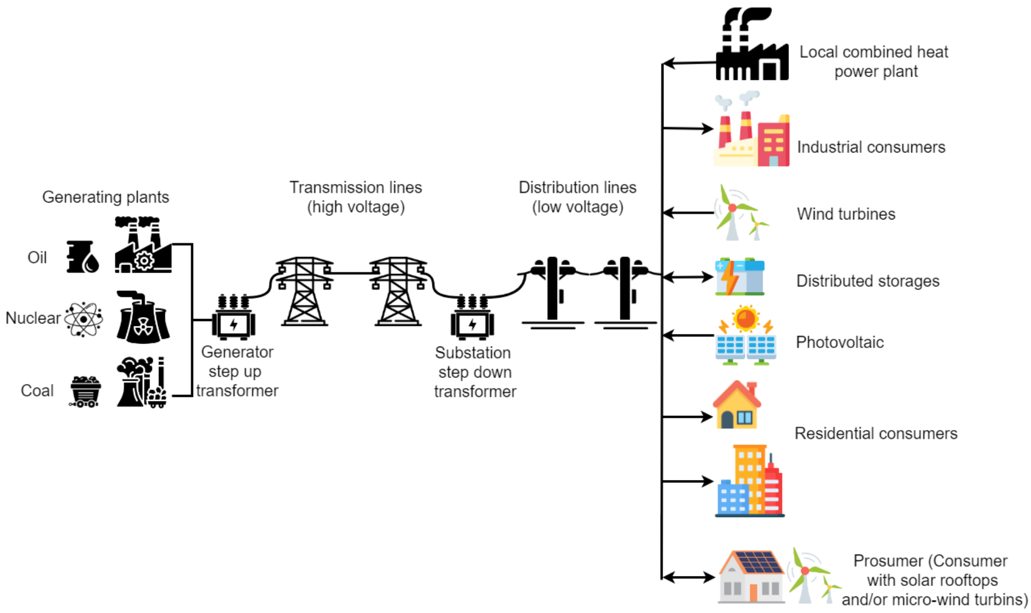

FIGURE 1.3: Distributed generation power system.

1.1.3 Smart grid

The proliferation of distributed energy resources has several advantages including:

- Lowering the carbon emissions
- Decreasing the energy transmission losses and cost
- Decreasing the load placed on the main grid, by meeting a portion of the demand through local energy generation.

However, since solar and wind are the most widely utilized sources and their generation fluctuates and depends on weather conditions; switching the grid's energy production from traditional approaches to full dependence on RESs cannot totally ensure energy balance. Furthermore, incorporating such RESs into the power system with its real-time operation is highly difficult [11], their power fluctuation can lead to voltage violation, reverse power flow, missing transmission grid capacity, or insufficient generation adequacy [12–14]. Energy storage systems (ESSs) may be utilised as a critical solution to alleviate the challenges connected with RESs while integrating them into the power system network [15]. ESSs are intended to be charged during periods of low energy demand and discharged during times of high consumer demand [16]. Accordingly, EESs refers to a process of converting electrical energy from an electrical power network into a form that may be stored and converted back to electrical energy as necessary [17]. The integration of ESSs enables stable renewable generation and rapid regulation.

To ensure the smooth operation of power systems, RESs and ESSs must be interconnected to the utility grid and managed utilising sensing capabilities combined with information and communication technology, resulting in Smart Grid [18]. As stated by the National Institute of Standards and Technology (NIST), USA, the smart grid (SG) is " *A modernized grid that enables bidirectional flows of energy and uses two-way communication and control capabilities that will lead to an array of new functionalities and applications*". SG, also known as intelligent grid, is an advancement of the centralised grid that is currently being investigated, developed, and installed throughout the world. The SG involves bidirectional communication and power flow between the utility supplier and its consumers, advanced smart devices and smart houses, smart meter technology, advanced communication and control technologies, and computation intelligence [19–21]. Figure 1.4 represents the structure of Smart Grid.

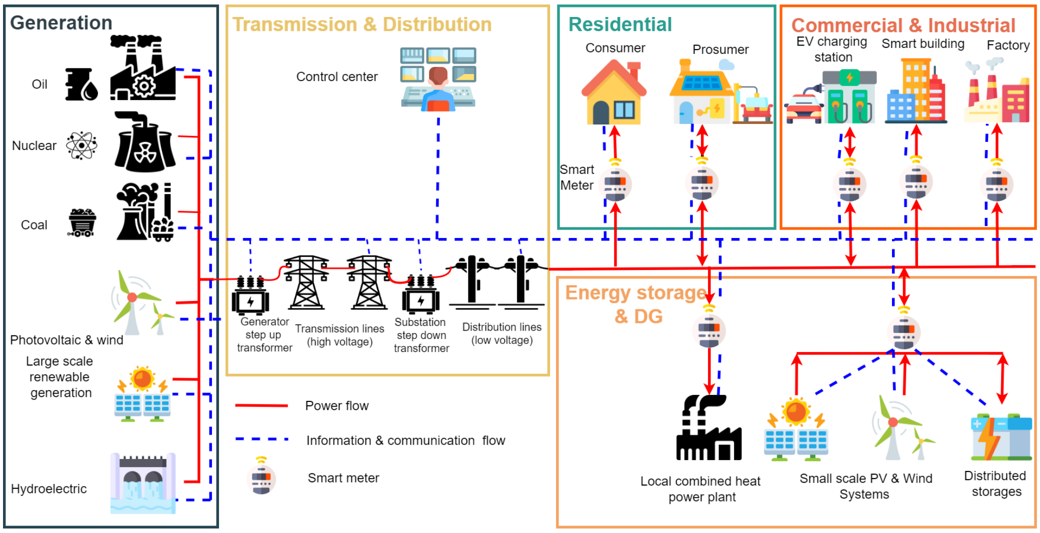

FIGURE 1.4: Smart Grid structure.

Various strategies, such as Demand Response (DR) technology and home energy management systems (HEMS), were proposed in the SG using information and communication technology to increase energy efficiency and create successful coordination between local distributed renewable generation units and power systems. In DR, the utility grid uses real-time electricity prices to persuade consumers to reduce their demand. Consumers, on the other hand, use HEMS and try to schedule their consumption based on real-time pricing and their consumption information in order to minimise their electricity bills [22]. DR and HEMS lower consumers' electricity bills and shift electricity demand from on-peak to off-peak periods.

A number of initiatives have been implemented in an effort to further minimise the carbon footprint and reliance on the main grid. Feed-In Tariffs [23], carbon taxes, and other financial instruments have all been proposed in many nations as ways to promote the development and penetration of renewable energy generation and encourage traditional consumers to become prosumers. A prosumer is an active consumer equipped with RESs like rooftop solar panels, micro-wind turbines, and domestic battery storage, and actively controls their energy consumption, production, storage and share [24]. Figure 1.5 represents an illustration of consumers and prosumers in the SG. The power generated by RESs is capable of not only meeting load requirements but also of feeding excess power produced to the electricity grid when supply exceeds load demand. Prosumers inject their excess and unused power into the grid using Feed-in-Tariff rate scheme (FiT)[23]. FiT is a price-driven strategy designed to encourage the increased use of RESs, enables prosumers to sell excess surplus energy to the grid (or, alternatively, to retailers) at a fixed price per unit of energy, and can also purchase energy from the grid if there is a shortage [23, 25].

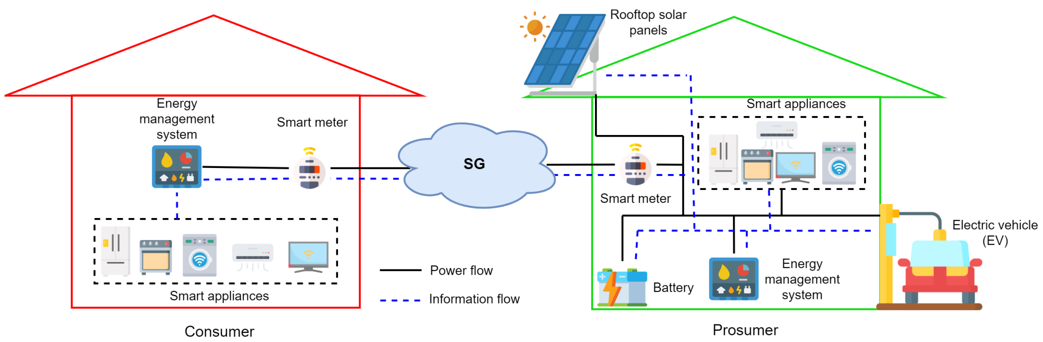

FIGURE 1.5: Illustration of Consumers and Prosumers in SG.

1.1.4 Peer to peer energy trading system

With the FiT scheme, prosumers in most countries now have two alternatives for their excess energy production: they may either inject it into the grid for monetary compensation (FiT) or store energy in a battery storage device for later use. Because of the fast and unexpected penetration of small-scale renewable energy generators by consumers, governments started reducing the FiT rates. The substantial disparity between the rising retail prices and FiT rates for consumers has resulted in the closure and decline of FiT in many countries, making investment profitability questionable [26]. Batteries, on the other side, remain excessively expensive and unprofitable for the majority of consumers [27]. Therefore, it is essential to create prosumer-centric schemes that can increase prosumers economic benefits and motivate them to use distributed RESs more effectively.

In this regard, Peer-to-Peer Energy Trading (P2PET) has been proposed as a novel market paradigm which enables a direct electricity exchange among prosumers and consumers without the interaction of a central authority unit (such as a utility company) while increasing their economic benefits [28]. Apart from injecting the electricity into the grid at a given price defined by the grid operator (FiT), P2PET allows prosumers to sell their surplus electricity to a set of trading partners that could be consumers who do not have RESs such as PV systems or other prosumers whose current demand exceeds their generation [29].

The primary focus of P2PET is to disrupt the centralised electrical grid architecture by enabling direct energy delivery and communication amongst different prosumers with distributed RESs. P2PET has the ability to benefit prosumers, consumers, and the utility grid. Consumers and prosumers with energy needs can purchase energy from other prosumers at a cheaper rate compared to utility grid tariffs, while prosumers with a surplus can increase their income by selling their excess power at a higher price than FiT rates [30]. Furthermore, it permits them to set their own selling and purchasing prices as well as the energy source. Accordingly, P2PET is a decentralized, open and competitive energy market. The electricity market is no longer monopolised by a limited number of large-scale utility corporations because of P2PET. Figure 1.6 represents the concept of P2PET system.

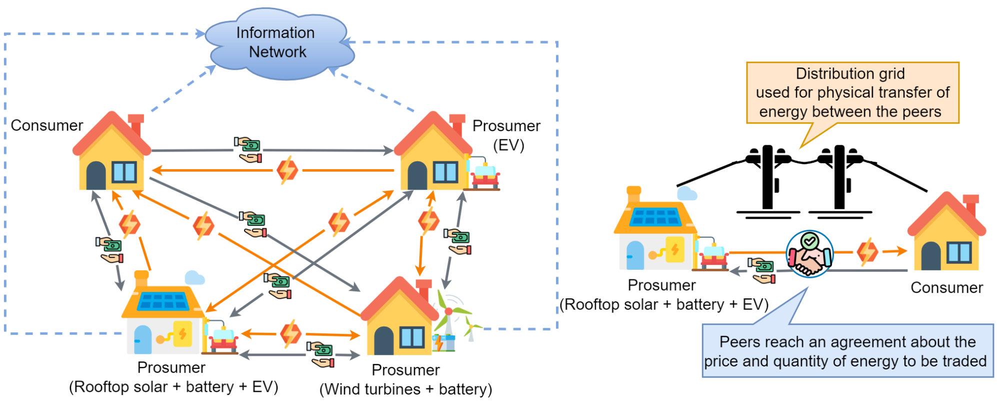

Figure 1.6: Peer-to-Peer Energy Trading.

In addition to the created financial benefits for individual consumers and prosumers,

P2PET can also maximize the advantages of the distributed generation, such as making better use of RESs, reducing the dependency on the main grid, keeping the power system resilient to outages and stabilizing the electricity supply [31, 32]. Since most P2PET markets are anticipated to emerge in grid-connected systems [33], they must fit and complement the current energy systems [34].
P2PET platforms have been created in industrialised countries including sonnenCommunity in Germany [35], Piclo in United Kingdom [36], Vandebron in Netherlands [37], PowerLedger in Austrilia, Yeloha [38] and TransActive grid [39] in USA.

1.1.5 Energy Internet

Despite the usage of an intelligent network with many interesting features, current research reveals that the SG still has considerable limits including the insufficient utilisation of energy forms such as chemical, biomass, and heat systems, the reliance on existing structures, that further outcomes in inefficient routing or scheduling, and the security vulnerabilities [40, 41]. The concept of Energy Internet (EI) has emerged in recent years, with the objective of reducing and eliminating many of the SG's concerns. EI, also known as the Internet of Energy, Global Energy Internet, and the Future Smart Grid was initially proposed by Rifkin and Tsoukalas's studies. The American economist *Jeremy Rifkin* initially put out the idea of EI as the third industrial revolution in his book *'The third industrial revolution: how lateral power is transforming energy, the economy, and the world'* [42]. According to *Jeremy Rifkin*, the EI is an energy system integrated with internet technology to make efficient use of renewable energy while enhancing energy efficiency and reliability of the power system. While Tsoukalas envisioned and introduced the EI as the SG's successor [43, 44] EI can be viewed as a multi-energy correlated network that connects multiple energy networks such as power grid, natural gas network, cooling and heating system, energy storage systems, distributed energy generation, and different loads, etc [45–47]. EI incorporates current SGs, the Internet of Things (IoT), renewable energy, storage devices, electric vehicles (EV), big data processing, and other advanced technologies such as smart monitoring and intelligent management [44, 48, 49]. Figure 1.7 represents a vision of the EI. While Table 1.1 provides a comparison between the SG and EI.
Today, the EI is the focus of extensive, continuous research. The literature on EI encompasses a variety of interpretations, conceptualizations, models, and perspectives. Although all proposed EI models have many similar characteristics, no clear, exact, and comprehensive global definition of EI exists. However, there is a consensus that

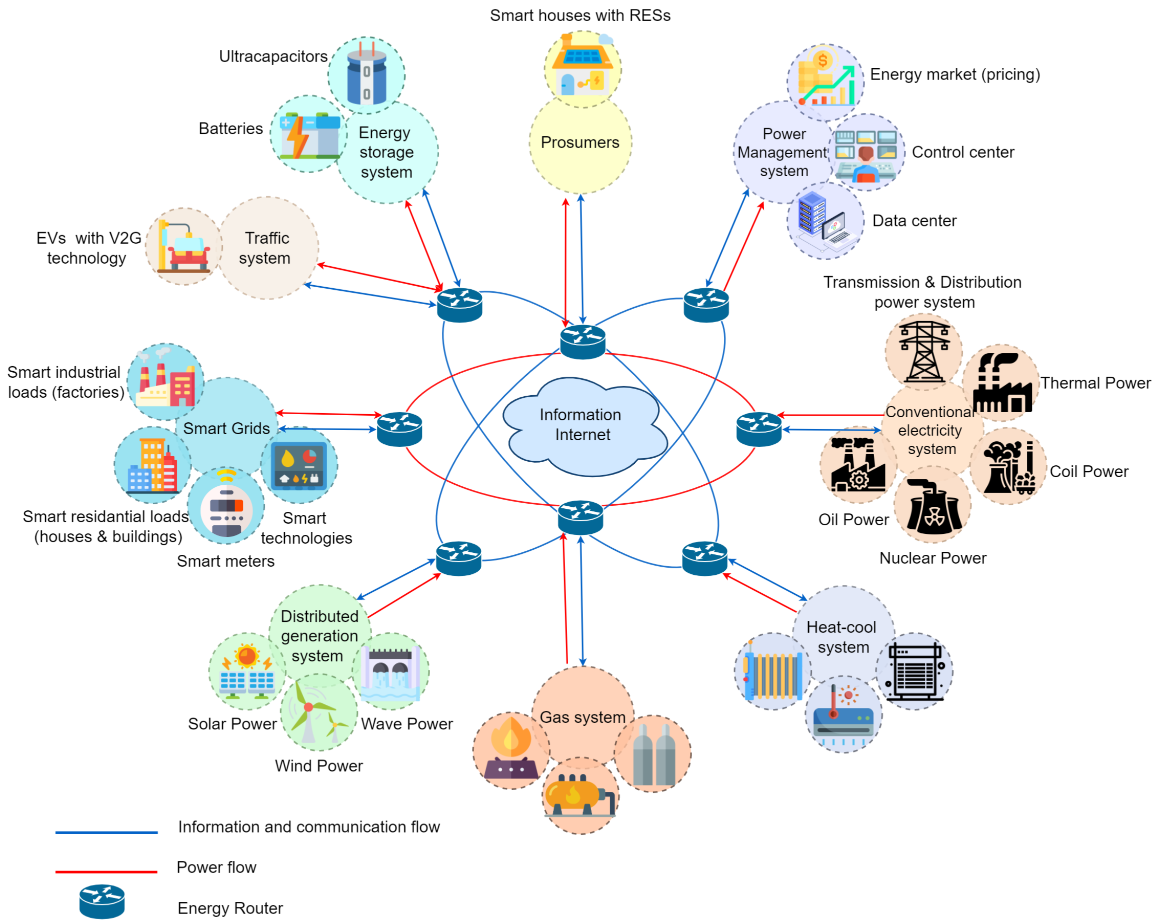

Figure 1.7: Vision of the Energy Internet.

the main focus of EI is to provide a sustainable and robust energy system that enhances access to scalable and distributed RESs and increases the efficiency of energy transmission. Simply, EI is the Internet of energy systems for large-scale energy sharing. The EI concept was inspired by the information internet. As a result, certain aspects of the information internet, such as plug-and-play mechanisms, information routers, open-source software platforms, and so on, have been imitated by the EI [51, 52]. However, EI sets itself apart in terms of network structure, features, services offered, various equipment types, and how it employs internet technology for information exchange to promote bidirectional power and money transfers [45, 53]. Table 1.2 shows a comparison between features of information internet and EI.

Currently, there is no operational EI model around the world. However, several EI-related projects have been launched in industrialised nations, such as the future renewable electric energy delivery and management (FREEDM) system project in USA [54], the E-energy project in Germany [55], the digital-power grid project in Japan [56].

As previously stated, the EI supports a variety of energy sources and forms. The energy flow in this study is stored and distributed as electrical energy. Also, the terms

Table 1.1: Comparison between SG and EI

Smart Grid	**Energy Internet**
■ Electric power system	■ Electric power system, transportation system, natural gas system
■ One type of energy (electric energy)	■ All types of energy (Electric energy, thermal energy and chemical energy)
■ Bidirectional information and communication flow	■ Bidirectional information and communication flow
■ Information system is based on industrial control system	■ Uses an open information network (Internet)
■ Feed-in-tariff scheme for energy sharing between prosumers and utility grid	■ Peer-to-Peer energy trading market where prosumers can share energy among themselves and with the utility grid
■ Distributed generation	■ Distributed generation
■ Smart meters are widely used	■ Energy Routers are the core component
■ Cover a small-scale energy system (regional system)	■ Wide-scale energy system (internet of power systems)
■ Researches focus on local energy consumption and control	■ Focus on creating an interconnected, robust and reliable power system with an increase of energy efficiency (generation, transmission, and consumption) and an efficient use of distributed RESs
■ International standards available, such as IEC 61850 [50]	■ No standards are available

Table 1.2: Comparison between EI and Information Internet

Information Internet	**Energy Internet**
■ Share information (Data)	■ Share energy (Electricity)
■ Information generation using Servers (Application servers, web servers, etc)	■ Energy generation using renewable and non-renewable distributed energy sources
■ Access for all	■ Access for all
■ Two-way of information and communication	■ Two-way of information, communication and power flow
■ Connects different computers and servers	■ Connects different forms of energy networks
■ Communication subnet (wired and wireless)	■ Transmission and distribution power lines
■ Mesh network	■ Mesh network
■ Storage using buffers, short-term or long-term memory	■ Storage using batteries, ultra-capacitors
■ Data is constantly created, retransmitted and stored	■ Energy can not be regenerated and retransmitted but it can be stored
■ Controls nodes and Routers	■ Controls nodes, smart meters and Energy Routers
■ Only information internet	■ Combines IoT, information internet, large data processing, power electronics, smart technologies and devices.

energy and power are used to refer to electricity.

1.1.5.1 Structure of Energy Internet

The idea behind the EI is to connect all different types of distributed energy resources in a way that is open and interconnected, much like the Internet, to enable bidirectional power flow and large-scale P2PET [57]. The architecture of the EI is similar to that of the information Internet and comprises large and small-scale distributed power generation systems (e.g., solar, wind, combined heat and power, geothermal), conventional energy power plants, ESSs (advanced batteries and super capacitors), EVs, consumers, also referred to as loads (e.g., smart homes, buildings, industrial users), and prosumers (consumers equipped with RESs such as rooftop solar panels or micro wind turbines) connected in a mesh network through energy routers [57–60]. Energy Routers (ERs) are considered to be the primary component of EI as they are responsible for energy routing in addition to other functionalities such as information exchange, energy conversion, scheduling and control, etc [10]. Since large-scale EI is structured into smaller-scale local area EIs [3] (microgrids), forming a hierarchy of three levels: distribution network level, microgrid level, and user level [10]. Consequently, energy transfers in EI are predicted to occur at different levels; hence, ERs are expected to be deployed at different levels [10, 57]. Based on their implementation level, ERs are classified into two categories: user-level ER and grid-level ER. The user-level ER is a low-voltage ER connected directly to the user and acts as a HEMS, providing coordinated control of the user's RESs, ESS, and loads [61, 62], and connecting the user (it could be house with or without RESs, EV charging station, an office, etc) to the grid. Consumers, prosumers, distributed energy sources, and ESSs at the microgrid level are connected through grid-level ERs, which are also used to interconnect several microgrids at the distribution network level. Figure 1.8 shows the EI structure with the two categories of ERs.

1.1.5.2 Key elements and technologies of Energy Internet

EI is one of the world's largest and most complicated infrastructures proposed by mankind. It provides a fresh concept and vision for boosting the performance of the electrical grid in power generation, transmission, distribution, consumption, storage, and monitoring. This section discusses critical technologies that can aid in the implementation of the EI.

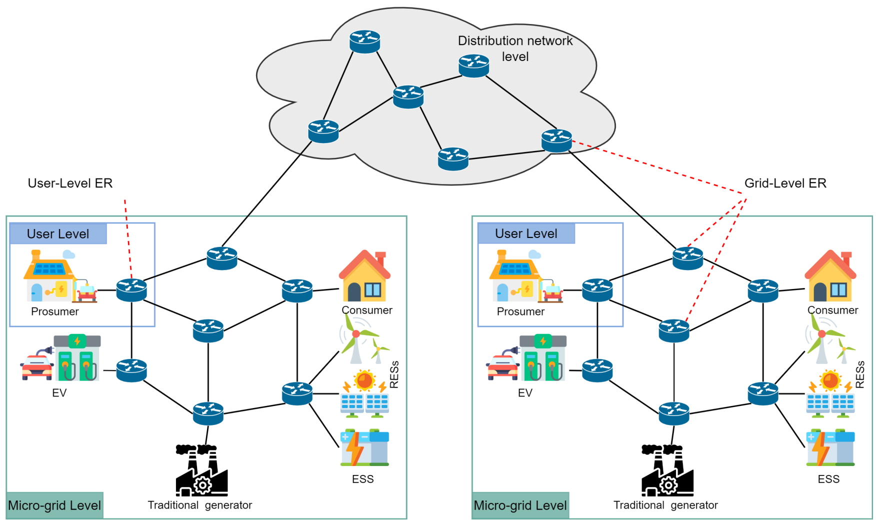

FIGURE 1.8: EI structure with the two categories of ERs.

1. **Smart Grid:** is a crucial dimension of the EI. It combines a connected power system, an intelligent network, and smart monitoring in order to enhance energy usage [63]. The spread of intelligence by the deployment of smart houses and buildings, with smart appliances, smart meters, and intelligent energy management systems, allows for more accurate monitoring and precise control of energy usage. Users may monitor and control the amount of power utilised by their household appliances by using smart HEMSs [64]. Smart meters work together with the smart HEMSs providing real-time information about energy consumption, rooftop solar production, available capacity of ESSs, energy pricing and much more [65]. For the EI, SG will offer energy prediction, control and observation.

2. **Energy Router:** is a fundamental and active technological component for achieving a functional EI infrastructure. It is often referred to as an electric energy router or power router, that combines information exchange and power transmission. ER is a sort of electrical equipment capable of multi-directional power transmission and active power flow regulation [66]. Real-time communication among power devices and dynamic adjustments of energy flows in transmission and distribution networks by rerouting energy flows are two of ER's main functions [67, 68]. The future renewable electric energy delivery and management system center (FREEDM) was the first to propose the ER concept [54]. In addition to the real-time information exchange and the dynamic routing of energy flows, ER is a multi-functional device that has other functionalities such as voltage regulation, multiform energy conversion, reactive power compensation, and power quality regulation [69]. These functions are still accomplished in

current electrical networks in Algeria by switches, disconnectors, transformers, and reclosers, most of which are operated manually.
In order to exchange energy effectively at the right frequency, electric current, and voltage, whether as direct current (DC) or alternating current (AC), ER must interact with the numerous attached users (such as distributed RESs, ESSs, loads), and other ERs [70].

ERs are still in their infancy and are the topic of significant research and development. As a consequence of continuous research on ER architecture, design modelling, functionalities, and control mechanisms, four different types of ER designs have been generated, which are described in further detail below.

- **Solid State Transformer based ER (SST-based ER):** is a commonly used ER model in several EI models. It is the first ER model that FREEDM center [54] has suggested. The SST-based ER converts different energy forms and voltage levels in the distribution network or microgrid [10]. As shown in Figure 1.9, SST-based ER consists of three principle modules: the energy management module (energy control center), power electronic conversion module (Solid State Transformer), and multiple plug-and-play interfaces [71].

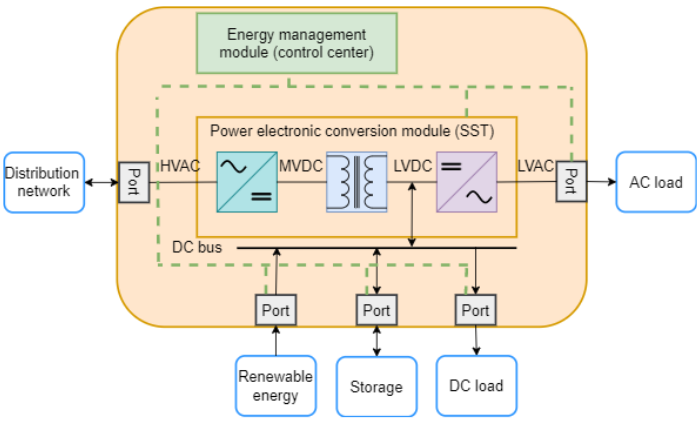

FIGURE 1.9: The structure of SST-based ER [10, 54, 68, 71]

Using information flow, the energy management module may realise communication, power routing, and management. There are two forms of communication: intra-communication, which occurs within the ER between the controller, solid-state transformer (SST), and each electrical port, and inter-communication, which occurs between various ERs [67]. The power electronic conversion module (SST) is a type of power electronic equipment, whose primary function is to convert electricity from the high voltage in transmission lines to various levels of low voltage that are appropriate for usage by electrical appliances. Actually, the SST has many more functionalities than just a voltage step-down function including power conversion, integration of RESs, and reactive power compensation [10, 54]. This SST is typically composed of a succession of sub-transformers interconnected in a three-stage topology to convert voltages [68]. The first stage is the high-voltage AC/DC power conversion stage, which converts the high-voltage alternating current (HVAC) to medium-voltage direct current (MVDC). The MVDC is then transformed to a regulated low-voltage direct current (LVDC) using the middle-frequency DC/DC converter stage, which generates a regulated DC bus and allows the direct connection of distributed energy sources such as RESs, ESSs, etc. Whereas the DC/AC inverter stage produces a low-voltage alternating current (LVAC) that can be utilized for connecting AC loads or grids. These three-stage sub-transformers are tied to a variety of electrical ports that serve as plug-and-play interfaces. Various electrical appliances as well as energy networks can be connected to each interface or port, as long as the combined power does not exceed the interface's capacity restrictions. The SST with three-stage topology provides isolation between its input and output ports, reducing the number of components engaged in power conversion and boosting the overall system's power density and reliability [72]. It has also the ability to regulate both active and reactive power, voltage compensation and fault isolation [71]. SST-based ER only supports electrical energy [73] and is suitable for transmission, distribution, and microgrid networks, indicating that it is a grid-level ER.

- **Multi-Port Converter based ER (MPC-based ER)** is constructed from a control center and a set of ports with bidirectional converters interconnected with a common DC bus that serves as an energy transmission intermediary. As shown in Figure 1.10, the two types of MPC-based ER are DC MPC-based ER and AC/DC MPC-based ER (hybrid MPC-based ER). The DC MPC-based ER has only DC ports or interfaces and routes energy through DC/DC converters. AC/DC MPC-based ER, on the other hand, uses AC/DC hybrid power ports to route energy through AC/DC, DC/AC, and DC/DC converters [74]. MPC-based ER allows the connection and control of all kinds of DESs (RESs,ESSs, . . .) and loads and attains a higher degree of reuse and integration [10]. It is usually used in low-voltage home distribution systems and serves as an interface between the consumer and the distribution grid. MC-based ER is now referred to as a "home energy router" since it is equipped with home energy management techniques that allow for intelligent power flow routing and control within the home [75, 76].

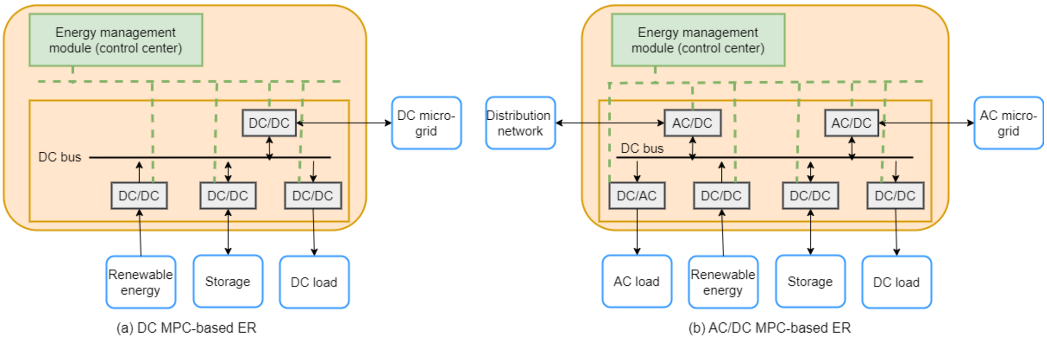

FIGURE 1.10: The structure of MPC-based ER, (a) DC MPC-based ER, (b) AC/DC MPC-based ER [10, 68, 71, 74]

- **Power Line Communication based ER (PLC-based ER)** is depicted in Figure 1.11, where energy and information can be transmitted over the same transmission line. The use of PLC technology in the ER has the following benefits: no need to rewire the network, lower ER volume and cost, and lower communication costs [68]. However, It has also significant disadvantages, including loud noise, constrained bandwidth, signal attenuation, low transmission rate, and no communication fallbacks in the incident that the power line is broken or damaged [73, 77]. The PLC-based ER's main principle is to send power in the form of energy packets [73]. Each energy packet would be preceded by a header containing the address of the source and destination devices and ended with a footer that may contain the synchronisation signal for the ER [78–80], similar to an information packet on the internet. PLC-based ER makes use of multipath transmission and time division of energy flows [81], which is not possible with conventional PLC technology. By using the time-division multiplexing (TDM) mechanism, energy packets are multiplexed throughout a transmission line. Then, individual energy packets are separated out at the receiving end of the transmission line using ER and routed to the appropriate end users (load destination).
- **Switch Array based ER (SA-based ER)** is a newly suggested design that is primarily centred on a switch array. It functions as a HEMS and is typically used in low-voltage household distribution systems. As shown in Figure 1.12, SA-based ER is composed of input and output ports for power sources and loads respectively, two AC buses separated with a switch array, one of them is connected to the grid and loads while the other one is

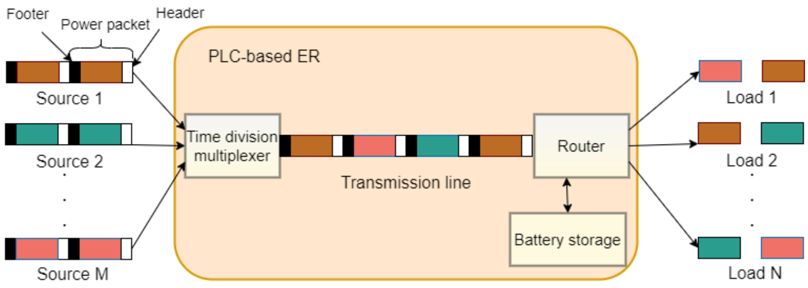

FIGURE 1.11: The structure of PLC-based ER [10, 68, 74, 81].

connected to the distributed energy sources such as RESs, ESSs, EVs, and small diesel generator, in addition to a DC bus with a AC/DC converter [82]. The switch array allows load-switching capabilities for efficient energy utilization by maximizing the use of renewable energy [83].

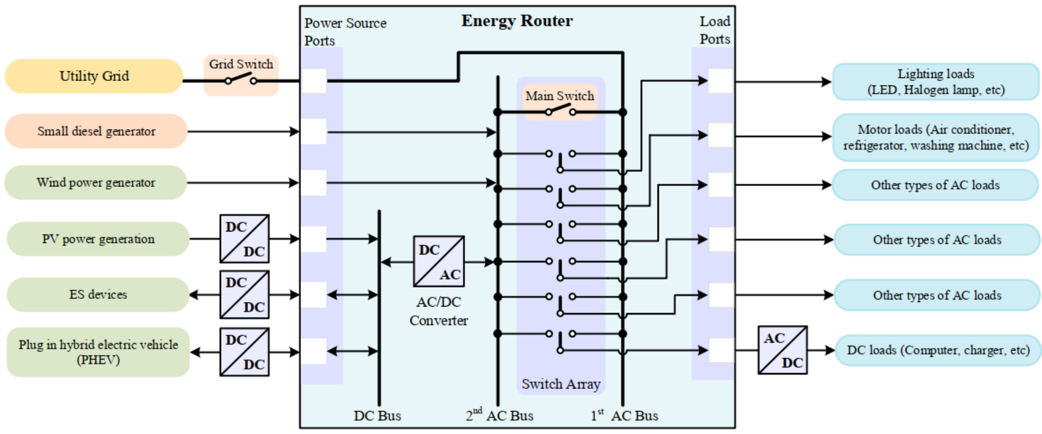

FIGURE 1.12: The structure of SA-based ER [82].

Table 1.3 represents a comparison between the different ER designs.
Despite the significant differences in the suggested models of ERs, they share comparable functional perspectives aimed at increasing large-scale renewable energy utilization and efficient power flow transmission. Currently, the development of ER is in the pilot implementation stage and still needs a lot of effort before it can be widely used.

3. **Distributed energy sources (DESs):** are the cornerstone of EI including small and modular energy sources with a limited capacity of 30 MW or less and are often situated close to the end-users. These DESs are classified into three different categories:

- **Renewable energy sources** such as rooftop solar panels, wind turbines, micro-hydro plants, biomass generators, and fuel cells.

TABLE 1.3: Comparison between the different ERs designs

ER Model	**ER Components**	**ER Functions**	**Application level**	**Proposed ERs**
■ SST based ER	■ Solid state transformer ■ DC/DC converter ■ AC/DC converter ■ Multiple Ports ■ DC bus ■ Control center	■ Bidirectional energy flow ■ Bidirectional information flow ■ Integration of multiple distributed energy sources ■ Flexibility control of active and reactive power ■ Conversion of multiple energy forms to satisfy multiple types of energy demand ■ Conversion of different voltage levels (voltage compensation) ■ Isolation between input and output ports	■ A grid level router used in: ■ Transmission system ■ Distribution system ■ Microgrid system	■ [67], [70], [72]
■ MPC based ER	■ DC/DC converter ■ AC/DC converter ■ Multiple Ports ■ DC bus ■ Control center	■ Bidirectional energy flow ■ Bidirectional information flow ■ Integration of multiple distributed energy sources ■ Conversion of multiple energy forms to satisfy multiple types of energy demand ■ Isolation between input and output ports ■ Acts as a home energy management system providing an intelligent control and routing of energy flows inside the home. ■ Provide bidirectional power flow among neighbors or main grid	■ Household distribution system (user level router)	■ [74], [75], [76], [84], [85]
■ PLC based ER	■ Time division multiplexer ■ Router ■ Multiple ports ■ Transmission line ■ Control center ■ Battery storage	■ Bidirectional energy flow ■ Bidirectional information flow ■ Integration of multiple distributed energy sources ■ Use the energy packet mode ■ Use the time division multiplexing mechanism ■ Information and energy are transmitted in the same transmission line ■ Acts as a home energy management system providing an intelligent control and routing of energy flows inside the home. ■ Provide bidirectional power flow among neighbors or main grid ■ Provide an ER with lower volume and cost and network with simple wiring	■ Household distribution system (user level router)	■ [81]
■ SA based ER	■ Smart switches ■ AC/DC converter ■ Multiple ports ■ DC bus ■ AC bus ■ Control center	■ Bidirectional energy flow ■ Bidirectional information flow ■ Integration of multiple distributed energy sources ■ Optimize the use of renewable energy by the switch array. ■ Acts as a home energy management system, providing intelligent control and routing of energy flows inside the home. ■ Provide bidirectional power flow among neighbors or main grid ■ Operates in connected and isolated modes.	■ Household distribution system (user level router)	■ [82], [83], [86]

- **Non-renewable energy sources** such as natural gas turbines, combustion turbines, diesel generators and micro-turbines.
- **Energy storage systems** such as batteries and aggregated EVs.

The dependency on conventional fossil fuel-based generating systems decreases as more and more RESs are incorporated into the EI. Since these RESs are becoming more affordable and with low or no carbon emissions, there is now a tremendous increase in their utilization worldwide. RESs may be used to generate electricity, provide cold/heat, and provide other energy services that traditional energy sources provide [8]. Wind and photovoltaic energy are the most advanced, cost-effective, and widely employed RESs. The wind power system, which uses the wind source to generate electricity, is regarded as the first to be competitive with traditional power plants. Wind turbines transform the kinetic energy of the wind into mechanical power, which is subsequently converted into electricity by generators. The size of the wind turbine and the wind speed affect the power production. The most pervasive and plentiful energy source on the planet is solar energy, and grid-connected PVs are now the renewable energy technology with the greatest growth rate, increasing by 40 % annually year over year [8]. In a solar power system or photovoltaic system, solar panels generate DC energy by absorbing sunlight through photovoltaic cells composed of semiconductor materials and converting it to usable AC energy with the aid of inverter technology.
Since RESs have not been sufficiently developed to supply the entire demand, and their energy output is extremely variable and unpredictable due to climate and geographical location, RESs must be integrated alongside other complementary technologies such as energy storage systems. However, the integration of DESs brings significant challenges to EI including commercial, technical, and safety issues [87], among which we mention the voltage and frequency fluctuations, the increasing power losses, the high computation burden, and the communication topologies [88, 89]. For an efficient and sustainable EI, DESs specially RESs should be integrated with advanced control, metering, communication, and other improved related technologies that can promote the development of renewable energy technologies, such as energy storage, DC, and power electronics technologies

4. **Energy storage systems (ESSs):** a substantial portion of the EI consists of distributed ESSs, whether they are in a fixed or mobile installation. ESSs can be found in EVs, residential, commercial, or industrial buildings, either individually or as a group [90]. As previously mentioned, the incorporation of

RESs into EI brings new challenges in energy management due to their fluctuation, variability, intermittency, and dependence on weather conditions. For instance, wind turbines may perform poorly in calm weather, solar panels may be unproductive in cloudy weather, and RESs may occasionally produce too much energy, overloading the system. As a result, ESSs are seen as a groundbreaking solution to RESs integration issues, to optimize energy management, and to balance energy generation and consumption [91]. ESSs are primarily intended to gather energy from numerous sources, convert it into another form, and store it as required for a variety of uses. ESSs serve as an energy buffer that can be installed either by the utility company as a backup supply or by the consumer as a battery backup, they charge during low energy cost period and discharge during high cost period, which lowers the cost of electricity for users by supplying power during times of peak demand and generates some financial benefits for users by trading their excess energy to the grid [90]. Furthermore, it provides grid support during peak hours by ensuring an uninterrupted power supply to avoid potential blackouts. In terms of the forms of stored energy, electrical energy storage techniques are mechanical, chemical, thermal, kinetic mechanical, electrochemical, and electric-magnetic field storage [92]. There are now a variety of energy storage technologies available, including flywheel energy storage devices, supercapacitors, compressed air, pumped hydro, and small-scale batteries. Authors in [91] provide a classification of ESSs based on the form of energy stored.

ESSs can be used in EI to reduce peak demand, address the intermittent nature of a large share of RESs, enhance the capability of grid frequency regulation, create a reliable supply and improve grid reliability, stability and efficiency [93, 94]. By 2030, the need for ESSs is predicted to quadruple from its current level [95].

5. **Electric Vehicles integration (EVs):** The majority of the energy used in today's transportation system comes from fossil fuels like gasoline and diesel. Transportation systems are a major source of air pollution, so many countries are electrifying their transportation systems by introducing electric vehicles as a renewable energy alternative for the transportation sector. Electricity for EV charging stations can be supplied from the grid or directly from a PV system which increases the use of RESs [96]. EVs use one or multiple batteries, fuel cells, and ultracapacitors as energy sources [97]. With the introduction of EVs, plans were established to employ EV batteries as mobile energy storage units in order to reap the full benefits of EV integration in grid infrastructure. Therefore, according to their charging state EVs can be both consumers and producers

(prosumers) in the grid since they have the ability to store energy using their batteries and feed it back into the system as required [98]. This is known as vehicle-to-grid technology (V2G). V2G technology creates a bidirectional energy flow between EV and the grid, allowing the EV to serve as a backup power supply in the grid by supplying power during peak demand periods [99].
EVs are critical components of the EI since they connect a transportation network to an electrical network. The integration of EVs with V2G technology increases the usage of renewable energy, lowers greenhouse gas (GHG) emissions for the transportation industry, provides potential income for vehicle owners, and enhances grid stability, reliability, efficiency, and power quality [100, 101]. However, uncoordinated widespread EVs usage has the potential to alter the load profile, change the scheduling of power sources, reduce the quality of the electricity, and lead to other issues with power regulation [97, 102]. Hence, intelligent and efficient EV energy management systems are required for efficient EV integration in the EI.

6. **Plug-and-play interface:** An open interface between electronic components and the EI is the plug-and-play interface. It simplifies communication so that EI-connected devices may be identified anytime, anywhere. It aids in the quick and simple detection of power devices such as loads, DERs as soon as they are connected to the EI, much like information transfer using an USB device in personal computers [53, 73]. There are many interface types (AC/DC) that the plug-and-play interface can have. In an EI, plug-and-play functionality is vital to automatically connect the different DESs and loads to the grid.

7. **Energy conversion and multi-energy interconnection:** The EI is a multi-energy network that connects networks for gas, heat, and electricity. The integration of diverse forms of energy enables the optimization of the entire energy system [93]. Multiple forms of energy conversion, such as the conversion of heat/electric power into chemical/mechanical energy and storing it for later use, power-to-gas systems, combined heat and power systems, and power-to-heat systems, permit the coordinated operation of several energy networks and improve the utilization of energy resources.

8. **Reliable communication technologies:** The combination of energy and communication infrastructure is critical to the success of EI. The bidirectional flow of information between energy components, customers, prosumers, and the utility grid will increase the amount of data that must be transferred and processed [93]. Also, efficient P2PET and efficient operation of EI will need a secure,

reliable, fast and efficient information collection, processing and transmission. Therefore, advanced information and communication technologies are required.

9. **Peer-to-Peer energy trading platforms:** P2PET (detailed in Section 1.1.4) provides several potential advantages, including the potential to decrease peak demand, promote the deployment of RESs, lower overall operating and investment costs, especially for ESSs, give consumers and prosumers options that are consistent with community values (prosumers are free to autonomously choose their energy-sharing settings, including how much energy to give and at what price, as well as who and when to share it with), and enhance energy efficiency and reliability of the grid [28, 103, 104]. To encourage prosumers to trade their redundant energy and to build a secure and trustworthy decentralized energy market, effective P2PET platforms are required. Recently, numerous researchers have been working on designing P2PET platforms and relevant technologies, such as game theory, auction theory, and blockchain have been used.

1.2 Energy routing problem

The EI is primarily reliant on P2PET amongst prosumers, resulting in a convoluted power flow characteristic of the entire system in which power flows from several sources via multiple paths. Since electricity is transferred between prosumers or energy trading pairs through the physical distribution network, uncoordinated energy injection and exchange between prosumers have the potential to exceed the network voltage limit [33], create the reverse power flow [105], violates power lines capacity and overheads the power system [106], jeopardizing the network's safe and efficient functioning [107]. Additionally, throughout the power transmission process in P2PET, power losses in the network lines are unavoidable [108] and will increase with the increasing number of P2P energy transactions between prosumers. The construction of several redundant power lines between the prosumers is the first method that proposes itself for reducing power losses, voltage, and capacity violations; however, this method raises the cost and complexity of the power grid. Hence, the key question that has yet to be answered is: how to establish the optimal power delivery path for a certain power transaction between prosumers to maintain the stability of the power grid? This introduces the energy routing problem.

The energy routing problem is defined as the problem of determining an efficient transmission path with the least transmission losses for transporting power between energy trading pairs that may be situated in various geographical locations [2, 3]. The effective transmission of power over the complicated EI is significantly dependent on the deployment of an efficient energy routing algorithm. In several regards, energy routing varies from data routing and optimal power flow (OPF) problems. The most significant differences are summarized in Table 1.4.

TABLE 1.4: Comparison between Information routing, energy routing, and optimal power flow problem.

Information routing problem	Energy routing problem	Optimal power flow problem
■ In the Information Internet	■ In the EI	■ In the traditional power system
■ The objective is to determine the optimum transmission path for data between network nodes	■ The objective is to determine the best transmission path for P2P energy trading pair	■ The objective is to identify the optimal operating parameters (such as voltage, injected power, etc) to minimize the operation and generation cost of energy
■ Minimize distance, cost, or time for data delivery between 2 or more nodes	■ Minimize the power transmission loss between a specific energy trading pair	■ Reduce the overall transmission loss of all power supplies in a centralized manner.
■ Information routing is demand dominated	■ Energy routing is demand dominated	
■ The source and destination of the data packet are predefined	■ The source of energy in energy request is not predefined	
■ The waste data packet can be regenerated	■ The waste energy can not be regenerated	
■ It is possible to buffer, save or delay the data during the transmission process.	■ There is no possibility of buffering, saving, or delaying the energy during energy transmission.	
■ Overflow can result in significant time delays and data packet loss.	■ Energy overflow may cause overheating, devices destruction, or even a complete system shutdown.	

In conjunction with power conversion and regulation functions, ERs should be outfitted with precise energy routing algorithms to properly transmit power in the network. Energy routing algorithms have three major challenges [57, 109]: subscriber matching, finding an efficient path, and transmission scheduling.

1.2.1 Subscriber matching (Pair matching)

Energy routing is driven by demand and occurs when consumers who are short on energy, also known as buyers in P2PET, submit energy requests to the ER [1].Since the consumer does not know in advance from which supplier -also referred to as producer or seller- they will purchase their needed energy, the energy requests do not include a destination address. Consumers choose to engage in energy trading with the best suppliers who can meet their power needs. Suppliers or sellers, on the other hand, are free to decide how and with whom they will exchange their excess energy.

Therefore, how to match various energy buyers and sellers is a critical question that must be solved. For that, an appropriate subscriber matching mechanism is required to match producers and consumers with different demand and supply requirements creating what we know as power transactions, where each power transaction contains the source and the destination with the power amount to be transmitted.
It is important to note that energy routing can occur between one consumer and one producer (one-to-one mode) or it can occur between one consumer and several producers, as is the case for heavy loads like EVs, where a single producer cannot meet the EV's energy needs; one producer could also supply several consumers at the same time (many-to-many mode) [1]. As a result, energy routing protocols should have an efficient subscriber matching phase between producers and consumers.

1.2.2 Energy efficient path

Power exchange in a P2PET system may increase losses [106] since power signals are acutely vulnerable to transmission loss. Numerous variables, like the impedance of the power lines, energy conversion losses, pre-existing power in power lines, etc., can have an impact on power transmission loss (detailed in Chapter 3). However, many energy trading algorithms do not provide sufficient technical arguments for how they avoid or even ignore the losses brought on by P2P energy transactions. EI is also a mesh network with various energy transmission paths that may be utilized to transport power between pairs. Each path suffers from power transmission loss. As a result, it is vital to limit transmission loss by determining the most energy-efficient path for transmitting power between trading pairs. The energy-efficient path is the path with minimum power loss (detailed in Chapter 3). It is important to note that the path with the least power loss is not always feasible for power transmission if the power lines and ERs constructing the path cannot sustain the power rate, type, and capacity of the power to be transferred, since this may result in overheating and failure [1]. Therefore, energy routing protocols should provide a valid energy-efficient path taking into account the physical constraints of the grid network.

1.2.3 Transmission scheduling (congestion management)

Transmission congestion compromises the reliability, safety, and stability of power systems, as well as their economic viability, and it worsens with the growing incorporation of distributed RESs [110]. Congestion arises when transmission networks fail to transfer all intended power transactions based on the load demand owing to system operational limitations breaches [111]. Congestion also occurs when electricity flows in a transmission line exceed its capacity limit, resulting in an overload (overflow) [112]. An overload can cause catastrophic damage to system equipment (due to overheating), as well as outages, blackouts, and a complete system to breakdown. The fundamental reason for transmission congestion and overflow, according to various definitions, is the transmission network's physical and system limits.

The unregulated and unrestricted energy transactions in the P2PET system may generate network congestion [113]. Since determining the energy-efficient path for different energy transactions without considering the network's physical capacity constraints may result in overloading the path in the event that the transmitted power exceeds the capacity of the path [109]. Congestion can also be caused when there are simultaneous power transmissions between pairs where each pair chooses its transmission path independently of the others at the same time [3]. Therefore, routing all P2P energy transactions in the EI becomes a difficult and complicated task. To this end, energy routing protocols should provide efficient congestion management schemes that prevent power systems from becoming congested and ensure safe and efficient energy transmission.

As a result, for efficient P2PET in EI, the designed energy routing protocols have to provide three main functions: subscriber matching, an energy-efficient path, and transmission scheduling.

1.3 Conclusion

This chapter has presented a detailed overview of the evolution of power systems, from traditional grids to the introduction of the EI. It described the structure, main components, and technologies of the EI, with a special emphasis on ERs and their categorization. The chapter followed by outlining the thesis's main topic: energy routing and its associated challenges, including subscriber matching, energy-efficient path, and transmission scheduling. Energy routing algorithms that successfully handle these three crucial challenges must be developed to accomplish efficient energy transfer within the EI. The following chapters will review the literature on energy routing algorithms, analyze their efficacy in addressing energy routing challenges, and introduce new energy routing approaches to optimize energy routing within the EI.

Chapter 2

Energy Routing Algorithms in Energy Internet: An Overview

The problem of energy routing in EI has received a lot of attention in recent years from the scientific community, and several energy routing algorithms have been proposed. Therefore, this chapter provides an overview of research that has studied energy routing algorithms. We give a detailed study of existing power routing algorithms, as well as a novel classification of them, which can benefit a large audience with an interest in this field of study.

2.1 Classification of energy routing protocols

The ability to safely pack and transfer energy units where and when needed is the most desired aspect of the EI. Therefore, several energy routing algorithms have been suggested in the literature to enable effective power transfer in EI. It is notable that both the virtual circuit mode and the energy packet mode have been employed for energy transmission in different energy routing protocols. Energy is split into several energy packets in the energy packets transmission mode, and each energy packet can be sent from the source to the load along different paths [114, 115] depending on the state of the grid. This mode of energy transmission allows high utilization of power lines, but it could increase the switching power loss of converters resulting from the path-changing process [1]. When operating in virtual circuit mode, a virtual circuit is established between the source of energy and the load by reserving all necessary ER ports and transmission lines along the transmission path [116]. Energy is then delivered through this circuit until the load is disconnected. It uses fewer power lines than energy packet mode [1]. As energy transmission between loads and sources is typically continuous unless the load is unplugged, the virtual circuit mode is the most often used transmission mode in many algorithms.

According to the literature currently available, Five different methods are used to create energy routing algorithms: EVs-based, Graph theory, Game theory, Auction theory, and optimization-based algorithms. Figure 2.1 shows the classification of different energy routing protocols.

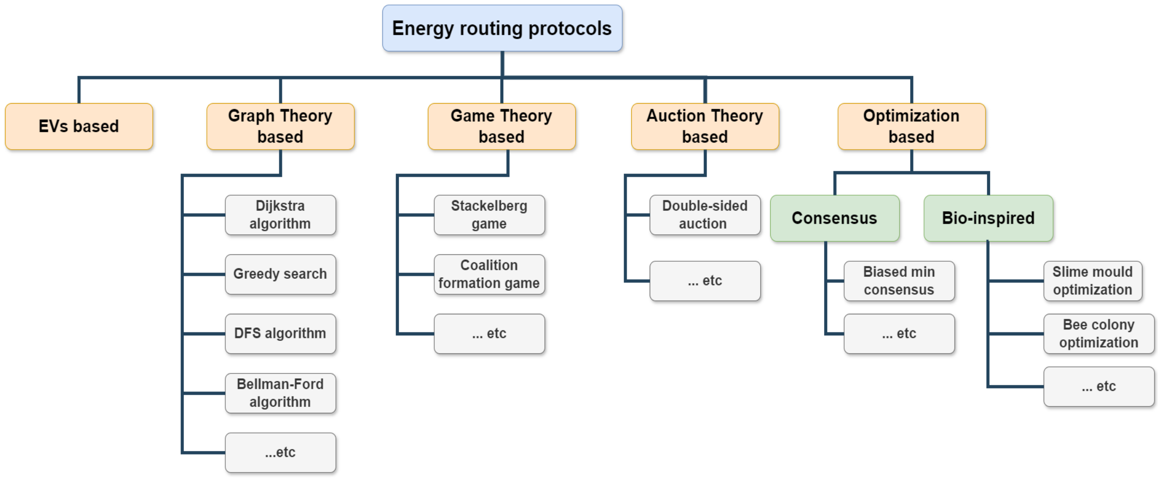

FIGURE 2.1: Classification of energy routing protocols in EI.

2.1.1 EVs-based routing algorithms

With the advent of EVs with energy storage capabilities, some researchers have advocated using EVs in power transmission to facilitate effective power transfer in the EI, which develops the Electric Vehicle Energy Internet (EVEI)[117]. Instead of utilizing power lines to carry energy, EVs in EVEI are used to store, transfer, and distribute energy from RESs toward consumers that require it. In the planned EVEI, battery-powered charging stations serve as ERs to take energy from one EV and deliver it to another EV. Authors in [98] proposed a heuristic energy routing algorithm in EVEI. The algorithm determines the best path to transport renewable energy using EVs from generation points to the charging station to be used by other EVs. The EVEI is represented by a hypergraph, and the best path is the path with the minimum power loss. Power loss occurs at each charge-discharge process of the EV and it is about 10% for each charge-discharge [118]. Authors in [119] prove that the routing and charging-discharging process of EVs is an NP-hard problem and introduce a distributed approximate algorithm that determines the routing with the scheduling of EVs charging-discharging process.

Even though the EV-based power routing was the first technique for power transmission proposed in the EI, using EVs to transport energy has some drawbacks, such as a lengthy charging and discharging process, issues with traffic, the need for more ESSs and charging stations which increase the cost, and the most important is that energy transmission using EVs taking a long time compared to transmitting energy through power lines.

2.1.2 Graph theory-based routing algorithms

Graph-based approaches are one of the strategies used to create energy routing algorithms. The majority of the routing algorithms in this category are concerned with locating the energy-efficient path, with the physical transportation network being represented by a graph and the energy-efficient path issue being defined as the graph theory shortest path problem. Basically in the graph network, nodes represent the ERs and edges are the power lines that connect these ERs. It could be a directed or underacted, weighted or unweighted graph. Several shortest path algorithms have been used to solve the energy efficient path problem, such as the Dijkstra algorithm, Bellman-Ford algorithm, Depth First Search algorithm (DFS), exhaustive search algorithm, etc.

An energy routing protocol for an energy local area network is put forward in [1]. This protocol introduces an energy-efficient path algorithm with a source allocation mechanism for heavy loads. The efficient path algorithm runs in two phases. As previously stated in graph theory-based algorithms, the network is represented as a graph in the first phase, and to prevent overflow and congestion problems, any power lines and ERs that do not satisfy the load power are removed from the graph before computing the path. In the second phase, the energy minimum loss path is calculated after traversing and comparing all the possible paths. For the source allocation mechanism for heavy loads, a combination of source sets is created, and the number of sources in each set should be fewer as possible. The best set with the amount of power to get from each source in the set is determined based on the total transmission power loss caused. The routing protocol is dynamic and uses the OSPF for information exchange but the efficient path algorithm is exhaustive and time-consuming, especially in huge networks, the source allocation for heavy load cases has a high complexity and is time-consuming since it compares all the possible set combinations, also the congestion management technique used could remove the minimum loss path.

Dijkstra algorithm has been used in [120, 121] to solve the energy-efficient path problem. In [120] authors firstly suggested a modified minimum spanning tree method that determines the ideal cable architecture between ERs in EI in order to decrease the complexity of power line connections and EI building costs. Then, the Dijkstra algorithm is used to determine the non-congestion minimum loss path between energy trading pairs. However, the aforementioned algorithm assumes the load and source pairs of an energy transaction directly, which is not optimal when there are several loads and sources present at the same time. While an energy routing mechanism based on real-time transactions was proposed by authors in [121]. To match suppliers and buyers in the energy network, writers created a real-time subscriber matching mechanism in the initial stage of the algorithm. Based on the price and transmission time, the subscriber matching mechanism identifies the source and destination of power flow as well as its amount and transmission time. The proposed mechanism is executed by the producer or the consumer that sends its bidding information including the available or requested power amount to other ERs in the network. After determining the energy trading pairs, the Dijkstra algorithm is used to compute the minimum energy loss path for each pair from their own perspectives. The power packet method was employed to tackle the transmission scheduling and congestion problem. In other words, when there is congestion, energy is split and a portion of it is delivered over the optimal path, while the remainder is sent through the sub-optimal path. The subscriber matching is based only on the price and is carried out at each node following its perspectives, which reflects the convenience of either the producer or the consumer. Other factors, such as power loss, the profitability of the two sides of the pair, etc., should also be taken into consideration in the subscriber matching process. Hemalatha, et al. [122] used the Bellman-Ford algorithm to find the energy minimum loss path with alternating paths between generation units and end users for reconfiguring the electricity system in the event of outages or blackouts. The Bellman-Ford algorithm is a single-path method that requires more time to compute in a large network than the Dijkstra algorithm does.

Razi, et al. propose a centralized graph theory-based energy routing protocol in [2]. In contrast to the previously mentioned energy routing protocols, which focus on minimizing the power loss of an energy transaction, the proposed protocol focuses on minimizing the total energy loss resulting from all energy transactions in the system and addresses the simultaneous multi-source and multi-load scenario. The protocol treats subscriber matching, energy-efficient path, and transmission scheduling problems. In the subscriber matching process, a combination of loads is created in which each load has a different priority in each set (containing all the loads in the network) to determine which load should be satisfied in the first place to get the total minimum power loss. Then for each load in each set, starting with the load with the highest priority all the possible paths to the different energy sources are calculated using the

Depth-First Search traversing algorithm (DFS). After that, the best source for each load in the set is the source with the minimum loss path. The same process is repeated for each set. The optimal solution is obtained by comparing the different set's solutions. For congestion management, the protocol uses the energy packet mode. To put it another way, the protocol identifies energy sources and schedules energy transactions in accordance with the overall power loss experienced by the network. Despite the method's advantages, many details were not considered in subscriber matching such as the price, profit, and the strategic decision-making of peers. Furthermore, centralized routing methods put all of the computational efforts on a control center which demands high computational resources and time, especially in large systems, which makes them unsuitable for real-time energy trading.

Unlike previous studies, and in order to avoid the congestion resulting from simultaneous energy transmissions, authors in [3] proposed a semi-decentralized energy routing algorithm to solve the minimum loss transmission problem. The proposed algorithm is divided into two parts: the fully distributed part and the centralized part. In the fully distributed part each pair in the proposed routing protocol searches for the minimum loss path in a fully decentralized way without considering the path selection of other pairs. In order to determine the minimum loss path, first the DFS is used to get all the paths that connect the pair. Then, the optimal path selection problem is formulated as a non-linear programming problem and solved by using the Lagrange multipliers method, which yields a multipath solution with splitting energy. After each pair independently selects the optimal paths, paths information are sent to the network control center to check for path overlapping cases. This process represents the centralized part in which if a path overlapping occurs between multiple pairs, the network control center centrally creates a coalition between all the affected pairs with the objective of minimizing the total transmission loss by recalculating new paths for them. The matching process was not examined in this study.

2.1.3 Game theory-based routing algorithms

Game theory is a mathematical technique that examines how players make strategic decisions in competitive situations where each player's choice of action influences and depends on that of the other players [123]. As P2PET in EI provides a competitive energy market among prosumers with conflicting interests, game theory has been extensively used as a useful analytical tool for modelling and analyzing prosumers interactions in the P2PET system. This category of energy routing algorithms primarily addresses the subscriber matching problem. In which prosumers (producers and consumers) compete in a game (such as the Stackelberg game, the Coalition game, etc.) to establish the trading pairs while maximizing their benefits. The authors of [34] suggested a P2P energy trading strategy based on a Stackelberg game to demonstrate how selling energy between peers might assist the centralized power grid in lowering generating costs during peak demand periods. In this Stackelberg game, the centralized power system (center) represents the leaders while prosumers are the followers. Under the suggested strategy, prosumers would only participate in P2P energy trading when the grid price is extremely high during peak hours. Prosumers use a double auction scheme to participate in a coalition formation game to form two different coalitions. In the first one, prosumers exchange their energy using the auction price, and the subscriber matching technique employed is the same as presented in [33]. While the second coalition comprises the remaining prosumers, they trade at a mid-market price, and the subscriber matching process is the same as in [124]. The fundamental drawback of this protocol is that prosumers are only permitted to exchange energy with one another during peak hours; otherwise, they must trade energy with the centralized power grid (FiT scheme). Furthermore, the matching process did not consider network constraints (voltage and capacity constraints), power losses of power transactions, social welfare, etc.

Another P2PET mechanism was proposed in [33]. In which the suggested subscriber matching algorithm prioritizes participating prosumers (sellers and buyers) by arranging them according to the lowest selling price for sellers and registration order for buyers. In the second phase of the algorithm, sellers' supply and buyers' demand are adjusted to achieve a balance between overall demand and supply. Each buyer on the buyers set will be matched with one or more sellers from the sellers set in the final phase according to their demand. The mid-market rate method is used to determine the trading price of each energy transaction, as a result, each power transaction has its trading price. The energy transaction pairs are constructed in a centralized manner based on the sellers' and buyers' priorities given by the selling price and registration order of buyers. As more prosumers join the network, the protocol's execution time will highly increase. The collapse of the central unit also results in the breakdown of the whole energy trading system. Furthermore, power losses and network limits (such as capacity and voltage restrictions) are not taken into account in this study.

Authors in [30, 124] introduce P2PET strategies based on canonical coalition games to match producers and consumers in EI. In the first scheme, prosumers trade their energy using a mid-market rate price mechanism (a price between the FiT and grid market prices). While in the second scheme, authors assume the absence of storage devices, therefore, the peer-to-peer energy trading occurs only during sunshine hours employing a mid-market rate price mechanism. The authors of these studies, like many others that have suggested P2PET strategies, did not detail how peers are matched in their suggested schemes.

2.1.4 Auction theory based routing algorithms

On the other hand, prosumers in auction-based techniques participate in the market by submitting offers/bids to an auctioneer, the auctioneer determines the price, power amount, and the two trading sides of each energy transaction. An auction mechanism is suggested in [125] with the goal of increasing sellers' profits in P2PET. Where transmission costs, buyers' bid , and operating costs are taken into consideration. Based on their profit, suppliers can choose whether to sell or conserve their energy under the suggested mechanism. Peers are matched using a profit maximization algorithm, in which the supplier arranges buyers' demand in ascending order and selects the lowest demand as the selling energy in the first phase. In the second phase, the supplier calculates its profit based on buyers' bid, transmission cost, and operating cost for each buyer and chooses the buyer with the highest profit that meets the line and capacity constraints. The algorithm is repeated until the supplier's surplus energy is sold or the profit goes negative. The suggested approach is supplier-centric, with the goal of increasing supplier profits while disregarding buyer interests. Furthermore, the process is intended for a single supplier with several buyers, which is not the case in practice. Lines capacity constraints are considered in this work, however, the path selection approach is not described.

Another double-sided auction mechanism is proposed in [126], in which sellers with surplus energy submit their offers to the auctioneer and buyers bid on the demand. The auctioneer matches sellers and buyers by determining the energy amount to be traded in conjunction with the trading price. The auction begins only if the buyer's bid exceeds the seller's offer; otherwise, no transaction occurs between the seller and buyer. The auction method establishes a trading price range, and consumers who fall outside of this range are excluded from the auction and do not participate in the trading market. For the purpose of matching peers, a group of buyers is formed for each seller whose bid is higher than the seller's offer. Using the same principle, a group of sellers is formed for each buyer. The suggested system addresses two distinct scenarios. In the first, the total demand exceeds the total surplus energy; the auctioneer ranks the sellers in ascending order depending on their offers. The auctioneer then selects for each seller from its buyers' group the buyer with the equal demand of the seller's surplus energy; otherwise, the selected buyer is the one with the greatest demand from the group. This loop will be continued until the seller's surplus energy is depleted. For the second scenario, the total demand is lower than the total surplus energy; buyers are arranged in descending order according to their demand. The auctioneer selects for each buyer from its sellers' group the seller with the equal surplus energy as the buyer's demand; otherwise, the seller with the least offer from the group is chosen. This sequence will be repeated until the buyer's demand is fulfilled. Using the random value approach, the auctioneer chooses a random price between the seller-buyer pair's offer and bid to determine the trading price for each created pair. In this study, prosumers primarily trade among themselves, leaving some sellers without the opportunity to sell their excess energy and certain buyers without the ability to satisfy their needs. Network constraints are not considered during the matching process.

2.1.5 Constrained optimization-based routing algorithms

The technique of maximizing or minimizing an objective function with regard to one or more variables while taking into account the constraints of those variables is known as constrained optimization. In EI, the energy routing problem in many research has been considered as a constrained optimization problem that aims for example to minimize the power losses, maximize the profit, minimize the energy cost, etc. Several optimization techniques have been used to solve the energy optimization problem such as consensus, bioinspired, and new optimization techniques such as the work in [127]. Since a multi-agent system (MAS) is defined as a collection of computational units known as agents with some level of autonomy and the capacity to make autonomous decisions, the energy network is typically depicted as a MAS in optimization-based routing protocols in several studies [128, 129]. The agents possess intelligence; they can observe their surrounding environment and behave to achieve goals in accordance with environmental performance metrics [130].
Khorasany et al [127] introduced another subscriber matching and negotiation mechanism in P2PET. This mechanism allows prosumers to agree on the quantity of energy to be exchanged as well as the trading price while optimizing their economic surplus. The authors assume the existence of a public database where any prosumer may publish his offer and browse the offers of other prosumers. In trade, sellers begin by offering their maximum generation capability, while buyers submit their minimal demand. Grid operator compensates power losses during energy exchange for transaction fees that are split evenly between the supplier and buyer. Each buyer constructs a vector of potential partners by ranging in ascending order all sellers that can provide its energy demand according to their price offering while considering transaction fees.

Following that, the buyer submits its vector to the selected sellers and negotiates the amount and price of energy with them. The negotiation mechanism used a greediness factor. After receiving the buyers' vector seller does the same process except for the range, in this case, is in descending order. Prosumers who did not match in the P2PET trades with the grid operator.

2.1.5.1 Consensus-based routing algorithms

As far as we are aware, very few researchers have suggested consensus-based solutions to energy routing issues. Most of them focused on the problem of choosing an energy-efficient path. Authors in [131] introduce a new discrete biased-min consensus algorithm to solve the energy routing problem. In this work, the energy routing problem is formulated as an optimal routing discovery problem. The algorithm determines the best supplier with the energy minimum loss path while avoiding line congestion. The DC-micro grid is represented by an undirected graph. Consumers send energy requests to other prosumers by using a discrete max consensus algorithm. Prosumers with surplus energy (suppliers) calculate the minimum transmission loss by using the discrete biased-min consensus. The minimal loss path is found by recursively searching the communication network for the parent nodes. Finally, consumers use the discrete min consensus algorithm to choose the supplier with the minimum transmission loss. For congestion control, the power loss of power lines that could not transport the entire quantity of energy is set to infinity. The proposed algorithm provides a single path for each energy transaction and ignores power lines with limited capacities. Additionally, the authors did not address the heavy load scenario.
Another discounted min-consensus algorithm is proposed by Yinliang et al in [129] to solve the energy routing problem. The algorithm determines the best supplier with the minimum power loss. It has similar steps to the previous one [131] and replaces the discrete biased min consensus with the new discount min consensus algorithm. Additionally, the algorithm handles the heavy load situation and creates a combination of power suppliers for the heavy load. When the selected source with the lowest power loss is inadequate to meet the consumer demand, the algorithm determines the remaining demand power and runs the calculation again with the new demand. The cycle continues until the consumer demand is met. For congestion management, the power loss ratio of power lines that couldn't transfer the full amount of power is adjusted to the value one to prevent them from being part of the path. The presented algorithm is adaptive to topology changes and requires just information transmission between neighbors via P2P communication. The transmission loss of a path is directly

related to the transmission loss of power lines and ERs (detailed in Chapter ??); however, the power loss of ERs is not factored in this method. Furthermore, neither of the protocols [129, 131] takes into account simultaneous energy transmission, which might lead to power system congestion.

2.1.5.2 Bio-inspired based routing algorithms

The aforementioned algorithms based on different methods such as consensus, game theory, graph theory, etc, consider the energy routing problem as an optimization problem and aim to find the optimal solution for it. However, the major disadvantage of these algorithms is the increasing time required for obtaining the solution, particularly in large complex systems. Recently in order to reduce the computational complexity, nature-based algorithms also known as bio-inspired algorithms have evolved to solve the energy routing problem [132]. As is well known, bio-inspired algorithms are metaheuristics that compromise optimality to find a near-optimal solution for the most challenging optimization problems with less computational effort. The application of metaheuristic algorithms in energy routing is new, and only a few protocols have been established such as the slime mould optimization-based energy routing protocol proposed in [133]. The protocol provides a subscriber matching mechanism between the prosumers with the minimum cost energy path. The minimum cost path is obtained by using the slime mould optimization algorithm. The path cost is the sum of the cost of power lines constructing the path. The authors didn't go into detail on how the cost of power lines is calculated. For the subscriber matching based on the requirement and cost of energy, the proposed slime mould algorithm combined with the Hungarian matching algorithm to determine the best supplier for each consumer. The power losses of energy transactions are not considered in this work.
A bee colony-based energy routing algorithm is introduced in [134]. The suggested algorithm aims to reduce the total power losses and costs of the whole network. It chooses the best producer for each consumer while minimizing the energy transmission cost. The cost of the path depends on the power loss of the path and the energy price of the producer. The proposed algorithm is executed at the central controller, this later determines a set of producers for each consumer with the energy minimum loss path between them. The producer is chosen for subscriber matching based on its pricing and transmission power loss to the consumer. Since population-based metaheuristic methods provide a set of feasible solutions with the best one between them, in the case where the consumer is a heavy load, the algorithm selects the solution (producer) with the highest available power and the lowest power loss as the first

source to get energy from, and the remaining power is supplied by the other solutions. Furthermore, in the multi-producer multi-consumer scenario, the algorithm creates a combination of consumers where the consumer priority differs in each set, and it gives the preference of minimizing price rather than minimizing power loss in cases where the available power exceeds the demand, whereas in the opposite case, the preference is to minimize power loss. Another artificial bee colony-based energy efficient path algorithm is proposed by the work in [132], where minimum loss energy transmission paths are determined based on the energy losses of ERs and power lines. The proposed protocol used both virtual circuits and energy packet transmission modes. Subscriber matching was not considered in this work.

According to the literature featured in this chapter, the majority of the algorithms given as a solution for the energy routing problem addressed energy-efficient path and transmission scheduling issues (congestion). Nevertheless, initiatives that promoted P2PET platforms and designs focused on the subscriber matching process. As shown in Table 2.1, authors in different works proposed the use of deterministic methods such as Dijkstra, DFS, Bellman-Ford, and exhaustive search traversal algorithms for determining the minimum energy loss path. These algorithms provide a single minimum loss path. The fundamental drawback of these algorithms is that it takes more time to find the solution to huge and complicated power systems. For that, several academics have recently focused on the application of bio-inspired algorithms.
Moreover, without proper technical explanations, most of the algorithms that solved the subscriber matching issue (see table Table 2.2), which are based on game theory, auction theory, and so on, ignored the energy losses incurred by P2P energy transactions. Since P2PET markets are expected to be developed in grid-tied systems, matching participants in EI without considering routing and grid constraints could lead to an increase in power losses, congestion issues, and even the failure of the system. Therefore, grid constraints and power losses should be integrated into the matching process.
There are currently few studies on congestion management in the distribution system that take P2PET into account. In fact, energy routing is a useful method for avoiding congestion and scheduling energy transactions in the EI. As shown in Table 2.3, according to the works cited in this chapter, two congestion management techniques are employed by the various protocols to schedule energy transactions and prevent congestion problems.

- **Method 1:** To prevent congested lines from being part of the selected path, all the power lines and ERs that could not transmit the power are ignored

TABLE 2.1: A comparison of existing energy-efficient paths algorithms

Ref	Year	Based on	Algorithm	Structure	Weaknesses
[1]	2017	Graph theory	exhaustive search traversal algorithm	Decentralized	High complexity, high computation time, the optimal path could be removed by using the proposed congestion method
[120]	2018	Graph theory	Dijkstra Algorithm	Decentralized	The source and load pairs are directly assumed, Dijkstra is a single path algorithm with high complexity in large networks
[121]	2019	Graph theory	Dijkstra Algorithm	Decentralized	Dijkstra is a single path algorithm with high complexity in large networks.
[122]	2012	Graph theory	Bellman-Ford algorithm	Centralized	Did not consider the existence of P2P energy transactions, only for the reconfiguration of the power system.
[2]	2020	Graph theory	DFS algorithm	Centralized	High computation complexity and time, complex selection routing algorithm that compares all the possible paths (exhaustive search algorithm).
[3]	2022	Graph theory	DFS with Lagrange multiplier method	Semi-decentralized	Compares all the possible paths before determining the best one, resulting in considerable time delay for large systems.
[131]	2018	Consensus	Discrete biased min consensus algorithm	Decentralized	ignore paths with small capacities, heavy load case is not considered.
[129]	2019	Consensus	Discounted min consensus algorithm	Decentralized	Power losses of ERs are not factored, possible power congestion resulting from simultaneous transmissions between different pairs.
[133]	2020	Bio-inspired	slime mould algorithm	Decentralized	Power losses of ERs and power lines are not included in the cost of the paths, possible power congestion resulting from simultaneous transmissions between different pairs.
[134]	2022	Bio-inspired	bee colony based algorithm	Centralized	The obtained solution in large networks are near-optimal solutions.

TABLE 2.2: A comparison of existing subscriber matching strategies

Ref	Year	Algorithm	Metrics	Structure	Weaknesses
[121]	2019	Optimization function	Producers price	Decentralized	Subscriber matching based on price only.
[2]	2020	Optimization function	Power losses between producers and consumers	Centralized	High computation complexity and time, creates an of satisfying loads after comparing all possible situations, subscriber matching based on power loss only without considering prices and preferences of prosumers.
[34]	2019	Cooperative coalition formation game	financial benefits (price, with power amount)	Centralized (auctioneer)	Power transmission losses, and preferences of prosumers are not considered, Prosumers engage in P2PET in peak hours only.
[33]	2019	Optimization	price, power amount	Centralized	High complexity and computation time, matching based on perspectives of central unit only, transmission losses, energy routing are not considered.
[125]	2019	An auction mechanism	Seller profit, line capacity constraints, buyer bid offer	Centralized	Works only for single supplier and multiple buyers case, based on the supplier preferences only.
[126]	2021	An auction mechanism	buyer's demand and bid, seller's profit and surplus energy	Centralized (Auctioneer)	High complexity and computation time, power losses and network constraints are not considered, in some cases, multiple prosumers are not allowed to trade.
[127]	2020	Optimization	Prosumers offers, transaction fees	Decentralized	
[131]	2018	Discrete min consensus algorithm	Transmission power losses	Decentralized	price, profit and perspectives of prosumers are not considered.
[129]	2019	Discrete min consensus algorithm	Transmission power losses	Decentralized	price, profit and perspectives of prosumers are not considered.
[133]	2020	Slime mould algorithm with Hungarian matching algorithm	Cost of the path	Decentralized	Power losses of energy transactions is not considered, authors did not detail the factors used in the path cost.
[134]	2022	Bee colony based algorithm	Producers price and power losses	Centralized	Sacrifice the optimality of solutions with the fast procedure.

TABLE 2.3: A comparison of existing congestion management techniques

	Congestion management methods	
	Method 1	**Method 2**
References	[1], [131], [129]	[120], [121], [2], [3], [134]
Weaknesses	Power lines with small capacities are ignored leading to unevenly distributed transfer of energy between them, which could result in higher losses and possible network congestion. Its effectiveness can not be guaranteed in simultaneous power transmission by different pairs	Guaranty the congestion prevents in the single trading pair case only, otherwise overlapping paths could occur, resulting in higher losses and possible network congestion.

and deleted from the graph network before calculating the efficient path [120]. Following the same principle with a slight change, instead of deleting power lines that could not transmit the power, set their power loss ratio to the value 1 or infinity before calculating the efficient path [129, 131]. Transmit power using virtual circuit mode.

- **Method 2:** After calculating the energy-efficient path, if it is insufficient to transmit the whole amount of energy, another or more paths are added to transport the power. The power, in this case, is split into energy packets; the efficient path transmits its maximum capacity and the remaining power is transmitted through the added paths (sub-optimal paths).

Additionally, energy routing protocols suggested in the literature are separated into two structures: centralized and distributed, with each structure having its own advantages and disadvantages. A control center unit performs energy routing, including subscriber matching, energy-efficient path, and transmission scheduling, in centralized energy routing algorithms. This control center designs carefully energy routing from the perspective of the entire system, ensuring that system power losses are kept to a minimum, physical limits of EI are met, and congestion concerns are avoided efficiently. The solutions found are globally optimal. Nevertheless, the fundamental drawback of centralized algorithms is that all of the network's computational requirements are placed on a single unit, which expands execution time, especially for large-scale systems, and necessitates a lot of communication that can violate network users' right to privacy. Besides that, decisions in energy management, particularly subscriber matching, are made primarily based on the preferences of the control center, which contradicts the concept of P2PET, in which participants play an active

TABLE 2.4: A comparison of the solving problems by the existing energy routing protocols

Ref	Year	Solved Problem			
		Subscriber Matching	Energy Efficient Path	Transmission Scheduling	Heavy load scenario
[1]	2017		✓	✓	✓
[120]	2018		✓	✓	
[121]	2019	✓	✓	✓	
[122]	2012		✓		
[2]	2020	✓	✓	✓	✓
[3]	2022		✓	✓	✓
[34]	2019	✓			
[33]	2019	✓			
[125]	2019	✓			
[126]	2021	✓			
[131]	2018	✓	✓	✓	
[129]	2019	✓	✓	✓	✓
[133]	2020	✓	✓		
[134]	2022	✓	✓	✓	✓

role in the P2PET market. Power systems with P2PET markets are very dynamic, and centralized approaches may be ineffective in dealing with unanticipated topological changes. As a result, various studies have looked into decentralized routing algorithms.

Subscriber matching, energy-efficient path, and transmission scheduling are all accomplished at the level of distinct ERs individually in decentralized energy routing algorithms. In this structure, ERs (or players) make decisions based on their own perspectives without taking into account the decisions of other participants. This will reduce the control center's computational burden. In contrast to a centralized structure, the provided solutions are not necessarily globally optimal. As calculating the paths and contracting the energy transactions at the same time by different ERs individually may result in overlapping paths. The overlapping path situation will result in a larger overall transmission loss for every extra unit of power added and even line congestion (detailed in Chapter 3).

Contrary to popular assumption, power routing does not just examine the search for the least loss paths between sources and loads in a power network; rather, it compromises the matching of power sources and loads with the selection of the non-congestion least loss paths. Energy routing protocol should combine the subscriber matching process with the selection of non-congested least loss paths. Table 2.4 resumes the solved problems by each routing protocol. Furthermore, energy routing decisions are time-consuming when compared to power transmission over transmission lines; additionally, matching market participants in a P2PET system should be in near real-time to ensure power availability; thus, energy routing protocols with low computational time are required.

2.2 Conclusion

This chapter analyzed, categorized, and assessed the strengths and drawbacks of the existing energy routing algorithms within the EI. While the majority of the energy routing algorithms focus on identifying non-congested energy-efficient paths, subscriber matching is typically addressed in separate P2PET studies. Only a few algorithms address all three essential routing issues: subscriber matching, energy-efficient paths, and transmission scheduling (congestion control). However, these algorithms frequently focus on either power losses or trading costs, while disregarding other P2PET criteria in the EI. Future energy routing algorithms should consider various aspects to create a more holistic and efficient EI.

Part II

Contributions

Chapter 3

System description and problem formulation

This chapter is an introduction to our many contributions. It explains the basic hypotheses on which our study is founded, and summarizes the aspects shared by the three chapters 4, 5, and 6.

3.1 System components and parameters

EI is one of the world's largest and most complicated infrastructures proposed by mankind. It is a multi-energy network that connects electrical power grids, natural gas networks, and cooling and heating systems. As previously mentioned, the energy flow in this study is stored and distributed as electrical energy.

In this thesis and as shown in Figure 3.1, EI is considered as a mesh network that connects by using ERs and power lines: large and small-scale distributed power generation systems (such as solar and wind power plants, combined heat and power plants, and geothermal power plants), conventional energy power plants (referred to as traditional producers), ESSs (advanced batteries and super capacitors), EVs with their charging stations, consumers (referred to as loads such as smart homes, hospitals, buildings, and industrial users) and prosumers. Prosumers are proactive consumers who have RESs; in this work, they are referred to as smart houses with rooftop solar panels or micro-wind turbines and ESS. Prosumers can participate in the EI as both producers and consumers of energy. They serve as producers when there is an excess of their local energy production; when there is a shortage, they behave as consumers. Figure 3.1 shows an example of the desired structure of the EI with ERs.

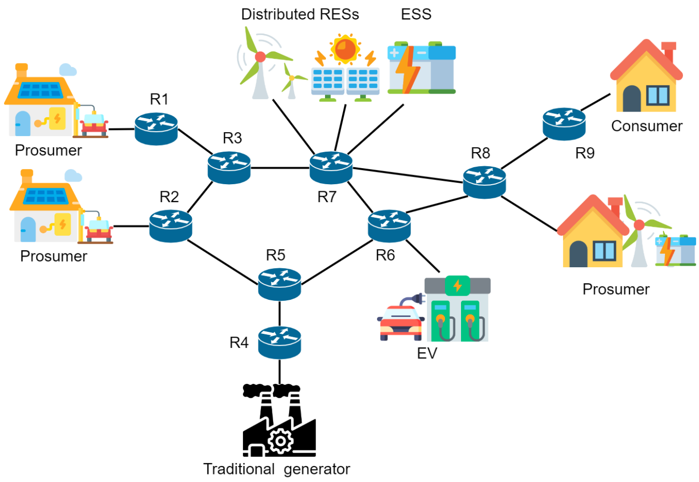

FIGURE 3.1: An example of the desired structure of the EI with ERs.

The time of RESs generation, at the prosumer level, relies on weather conditions (electricity output from solar plants depends on the quantity of direct sunshine, while power production from wind turbines depends on wind speed), and it often only partially fulfils the household demand. Therefore, prosumers have three alternatives for their excess RESs production: store it in a battery storage system for later use, or trade it with the utility company and inject it into the grid for monetary compensation (FiT scheme), or, through the P2PET market, prosumers may sell their excess energy to neighbors who do not own a RESs system (consumers) or whose current consumption exceeds their production (other prosumers). As the financial benefits of trading energy with the utility company are limited, prosumers choose to store energy for later use if they have ESSs, which are still costly, or trade it with other prosumers and consumers in the network rather than selling it to the utility company using the FiT scheme.

Moreover, we assume that consumers who do not own a RESs system or prosumers with a shortage of energy generation prefer to buy energy from neighboring prosumers with surplus generation at low unit prices rather than buying from the utility company at high unit prices. While the utility company serves as a backup trader in the P2PET market, it either provides unlimited electricity supply to the grid using traditional power plants or through distributed power generation systems when prosumers' local RESs do not generate enough electricity to cover local demand. It has unlimited storage capacity to absorb surplus electricity bought from the prosumers when their local production surpasses local demand, this will maintain the stability of the system.

The majority of P2PET projects and initiatives today physically transport energy across distribution networks set up by the traditional grid (utility companies); hence, P2PET markets need to be beneficiary to utility companies. In the proposed EI, we assume that prosumers or trading peers should pay a subscription fee to the utility company to access its network for P2PET.

It is vital to note that throughout the rest of this thesis, we adopt the terms producers or sellers for prosumers with excess energy, and the terms consumers and buyers for prosumers with a shortage of energy.

ERs are essential for establishing a networked P2PET system and managing bidirectional data and power flow. They can have several legs (connected to multiple power lines) that enable the construction of a distribution network with multiple energy distribution paths (a mesh topology). Due to the fact that RESs, ESSs, consumers, and prosumers may have diverse requirements for interface types (AC or DC), voltage levels, power levels, and power quality criteria, and considering that the power distribution architecture in the EI can use a DC interface through low-voltage (LV) or medium-voltage bus (MV), AC interface, or a combination of both, this thesis introduces a hybrid AC/DC power distribution architecture. The basic aim is to reduce the requirement for energy conversion between AC and DC forms, thereby increasing efficiency. This is accomplished by deploying multi-port SST-based ERs. Figure 1.9 in Chapter 2 represents the used multi-port SST-based ER structure, while Table 3.1, and Table 3.2 show the ERs and power lines parameters used in the network in Figure 3.1.

TABLE 3.1: Energy router parameters used in the EI system in Figure 3.1

ER	**Capacity P^C_{ER} (kW)**	**Efficiency (eff)**	**ER**	**Capacity P^C_{ER} (kW)**	**Efficiency (eff)**
R_1	20	0.98	R_6	18	1
R_2	15	0.98	R_7	20	1
R_3	10	1	R_8	18	0.98
R_4	15	0.98	R_9	20	0.98
R_5	15	1			

TABLE 3.2: Power line parameters used in the EI system in Figure 3.1

Power line	**Capacity P^C_{line} (kW)**	**Resistance (Ω)**	**Voltage (V)**
L_{1-3}	30	0.6	400
L_{2-3}	20	0.64	400
L_{2-5}	20	0.51	400
L_{3-7}	45	0.94	400
L_{4-5}	24	0.19	400
L_{5-6}	20	0.45	400
L_{6-7}	40	0.24	400
L_{6-8}	30	0.21	400
L_{7-8}	30	0.21	400
L_{8-9}	32	0.6	400

As shown in Figure 3.1, EI is a mesh network where energy flows from multiple sources through multiple paths with bidirectional power and information flows. As

energy routing is driven by demand and the energy source is unknown in advance, ERs are needed to store power information tables about all connected devices, ERs, and power lines rather than the minimum loss path routing tables [57]. Furthermore, EI is a dynamic network in which many metrics can change, such as energy generation, consumption, prices, trading pairs, transmission paths, connected and disconnected components, the availability of power lines and ERs capacities, etc. With all these changes, the EI network has to stay up to date. Therefore, ERs must share any change in the network by updating their storing tables and sharing them with each other.
In this thesis, we assume that information exchange and energy forwarding are handled by the ERs. Using the energy routing protocol, the ER will autonomously select the trading pairs (producers-consumers) with the non-congestion minimum loss path between them.

3.2 Graph theory model of the system

Graph theory has been widely and successfully used to model diverse systems in a variety of domains. The system objects are represented by a set of nodes, and the particular relationships between some of the pairs of objects are stated by lines connecting these pairs of nodes. Recently, graph theory has been increasingly applied to model the power system in order to solve the energy routing problem (see Chapter 2). EI in this thesis is represented by a connected undirected weighted graph $G = \{V, E, W\}$, where:

- V is the set of nodes in G, which represents the energy routers of the network $V = \{R_1, R_2, \ldots, R_n\}$.
- E is the set of edges in G, which represents the transmission lines (power lines) connecting ERs, $E = \{L_{ij}, \ldots\}$, where L_{ij} is the power line that connects router R_i to router R_j. Two nodes (ERs) R_i, R_j of G are adjacent, if $L_{ij} \in E$.
- W describes the adjacency matrix of the network $W = (w_{ij})_{n\times n}$, which reflects the network topology with the weights of both ERs and power lines of EI as shown in equation (3.1).

$$w_{ij} = \begin{cases} w_{L_{ij}} & L_{ij} \in E \\ w_{R_i} & i = j \\ \infty & L_{ij} \notin E \end{cases} \tag{3.1}$$

Weight $w_{i,j}$ may have varied meanings depending on the demands of various optimization objectives. In this study, $w_{L_{ij}}$ is the weight of the edge L_{ij}, which represents the power loss of the power line that connects energy routers R_i and R_j. While w_{R_i} is the weight of ER R_i, which represents its power loss. Both weights of power lines and ERs are determined by equations (3.4), (3.5) and (3.6)

Figure 3.2 represents the graph model of the EI shown in Figure 3.1.

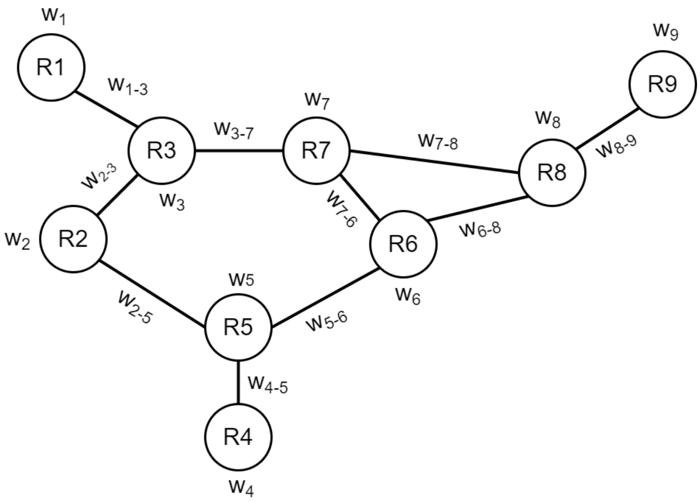

FIGURE 3.2: Graph model of the EI shown in Figure 3.1.

3.3 Mathematical model of the concerned problem

Typically, energy management problems are solved as an optimization problem with one or more objective functions and multiple constraints. One of EI's energy management difficulties is the energy routing problem. Routing energy from sources to loads in the EI, as indicated in Chapter 1, entails matching loads to energy sources and selecting a non-congestion path with minimum energy loss between the matched peers.

EI is a mesh network. There may be many paths to transmit energy between energy trading prosumers (sources and loads). Each path suffers from power transmission loss. The minimum loss path is the path with the minimum energy transmission loss. In our case, the weight on each edge and a node represents the power loss; therefore, finding the path with the minimum energy transmission loss is the selection of the minimum-weighted path. $W_{Total}^{p:s\rightarrow l}$ (in Equation (3.2)) represents the power transmission loss of a path p from the source s to the load l.

$$f = min(W_{Total}^{p:s\rightarrow l}) \tag{3.2}$$

The power transmission loss of a path is determined by two major factors: the power line losses ($w_{i,j}$) and the ER losses (w_i) that comprise the path.

$$W_{Total}^{p:s\rightarrow l} = \sum_{R_i \in p} w_i + \sum_{L_{i,j} \in p} w_{i,j} \tag{3.3}$$

The power loss in an ER is determined by the amount of power transmitted through it, the conversion efficiency of its electronic converters, and the power cable transmission losses. For simplicity, based on previous studies in the literature ([1, 3, 120, 121, 135]), the conversion efficiency of ER electronic converters is assumed to be constant. Because the power cables inside the ER are relatively short, power losses are omitted. Therefore, the ER power loss is a linear function of the transmitted power (Equation (3.4)). Where eff_i, P_{s-l} represent the conversion efficiency of energy router R_i and the transmitted power from the source s to load l, respectively.

$$w_i = (1 - eff_i) \times P_{s-l} \tag{3.4}$$

It should be noted that in AC transmission systems, the power line loss is proportional to the active and reactive power. The resistance value is significantly higher than the inductance value on low-voltage transmission lines because of the lower conductor cross-sectional area and conductor spacing. The inductance value may be neglected in this case, therefore, the loss is mostly influenced by active power. While the power line loss in DC transmission systems is essentially proportional to the active power. Therefore, the power line loss between ERs R_i and Rj is calculated using Equation (3.5).

$$w_{ij} = \frac{r_{ij}}{V_{ij}^2} \times P_{s-l}^2 \tag{3.5}$$

Where, r_{ij}, V_{ij} and P_{s-l} denotethe resistance, voltage, and transmitted power of the power line that connects ERs R_i and R_j, respectively. In fact, Equation (3.5) is not applicable in the presence of a pre-existing power (P_{ij}) in the power line. Equation (3.6) is used in this instance to compute the loss on the power line.

$$w_{ij} = \frac{r_{ij}}{V_{ij}^2} \times \left[(P_{s-l} + P_{ij})^2 - P_{ij}^2\right] \tag{3.6}$$

The total power loss of a transmission path between two prosumers (source-load pair) is the sum of the power losses of all ERs and power lines that build the path (see Equation (3.3)). However, the transmitted power can be split into multiple energy packets and transmitted through different paths (N_p). In this case, the total transmission loss is the sum of the transmission losses of the different paths used to transmit the total power. It is calculated using Equation (3.7), where $W_{Total}^{p_k:s\to l}$ denotes the transmission loss of the k^{th} path.

$$TL_{Total}^{s\to l} = \sum_{k=1}^{N_p} \left(W_{Total}^{p_k:s\to l} \right) \tag{3.7}$$

Finding the minimal loss path does not imply that it will be used to transport energy; rather, the energy minimum loss path must meet the following constraints:

- A path's power loss should be less than the transmitted energy.

$$W_{Total}^{p:s\to l} < P_{s-l} \tag{3.8}$$

- The transmitted power should not surpass the path's maximum capacity. It is the minimum between the lowest interface capacity of ERs and the lowest capacity of power lines that formed the path.

$$P_{s-l} \leq min \left(P_{s\to l}^{Lines\_c}, P_{s\to l}^{ERs\_c} \right) \tag{3.9}$$

- A power line's total power transferred should not exceed its available capacity.

$$\sum P_{(R_i,R_j)} \leq P_{(L_{i,j})}^{c} \tag{3.10}$$

- The total power flowing into the same ER interface should not surpass the interface capacity.

$$\Sigma P_{(R_i,R_j)} \leq P_{R_i}^{c} \tag{3.11}$$

- In case the power is transmitted in different paths, the total power loss of different paths should not exceed the transmitted power.

$$\sum_{k=1}^{N_p} \left(W_{Total}^{p_k:s\to l} \right) < P_{s-l} \tag{3.12}$$

- Every time the preexisting or transmitted power is altered in the network, the available capacity of ERs and power lines must be updated in order to adapt to real-time power transactions and avoid congestion. The ERs and power lines capacities are updated using Equations (3.13) and (3.14).

$$\begin{gathered} P^{c}_{(L_{i,j})} = P^{c}_{(L_{i,j})} - \sum_{k=1}^{N_p} P^{k}_{(L_{i,j})} \\ P^{c}_{(L_{i,j})} \leq P^{Tc}_{(L_{i,j})} \end{gathered} \tag{3.13}$$

$$\begin{gathered} P^{c}_{(R_i)} = P^{c}_{(R_i)} - \sum_{k=1}^{N_p} P^{k}_{(R_i)} \\ P^{c}_{(R_i)} \leq P^{Tc}_{(R_i)} \end{gathered} \tag{3.14}$$

where, $P^{c}_{(L_{i,j})}$ and $P^{c}_{R_i}$ denotes the available capacity of power line $L_{i,j}$ and energy router R_i respectively, while $P^{Tc}_{(L_{i,j})}$ and $P^{Tc}_{R_i}$ are their maximum capacities. $P^{k}_{(L_{i,j})}$ and $P^{k}_{(R_i)}$ signifies the pre-existing power over power line $L_{i,j}$ and energy router R_i in the k^{th} path that includes them.

It is important to note that, to simplify the computation of power loss and the search for the lowest loss path, existing routing algorithms often assume that the transmitted power throughout the entire path is always constant. However, the resultant path power loss is higher than the actual path loss because, in the actual operation of the EI, the power progressively decreases with the transmission path, as illustrated in Figure 3.3.

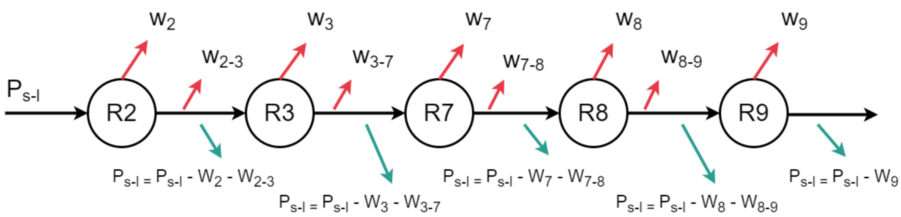

FIGURE 3.3: Graphical depiction of power conversion and transmission losses along the path.

For the subscribers matching process, there is no standard mathematical formulation of the problem, and different models have been proposed in the literature. In the different models, subscriber matching was treated as an optimization problem with different objective functions, some of them aimed at minimizing prices, others aimed at minimizing transmission losses, etc, taking into account different criteria.
Whenever the objective function is used in the subscriber matching modelization, it must adhere to the following constraints:

- If the source (producer) is matched with multiple loads (consumers), the total amount of selling electricity (P_{s-l}) should not exceed the existing power of the source (prosumer) (P_s).

$$0 \leq \sum_{l=1}^{k} P_{s-l} \leq P_s \tag{3.15}$$

- If the consumer is matched with multiple sources (prosumers), the total amount of buying electricity (P_{s-l}) should not exceed the demand energy of the load (consumer) (P_l).

$$0 \leq \sum_{s=1}^{k} P_{s-l} \leq P_l \tag{3.16}$$

- If the consumer is a heavy load that must be matched with several sources (prosumers), the number of sources should be kept as low as possible to reduce the complexity of the selection process while boosting the system's reliability, security, and robustness [1].

The power received by the load is less than the load demand due to transmission losses. These transmission losses should be considered in Equations (3.15) and (3.16) to ensure that loads receive their precise demand without deficit. Because the power sources are unknown in the first place, the power losses are initially unpredictable, in this case, the energy routing equations can only be solved recursively, significantly increasing the complexity and volume of the computations [2]. For this reason, the literature has basically moved away from incorporating losses in power equilibrium equations and instead assumes that these power transmission losses are compensated with the utility grid for a compensation fee, or compensated by the prosumers (energy sources), by setting aside a percentage of their output as a reserve for losses compensation. In this work, we presume that power transmission losses are compensated with the utility grid for a compensation fee paid by the consumer.
We assume that only one directional power flow is permitted between two ERs through the same power line (Power flow directional constraint PFD) since simultaneous bidirectional power flow between them might result in a reverse power flow and alter the direction and routing of the power flow.

3.4 Simulation tools and scenarios

Many analysis cases with various network architectures and scenarios have been implemented in Matlab R19a using a laptop with an i5-10210U CPU running at 2.11 GHz and 8G of RAM to evaluate and confirm the performance of our contributions. We selected Matlab for our simulations since it is the most commonly used simulation program in the literature to address the energy routing issue, as well as for its simplicity, modularity, and flexibility.

3.4.1 Basic data

Multiple EI structures ranging in size from small to big and complicated ones were employed in simulations to assess the efficiency of our suggested contributions. These EI structures are all drawn from the literature and are assumed to mimic real-world distributed systems. In addition to the network shown in Figure 3.1 with its parameters summarized in Tables 3.1 and 3.2; Figures 3.4, 3.5, and Tables 3.5, 3.6, 3.3, and 3.4 represent the networks structure, ERs, and power line parameters of the modified EI from the IEEE 14-Bus and IEEE 30-Bus systems used in [116] and [135], respectively. The network structures in Figures 3.2 and 3.5 are commonly employed

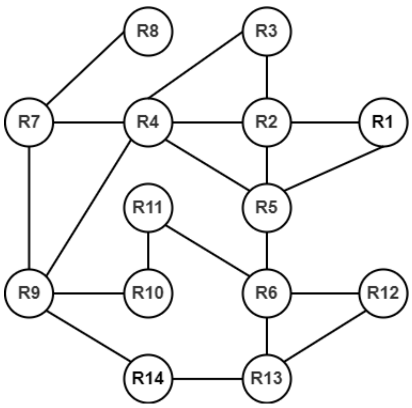

FIGURE 3.4: Graph model of the EI modified from IEEE 14-Bus system.

TABLE 3.3: Energy router parameters used in the EI system in Figure 3.4

ER	Capacity P_{ER}^{C} (kW)	Efficiency (eff)	ER	Capacity P_{ER}^{C} (kW)	Efficiency (eff)
R_1	32	0.98	R_8	65	0.97
R_2	130	0.97	R_9	65	0.98
R_3	130	0.98	R_{10}	65	0.98
R_4	130	0.96	R_{11}	32	0.99
R_5	130	0.97	R_{12}	65	0.97
R_6	32	0.98	R_{13}	130	0.98
R_7	65	0.98	R_{14}	130	0.98

TABLE 3.4: Power line parameters used in the EI system in Figure 3.4

Power line	**Capacity** P^C_{line} **(kW)**	**Resistance** **(Ω)**	**Voltage** **(V)**	**Power line**	**Capacity** P^C_{line} **(kW)**	**Resistance** **(Ω)**	**Voltage** **(V)**
L_{1-2}	65	0.01938	400	L_{6-11}	20	0.09498	400
L_{1-5}	32	0.05406	400	L_{6-12}	130	0.12291	400
L_{2-3}	130	0.04699	400	L_{6-13}	32	0.06615	400
L_{2-4}	32	0.05811	400	L_{7-8}	65	0.11021	400
L_{2-5}	130	0.05695	400	L_{7-9}	32	0.19038	400
L_{3-4}	70	0.15701	400	L_{9-10}	130	0.03181	400
L_{4-5}	70	0.0.1335	400	L_{9-14}	25	0.12711	400
L_{4-7}	70	0.01227	400	L_{10-11}	70	0.08205	400
L_{4-9}	32	0.01303	400	L_{12-13}	65	0.22092	400
L_{5-6}	65	0.11202	400	L_{13-14}	70	0.17093	400

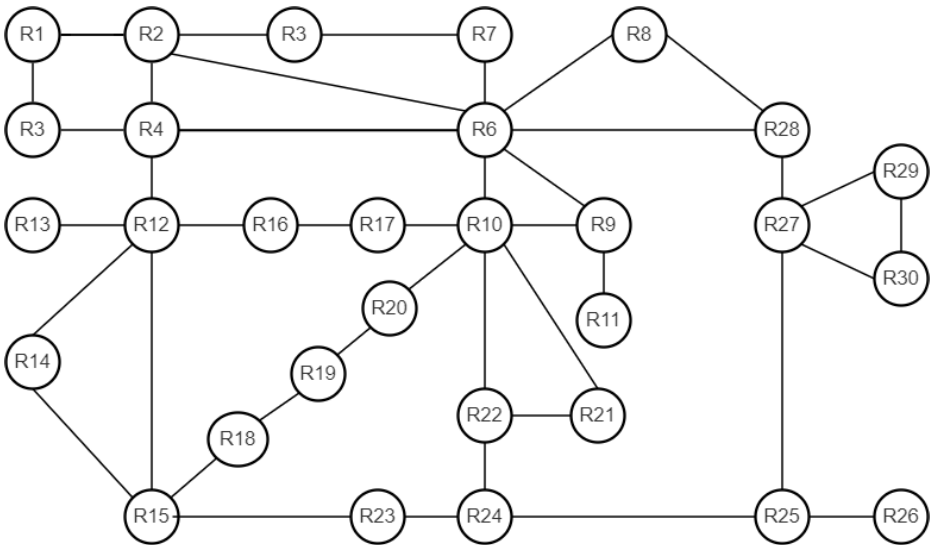

FIGURE 3.5: Graph model of the EI modified from IEEE 30-Bus system.

TABLE 3.5: Energy router parameters used in the EI system in Figure 3.5

ER	**Capacity** P^C_{ER} **(kW)**	**Efficiency** (eff)	**ER**	**Capacity** P^C_{ER} **(kW)**	**Efficiency** (eff)
R_1	130	0.98	R_{16}	32	0.98
R_2	130	0.98	R_{17}	32	0.98
R_3	130	0.98	R_{18}	16	0.98
R_4	130	0.98	R_{19}	32	0.98
R_5	130	0.98	R_{20}	32	0.98
R_6	130	0.98	R_{21}	32	0.98
R_7	130	0.98	R_{22}	32	0.98
R_8	32	0.98	R_{23}	16	0.98
R_9	65	0.98	R_{24}	16	0.98
R_{10}	65	0.98	R_{25}	16	0.98
R_{11}	65	0.98	R_{26}	16	0.98
R_{12}	65	0.98	R_{27}	65	0.98
R_{13}	65	0.98	R_{28}	65	0.98
R_{14}	32	0.98	R_{29}	16	0.98
R_{15}	32	0.98	R_{30}	16	0.98

TABLE 3.6: Power line parameters used in the EI system in Figure 3.5

Power line	**Capacity P^C_{line} (kW)**	**Resistance (Ω)**	**Voltage (V)**	**Power line**	**Capacity P^C_{line} (kW)**	**Resistance (Ω)**	**Voltage (V)**
L_{1-2}	130	0.0192	400	L_{12-13}	65	0.105	400
L_{1-3}	130	0.0452	400	L_{12-14}	32	0.1231	400
L_{2-4}	25	0.057	400	L_{12-15}	32	0.0662	400
L_{2-5}	130	0.0472	400	L_{12-16}	32	0.0945	400
L_{2-6}	25	0.0581	400	L_{14-15}	16	0.221	400
L_{3-4}	130	0.0132	400	L_{15-18}	16	0.1073	400
L_{4-6}	25	0.0119	400	L_{15-23}	16	0.1	400
L_{4-12}	65	0.257	400	L_{16-17}	16	0.0524	400
L_{5-7}	70	0.046	400	L_{18-19}	16	0.0639	400
L_{6-7}	130	0.0267	400	L_{19-20}	32	0.034	400
L_{6-8}	20	0.012	400	L_{21-22}	16	0.0116	400
L_{6-9}	65	0.522	400	L_{22-24}	16	0.115	400
L_{6-10}	32	0.351	400	L_{23-24}	16	0.132	400
L_{6-28}	32	0.0169	400	L_{24-25}	16	0.1885	400
L_{8-28}	32	0.0636	400	L_{25-26}	16	0.2544	400
L_{9-10}	65	0.1243	400	L_{25-27}	16	0.1093	400
L_{9-11}	65	0.0831	400	L_{27-28}	65	0.0678	400
L_{10-17}	32	0.0324	400	L_{27-29}	16	0.2198	400
L_{10-20}	32	0.0936	400	L_{27-30}	16	0.3202	400
L_{10-21}	32	0.0348	400	L_{29-30}	16	0.2399	400
L_{10-22}	32	0.0727	400				

in various studies conducted in the literature ([1, 2, 120, 121]. They are small, but they are beneficial for preliminary testing and development of energy routing protocols, they may not give a true depiction of how these energy routing protocols would behave on larger, more sophisticated EI networks. As EI is a large and complex network, it is critical to test energy routing protocols on a range of network sizes and topologies to assure their effectiveness and scalability in real-world circumstances. To further study and assess the effectiveness of energy routing algorithms for larger and more complicated EI networks, and given the lack of real data on EI networks, we opted to use simulated data. In particular, we used the IEEE 39 Bus [136], the IEEE 118 Bus and 201 Bus systems depicted in Figures 3.6, 3.7 and 3.8, respectively, where the parameters of the ERs and power lines have been established based on the values provided by the prior systems as summarized in Tables 3.7, 3.8, 3.9, 3.10, 3.11, 3.12, and 3.13.

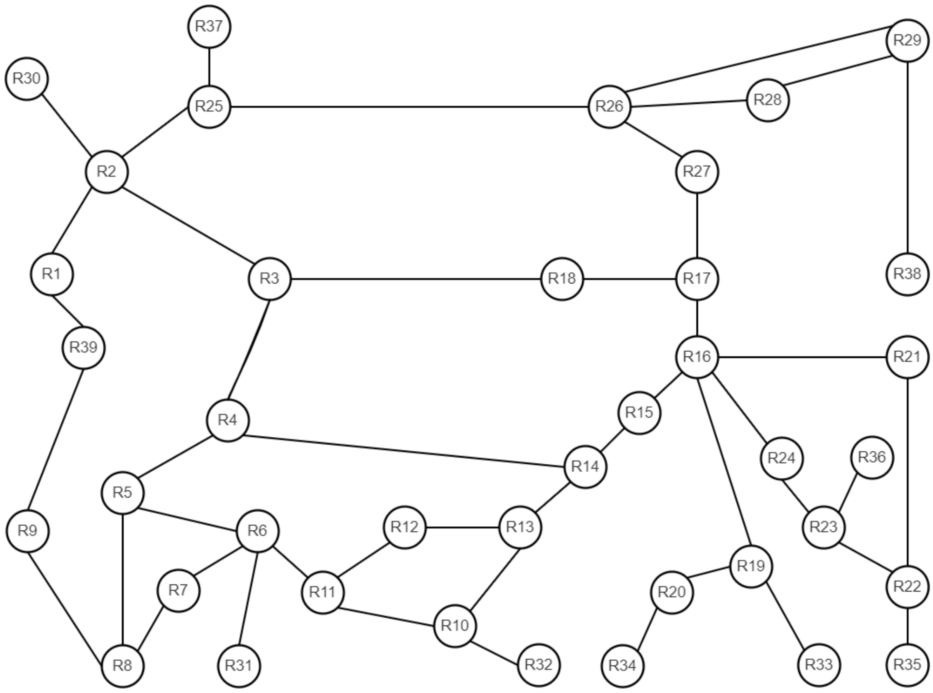

FIGURE 3.6: Graph model of the EI modified from IEEE 39-Bus system

TABLE 3.7: Energy router parameters used in the EI system in Figure 3.6

ER	**Capacity** P_{ER}^{C} **(kW)**	**Efficiency** (eff)	**ER**	**Capacity** P_{ER}^{C} **(kW)**	**Efficiency** (eff)
R_1	132	0.98	R_{21}	127	0.99
R_2	132	0.99	R_{22}	148	0.97
R_3	135	0.98	R_{23}	148	0.99
R_4	135	0.97	R_{24}	134	0.98
R_5	142	0.99	R_{25}	135	0.99
R_6	126	0.98	R_{26}	149	0.97
R_7	120	0.98	R_{27}	129	0.99
R_8	142	0.99	R_{28}	146	0.98
R_9	126	0.98	R_{29}	149	0.99
R_{10}	135	0.97	R_{30}	112	0.98
R_{11}	121	0.99	R_{31}	126	0.97
R_{12}	128	0.98	R_{32}	101	0.99
R_{13}	135	0.98	R_{33}	116	0.98
R_{14}	135	0.99	R_{34}	100	0.97
R_{15}	135	0.99	R_{35}	122	0.99
R_{16}	136	0.98	R_{36}	143	0.98
R_{17}	136	0.97	R_{37}	113	0.98
R_{18}	148	0.98	R_{38}	116	0.99
R_{19}	133	0.99	R_{39}	130	0.98
R_{20}	124	0.98			

TABLE 3.8: Power line parameters used in the EI system in Figure 3.6

Power line	Capacity P^C_{line} (kW)	Resistance (Ω)	Voltage (V)	Power line	Capacity P^C_{line} (kW)	Resistance (Ω)	Voltage (V)
L_{1-2}	132	0.1243	400	L_{14-15}	135	0.1050	400
L_{1-39}	130	0.0945	400	L_{15-16}	111	0.2399	400
L_{2-3}	127	0.1243	400	L_{16-17}	136	0.0340	400
L_{2-25}	110	0.3202	400	L_{16-19}	133	0.0452	400
L_{2-30}	112	0.3510	400	L_{16-21}	113	0.0348	400
L_{3-4}	135	0.2399	400	L_{16-24}	118	0.1050	400
L_{3-18}	121	0.2210	400	L_{17-18}	148	0.2399	400
L_{4-5}	120	0.2544	400	L_{17-27}	129	0.0120	400
L_{4-14}	122	0.1000	400	L_{19-20}	124	0.0119	400
L_{5-6}	126	0.0936	400	L_{19-33}	116	0.2198	400
L_{5-8}	142	0.2399	400	L_{20-34}	100	0.0324	400
L_{6-7}	120	0.1050	400	L_{21-22}	127	0.0324	400
L_{6-11}	104	0.0116	400	L_{22-23}	148	0.0524	400
L_{6-31}	126	0.0267	400	L_{22-35}	122	0.1320	400
L_{7-8}	115	0.2544	400	L_{23-24}	134	0.0348	400
L_{8-9}	129	0.0727	400	L_{23-36}	143	0.0119	400
L_{9-39}	120	0.0192	400	L_{25-26}	135	0.0936	400
L_{10-11}	121	0.0169	400	L_{25-37}	113	0.1320	400
L_{10-13}	135	0.0936	400	L_{26-27}	113	0.3510	400
L_{10-32}	101	0.0662	400	L_{26-28}	100	0.0119	400
L_{11-12}	117	0.0662	400	L_{26-29}	149	0.1000	400
L_{12-13}	128	0.0452	400	L_{28-29}	146	0.0169	400
L_{13-14}	135	0.1231	400	L_{29-38}	116	0.2544	400

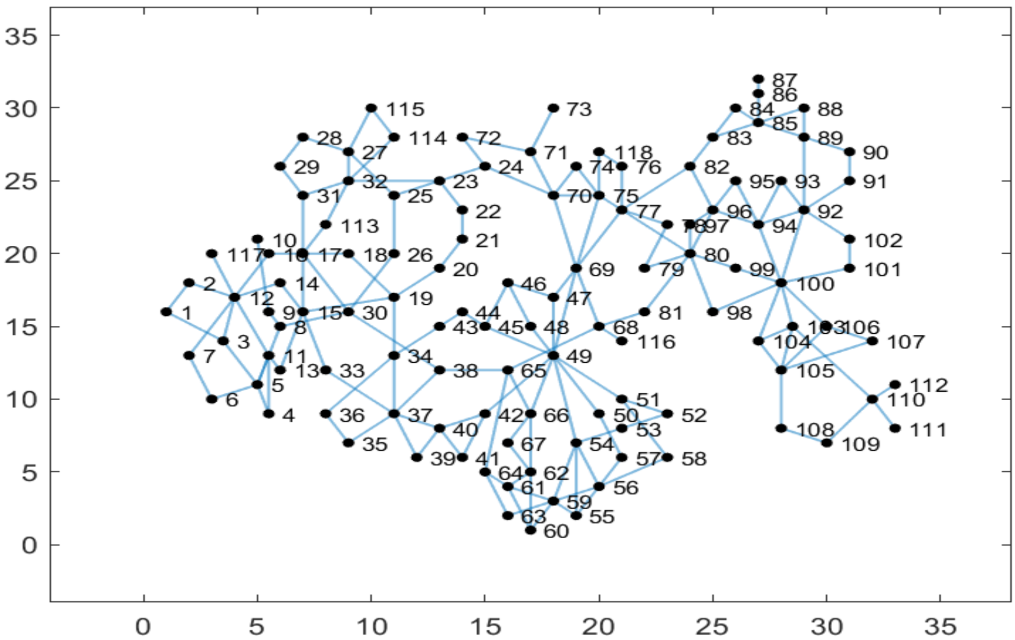

FIGURE 3.7: Graph model of 118-Bus distribution system.

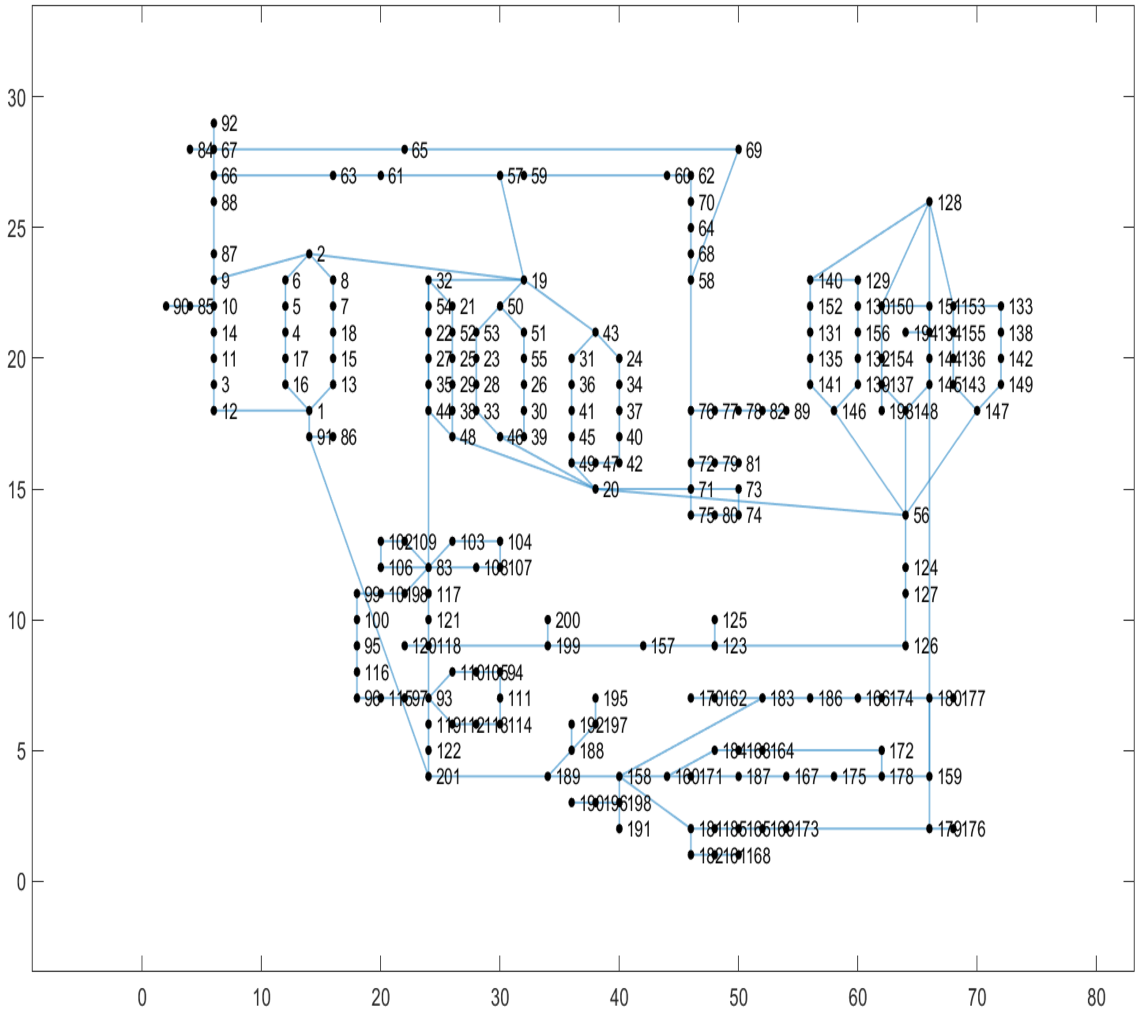

FIGURE 3.8: Graph model of 201-Bus distribution system.

TABLE 3.9: Energy router parameters used in the EI system in Figure 3.8 part 1.

ER	Capacity P_{ER}^{C} (kw)	Efficiency (eff)	ER	Capacity P_{ER}^{C} (kw)	Efficiency (eff)	ER	Capacity P_{ER}^{C} (kw)	Efficiency (eff)	ER	Capacity P_{ER}^{C} (kw)	Efficiency (eff)
R_{1}	130	0.98	R_{28}	65	0.98	R_{55}	16	0.99	R_{82}	32	0.97
R_{2}	130	0.99	R_{29}	16	0.99	R_{56}	16	0.97	R_{83}	16	0.99
R_{3}	130	0.98	R_{30}	16	0.98	R_{57}	65	0.99	R_{84}	16	0.98
R_{4}	130	0.97	R_{31}	130	0.98	R_{58}	65	0.98	R_{85}	16	0.99
R_{5}	130	0.99	R_{32}	130	0.99	R_{59}	16	0.99	R_{86}	16	0.97
R_{6}	130	0.98	R_{33}	130	0.98	R_{60}	16	0.98	R_{87}	65	0.99
R_{7}	130	0.98	R_{34}	130	0.97	R_{61}	130	0.98	R_{88}	65	0.98
R_{8}	32	0.99	R_{35}	130	0.99	R_{62}	130	0.99	R_{89}	16	0.99
R_{9}	65	0.98	R_{36}	130	0.98	R_{63}	130	0.98	R_{90}	16	0.98
R_{10}	65	0.97	R_{37}	130	0.98	R_{64}	130	0.97	R_{91}	130	0.98
R_{11}	65	0.99	R_{38}	32	0.99	R_{65}	130	0.99	R_{92}	130	0.99
R_{12}	65	0.98	R_{39}	65	0.98	R_{66}	130	0.98	R_{93}	130	0.98
R_{13}	65	0.98	R_{40}	65	0.97	R_{67}	130	0.98	R_{94}	130	0.97
R_{14}	32	0.99	R_{41}	65	0.99	R_{68}	32	0.99	R_{95}	130	0.99
R_{15}	32	0.99	R_{42}	65	0.98	R_{69}	65	0.98	R_{96}	130	0.98
R_{16}	32	0.98	R_{43}	65	0.98	R_{70}	65	0.97	R_{97}	130	0.98
R_{17}	32	0.97	R_{44}	32	0.99	R_{71}	65	0.99	R_{98}	32	0.99
R_{18}	16	0.98	R_{45}	32	0.99	R_{72}	65	0.98	R_{99}	65	0.98
R_{19}	32	0.99	R_{46}	32	0.98	R_{73}	65	0.98	R_{100}	65	0.97
R_{20}	32	0.98	R_{47}	32	0.97	R_{74}	32	0.99	R_{101}	65	0.99
R_{21}	32	0.99	R_{48}	16	0.98	R_{75}	32	0.99	R_{102}	65	0.98
R_{22}	32	0.97	R_{49}	32	0.99	R_{76}	32	0.98	R_{103}	65	0.98
R_{23}	16	0.99	R_{50}	32	0.98	R_{77}	32	0.97	R_{104}	32	0.99
R_{24}	16	0.98	R_{51}	32	0.99	R_{78}	16	0.98	R_{105}	32	0.99
R_{25}	16	0.99	R_{52}	32	0.97	R_{79}	32	0.99	R_{106}	32	0.98
R_{26}	16	0.97	R_{53}	16	0.99	R_{80}	32	0.98	R_{107}	32	0.97
R_{27}	65	0.99	R_{54}	16	0.98	R_{81}	32	0.99	R_{108}	16	0.98

TABLE 3.10: Energy router parameters used in the EI system in Figure 3.8 part 2.

ER	**Capacity** P_{ER}^{C} **(kw)**	**Efficiency** (eff)	**ER**	**Capacity** P_{ER}^{C} **(kw)**	**Efficiency** (eff)	**ER**	**Capacity** P_{ER}^{C} **(kw)**	**Efficiency** (eff)	**ER**	**Capacity** P_{ER}^{C} **(kw)**	**Efficiency** (eff)
R_{109}	32	0.99	R_{133}	65	0.98	R_{157}	130	0.98	R		
R_{110}	32	0.98	R_{134}	32	0.99	R_{158}	32	0.99	R		
R_{111}	32	0.99	R_{135}	32	0.99	R_{159}	65	0.98	R_{181}	130	0.98
R_{112}	32	0.97	R_{136}	32	0.98	R_{160}	65	0.97	R_{182}	130	0.99
R_{113}	16	0.99	R_{137}	32	0.97	R_{161}	65	0.99	R_{183}	130	0.98
R_{114}	16	0.98	R_{138}	16	0.98	R_{162}	65	0.98	R_{184}	130	0.97
R_{115}	16	0.99	R_{139}	32	0.99	R_{163}	65	0.98	R_{185}	130	0.99
R_{116}	16	0.97	R_{140}	32	0.98	R_{164}	32	0.99	R_{186}	130	0.98
R_{117}	65	0.99	R_{141}	32	0.99	R_{165}	32	0.99	R_{187}	130	0.98
R_{118}	65	0.98	R_{142}	32	0.97	R_{166}	32	0.98	R_{188}	32	0.99
R_{119}	16	0.99	R_{143}	16	0.99	R_{167}	32	0.97	R_{189}	65	0.98
R_{120}	16	0.98	R_{144}	16	0.98	R_{168}	16	0.98	R_{190}	65	0.97
R_{121}	130	0.98	R_{145}	16	0.99	R_{169}	32	0.99	R_{191}	65	0.99
R_{122}	130	0.99	R_{146}	16	0.97	R_{170}	32	0.98	R_{192}	65	0.98
R_{123}	130	0.98	R_{147}	65	0.99	R_{171}	32	0.99	R_{193}	65	0.98
R_{124}	130	0.97	R_{148}	65	0.98	R_{172}	32	0.97	R_{194}	32	0.99
R_{125}	130	0.99	R_{149}	16	0.99	R_{173}	16	0.99	R_{195}	32	0.99
R_{126}	130	0.98	R_{150}	16	0.98	R_{174}	16	0.98	R_{196}	32	0.98
R_{127}	130	0.98	R_{151}	130	0.98	R_{175}	16	0.99	R_{197}	32	0.97
R_{128}	32	0.99	R_{152}	130	0.99	R_{176}	16	0.97	R_{198}	16	0.98
R_{129}	65	0.98	R_{153}	130	0.98	R_{177}	65	0.99	R_{199}	32	0.99
R_{130}	65	0.97	R_{154}	130	0.97	R_{178}	65	0.98	R_{200}	32	0.98
R_{131}	65	0.99	R_{155}	130	0.99	R_{179}	16	0.99	R_{201}	32	0.99
R_{132}	65	0.98	R_{156}	130	0.98	R_{180}					

Table 3.11: Power line parameters used in the EI system in Figure 3.8 part 1.

Power line	Capacity P_{line}^{C} (Kw)	Resistance (Ω)	Voltage (V)	Power line	Capacity P_{line}^{C} (Kw)	Resistance (Ω)	Voltage (V)	Power line	Capacity P_{line}^{C} (Kw)	Resistance (Ω)	Voltage (V)
L_{1-12}	130	0.0192	400	L_{19-57}	16	0.1073	400	L_{33-46}	65	0.0522	400
L_{1-13}	130	0.0452	400	L_{20-46}	16	0.1	400	L_{34-37}	32	0.0351	400
L_{1-16}	25	0.057	400	L_{20-48}	16	0.0524	400	L_{35-44}	32	0.0169	400
L_{1-91}	130	0.0472	400	L_{20-49}	16	0.0639	400	L_{36-41}	32	0.0636	400
L_{2-6}	25	0.0581	400	L_{20-56}	32	0.034	400	L_{37-40}	65	0.1243	400
L_{2-8}	130	0.0132	400	L_{20-71}	16	0.0116	400	L_{38-48}	65	0.0831	400
L_{2-9}	25	0.0119	400	L_{21-32}	16	0.115	400	L_{39-46}	32	0.0324	400
L_{2-19}	65	0.0257	400	L_{21-52}	16	0.132	400	L_{40-42}	32	0.0936	400
L_{3-11}	70	0.046	400	L_{22-27}	16	0.1885	400	L_{41-45}	32	0.0348	400
L_{3-12}	130	0.0267	400	L_{22-54}	16	0.2544	400	L_{42-47}	32	0.0727	400
L_{4-5}	20	0.012	400	L_{23-28}	16	0.1093	400	L_{44-48}	65	0.1050	400
L_{4-17}	65	0.0522	400	L_{23-53}	65	0.0678	400	L_{45-49}	32	0.1231	400
L_{5-6}	32	0.0351	400	L_{24-34}	16	0.2198	400	L_{47-49}	32	0.0662	400
L_{7-8}	32	0.0169	400	L_{24-43}	16	0.3202	400	L_{50-51}	32	0.0945	400
L_{7-18}	32	0.0636	400	L_{25-29}	16	0.2399	400	L_{50-53}	16	0.221	400
L_{9-10}	65	0.1243	400	L_{25-52}	130	0.0192	400	L_{51-55}	16	0.1073	400
L_{9-87}	65	0.0831	400	L_{26-30}	130	0.0452	400	L_{56-124}	16	0.1	400
L_{10-14}	32	0.0324	400	L_{26-55}	25	0.057	400	L_{56-146}	16	0.0524	400
L_{10-85}	32	0.0936	400	L_{27-35}	130	0.0472	400	L_{56-147}	16	0.0639	400
L_{11-14}	32	0.0348	400	L_{28-33}	25	0.0581	400	L_{56-148}	32	0.034	400
L_{13-15}	32	0.0727	400	L_{29-38}	130	0.0132	400	L_{57-59}	16	0.0116	400
L_{15-18}	65	0.1050	400	L_{30-39}	25	0.0119	400	L_{57-61}	16	0.115	400
L_{16-17}	32	0.1231	400	L_{31-36}	65	0.0257	400	L_{58-68}	16	0.132	400
L_{19-32}	32	0.0662	400	L_{31-43}	70	0.046	400	L_{58-69}	16	0.1885	400
L_{19-43}	32	0.0945	400	L_{32-54}	130	0.0267	400	L_{58-76}	16	0.2544	400
L_{19-50}	16	0.221	400	L_{32-83}	20	0.12	400	L_{59-60}	16	0.1093	400

TABLE 3.12: Power line parameters used in the EI system in Figure 3.8 part 2.

Power line	**Capacity** P_{line}^{C} **(Kw)**	**Resistance** **(Ω)**	**Voltage (V)**	**Power line**	**Capacity** P_{line}^{C} **(Kw)**	**Resistance** **(Ω)**	**Voltage (V)**	**Power line**	**Capacity** P_{line}^{C} **(Kw)**	**Resistance** **(Ω)**	**Voltage (V)**
L_{60-62}	65	0.0678	400	L_{83-103}	32	0.1231	400	$L_{103-104}$	65	0.0257	400
L_{61-63}	16	0.2198	400	L_{83-106}	32	0.0662	400	$L_{104-107}$	70	0.046	400
L_{62-70}	16	0.3202	400	L_{83-108}	32	0.0945	400	$L_{105-110}$	130	0.0267	400
L_{63-66}	16	0.2399	400	L_{83-109}	16	0.221	400	$L_{107-108}$	20	0.012	400
L_{64-68}	130	0.0192	400	L_{83-117}	16	0.1073	400	$L_{111-114}$	65	0.0522	400
L_{64-70}	130	0.0452	400	L_{85-90}	16	0.1	400	$L_{112-113}$	32	0.0351	400
L_{65-67}	25	0.057	400	L_{86-91}	16	0.0524	400	$L_{113-114}$	32	0.0169	400
L_{65-69}	130	0.0472	400	L_{87-88}	16	0.0639	400	$L_{117-121}$	32	0.0636	400
L_{66-67}	25	0.0581	400	L_{91-201}	32	0.034	400	$L_{118-120}$	65	0.1243	400
L_{66-88}	130	0.0132	400	L_{93-97}	16	0.0116	400	$L_{118-121}$	65	0.0831	400
L_{67-84}	25	0.0119	400	L_{93-110}	16	0.115	400	$L_{118-199}$	32	0.0324	400
L_{67-92}	65	0.0257	400	L_{93-112}	16	0.132	400	$L_{119-122}$	32	0.0936	400
L_{71-72}	70	0.046	400	L_{93-118}	16	0.1885	400	$L_{122-201}$	32	0.0348	400
L_{71-73}	130	0.0267	400	L_{93-119}	16	0.2544	400	$L_{123-125}$	32	0.0727	400
L_{71-75}	20	0.012	400	L_{94-105}	16	0.1093	400	$L_{123-126}$	65	0.1050	400
L_{72-76}	65	0.0522	400	L_{94-111}	65	0.678	400	$L_{123-157}$	32	0.1231	400
L_{72-79}	32	0.0351	400	L_{95-100}	16	0.2198	400	$L_{124-127}$	32	0.662	400
L_{73-74}	32	0.0169	400	L_{95-116}	16	0.3202	400	$L_{126-127}$	32	0.0945	400
L_{74-80}	32	0.0636	400	L_{96-115}	16	0.2399	400	$L_{128-140}$	16	0.212	400
L_{75-80}	65	0.1243	400	L_{96-116}	130	0.0192	400	$L_{128-150}$	16	0.1073	400
L_{76-77}	65	0.0831	400	L_{97-115}	130	0.0452	400	$L_{128-153}$	16	0.1	400
L_{77-78}	32	0.0324	400	L_{98-101}	25	0.057	400	$L_{128-159}$	16	0.0524	400
L_{78-82}	32	0.0936	400	L_{99-100}	130	0.0472	400	$L_{129-130}$	16	0.639	400
L_{79-81}	32	0.0348	400	L_{99-101}	25	0.0581	400	$L_{129-140}$	32	0.034	400
L_{82-89}	32	0.0727	400	$L_{102-106}$	130	0.0132	400	$L_{130-156}$	16	0.0116	400
L_{83-98}	65	0.1050	400	$L_{102-109}$	25	0.0119	400	$L_{131-135}$	16	0.115	400

Table 3.13: Power line parameters used in the EI system in Figure 3.8 part 3.

Power line	**Capacity** P^C_{line} **(Kw)**	**Resistance (Ω)**	**Voltage (V)**	**Power line**	**Capacity** P^C_{line} **(Kw)**	**Resistance (Ω)**	**Voltage (V)**	**Power line**	**Capacity** P^C_{line} **(Kw)**	**Resistance (Ω)**	**Voltage (V)**
$L_{131-152}$	16	0.132	400	$L_{157-199}$	32	0.0936	400	$L_{172-178}$	130	0.0472	400
$L_{132-139}$	16	0.1885	400	$L_{158-160}$	32	0.0348	400	$L_{173-179}$	25	0.0581	400
$L_{132-156}$	16	0.2544	400	$L_{158-181}$	32	0.0727	400	$L_{174-180}$	130	0.0132	400
$L_{133-138}$	16	0.1093	400	$L_{158-183}$	65	0.1050	400	$L_{175-178}$	25	0.0119	400
$L_{133-153}$	65	0.0678	400	$L_{158-189}$	32	0.1231	400	$L_{176-179}$	65	0.0257	400
$L_{134-144}$	16	0.2198	400	$L_{158-198}$	32	0.0662	400	$L_{177-180}$	70	0.046	400
$L_{134-151}$	16	0.3202	400	$L_{159-178}$	32	0.0945	400	$L_{181-182}$	130	0.0267	400
$L_{134-194}$	16	0.2399	400	$L_{159-179}$	16	0.221	400	$L_{181-185}$	20	0.012	400
$L_{135-141}$	130	0.0192	400	$L_{159-180}$	16	0.1073	400	$L_{183-186}$	65	0.0522	400
$L_{136-143}$	130	0.0452	400	$L_{160-171}$	16	0.1	400	$L_{188-189}$	32	0.0351	400
$L_{136-155}$	25	0.057	400	$L_{160-184}$	16	0.0524	400	$L_{188-192}$	32	0.0169	400
$L_{137-148}$	130	0.0472	400	$L_{161-168}$	16	0.0639	400	$L_{188-197}$	32	0.0636	400
$L_{137-154}$	25	0.0581	400	$L_{161-182}$	32	0.034	400	$L_{189-201}$	65	0.1243	400
$L_{137-193}$	130	0.0132	400	$L_{162-170}$	16	0.0116	400	$L_{190-196}$	65	0.0831	400
$L_{138-142}$	25	0.0119	400	$L_{162-183}$	16	0.115	400	$L_{191-198}$	32	0.0324	400
$L_{139-146}$	65	0.0257	400	$L_{163-164}$	16	0.132	400	$L_{195-197}$	32	0.0936	400
$L_{140-152}$	70	0.046	400	$L_{163-184}$	16	0.1885	400	$L_{196-198}$	32	0.0348	400
$L_{141-146}$	130	0.0267	400	$L_{164-172}$	16	0.2544	400	$L_{199-200}$	32	0.0727	400
$L_{142-149}$	20	0.012	400	$L_{165-169}$	16	0.1093	400				
$L_{143-147}$	65	0.0522	400	$L_{165-185}$	65	0.0678	400				
$L_{144-145}$	32	0.0351	400	$L_{166-174}$	16	0.2198	400				
$L_{145-148}$	32	0.0169	400	$L_{166-186}$	16	0.3202	400				
$L_{147-149}$	32	0.0636	400	$L_{167-175}$	16	0.2399	400				
$L_{150-151}$	65	0.1243	400	$L_{167-187}$	130	0.0192	400				
$L_{150-154}$	65	0.0831	400	$L_{169-173}$	130	0.0452	400				
$L_{153-155}$	32	0.0324	400	$L_{171-187}$	25	0.057	400				

3.4.2 Analyses scenarios

In real-world electric systems, unexpected events can occur, such as an overflow in a power line, sudden changes in the grid parameters, etc. In order to ensure the reliability, robustness, and efficiency of an energy routing algorithm in EI, it is essential to validate its performance under different scenarios and conditions. For that, we propose the following simulation cases:

- **Case 1: Single predetermined source-load pair:**
  In this case, to assess the path selection phase of the different energy routing algorithms, it is assumed that the source-load trading pair and the required energy transfer amount (the energy transactions) are fixed and predefined before the path selection phase. The different EI networks introduced earlier in this chapter are used for simulation. Within each network, the nodes (ERs) located at the opposite edges of the graph were deliberately chosen as source-load trading pairs to expand the array of potential paths between these selected pairs. This allows a thorough assessment of the routing algorithms' ability to select the most efficient path among a variety of available paths, particularly in large networks.

- **Case 2: Single load multiple sources**
  Since matching loads with sources and creating energy transactions is a significant phase of the energy routing algorithms, this case is dedicated to investigating the matching decisions made by the different algorithms. Therefore, it presupposes the existence of a single load with multiple energy sources in the network that could fulfil the energy request by the load.

- **Case 3: Heavy load (multi-source consumer)**
  A heavy-load, also known as a multi-source consumer, is a consumer whose demand cannot be met by a single energy source (producer-prosumer), and in this situation, many producers should be chosen to meet its energy request.

- **Case 4: Multi-loads multi-sources**
  In this particular scenario, the presence of multiple consumers and producers in the network is assumed, with the possibility of having a non-overlapping, overlapping, or simultaneous transmission schedule.

  - **Case 4-1: Non-overlapping transmission time**
    The network consumers have different transmission times which means it does not have any overlap. Taking as an example the network in Figure 3.1, assuming that we have two consumers connected to R_1 and R_2, with T_1

(9:00-10:00) and T_2 (11:00-12:00) as the transmission time of consumers connected to R_1 and R_2 respectively. As T_1 and T_2 do not have any overlap, the energy source and energy transmission path taken by the first consumer will not affect the second one.

- **Case 4-2: Overlapping transmission time** Unlike the previous case, the network consumers, in this case, have a partially overlapping transmission time (for example T_1 from 10:00 to 11:00, T_2 from 10:20 to 11:20). In this case, the pre-existing power over the power lines selected for the first transaction in T_1 will be increased. This will lead to major changes in the power loss in those lines. As a result, the decision made by early consumers with earlier transmission time will influence the path and source selection of later consumers with late transmission time.
- **Case 4-3: Simultaneous transmission time**
  Whereas the network consumers in this case have the same energy transmission time. The multiple consumers could choose the same producer. Also, path overlapping may occur when consumer and producer pairs choose their transmission paths independently at the same time. An example of an overlapping transmission path is shown in Figure 3.9, where the selected transmission paths between $R_1 - R_9$ and $R_2 - R_8$ overlap. This will increase the power loss of the paths and could even lead to an overflow, congestion problem, or reverse power flow in cases where the path is selected to transmit power in opposite directions (detailed in Chapter 5).

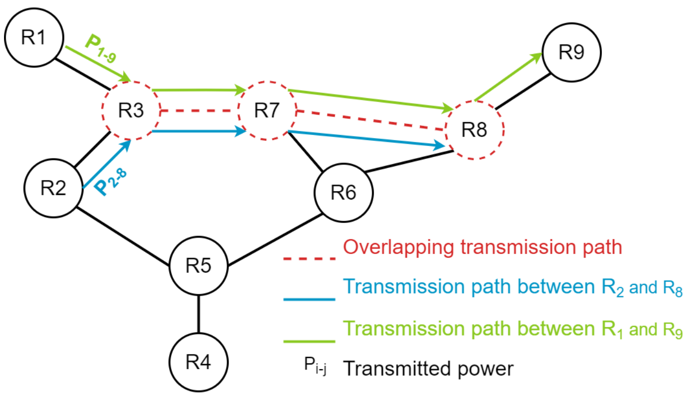

FIGURE 3.9: Diagram illustrating the scenario of path overlapping between multiple energy trading pairs.

It's worth noting that all of these distinct scenarios have been implemented within the different EI architectures outlined earlier in this chapter.

3.5 conslusion

This chapter provided the groundwork for our proposed energy routing approaches. We investigated several EI topologies, identified essential components and factors, created a graph theory model, and introduced a mathematical model of energy transmission losses to address the energy routing problem. Finally, we selected appropriate simulation tools and scenarios to evaluate our suggested solutions. The following chapters use this groundwork to introduce and evaluate the proposed energy routing approaches.

Chapter 4

Hybrid Energy Routing Protocol for EI

The work in this chapter has been published in Energies Journal since 2021 [137]: HEBAL, Sara, MECHTA, Djamila, HAROUS, Saad, et al. Hybrid energy routing approach for energy internet. Energies, 2021, vol. 14, no 9, p. 2579.

To ensure a controllable and reliable EI, this chapter first presents a P2PET scheme and introduces a new energy routing protocol based on meta-heuristic algorithms called the hybrid energy routing protocol in Energy Internet. The proposed protocol addresses the three energy routing issues: subscriber matching, energy-efficient paths, and transmission scheduling. In which the best producers for each consumer with the non-congested minimum loss path are determined. In contrast to prior research, multiple networks with varying sizes and scenarios have been used to evaluate the performance of the energy routing protocol in complex networks in terms of power losses, cost, and computation time and compared to existing algorithms in the literature. The simulation results demonstrate the effectiveness of the suggested energy routing protocol.

4.1 Introduction

The most coveted feature of the EI is the ability to accurately package and deliver energy units when and where required. Accordingly, the performance of EI relies on the proper and effective transfer of power, a process that is highly impacted by the implementation of appropriate energy-routing algorithms. Thus, ERs within the EI need to be equipped with effective energy-routing protocols. Most of the energy routing algorithms stated and discussed in Chapter 2 address the energy routing problem as an optimization problem, employing diverse deterministic approaches such as graph theory, game theory, and consensus to find the optimal solution. Nevertheless, the significant drawback of these deterministic methods, particularly when applied to large and complex systems, is the increasing time involved in achieving a solution. As a result, as mentioned in Chapter 2, as bio-inspired algorithms provide high-quality solutions for complex optimization problems in low computational time, several recent researchers have resorted to bio-inspired algorithms to handle the energy routing problem, with the aim of reducing computational complexity. Motivated by these analyses, we propose in this chapter a hybrid energy routing protocol that uses ACO and PSO algorithms to select the best producer for each consumer with the non-congested minimum loss path. The proposed protocol is detailed in Section 4.2. Evaluation and numerical simulation of the developed energy routing protocol are discussed in Section 4.3. This section investigates various scenarios involving networks of varying sizes, with a special emphasis on larger networks that have not been previously studied.

4.2 Hybrid energy routing protocol in Energy Internet

The energy routing problem is different from the data routing problem (as outlined in Table 1.4). Thus, the particular features of energy routing must be taken into consideration while designing energy routing protocols. By considering these features, we conceptualized in this chapter the energy routing problem as an optimization problem. The main objective of this optimization is to minimize both power transmission losses and the cost of energy between producers and consumers in the EI. In fact, the EI network architecture, components, and parameters used are described in detail in Chapter 3. In order to solve the energy routing problem, we start our contributions by introducing a centralized P2PET architecture. This architecture features a key component known as the “Broker” (refer to Figure 4.1) and aims to provide a controllable energy trading system. A thorough discussion of the broker’s functions will be furnished in the following section. The remaining contributions of the proposed hybrid energy routing protocol are resumed as follows:

- A subscriber matching mechanism is introduced to match producers and consumers while taking into consideration, the energy available, demand, and network physical constraints aiming to minimize both energy cost and transmission losses.

- An energy PSO algorithm is introduced to determine the amount of power to get from a set of producers for a heavy load (multi-source consumer) while minimizing the total power cost and transmission losses. The aim of using the PSO is to get an efficient and less computational subscriber matching algorithm.

- A pruning mechanism is used to prevent congestion issues.

- An ACO-based energy routing algorithm is proposed to find the least loss path between a trading pair [138].

4.2.1 Subscriber Matching Mechanism

The subscriber matching mechanism allows the construction of energy transactions, including the trading pair of consumer-producer and the traded power amount. In the proposed centralized P2PET architecture, it is assumed that the Broker maintains the producers' and consumers' profiles, encompassing information such as energy pricing, transmission duration, and the quantity of available/required power. To avoid the possibility of a single point of failure in the broker system, we have included a backup broker who will smoothly take over in the case of a detected failure. Additionally, it is presumed that the energy trading process adopts an intraday trading strategy , in which the trading interval occurs before the actual consumption and delivery time by a predetermined time frame, such as 30 minutes. The intraday trading will ensure power availability at the producer level, decrease the need for large-capacity batteries, and allow participants to adapt quickly to the dynamic fluctuations of energy availability, demand, and system conditions. The following steps outline the proposed subscriber matching mechanism:

- Prosumers, who generate more energy than they consume, known as producers or sellers, communicate with the broker by providing critical information comprising the amount of available energy, the time frame, and the energy trading price at the beginning of the trading slot.

- Prosumers, who generate less energy than they consume - essentially those in need of more energy - as well as conventional consumers without RESs, submit

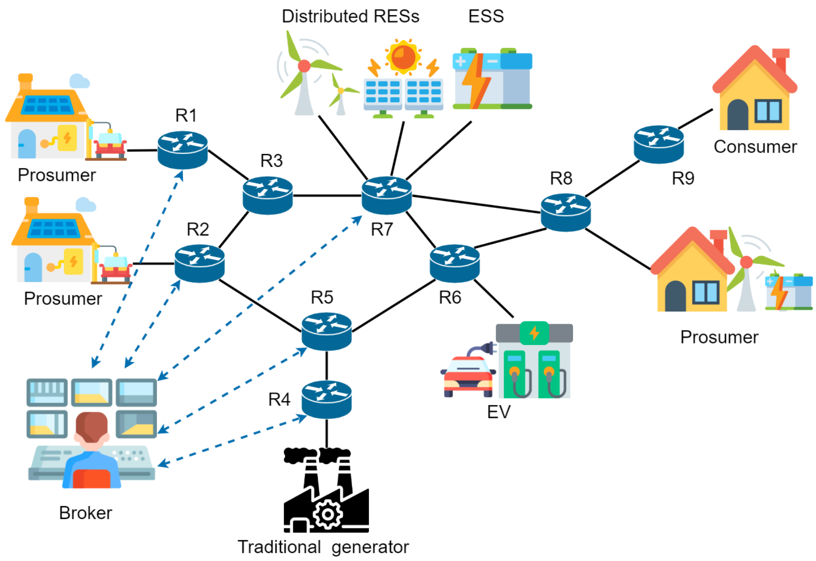

FIGURE 4.1: An example of the proposed centralized P2PET architecture.

an energy request indicating the required energy amount and time frame to their directly associated ERs.

- The associated ER forwards this energy request to the broker.

- The broker evaluates energy requests based on their submission time and creates a list of all producers/prosumers who can supply the whole needed energy within the stipulated timeframe for each consumer request, and in this case, the consumer is a "mono-source". Otherwise, if there isn't a producer/prosumer who can fulfil the consumer's energy request in the system, the consumer is classified as a "heavy-load" or "multi-source consumer" that needs multiple sources to meet its request. In such cases, the broker generates a list of all available producers/prosumers whose timelines align with the consumer's time frame.

- The generated list is forwarded by the broker to the ER associated with the consumer.

- Once the ER associated with the consumer receives the list of possible producers, it runs the subscriber matching mechanism to decide from which producer the energy will be purchased. As illustrated in Algorithm 4.1, the matching mechanism relies on the consumer type, which is defined by the list of potential producers and their surplus power.

- In the **Mono-source consumer** case, each producer in the list can supply the whole demand of the consumer. The ER uses the first case in the subscriber

Algorithm 4.1: Subscriber Matching Mechanism

```
Input: c                                              // the identify of consumer
       P_c                                            // the requested energy of consumer
       L                                              // the list of possible producers
Output: Fitness                                       // the Fitness value
/* check if the consumer is a heavy load                                        */
Fitness ← 0
if !heavyLoad(c) then
    /* case 1: Mono-source consumer                                             */
    for i ← 1 to l do
                                              // l:the number of producers in list L
        cost_p ← calculatecost(L(i), P_c)
        W_{c↔p} ← ACObasedERP(L(i), c, P_c)
        Fitness_p(i) ← α × W_{c↔p} + (1 − α) × Cost_p
    /* Select the best producer with min Fitness                                */
    Fitness = min(Fitness_p)
else
    /* case 2: Heavy load (multi-source consumer)                               */
    C_n^c ← createCombination(P_c, L)
    for i ← 1 to m do
        /* Determine the power amount to get from each set to achieve the minimum
           Fitness                                                              */
        Fitness_s(i) ← EPSOA(C_c^n(i), c, P_c)
    /* Select the best producers set with the min Fitness                       */
    Fitness ← min(Fitness_s)
```

matching mechanism and calculates the fitness value ($Fitness_p$) to each producer p in the potential producers' list using Equation (4.1).

$$Fitness_p = \alpha \times W_{c \leftrightarrow p} + (1 - \alpha) \times Cost_p \tag{4.1}$$

$$Cost_p = Price_p \times P_c \times Time \tag{4.2}$$

Where: $0 \leq \alpha \leq 1$, $cost_p$ and $W_{c \leftrightarrow p}$ symbolize, in sequence, the energy cost and the power transmission loss of the minimum loss path between the consumer and the producer. The minimum loss path is generated by the ACO-based energy routing protocol described in detail in Section 4.2.2. As indicated in Equation (4.1), the objective function involves two criteria that need to be minimized: energy cost and energy transmission losses. These two criteria are connected through a factor denoted as "α", which indicates the relevance (weight) assigned to each criterion, according to the broker's preferences. The broker adjusts the α value depending on the overall system generation and demand. If the total energy generation exceeds the total demand, the broker reduces the α value while prioritizing cost. On the contrary, if the total energy generation falls short of demand, the broker raises the α value, prioritizing the minimization of power loss.

- Based on Equation (4.3), the ER selects the producer with the lowest fitness value. It informs the broker to validate the created energy transaction and updates its data.

$$Minimize\left(\sum_{p\in L} Fitness_p\right) \tag{4.3}$$

- The ER creates the virtual circuit for the selected producer. Each ER in the virtual circuit will update its data and share it with the rest of the ERs in the system.

- Whereas, in **Multi-source consumer (heavy load)** case, none of the potential producers can fulfil the entire required energy amount. Consequently, the subscriber matching mechanism executed by the ER will opt for multiple producers to satisfy the consumer's energy request. As outlined in references [1, 2], it is advisable to keep the number of producers selected for a single consumer as minimal as feasible. This will reduce the complexity of the subscriber matching system while increasing grid stability and assuring its security and durability. Therefore, it is assumed that a single consumer cannot obtain energy from more than three producers.

- Using the list of potential producers (L), First, a combination set C_n^c of producers is formed.

$$C_n^c = \begin{pmatrix} S_1 \\ S_2 \\ \dots \\ S_m \end{pmatrix}_{m\times 1} = \begin{pmatrix} p_{11} & p_{12} & \dots & p_{1n} \\ p_{21} & p_{22} & \dots & p_{2n} \\ \dots & \dots & \dots & \dots \\ p_{m1} & p_{m2} & \dots & p_{mn} \end{pmatrix}_{m\times n}$$

Each set S in the combination set C_n^c consists of a specific number of producers (n), whose combined available power is sufficient to fulfill the consumer's energy request (Equation (4.4)). The construction of this combination set enables strategic power transmission scheduling between the customer and the selected producers. This involves identifying the best sequence of producers to start with, with the aim of minimizing both total power loss and energy costs. This strategy has the ability to greatly reduce total power loss and congestion in the system.

$$\Sigma_{k=1}^{n} P_k >= P_c, k \in L \tag{4.4}$$

- The energy particle swarm optimization algorithm (EPSOA) is then used to determine the required power amount to get from each producer within set S_k to satisfy consumer demand while minimizing the fitness value of the set (see Equation 4.5).

$$Fitness_{S_k} = \Sigma_{i=1}^{n} Fitness_{p_i} \tag{4.5}$$

- This step is repeated for each set S_k present in C_n^c, and the set with the minimum fitness is selected to power the consumer (Equation (4.6)).

$$Fitness_{min} = min_{k=1...m}(Fitness_{S_k}) \tag{4.6}$$

- The suggested energy particle swarm optimization algorithm (EPSOA) is depicted in algorithm 4.2. The EPSOA starts with the generation of k particles. Each particle (X_i) represents the amount of power allocated by each producer in the set S to meet the energy demand of the consumer. The initial power amount allocated from producers 1 to $(n-1)$ in the set S is chosen randomly within their generation boundaries, while the n^{th} producer delivers the remaining power to meet the consumer's demand. The algorithm calculates the fitness value for each particle by employing Equations (4.5) and (4.1). It then initiates the pbest (personal best) and gbest (global best) values and proceeds to adjust the position (X) and velocity (V) of each particle in every iteration using Equations (4.7) and (4.8) while respecting the following constraints.

$$X_i^{t+1} = X_i^t + V_i^{t+1} \tag{4.7}$$

$$V_i^{t+1} = wV_i^t + C_1 r_1[pbest_i^t - X_i^t] + C_2 r_2[gbest^t - X_i^t] \tag{4.8}$$

C1: The particle's total power should be equal to the consumer's energy demand.

$$\Sigma_{j=1}^{n} X_{ij} = P_c$$

C2: The extracted power from producer j inside particle i must be within the capacity of the producer, which corresponds to its available power.

$$0 \leq X_{ij} \leq P_{p_j}$$

Algorithm 4.2: Energy Particle Swarm Optimization

Input: c, P_c, S
Output: $gBest$
Initialize the PSO parameters $(k, n, C_1, C_2$, and $w)$
/* Initialize the random positions of each particle (X_i) */

for *each particle i in the swarm* **do**
    Initialize randomly its position (X_i) while respecting constraints C1 and C2
    Initialize velocity (V_i) randomly
    for *each producer j in the set S* **do**
        Calculate the Cost of getting X_{ij} power amount from producer j, according to Equation (4.2)
        Calculate the best path for transmitting X_{ij} power amount from producer j using ACO-based energy routing protocol
        Evaluate the fitness value ($Fitness(X_{ij})$), according to Equation (4.1)
        Evaluate the fitness value ($Fitness(X_i)$) of the position X_i, according to Equation (4.5)
    Initialize $pBest$ to its initial position $pbest(i) \leftarrow X(i)$
Initialize the $gbest$ as the particle with the minimum fitness value
/* Repeat until terminal criteria is met */

$ite \leftarrow 1$
while $(ite <= maxit)$ && *!(error criteria)* **do**
    for *each particle i in the swarm* **do**
        Update particles's velocity V_i according to Equation (4.8)
        Update particle's position X_i according to Equation (4.7)
        Use a limiter to ensure that the new particle's position X_i respect constraints C1 and C2
        for *each producer j in the set S* **do**
            Calculate the Cost of getting X_{ij} power amount from producer j, according to Equation (4.2)
            Calculate the best path for transmitting X_{ij} power amount from producer j using ACO-based energy routing protocol
            Evaluate the fitness value ($Fitness(X_{ij})$), according to Equation (4.1)
            Evaluate the fitness value ($Fitness(X_i)$) of the position X_i, according to Equation (4.5)
        if $Fitness(X_i) < Fitness(pBest_i)$ **then**
            Update the $pBest$ of particle i: $pBest(i) \leftarrow X_i$
            if $Fitness(X_i) < Fitness(gBest)$ **then**
                Update the $gBest$ of the swarm: $gbest \leftarrow X_i$
    $i \leftarrow i + 1$

- The ER determines the best set of producers with all necessary data, including the required power from each producer and the best path to each producer inside the best set. Similarly to the mono-source consumer case, the ER informs the broker of its trading decision. Following broker approval, the ER performs the necessary updates, establishes the circuits, and begins energy transfer from the selected producers.

The consumer-producer pairs generated by the subscriber matching mechanism must comply with the constraints (3.15) and (3.16).

4.2.2 ACO-based Energy Routing Algorithm

Most of the energy-routing algorithms used in the literature to find the energy minimum loss path between a trading pair use graph theory methods, which have high computational time in huge networks. In order to address the computational complexity, we proposed the use of metaheuristic algorithms to solve this problem. As the Ant Colony Optimization algorithm (ACO) has shown effective applicability in solving a wide range of routing problems, including Wireless Sensor Network Routing [139], Vehicle Routing Problem [140], and Traveling Salesman Problem [141], etc. We propose an ACO-based energy routing algorithm in this section. The proposed algorithm is executed by ERs to determine the non-congestion energy-efficient transmission path between a trading pair (the producer-consumer pair). As detailed in Chapter 3, the energy-efficient transmission path is the energy minimum loss path (see Equation (3.2)), while the total energy loss along a transmission path connecting a consumer-producer pair is the sum of power losses along all ERs and power lines constituting the path (see Equation (3.3)). As highlighted in Chapter 3, it's crucial to emphasize that the energy minimum loss path should satisfy the constraints (3.8),(3.9),(3.10),(3.11) and (3.12).
The flowchart depicted in Figure 4.2 illustrates the fundamental concept and implementation of the proposed ACO-based energy routing protocol. While the relevant parameters are presented in Table 4.1. The sequential steps of the ACO-based energy routing algorithm are as follows:

1. Initially, following the explanation provided in chapter Chapter 3, the ERs use network information and graph theory concepts to construct a connected undirected weighted graph that serves as a representation of the network power system.

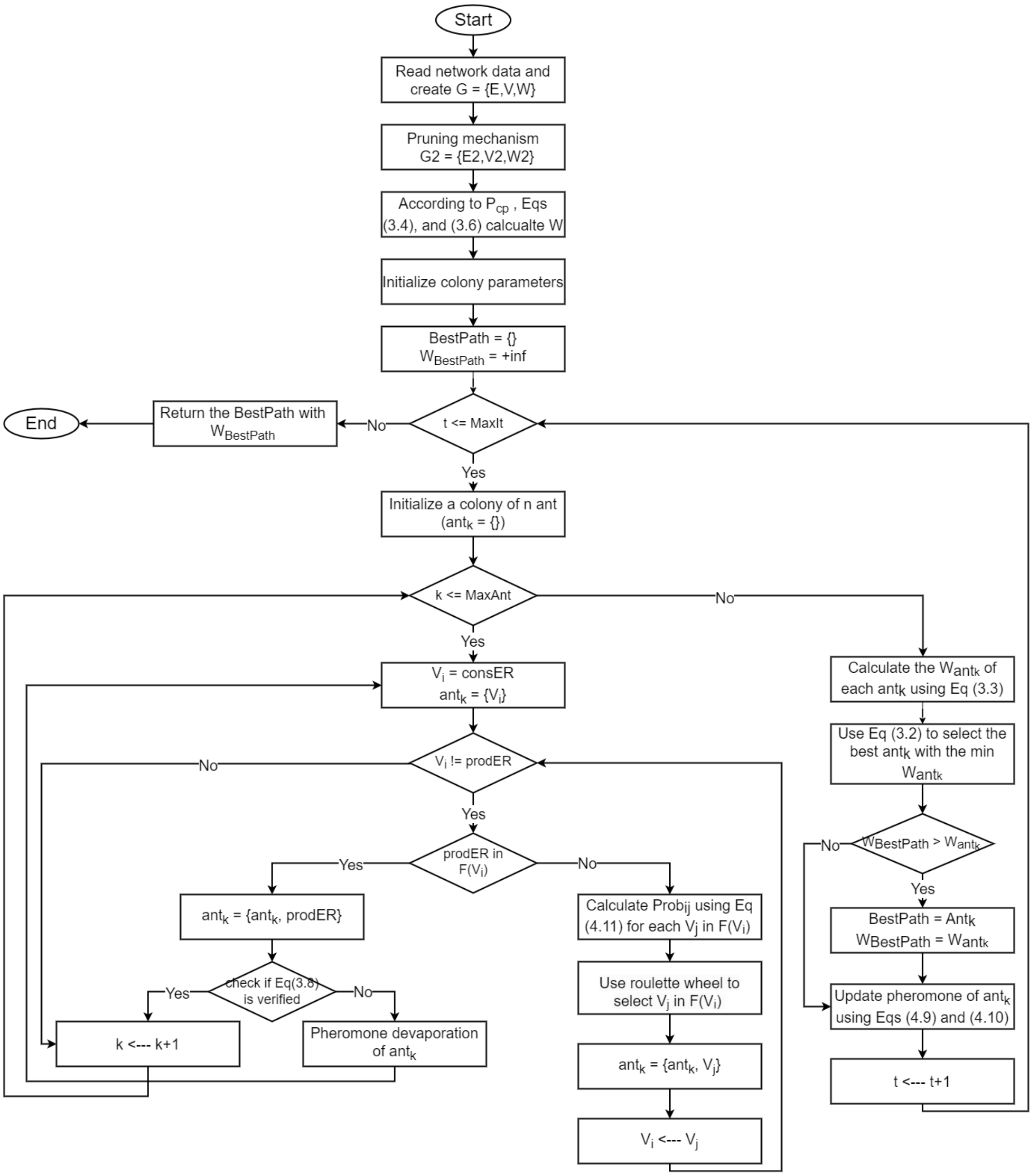

FIGURE 4.2: ACO-based energy routing protocol (ACO-ERP).

2. Upon receiving the energy transaction information including the transmitted power amount P_{cp}, and the producer identity, a pruning mechanism is initiated. This mechanism is executed before the energy minimum loss path selection and aims to prevent the power system from congestion and failure. It involves applying constraints (3.9),(3.10), and (3.11) to remove all power lines and ERs that are incapable of transmitting P_{cp}. Consequently, a new sub-graph denoted $G2$ is deducted.

3. According to P_{cp} and using Equations (3.4) and (3.6), the power loss of each power line and ER in the $G2$ is calculated.

TABLE 4.1: ACO-ERP's flowchart parameters

Symbol	Description
$G = \{E, V, W\}$	The EI corresponding graph model, E, V, W represents the set of nodes and edges that consist of the graph G with their weights, respectively.
$G2 = \{E2, V2, W2\}$	The new graph of EI resulting from the pruning mechanism.
P_{cp}	The transmitted power between the producer-consumer pair
$BestPath$	The energy-efficient path (energy minimum loss transmission path)
$W_{BestPath}$	The total power loss of $BestPath$
$maxIt$	Iterations maximum number
$maxAnt$	Ants maximum number
ant_k	The k^{th} path, which is the energy transmission path between the consumer-producer pair determined by an ant k
W_{ant_k}	The total power loss of the path k
$consER$	The consumer associated ER
$prodER$	The producer associated ER
V_i	The current node (ER) where the ant is allocated
V_j	A neighbor of node V_i (ER_i)
$F(V_i)$	A set of one-hop neighbors of a node V_i (ER_i)

4. The minimum path selection method is founded on ACO principles. Consumers and producers/prosumers, in this metaphor, perform the roles of an ant nest and a food source, respectively. Ants are used to identify the best path between them. They communicate and move toward the food source using a chemical signal called a pheromone. The path with the highest concentration of pheromone becomes the favoured option used by ants among the various paths, typically indicating the shortest path. Certain ants release more pheromones in nature when the food source is plentiful or of higher quality, and the path is extremely efficient. Consequently, the pheromone level on a path is precisely proportional to its power transmission loss. Equation (4.9) reflects the quantity of pheromone deposition on an edge (power line) L_{ij} by ant k, where W^{path} represents the power transmission loss associated with the transmission path that includes the line L_{ij}.

$$\Delta t_{ij}^{k} = \frac{1}{W^{path}} \tag{4.9}$$

When ant k chooses the line L_{ij}, the amount of pheromone on that particular line is adjusted per Equation (4.10), where n stands for the number of ants that have selected the line L_{ij}.

$$\tau_{ij}^{k} = \Sigma_{k=1}^{n} \Delta t_{ij}^{k} \tag{4.10}$$

The ER establishes the ant colony's initial settings during this step, comprising the number of iterations, the number of ants, and the initial pheromone concentration.

5. Each ant moves along the graph, from one node to the next (beginning with the consumer-associated ER) until it reaches the producer-associated ER (the destination node). Using the roulette wheel method, the subsequent node (ER) is chosen by computing a probability for each neighbouring node. As outlined in Equation (4.11), two factors impact this probability: the concentration of pheromone associated with the probably next node and the power loss sustained when travelling to that node, where α and β are two parameters that control, respectively, the importance of the pheromone intensity (τ_{ij}) and the quality of the power line (η_{ij}). F_i is the list of neighbors of node v_i in the graph $G2$, while Equation (4.12) outlines the quality of the power line L_{ij}.

$$Prob_{ij} = \frac{(\tau_{ij})^{\alpha}\,(\eta_{ij})^{\beta}}{\Sigma_{j\in F_i}\,(\tau_{ij})^{\alpha}\,(\eta_{ij})^{\beta}} \tag{4.11}$$

$$\eta_{ij} = \frac{1}{w_i + w_{ij}} \tag{4.12}$$

6. When an ant's selected path violates the constraint (3.8), indicating that the power loss of this selected path exceeds the transmitted power, a mechanism called "pheromone devaporation" is initiated. In this mechanism, the pheromone level associated with this path is reduced by 5% to discourage other ants from selecting the same path.

7. The method iterates several times, with each iteration comprising the selection of an energy-efficient path (denoted by set S in Figure 4.2). Concurrently, the pheromone level is adjusted in accordance with Equations (4.9) and (4.10).

8. As specified by Equation (3.2), the most energy-efficient path within set S is the one with the least power transmission loss.

A virtual circuit is established using the selected energy-efficient path for the transfer of energy between the producer-consumer pair. The adoption of the pruning process, as well as information sharing between ERs during circuit generation, along with capacity constraint validation prior to circuit construction, successfully mitigates congestion and overhead problems.

4.3 Numerical Simulation and Result Analysis

In this section, detailed numerical simulations will be employed to assess the performance of the proposed hybrid energy routing protocol in different scenarios using different EI networks, covering the three main energy routing problems: subscriber matching, energy-efficient path, and transmission scheduling.
It's important to note that within this context, as mentioned in Chapter 3, a "load" refers to shortage-energy prosumer , while a "source" refers to a surplus-energy prosumer . Additionally, if an ER is directly linked to a load, it is considered as a load. On the contrary, if it's connected to an energy source, it is considered an energy source in the network.

4.3.1 Single predetermined source load pair

To initiate the evaluation process of the proposed energy routing algorithm, we start by evaluating the performance of the ACO-based energy routing algorithm in small and large networks. For that, the networks described in Chapter 3 in Figures 3.5, 3.7 and 3.8 with their detailed parameters in Tables 3.5, 3.6, 3.9, 3.10, 3.11,3.12, and 3.13 are used for simulation to allow a comparison between the energy routing algorithms in [2], [1], and the proposed ACO-based energy routing algorithm in this chapter. As illustrated in Tables 4.2 and 4.3 the source load pair and the amount of transmitted power are determined in each network. It is assumed that the preexisting power in this case equals zero.
In the network in Figure 3.5, the scenario of power transmission from ER_1 to ER_{26} is simulated for two power levels, 10 kW and 2 kW. The simulation results are given by Tables 4.2, 4.3, in which it can be seen that irrespective of the growing power loss caused by the increasing amount of transmitted power between ER_1 and ER_{26}, exhaustive search algorithm in [1], DFS algorithm in [2], and the proposed ACO-based algorithm choose the same single transmission path ($1 \rightarrow 2 \rightarrow 6 \rightarrow 28 \rightarrow 27 \rightarrow 25 \rightarrow 26$) for both 2 kW and 10 kW since there are no other single paths in the network with a lower loss than the currently selected path. It is notable that the ACO-based algorithm demonstrated a 61.4 % reduction in computational time compared to the exhaustive search algorithm, and 54.4% compared to the DFS algorithm.
The power line L_{25-27} initially has a capacity of 16 kW. A pre-existing power of 10 kW on this line decreases its capacity to 6 kW, restricting the capacity of the path $1 \rightarrow 2 \rightarrow 6 \rightarrow 28 \rightarrow 27 \rightarrow 25 \rightarrow 26$ to 6 kW, making it unable to transmit the required 10 kW between ERs 1 and 26. Choosing this path will overload the power line

TABLE 4.2: Simulation results of single predetermined source load pair in multiple networks (Exhaustive-search [1], DFS [2]).

Network	Traiding pair	Transmitted power (kW)	Evaluation parameters	Exhaustive search	DFS
3.5	$1 \rightarrow 26$	2	**Path**	$1 \rightarrow 2 \rightarrow 6 \rightarrow 28 \rightarrow 27 \rightarrow 25 \rightarrow 26$	$1 \rightarrow 2 \rightarrow 6 \rightarrow 28 \rightarrow 27 \rightarrow 25 \rightarrow 26$
			TL (kW)	0.293	0.293
			CT (s)	2.25	2.24
		10	**Path**	$1 \rightarrow 2 \rightarrow 6 \rightarrow 28 \rightarrow 27 \rightarrow 25 \rightarrow 26$	$1 \rightarrow 2 \rightarrow 6 \rightarrow 28 \rightarrow 27 \rightarrow 25 \rightarrow 26$
			TL (kW)	1.728	1.728
			CT (s)	2.28	2.10
		10 $P_{L_{27-25}} = 10$ kW	**Path**	$1 \rightarrow 2 \rightarrow 6 \rightarrow 10 \rightarrow 22 \rightarrow 24 \rightarrow 25 \rightarrow 26$	$1 \rightarrow 2 \rightarrow 6 \rightarrow 28 \rightarrow 27 \rightarrow 25 \rightarrow 26$ $1 \rightarrow 2 \rightarrow 6 \rightarrow 10 \rightarrow 22 \rightarrow 24 \rightarrow 25 \rightarrow 26$
			TL (kW)	2.261	1.885
			CT (s)	2.08	4.36
3.7	$28 \rightarrow 58$	5	**Path**	$28 \rightarrow 27 \rightarrow 32 \rightarrow 23 \rightarrow 24 \rightarrow 70 \rightarrow 69 \rightarrow 49 \rightarrow 51 \rightarrow 58$	$28 \rightarrow 27 \rightarrow 32 \rightarrow 23 \rightarrow 24 \rightarrow 70 \rightarrow 69 \rightarrow 49 \rightarrow 51 \rightarrow 58$
			TL (kW)	1.083	1.083
			CT (s)	1080	980
	$112 \rightarrow 117$	14	**Path**	$112 \rightarrow 110 \rightarrow 103 \rightarrow 100 \rightarrow 98 \rightarrow 80 \rightarrow 81 \rightarrow 68 \rightarrow 65 \rightarrow 38 \rightarrow 30 \rightarrow 17 \rightarrow 16 \rightarrow 12 \rightarrow 117$	$112 \rightarrow 110 \rightarrow 103 \rightarrow 100 \rightarrow 98 \rightarrow 80 \rightarrow 81 \rightarrow 68 \rightarrow 65 \rightarrow 38 \rightarrow 30 \rightarrow 17 \rightarrow 16 \rightarrow 12 \rightarrow 117$
			TL (kW)	5.874	5.874
			CT (s)	1075	970
3.8	$92 \rightarrow 176$	15	**Path**	$92 \rightarrow 67 \rightarrow 65 \rightarrow 69 \rightarrow 58 \rightarrow 76 \rightarrow 72 \rightarrow 71 \rightarrow 20 \rightarrow 56 \rightarrow 147 \rightarrow 143 \rightarrow 136 \rightarrow 155 \rightarrow 153 \rightarrow 128 \rightarrow 159 \rightarrow 179 \rightarrow 176$	$92 \rightarrow 67 \rightarrow 65 \rightarrow 69 \rightarrow 58 \rightarrow 76 \rightarrow 72 \rightarrow 71 \rightarrow 20 \rightarrow 56 \rightarrow 147 \rightarrow 143 \rightarrow 136 \rightarrow 155 \rightarrow 153 \rightarrow 128 \rightarrow 159 \rightarrow 179 \rightarrow 176$
			TL (kW)	6.721	6.721
			CT (s)	864	629
	$201 \rightarrow 69$	12	**Path**	$201 \rightarrow 91 \rightarrow 1 \rightarrow 12 \rightarrow 3 \rightarrow 11 \rightarrow 14 \rightarrow 10 \rightarrow 9 \rightarrow 87 \rightarrow 88 \rightarrow 66 \rightarrow 67 \rightarrow 65 \rightarrow 69$	$201 \rightarrow 91 \rightarrow 1 \rightarrow 12 \rightarrow 3 \rightarrow 11 \rightarrow 14 \rightarrow 10 \rightarrow 9 \rightarrow 87 \rightarrow 88 \rightarrow 66 \rightarrow 67 \rightarrow 65 \rightarrow 69$
			TL (kW)	3.738	3.738
			CT (s)	506	478

L_{25-27} and create congestion. To avoid congestion issues, the proposed ACO-based algorithm uses a pruning mechanism that prunes out the ERs and power lines that couldn't carry the 10 kW, including the power line L_{25-27}. As a result, a different path ($1 \rightarrow 2 \rightarrow 6 \rightarrow 10 \rightarrow 22 \rightarrow 24 \rightarrow 25 \rightarrow 26$) was chosen, although with a larger transmission loss (2.261 kW). This path, on the other hand, had a capacity of 16 kW, allowing the 10 kW to be successfully transmitted. The same results are obtained with the algorithm in [1] but with more execution time. The DFS algorithm in [2] uses the data packet mode and executes the algorithm multiple times to find multiple paths to transmit the power in multiple paths. This results in more execution time, especially in large and complex networks, making it unfeasible for real-time and near-real-time energy trading.

Networks in Figures 3.7 and 3.8 are used to evaluate the proposed energy routing algorithm's efficacy on large networks that offer a vast array of power routing options (paths) compared to the first network. As shown in Tables 4.2 and 4.3 different trading pairs with different power transmission amounts are used in each network. The results show that the ACO-based energy routing algorithm outperforms the exhaustive search and DFS algorithms in larger networks, giving the minimum energy loss path with much less computing time (50% less), making it ideal for near-real-time and real-time energy routing in vast networks. Even the poorest solution discovered by the ACO-based energy routing algorithm represents a path that falls within the top 10% of the best paths within the network.

TABLE 4.3: Simulation results of single predetermined source load pair in multiple networks (the proposed ACO-based algorithm).

Network	Trading pair	Transmitted power (kW)	Evaluation parameters	The proposed ACO-based algorithm	
				Best	Worst
3.5	$1 \rightarrow 26$	2	**Path**	$1 \rightarrow 2 \rightarrow 6 \rightarrow 28 \rightarrow 27 \rightarrow 25 \rightarrow 26$	-
			TL (kW)	0.293	-
			CT (s)	0.83	-
		10	**Path**	$1 \rightarrow 2 \rightarrow 6 \rightarrow 28 \rightarrow 27 \rightarrow 25 \rightarrow 26$	-
			TL (kW)	1.728	-
			CT (s)	0.88	
		10 $P_{L_{27-25}} = 10$ kW	**Path**	$1 \rightarrow 2 \rightarrow 6 \rightarrow 10 \rightarrow 22 \rightarrow 24 \rightarrow 25 \rightarrow 26$	-
			TL (kW)	2.261	-
			CT (s)	1.1	-
3.7	$28 \rightarrow 58$	5	**Path**	$28 \rightarrow 27 \rightarrow 32 \rightarrow 23 \rightarrow 24 \rightarrow 70 \rightarrow 69 \rightarrow 49 \rightarrow 51 \rightarrow 58$	$28 \rightarrow 27 \rightarrow 25 \rightarrow 2324 \rightarrow 70 \rightarrow 69 \rightarrow 49 \rightarrow 51 \rightarrow 58$
			TL (kW)	1.083	1.093
			CT (s)	9.67	11.30
	$112 \rightarrow 117$	14	**Path**	$112 \rightarrow 110 \rightarrow 103 \rightarrow 100 \rightarrow 98 \rightarrow 80 \rightarrow 81 \rightarrow 68 \rightarrow 65 \rightarrow 38 \rightarrow 30 \rightarrow 17 \rightarrow 16 \rightarrow 12 \rightarrow 117$	$112 \rightarrow 110 \rightarrow 103 \rightarrow 100 \rightarrow 98 \rightarrow 80 \rightarrow 81 \rightarrow 68 \rightarrow 65 \rightarrow 38 \rightarrow 30 \rightarrow 17 \rightarrow 15 \rightarrow 14 \rightarrow 12 \rightarrow 117$
			TL (kW)	5.874	6.109
			CT (s)	13.38	14.05
3.8	$92 \rightarrow 176$	15	**Path**	$92 \rightarrow 67 \rightarrow 65 \rightarrow 69 \rightarrow 58 \rightarrow 76 \rightarrow 72 \rightarrow 71 \rightarrow 20 \rightarrow 56 \rightarrow 147 \rightarrow 143 \rightarrow 136 \rightarrow 155 \rightarrow 153 \rightarrow 128 \rightarrow 159 \rightarrow 179 \rightarrow 176$	$92 \rightarrow 67 \rightarrow 66 \rightarrow 88 \rightarrow 87 \rightarrow 9 \rightarrow 10 \rightarrow 14 \rightarrow 11 \rightarrow 3 \rightarrow 12 \rightarrow 1 \rightarrow 91 \rightarrow 201 \rightarrow 189 \rightarrow 158 \rightarrow 181 \rightarrow 185 \rightarrow 165 \rightarrow 169 \rightarrow 173 \rightarrow 179 \rightarrow 176$
			TL (kW)	6.721	7.303
			CT (s)		
	$201 \rightarrow 69$	12	**Path**	$201 \rightarrow 91 \rightarrow 1 \rightarrow 12 \rightarrow 3 \rightarrow 11 \rightarrow 14 \rightarrow 10 \rightarrow 9 \rightarrow 87 \rightarrow 88 \rightarrow 66 \rightarrow 67 \rightarrow 65 \rightarrow 69$	
			TL (kW)	3.738	-
			CT (s)	21	-

4.3.2 Single load multiple sources

The process of matching energy sources to loads and establishing energy transactions is an integrated part of the energy routing protocol. To evaluate the matching process of the proposed energy routing protocol, taking the network depicted in Figure 3.5, we assume the presence of five sources ER_2, ER_6, ER_8, ER_{25}, and ER_{27} each with distinct power capacities of 18 kW, 12 kW, 11 kW, 15 kW, and 10 kW respectively. These energy sources are associated with different prices for supplying power, which are 0.056 \$/kWh, 0.078 \$/kWh, 0.068 \$/kWh, 0.065 \$/kWh and 0.041 \$/kWh, respectively, and must supply 10 kW power demand by load ER_{18}. We presume that all energy sources, except ER_8, have a similar transmission time as the load. As the transmission time of ER_8 doesn't align with the required timeframe of the load, the broker will exclude the ER_8 from the list of potential sources for load ER_{18} as it cannot provide the requested power within the necessary timeframe.

As depicted in Table 4.4, the work outlined in [121] consider the subscriber matching and energy-efficient path as two separate optimization problems where source-load pairs are formed prior to the selection of energy transmission paths. The matching process is primarily price-based, leading to the selection of ER_{27}, which offers the lowest price but incurs the highest power loss (1.584 kW) compared to other sources. On the other hand, the subscriber matching process employed in references [1] and [2] is power loss-based, where exhaustive search and DFS algorithms are first used to find the energy-efficient path to each potential source in the network, selecting the one with the minimal power transmission loss, which is in this case ER_6. However, it is important to highlight that ER_6 comes with the highest price. On the contrary, the proposed energy routing protocol incorporates both power loss and price considerations into a single objective function for subscriber matching. After receiving the list of possible producers from the broker, ER_{18} starts the matching process by calculating the fitness value of each energy source in the list and selecting the one with the minimum fitness value (see Table 4.5), in this case, ER_2. This selection offers more beneficial pricing (28.2%) than the methods in [1] and [2]. Additionally, it outperforms the algorithm's selection in [121] in terms of power efficiency (26.76% reduced power loss).

Table 4.4: Comparison of source selection in the case of single load multiple sources.

Algorithm	Energy source	Transaction power (kw)	Price ($/kw)	Transmission Path	Power loss (kw)
[1]	6	10	0.78	$6 \rightarrow 4 \rightarrow 12 \rightarrow 15 \rightarrow 18$	1.131
[121]	27		0.41	$27 \rightarrow 28 \rightarrow 6 \rightarrow 4 \rightarrow 12 \rightarrow 15 \rightarrow 18$	1.584
[2]	6		0.78	$6 \rightarrow 4 \rightarrow 12 \rightarrow 15 \rightarrow 18$	1.131
[137]	**2**		**0.56**	$2 \rightarrow 4 \rightarrow 12 \rightarrow 15 \rightarrow 18$	**1.160**

Table 4.5: The source selection of the proposed hybrid energy routing protocol in the case of single load multiple sources ($\alpha = 0.5$).

Load	**Transaction power (kw)**	**Energy source**	**Price ($/kw)**	**Transmission Path**	**Power loss (kw)**	**Fitness value**	**Selected source**
18	10	2	0.56	$2 \rightarrow 4 \rightarrow 12 \rightarrow 15 \rightarrow 18$	1.160	0.86	2
		6	0.78	$6 \rightarrow 4 \rightarrow 12 \rightarrow 15 \rightarrow 18$	1.131	0.95	
		25	0.65	$25 \rightarrow 24 \rightarrow 23 \rightarrow 15 \rightarrow 18$	1.329	0.98	
		27	0.41	$27 \rightarrow 28 \rightarrow 6 \rightarrow 4 \rightarrow 12 \rightarrow 15 \rightarrow 18$	1.584	1.004	

4.3.3 Heavy load (multi-source consumer)

A P2PET in EI permits a single source to power numerous loads. Similarly, a load can acquire the required power from one or more sources. To evaluate the performance of the proposed energy routing algorithm when dealing with heavy loads in the system, we assume the presence of an EV connected to ER_{17} with the same set of producers as mentioned earlier (ER_2, ER_6, ER_{25}, and ER_{27}). As per the European EV charging standard IEC 61851 [1], the power requirement of the EV is 22 kW and none of the network available sources can entirely fulfil this request, therefore the EV is classified as a heavy load. In this case, after receiving the ER_{17}' power request, the broker creates a list that contains all the possible producers that can transmit power at the same timeframe of ER_{17} ($L = \{ER_2, ER_6, ER_{25}, ER_{27}\}$). Given the power data from the sources in the set L, at least two sources are required to provide the load ER_{17}

with the requested power. By receiving the list L, ER_{17} creates a combination set C as follows:

$$C_2^{ER_{17}} = \begin{pmatrix} S_1 \\ S_2 \\ S_3 \\ S_4 \\ \dots \\ S_{12} \end{pmatrix}_{12\times1} = \begin{pmatrix} ER_2 & ER_6 \\ ER_2 & ER_{25} \\ ER_2 & ER_{27} \\ ER_6 & ER_2 \\ \dots & \dots \\ ER_{27} & ER_{25} \end{pmatrix}_{12\times2}$$

This specific combination creates a source allocation scheduling strategy, setting the priority order for assigning sources and paths, which reduces the total power loss. For each set S_i the ER_{17} invokes the EPSOA and determines the best set with the minimum fitness value that satisfies the EV power request. Table 4.6 summarizes the results of the computations, encompassing the selected sources and paths, transmission power, pricing, and power losses compared to other algorithms in the literature.

While Table 4.7 illustrates the selection of power sources and their power amounts in the ER17 context, depending on various values of α. When α is set to 1, the algorithm focuses on minimizing power loss in subscriber matching leading to the selection of ERs 6 and 2 due to their lowest transmission losses which is the same provided solution in the previous works [1] and [2]. Conversely, when α equals 0, the algorithm prioritizes the price and performs matching based only on it resulting in the selection of ERs 2 and 27 as they offer the lowest prices. However, our proposed algorithm aims to perform matching by considering power losses and prices at the same time. In this scenario, energy sources that offer the lowest prices have the highest energy losses, whereas those with the lowest losses typically come with the highest prices. Therefore, decreasing the α value reduces the energy drawn from ER_6 and raises the energy obtained from other low-priced sources (ER_2,ER_{27}) leading to a new solution with a small increase in power loss but a better price for prosumers. While algorithm [121] failed to generate a feasible solution for this scenario.

It is worth mentioning that in many P2PET systems proposed in the literature, the trading pairs must pay energy loss compensation fees to the utility grid to compensate for the energy losses resulting from the P2PET transactions [126, 142, 143], which increases the cost of trading in P2PET systems. Assuming a rate of 0.2 $/kW.h for 1 kW power loss, the total cost incurred by consumer ER_{17} in this scenario would be 1,93$ using [1], 1.95 $ using [2], and 1.87 $ using the proposed energy routing protocol. Clearly, the suggested matching algorithm yields the lowest overall energy cost, emphasizing the necessity of factoring in energy transmission loss as well as prosumer costs throughout the matching process.

TABLE 4.6: Comparison of source selection in the case of heavy load ($\alpha = 0.5$). NC: Not Considered.

Algorithm	Transaction pair	Transaction power (kw)	Price ($/kw)	Transmission Path	Power loss (kw)	Total power loss (kw)	Total price ($/kw)
[1]	6 - 17	12	0.936	$6 \rightarrow 10 \rightarrow 17$	1.065	2.2086	1.496
	2 - 17	10	0.56	$2 \rightarrow 4 \rightarrow 12 \rightarrow 16 \rightarrow 17$	1.1436		
[121]	NC	NC	NC	NC	NC	NC	NC
[2]	6 - 17	12	0.936	$6 \rightarrow 9 \rightarrow 10 \rightarrow 17$	1.148	2.2725	1.496
	2 - 17	10	0.56	$2 \rightarrow 6 \rightarrow 10 \rightarrow 17$	1.1245		
[137]	**2 - 17**	**13.840**	**0.775**	$2 \rightarrow 4 \rightarrow 12 \rightarrow 16 \rightarrow 17$	**1.6589**	**2.308**	**1.411**
	6 - 17	**8.16**	**0.636**	$6 \rightarrow 10 \rightarrow 17$	**0.6491**		

TABLE 4.7: α variation and source selection for heavy load case.

α	Transaction pair	Transaction power (kw)	Price ($/kw)	Transmission Path	Power loss (kw)	Total power loss (kw)	Total price ($/kw)
1	6 - 17	12	0.936	$6 \rightarrow 10 \rightarrow 17$	1.065	2.2086	1.496
	2 - 17	10	0.56	$2 \rightarrow 4 \rightarrow 12 \rightarrow 16 \rightarrow 17$	1.1436		
0.7	2 - 17	11.549	0.647	$2 \rightarrow 4 \rightarrow 12 \rightarrow 16 \rightarrow 17$	1.3463	2.235	1.462
	6 - 17	10.451	0.815	$6 \rightarrow 10 \rightarrow 17$	0.8887		
0.5	2 - 17	13.840	0.775	$2 \rightarrow 4 \rightarrow 12 \rightarrow 16 \rightarrow 17$	1.6589	2.308	1.411
	6 - 17	8.16	0.636	$6 \rightarrow 10 \rightarrow 17$	0.6491		
0.3	2 - 17	14.518	0.813	$2 \rightarrow 4 \rightarrow 12 \rightarrow 16 \rightarrow 17$	1.754	2.666	1.12
	27 - 17	7.482	0.307	$27 \rightarrow 28 \rightarrow 6 \rightarrow 10 \rightarrow 17$	0.912		
0	27 - 17	10	0.41	$27 \rightarrow 28 \rightarrow 6 \rightarrow 10 \rightarrow 17$	1.2926	2.6993	1.082
	2 - 17	12	0.672	$2 \rightarrow 4 \rightarrow 12 \rightarrow 16 \rightarrow 17$	1.4067		

4.3.4 Multi-loads multi-sources

To demonstrate the effectiveness of the proposed protocol in efficiently managing energy routing when dealing with numerous sources and loads, we'll be using the same electrical network system as previously outlined (Figure 3.5), with a small modification: the capacity of the power line L_{4-12} has been set at 17 kW to purposely induce congestion on that line. We'll proceed with the simulation using the same group of sources as described in the previous scenarios. The following power requests 4 kW, 22 kW, and 10 kW, must be supplied by these sources to the loads ER_{13}, ER_{17}, and ER_{18}, respectively. Different loads will have different transmission times, which can result in a variety of situations where the transmission times are either non-overlapping or overlapping.

4.3.4.1 Non-overlapping transmission time

The transmission times of the different loads in this scenario do not overlap. Therefore, the preexisting power in the network is considered to be 0 and the choice of a load will not affect the other one. It is presumed that sources ER_2, ER_6, ER_{25}, and ER_{27} could deliver an equivalent surplus of power during various load transmission times. This ensures a consistent array of choices for each consumer and allows the assessment of the algorithm's efficacy under diverse demands and situations. The energy source and transmission path chosen by each load, utilizing the proposed energy routing protocol, are illustrated in Table 4.8. A comparative analysis with the studies in [1], [121], and [2] is also provided.

TABLE 4.8: Comparison of source selection in the case of Multi-loads multi-sources with Non-overlapping transmission time. NC: Not Considered.

Algorithm	Transaction pair	Transaction power (kW)	Total Price ($/kW.h)	Transmission Path	Path capacity (kW)	Total Power loss (kW)
[1]	6 - 17	12	1.496	$6 \rightarrow 10 \rightarrow 17$	32	2.209
	2 - 17	10		$2 \rightarrow 4 \rightarrow 12 \rightarrow 16 \rightarrow 17$	16	
	6 - 18	10	0.78	$6 \rightarrow 4 \rightarrow 12 \rightarrow 15 \rightarrow 18$	16	1.132
	6 - 13	4	0.312	$6 \rightarrow 4 \rightarrow 12 \rightarrow 13$	17	0.335
[121]	? - 17	NC	NC	NC	NC	NC
	27 - 18	10	0.41	$27 \rightarrow 28 \rightarrow 6 \rightarrow 4 \rightarrow 12 \rightarrow 15 \rightarrow 18$	16	1.585
	27 - 13	4	0.164	$27 \rightarrow 28 \rightarrow 6 \rightarrow 4 \rightarrow 12 \rightarrow 13$	17	0.503
[2]	6 - 17	12	1.496	$6 \rightarrow 9 \rightarrow 10 \rightarrow 17$	32	2.273
	2 - 17	10		$2 \rightarrow 6 \rightarrow 10 \rightarrow 17$	20	
	6 - 18	10	0.78	$6 \rightarrow 4 \rightarrow 12 \rightarrow 15 \rightarrow 18$	16	1.132
	6 - 13	4	0.312	$6 \rightarrow 4 \rightarrow 12 \rightarrow 13$	17	0.335
[137]	6 - 17	8.16	1.411	$6 \rightarrow 10 \rightarrow 17$	32	2.308
	2 - 17	13.84		$2 \rightarrow 4 \rightarrow 12 \rightarrow 16 \rightarrow 17$	16	
	2 - 18	10	0.56	$2 \rightarrow 4 \rightarrow 12 \rightarrow 15 \rightarrow 18$	16	1.160
	2 - 13	4	0.224	$2 \rightarrow 4 \rightarrow 12 \rightarrow 13$	17	0.338

The table indicates that the algorithm consistently selects an energy source for each load that can provide the whole demand through a congestion-free path (with power flow below its maximum capacity). The matching method suggested in this chapter takes into account both path power loss and price, unlike the other three algorithms, which only take into account energy source prices [121] or transmission power loss [1] and [2]. It chooses energy sources that concurrently balance and optimize cost and power loss. The selected sources for the load ER_{17} are the same by the different algorithms but with different amounts of power. This slight difference in the amount of power provided by the proposed algorithm creates a gain in the cost by 5,68% compared to the solution provided by [1] and [2]. It also provides a gain cost of 28% for both ERs 18 and 13. Same for the power loss it provides a gain of 26,81% (425w) and 32,8% (165w) power saving for ERs 18 and 13, respectively compared with the solution provided by [121].

4.3.4.2 Overlapping transmission time

In this scenario, we presumed that the transmission times of various loads overlap, but with a considerable time delay between them. The transmission time for ER_{18}

begins after ER_{17}, whereas the transmission time for ER_{13} starts after ER_{18}, with a considerable time disparity between their respective beginning points. As depicted in Table 4.9, using the proposed energy routing protocol the selected sources by ER_{17} stay consistent with the non-overlapping case since there is no preexisting power in the system. However, by providing 13,84 kW from its energy availability the energy source connected to ER_2 is no longer a viable option for ER_{18} as its remaining power (4,16 kW) cannot fulfil its total demand. The broker list sent to ER_{18} contains ERs 25 and 27, from which based on their suggested prices and the actual network energy loss, the ER_{25} is chosen to power ER_{18}.

The paths allocated by the first trading pairs ($ER_6 - ER_{17}$, $ER_2 - ER_{17}$, $ER_{25} - ER_{18}$) decreases the capacity of the selected power lines and increases their power losses due to the change on lines pre-existing power from 0 to 8,16 kW, 10kW and 13,84kW (because of its quadratic function of pre-existing and transmitted power see Section 3.3). The capacity of the power lines L_{4-12} and L_{16-17} has decreased to 3,16 kW and 2,16 kW, respectively. This maximum capacity can not transmit the whole demand of ER_{13} (4 kw), therefore, they are pruned from the graph as depicted in Figure 4.3 before calculating the efficient paths using the proposed pruning mechanism. As the next best path that can transmit 10 kW between ERs 13 and 2 ($2 \rightarrow 6 \rightarrow 9 \rightarrow 10 \rightarrow 22 \rightarrow 24 \rightarrow 23 \rightarrow 15 \rightarrow 12 \rightarrow 13$) has a higher energy loss (998.55 kW), the ER turns to another energy source that provides better price and power loss which is ER_{27}.

The proposed energy routing protocol prevents congestion and overload successfully while minimizing price and energy transmission loss.

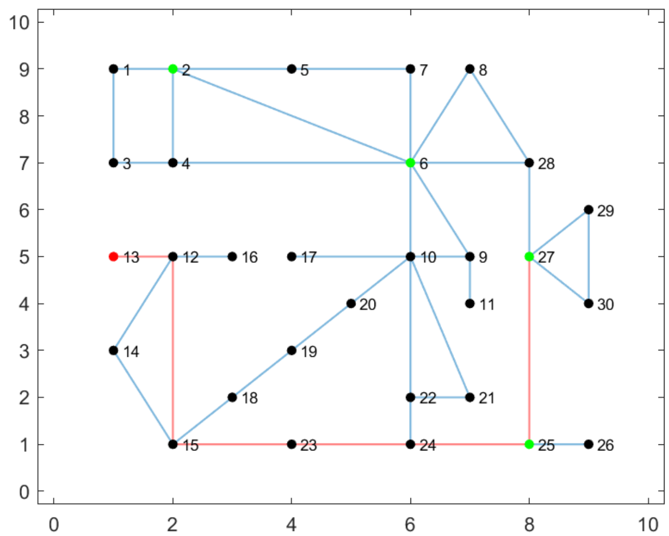

FIGURE 4.3: The source and path selected for ER_{13} using the proposed hybrid energy routing protocol.

TABLE 4.9: The source selection of the proposed protocol in the case of Multi-loads multi-sources with overlapping transmission time.

Transaction pair	Transaction power (kW)	Total Price ($/kW.h)	Transmission Path	Path capacity (kW)	Total Power loss (kW)
6 - 17	8.16	1.411	*6 → 10 → 17*	32	2.308
2 - 17	13.84		*2 → 4 → 12 → 16 → 17*	16	
25 - 18	10	0.65	*25 → 24 → 23 → 15 → 18*	16	1.330
27 - 13	4	0.164	*27 → 24 → 23 → 15 → 12 → 13*	6	0.840

4.3.4.3 Simultaneous transmission time

As previously stated, the proposed hybrid energy routing protocol is a decentralized protocol that operates at the connected consumer ER, taking into account the actual state of the network. In instances where different consumers have coincident transmission times, the protocol will be simultaneously executed by these consumers. Each consumer makes individual source and path selection decisions, potentially leading to the selection of the same energy source, path, or portions of the path by multiple consumers. This might lead to line congestion and conflicts over energy source use. To overcome this issue, when multiple consumers have selected the same producer, as in Table 4.8, even if its available power can satisfy all the consumers, it selects the initial consumer who placed the energy request, since the change in the preexisting power flow in certain power lines picked by the first consumer will increase their power loss, which may encourage the other consumers who had previously chosen this producer to move to a different producer who better matches their preferences. Therefore, we proposed that the producer select the initial consumer who placed the energy request, update his available energy amount, and inform the rest.

Taking the example in Table 4.8, assuming that ER_2 has received the energy requests of ERs 13, 18, and 17 in this order (based on their execution time). In this particular instance, the producer would opt to choose the initial consumer, ER_{13}, to meet his demand, validate the energy transaction, update its available energy, and inform the other consumers, ERs 18 and 17. Upon acquiring confirmation from the producer, consumer ER_{13} starts the virtual circuit allocation procedure. Each ER in the selected path ($2 \rightarrow 4 \rightarrow 12 \rightarrow 13$) updates its information and informs the other ERs in the network. Communication between ERs during the establishment of energy transmission circuits, as well as confirmation of capacity limits before path building, help to reduce congestion and overload in the power system.

ERs 18 and 17 take the new state of the network and execute the algorithm until they get an approved solution. Table 4.10 shows the selected energy sources and paths for each consumer compared with the centralized algorithm in [2]. The table depicts the noticeable superiority of our protocol compared to the centralized algorithm. First, unlike the centralized algorithm that determines all the pairs centrally while minimizing the total power losses in the network and ignoring the monetary benefits and preferences of consumers, the proposed protocol provides the consumers with freedom in selecting the producers that provide monetary benefits while minimizing the transmission losses. This leads to better total costs of 5% for ER_{17} and 6% for ER_{17}. Additionally, the centralized algorithm efficiently manages the congestion problem as it schedules the energy transactions, but the whole energy trading could break down if the central unit collapses, which could not happen in the decentralized protocol.

TABLE 4.10: Comparison of source selection in the case of simultaneous transmission time.

Algorithm	Transaction pair	Transaction power (kW)	Total Price ($)	Transmission Path	Total Power loss (kW)	Total Cost ($)
Centralized algo	6 - 17	12	1.496	$6 \rightarrow 9 \rightarrow 10 \rightarrow 17$	2.273	1.96
	2 - 17	10		$2 \rightarrow 6 \rightarrow 10 \rightarrow 17$		
	2 - 13	4	0.224	$2 \rightarrow 4 \rightarrow 12 \rightarrow 13$	0.338	0.291
	2 - 18	4	0.614	$2 \rightarrow 4 \rightarrow 12 \rightarrow 15 \rightarrow 18$	1.194	0.86
	25 - 18	6		$25 \rightarrow 24 \rightarrow 23 \rightarrow 15 \rightarrow 18$		
Proposed protocol	2 - 13	4	0.224	$2 \rightarrow 4 \rightarrow 12 \rightarrow 13$	0.338	0.291
	2 - 18	10	0.56	$2 \rightarrow 4 \rightarrow 12 \rightarrow 15 \rightarrow 18$	1.201	0.8
	27 - 17	10	1.346	$27 \rightarrow 28 \rightarrow 6 \rightarrow 9 \rightarrow 10 \rightarrow 17$	2.497	1.84
	6 - 17	12		$6 \rightarrow 10 \rightarrow 17$		

4.4 Conclusion

A hybrid energy routing protocol is proposed in this chapter to solve the energy routing problem in EI including subscriber matching, energy-efficient path and transmission scheduling. Power losses on network lines are an unavoidable part of power transmission in P2P energy trading. As a result, the load/energy source matching algorithm was designed to reduce both energy prices and energy transmission losses while remaining consistent with the physical characteristics of the power system, power availability, and demand. The heavy load case was considered and a PSO matching-based algorithm was used to determine the amount of power to get from each source to satisfy the demand. A pruning mechanism with an ACO-based energy routing algorithm was proposed to find a congestion-free path between a trading pair. The key findings of this study are that the suggested protocol is decentralized, allowing P2P energy market participants to make their own decisions while protecting their privacy and interests. It also reduces the computational strain on the system operator and prevents single-point failures. The suggested matching method integrates energy transmission losses and pricing into a single optimization problem, providing a good solution that minimizes both power loss and price. Using a broker will reduce the number of communication transactions inside the network. Furthermore, the proposed ACO-based energy routing algorithm has less computational time compared to other literature algorithms which is extremely desirable in large-scale networks. The pruning process, the consideration of the network's physical characteristics, and the information change between ERs in the power system all contribute to lowering congestion in power lines and ERs, ensuring the grid's safety and power supply reliability. Simulation findings in an EI network under various scenarios approved the effectiveness of the proposed energy routing protocol. The results, given in Table 4.11, illustrate various advantages of the suggested hybrid energy routing protocol. These findings establish it as a potential and practical routing option for energy trading on the emerging EI.

TABLE 4.11: A comparison of the solving problems, matching criterias, and simulation cases by the proposed Hybrid energy routing protocols and literature.

		Energy routing Algorithms			
		[1]	[121]	[2]	Proposed [137]
Solved Problem	**Subscriber Matching**		✓	✓	✓
	Energy Efficient Path	✓	✓	✓	✓
	Transmission Scheduling	✓	✓	✓	✓
Matching metrics	**Price**		✓		✓
	Power loss			✓	✓
	Energy availability and demand		✓	✓	✓
	Network physical characteristics			✓	✓
Simulation scenarios	**Heavy load scenario**	✓		✓	✓
	Non-overlapping transmission time	✓	✓	✓	✓
	Overlapping transmission time	✓	✓	✓	✓
	Simultaneous transmission time			✓	✓

Chapter 5

A semi-decentralized congestion-free multi-path energy routing for P2PET systems through Yen's algorithm and SQP.

This chapter focuses on tackling energy-efficient path and transmission scheduling issues by switching from single-path to multi-path power transmission. The energy routing issue is formulated as a non-convex, non-linear optimization problem. To address this problem, a combination technique is given that incorporates graph theory and non-convex nonlinear programming. This integrated technique consistently produces an efficient multi-path solution for a particular trading pair, taking into account the power flow direction constraint and precisely computing power losses during transmission. For those circumstances requiring simultaneous power transmissions from many energy trading pairs, a semi-decentralized algorithm with a new ranking concept is proposed. This algorithm is intended to control congestion and shift computational workloads to individual trading pairs (ERs) and the network system operator.

5.1 Introduction

Recently, there has been an increased emphasis on creating energy-routing algorithms for EI. Regardless of the method used to establish the energy transmission paths, as discussed in previous chapters, the energy routing algorithms suggested in the literature are often divided into two categories: centralized and decentralized algorithms. In centralized algorithms such as those described in [2, 122, 134], the energy transmission paths for all trading pairs are calculated by a network system operator (NSO). Generally, these centralized algorithms assign energy transmission paths and schedule the energy transactions in such a manner that the grid's overall power loss is minimized. The primary advantage is that this strategy ensures a global optimum solution with congestion relief even in simultaneous energy transmissions by multiple energy trading pairs. However, one important drawback is the concentration of computational efforts on the NSO, which requires significant computational resources and time, especially in larger systems. Furthermore, certain trading pairs may incur larger losses in the chosen path solution as they must renounce high-efficiency transmission paths for the benefit of other trading pairs to minimize total network losses. By contrast to centralized energy routing algorithms, decentralized energy routing algorithms, such as those described in [1, 120, 121, 133], allow energy trading pairs to calculate their trading paths according to their preferences, decreasing the computational burden on the NSO. Assigning paths locally by each energy trading pair while avoiding congestion using virtual circuits or energy packet mode can achieve congestion management locally from the local perspective of each trading pair. Nevertheless, the ability to provide congestion-free energy transmission in scenarios involving simultaneous power transmissions by several energy trading pairs is questionable and cannot be guaranteed, exposing a significant weakness of decentralized energy routing algorithms. According to Chapter 2, energy packet mode optimizes power line use and, in some situations, reduces energy transmission loss. The centralized and decentralized energy routing algorithms discussed above are single-path algorithms.

To overcome the shortcomings of the previous algorithms, certain researchers, as proven in the study provided in [3], have shifted from single-path centralized and decentralized algorithms to multi-path semi-decentralized algorithms that showed promising results in optimizing energy routing.

It is crucial to note that, according to our best knowledge, none of the existing energy routing algorithms in the literature have adequately calculated the power losses during the transmission process since the power gradually diminishes along the transmission path, as depicted in Figure 3.3. However, the proposed algorithms often assume that the transmitted power throughout the entire path is always constant to simplify the computation of power loss and the search for the lowest loss paths, leading to higher power losses than the real loss. Furthermore, P2PET systems physically transport energy across distribution networks set up by the traditional grid, where power lines are designed for unidirectional power flow and are unable to transfer electrical energy in two opposing directions simultaneously. It is vital to elucidate that bidirectional power flow in EI typically means that a specific power line can be used to transport power flow in two directions but not at the same time. This power line's physical limit is known as the power flow direction constraint (PFD), which has not been considered by all of the previously discussed energy routing algorithms. As shown in Figure 5.1, assuming that the energy trading pairs (ER_1,ER_6) and (ER_4,ER_3) select their transmission paths to transmit the traded power, as can be observed, the power line between ERs 2 and 5 is chosen to transmit simultaneously the traded power in opposite directions. This can result in reverse power flow, overloading the transmission line, voltage fluctuations, and equipment failures. This will affect the performance, efficiency, and reliability of the power grid. Therefore, to ensure the appropriate operation of the EI, the PFD constraint of each power line must be considered when performing energy routing.

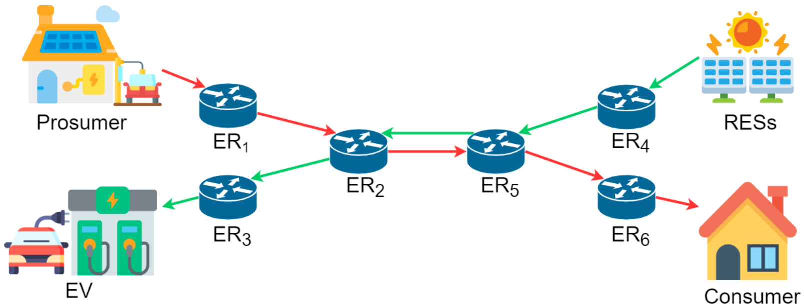

FIGURE 5.1: Diagram representing simultaneous bidirectional power flow in a power line case.

As a result of the preceding discussion, we have formulated the energy routing problem in this chapter as a non-convex, non-linear optimization problem. To solve this problem, we proposed a novel semi-decentralized multi-path energy routing algorithm that computes power losses accurately during path selection while respecting all the physical power system constraints, including the PFD constraint. The proposed semi-decentralized energy routing algorithm is divided into two phases: the local path discovery phase and the global path conflict resolution phase. The local path discovery phase represents the decentralized phase of the algorithm; it is executed at the trading pair ER level, where each trading pair chooses the transmission paths autonomously. In cases of conflict in the chosen energy transmission paths between the different energy trading pairs, the global path conflict resolution phase is invoked at the NSO level to solve this conflict and provide a global solution, which constructs the centralized part of the algorithm. The novel energy routing problem formulation is represented in Section 5.2. The proposed semi-decentralized multi-path energy routing algorithm is detailed in Section 5.3. Evaluation and numerical simulation of the developed energy routing algorithm are discussed in Section 5.4. This section investigates various scenarios involving networks of varying sizes, with a special emphasis on simultaneous transmission time scenarios.

5.2 Energy routing problem formulation

EI is a mesh network where many paths can be used to transmit energy between energy-trading prosumers (sources and loads). In the previous chapter, a single energy transmission path solution was proposed to transmit the total traded energy between energy-trading prosumers. The proposed solution provides congestion-free energy transmission paths while limiting the selection of power lines to those with significant capacity that can transmit the whole amount of traded power. This constraint may lead to disputes between trading pairs competing for access to these lines, while lower-capacity power lines are ignored. Instead of using a single energy transmission path to send the total traded power, the traded power can be split into multiple energy packets and transmitted through different paths. Therefore, building upon the energy routing problem formulation introduced in Chapter 3, we introduce an enhanced mathematical formulation of the problem that incorporates additional constraints for multi-path energy routing. The optimization problem of multi-path energy routing is defined by Equation (5.1).

$$min\left(TL_{Total}^{s\to l}\right) \tag{5.1}$$

Where $TL_{Total}^{s\to l}$ represents the total transmission loss of transmitting an amount of power between a trading pair $(s-l)$ through multiple paths. As outlined in Equation (3.7), it is the sum of the transmission losses of the different paths used to transmit the total power amount. The energy transmission loss of a path p is calculated using Equations (3.3), (3.4), and (3.6).

The multi-path energy routing must meet the constraints formulated as Equations

(5.2)-(5.8).

$$\text{s.t. } (3.8) - (3.12)$$

$$TP_{s-l} = \sum_{k=1}^{N_p} P_{s-l}^{k} \tag{5.2}$$

$$TL_{Total}^{s \to l} < TP_{s-l} \tag{5.3}$$

$$\sum_{k=1}^{Np} P_{s-l}^{k} + P_{ij} \leq P_{(L_{i,j})}^{Tc}, \quad \forall L_{i,j} \in E \tag{5.4}$$

$$\sum_{k=1}^{Np} P_{s-l}^{k} + P_{ij} \leq P_{(R_j)}^{Tc}, \quad \forall R_i \in V \tag{5.5}$$

$$P_{ij}^{total} = \sum_{(s-l) \in N} \sum_{k=1}^{Np} P_{s-l}^{k} + P_{ij}, \quad \forall L_{i,j} \in E \tag{5.6}$$

$$P_{ij}^{total} \times P_{ji}^{total} = 0, \quad \forall L_{i,j} \in E \tag{5.7}$$

$$0 \leq P_{s-l}^{k} \leq TP_{s-l} \tag{5.8}$$

Where:

- TP_{s-l} represents the total power amount that needs to be transmitted from the energy source s to the load l.
- P_{s-l}^{k} is the transmitted power through a path k from the source s to the load l.
- P_{ij}^{Total} depicts the total power sent over the power line L_{ij}, including the pre-existing power and power flows delivered along multiple paths involving different trading pairs that integrate the power line L_{ij}.

Constraints (3.8)-(3.12) ensure that the total power transferred along a particular path k is within the capacity of the ERs and power lines that comprise the path. Furthermore, these constraints ensure that the transmission power loss on the path is lower than the transmitted power over that particular path. The total amount of power transferred throughout the Np paths linking the source s and the load l must be equal to the overall power (TP_{s-l}) that flows initially from s (see Equation (5.2)). Simultaneously, the combined transmission loss across these paths must be lower than TP_{s-l} (refer to Equation (5.3)). A power line L_{ij} can be used by multiple paths to send power from s to l. Hence, the combined power transmitted across this line, together with the previous power, must comply with the maximum capacity of the power line and ERs in the extremities of this line as depicted by Equations (5.4) and (5.5).

As discussed in the section 5.1, a power line L_{ij}, cannot transmit simultaneous bidirectional power flows. The constraint (5.7) ensures that a power line L_{ij} may only transmit power in one direction at a time. If the overall power flow in the line from node i to node j is greater than 0 ($P_{ij}^{Total} > 0$), then the total power flowing in the opposite direction from node j to node i must be equal to zero.
The objective of the multi-path energy routing optimization problem is to define the best paths to select with the amount of power to send in each path so the total transmission energy loss is minimized (5.1). Equation (3.6) shows that power line loss increases quadratically with the amount of power flowing through it, resulting in a non-linear optimization problem. Furthermore, the PFD constraint in Equation (5.7) increases the complexity of the problem by defining a non-convex set, resulting in a non-convex nonlinear optimization problem.

5.3 Semi-decentralized multi-path energy routing through Yen's and SQP algorithms

The multi-path energy routing problem is a non-convex, non-linear optimization problem. Non-convex problems are more challenging, and a global solution is not guaranteed. To solve this problem, we proposed the use of a semi-decentralized energy routing algorithm where most routing decisions are made locally at the ER level with the central coordination of an NSO. We presume the existence of a P2PET communication platform where energy trading pairs are created (which is not considered in this work) and power system characteristics are shared. This communication platform allows ERs to submit their status information (including their capacities, conversion efficiency, and the information of their connected power lines and ERs) and to get a complete view of the network structure and status information. As illustrated in Figure 5.2, the proposed algorithm is divided into two phases: the local path discovery phase and the global path conflict resolution phase.

5.3.1 Local path discovery phase

This phase is executed at the trading pair associated ER; it could be at the source or the load side, according to the P2PET system policy. In this algorithm, we assumed that consumers are responsible for calculating their energy transmission paths. In the proposed semi-decentralized multi-path energy routing, we are not only selecting one or multiple paths but also optimizing the power flow distribution through the

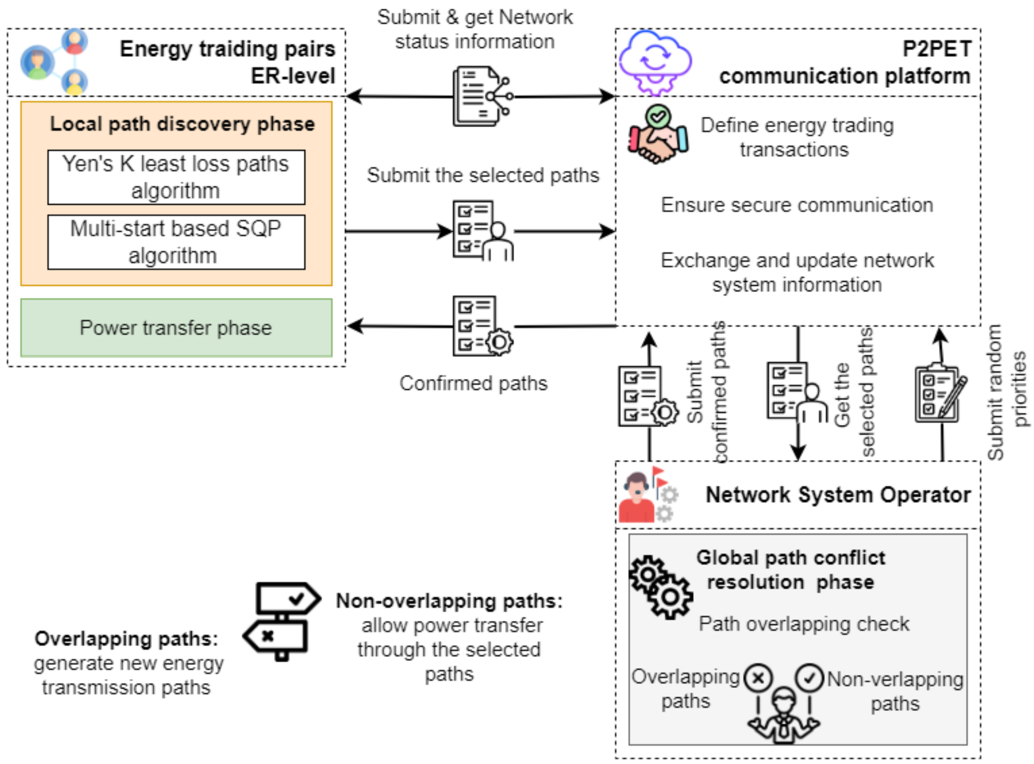

FIGURE 5.2: An overview of the proposed Semi-decentralized multi-path energy routing.

selected paths to minimize the total energy transmission loss. Therefore, the local path discovery phase is divided into two main algorithms: path enumeration and power distribution.

5.3.1.1 Modified Yen's k least loss paths-based path enumeration algorithm

Instead of finding all the possible paths between the trading pair, which increases the search space for the power dispatch algorithm, especially in huge and complex networks, we proposed the use of an updated version of Yen's k shortest path method, termed the Modified Yen's k energy least loss paths algorithm. The algorithm provides the k most promising paths to use for multi-path routing between the energy trading pairs. Traditional Yen's algorithm uses a cost parameter to determine the best k shortest paths [144] since, in our case, we do not know how the power will be distributed among the different paths in the initial phase, making the exact cost of the networks' ERs and power lines unknown as it has a quadratic relation to the amount of power transmitted through them (Equations (3.4) and (3.6)). Therefore, we proposed the use of a heuristic that represents the maximum power loss of transmitting the total power between the trading pair. We assumed that the total transmitted power would be transmitted through each ER and power line in the network, and we calculated their corresponding energy transmission losses. After determining the energy transmission loss of using each line and ER in the network, the modified Yen's k energy least loss paths algorithm invokes a modified bidirectional Dijkstra algorithm to select the k least loss paths. The modified bidirectional Dijkstra algorithm starts the search of the paths from both directions (energy source and load) simultaneously, reducing the Dijkstra algorithm's processing time, particularly in large networks. The path is formed when searches initiated from both the source and load sides converge at a midpoint. It integrates a filtering phase, where power lines with an existing power flow in the opposite direction as the algorithm search direction, saturated power lines, and ERs are selectively excluded at each step in the path discovery process.

The modified Yen's K least loss paths algorithm generates for the trading pair a set of the k most promising paths that do not have a reverse power flow, even the paths with small capacities.

Figures 5.3 and 5.4 illustrate the flowchart of the proposed Yen's k least loss paths and modified bidirectional Dijkstra algorithms, respectively.

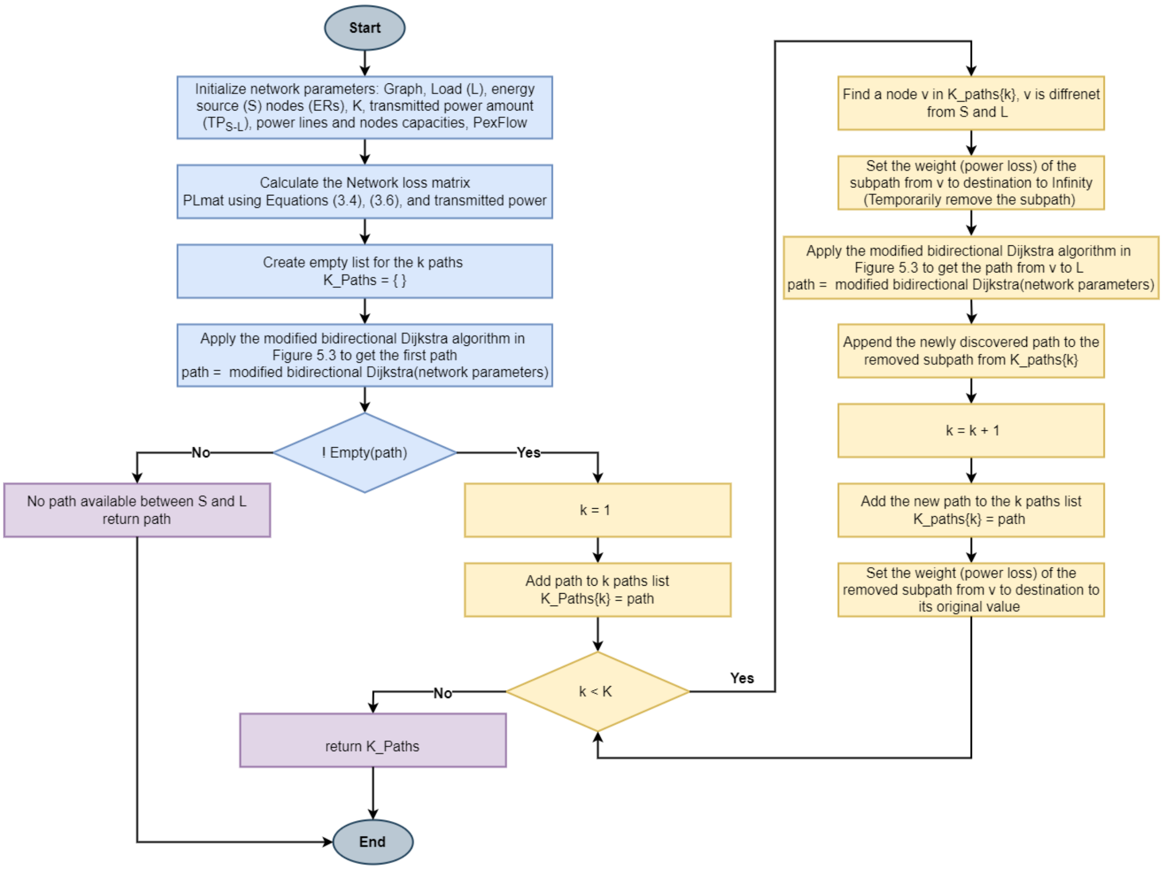

FIGURE 5.3: Flowchart of the Yen's K least loss paths algorithm.

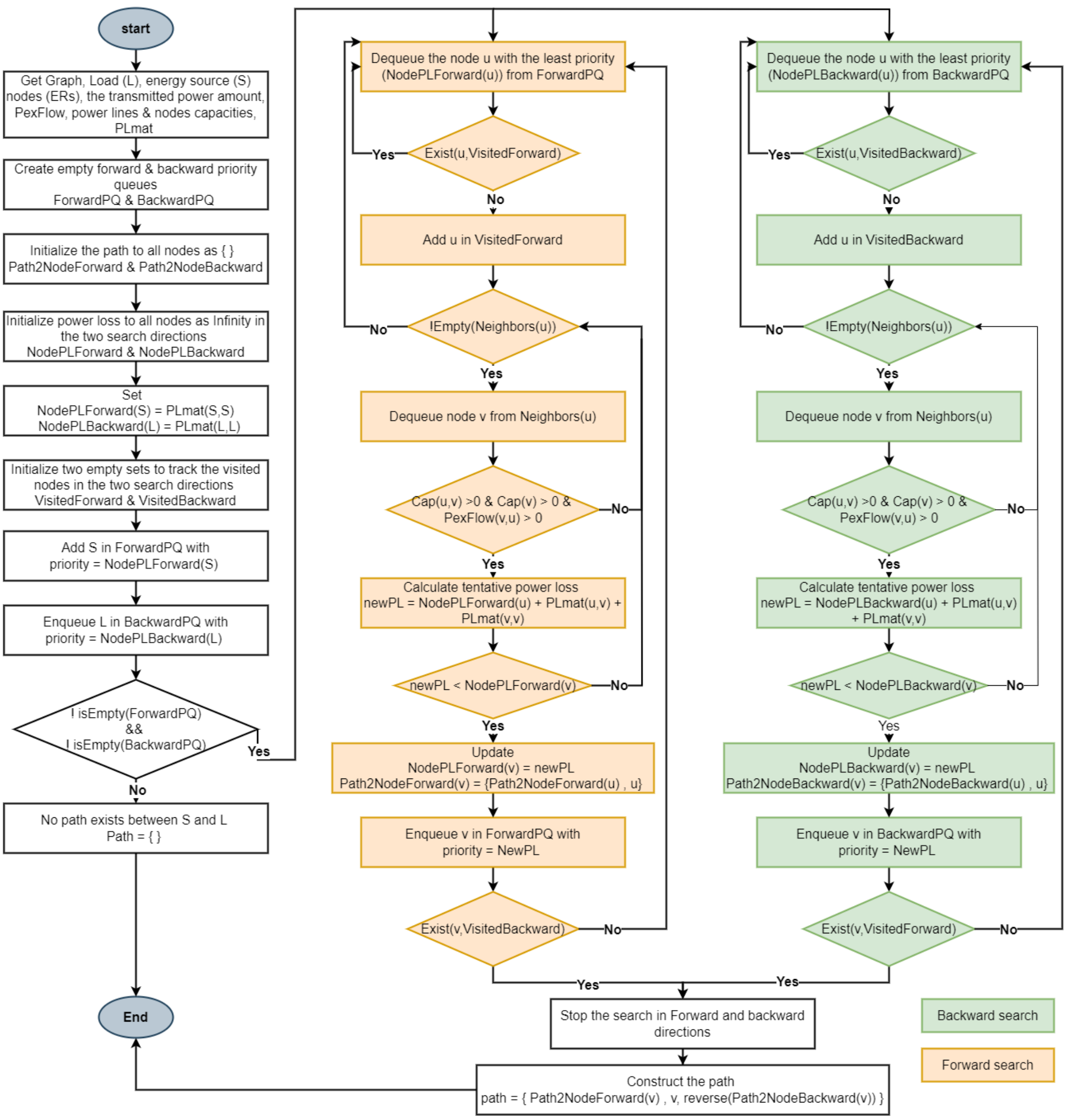

FIGURE 5.4: Flowchart of the Modified Bidirectional Dijkstra.

5.3.1.2 Power distribution-based SQP algorithm

After getting the k promising paths from the path enumeration algorithm for each trading pair, a power distribution algorithm is required to determine the selected paths from this set with the amount of power to send in each path. The selected paths should respect the PFD constraint (see Equation (5.7)), which makes the problem a non-convex non-linear optimization problem. Non-convexity provides the potential of having numerous local optima but it does not ensure the presence of a global optimum, thus it is difficult to identify whether the discovered solution is the global optimum or not. Sequential quadratic programming (SQP) is an efficient method to solve non-linear, constrained optimization problems with fast convergence. To prevent the SQP from getting stuck in a local optimal solution, we proposed the use of multi-start point SQP for the power distribution as shown in Algorithm 5.1. The use of multi-start points enhances the possibility of moving outside the local optimal by identifying an improved solution that is nearest to the global optimal solution. As illustrated in Algorithm 5.1, the multi-start point SQP is an iterative algorithm, and for faster execution, the proposed algorithm can be parallelized if the network's ERs are sufficiently powerful.

Algorithm 5.1: Multi-Start Point SQP Algorithm

Input: KPaths, KPathsCap, NetworkParameters

Output: $XBest, TL_{Total}^{XBest}$

```
/* Initialize a random solution */
```

$XBest \leftarrow$ generate a random solution in bounds of the k paths capacities

$TL_{Total}^{XBest} \leftarrow 0$

```
/* Determine the power loss of each selected path in XBest */
```

for i = *1* ***to*** K **do**

  $W^P \leftarrow$ compute loss of path i in the KPaths using Algotithm 5.2

  $TL_{Total}^{XBest} \leftarrow TL_{Total}^{XBest} + W^P$

  Update Network Prameters

while *stopping condition is not satisfied* **do**

  $X_0 \leftarrow$ generate a random solution in bounds of the k paths capacities

  $(TL_{Total}, X) \leftarrow$ Apply SQP on X_0

```
/* Update XBest */
```

  if $TL_{Total} < TL_{Total}^{XBest}$ **then**

    $XBest \leftarrow X$

    $TL_{Total}^{XBest} \leftarrow TL_{Total}$

$XBest$ is a vector of the amount of power to be transmitted through each path in the k paths selected by the path enumeration algorithm; if $XBest(i) > 0$ the path i is selected to transmit $XBest(i)$ kW; otherwise, the path is not selected. TL_{Total}^{XBest} represents the total transmission loss of the paths in $XBest$ to transmit the traded power between the energy trading pair.

It is important to mention that all the proposed energy routing algorithms discussed in the previous chapters assume that the transmitted power throughout the entire path is always constant to simplify the computation of power loss and the search for the lowest loss paths, while it gradually diminishes along the transmission path, which results in different energy transmission losses. Taking the network example in Figure 5.1, assuming that the transmitted power from ER_1 to ER_2 is denoted by P, the total power loss $W_{Total}^{p:1-2}$ is calculated using Equations (5.9)-(5.12).

$$w_{R_1} = (1 - eff_{R_1}) \times P \tag{5.9}$$

$$w_{L_{(1,2)}} = \frac{r_{L_{(1,2)}}}{V^2_{L_{(1,2)}}} \times \left[\left((P - w_{R_1}) + Pex_{L_{1,2}} \right)^2 - Pex^2_{L_{(1,2)}} \right] \tag{5.10}$$

$$w_{R_2} = (1 - eff_{R_2}) \times (P - w_{R_1} - w_{L_{(1,2)}}) \tag{5.11}$$

$$W_{Total}^{p:1-2} = w_{R_1} + w_{L_{(1,2)}} + w_{R_2} \tag{5.12}$$

Hence, to get the precise energy transmission loss for each path, the SQP algorithm uses Algorithm 5.2. As the solution in this case consists of a set of paths, it is critical to update the network's pre-existing power flow after computing the power loss for path i in the set before moving on to path $i + 1$. The SQP algorithm takes into consideration the constraints (3.8)-(3.12), (5.2)-(5.8) and returns the best set of paths found, the amount of power to send in each path and the total energy transmission loss.

Algorithm 5.2: Precise path power loss Algorithm

Input: P, Path, NetworkParameters
Output: W_{Total}^{p}
$W_{Total}^{p} \leftarrow 0$
for i = *1* ***to*** $(length(Path) - 1)$ **do**
    $w_{Path(i)} \leftarrow$ calculate $ER_{Path(i)}$ power loss using Equation (3.4), P, and NetworkParameters
    `/* Update the transmitted power` P `that enters the next power line */`
    $P \leftarrow P - w_{Path(i)}$
    $w_{Path(i,i+1)} \leftarrow$ calculate $L_{Path(i,i+1)}$ power loss using (3.6), P, and NetworkParameters
    `/* Update the transmitted power` P `that enters the` $ER_{Path(i+1)}$ `*/`
    $P \leftarrow P - w_{Path(i,i+1)}$
    $W_{Total}^{p} \leftarrow W_{Total}^{p} + w_{Path(i)} + w_{Path(i,i+1)}$
`/* Calculate the power loss of the last ER in the path */`
$w_{Path(end)} \leftarrow$ calculate $ER_{Path(end)}$ power loss using Equation (3.4), P, and NetworkParameters
$W_{Total}^{p} \leftarrow W_{Total}^{p} + w_{Path(end)}$

P is the transmitted power; $Path$ is the energy transmission path, which is a vector of the ERs that construct the path; and $NetworkParameters$ contains the network's power lines and ERs information, including voltage, resistance, efficiency, and pre-existing power.

At the end of the local path discovery phase, each ER submits to the P2PET communication platform the selected paths to use, along with the amount of power to send on each one.

5.3.2 Global path conflict resolution phase

The P2PET system is not totally independent from the grid; electricity power must be transmitted through utility grid lines [145]. Using the local path discovery phase to define transmission paths in a fully decentralized manner based on the perspectives of energy trading pairs at the ER level may result in overlapping paths in simultaneous power transmissions, increasing power loss, and perhaps causing congestion in the intersection parts, jeopardizing grid stability. Therefore, the NSO is used in our proposed algorithm to manage these risks.

After each ER submits its selected energy transmission paths and the amount of power to send through each path on the P2PET communication platform, the NSO extracts this information and invokes the global path conflict resolution phase. In this phase, the NSO checks for the presence of overlapping paths. If there is no path overlapping between the selected paths by the different trading pairs (ERs), the NSO sends a path confirmation to the pairs, permitting them to start the energy transfer. Otherwise, the NSO orders the conflicted trading pairs according to their priority ranking, assigns the path to the trading pair with the higher ranking, and then decreases this pair's ranking. In cases where two trading pairs have the same ranking, the NSO chooses one of them randomly. For the remaining trading pairs that did not get their selected paths, the NSO constructs new paths for each trading pair. Since fairness between the trading pairs is an important criterion that needs to be considered, we proposed two methods for generating the new paths:

- As the pre-existing power in the power lines has an impact on their transmission losses, the order of path allocation will influence the network total loss. This means that the order in which trading pairs are treated (affected new paths) can have a significant influence on network overall transmission loss. Consequently, in the first proposed method, the NSO selects the ideal sequence in which each pair is accommodated so the network total transmission losses are reduced. Assuming that we have two trading pairs (s_1, l_1) and (s_2, l_2), the NSO creates a combination set $\{\{(s_1, l_1), (s_2, l_2)\}, \{(s_2, l_2), (s_1, l_1)\}\}$. It starts with the first set $\{(s_1, l_1), (s_2, l_2)\}$ and allocates the paths for each trading pair according to their order in the set (affects new energy transmission paths for trading pair

(s_1, l_1), then for pair (s_2, l_2)) and does the same thing with the second set. After determining the total transmission loss of each set, it chooses the set with the lowest transmission loss.

As the new paths are allocated for the trading pairs based on the total network loss, this will favour some trading pairs at the expense of others (increasing the power loss for others); therefore, to create a fair situation, the total power loss of all the remaining trading pairs will be divided between them. Equation (5.13) illustrates the amount of power loss charged to each trading pair, where the fraction indicates the ratio of the network total power loss to the total transmitted power between all the pairs. TP_{s-l} denotes the transmitted power between a trading pair.

$$PL_{pair} = \frac{\sum_{(s-l)\in N} TL_{Total}^{s\to l}}{\sum_{(s-l)\in N} \sum_{k=1}^{N_p} P_{s-l}} \times TP_{s-l} \tag{5.13}$$

- In the second method, the NSO takes the remaining trading pairs randomly, one by one, and attributes new paths for each trading pair using the proposed semi-decentralized algorithm (local path discovery phase). The power losses charged to each pair are calculated using Equation (5.13).

The first method provides the minimum network energy transmission loss, which creates benefits for both trading pairs and the utility grid, as in the majority of P2PET systems, the utility grid compensates for the loss and bills the trading pairs. However, it takes a significant amount of time, which increases with the number of pairs and the network's size. As a result, the second method is better when dealing with a large number of trading pairs.

For the priority ranking concept, we assume that the NSO generates random priorities for all the prosumers, consumers, and producers in the network and distributes them with the utility grid prices at the beginning of the day. It uses the historical data

The priority of the trading pair is the mean of the consumer's and producer's priorities that construct the pair. Each time a trading pair gets the conflicted path (the overlapping path), its priority will decrease. This gives the remaining pairs (producers and consumers) a higher possibility of taking the desired paths in the next path-overlapping cases and prevents some trading pairs from dominating the power lines.

The energy trading pairs must obtain NSO approval before initiating a power transfer; this ensures system stability and appropriate risk management.

5.4 Numerical Simulation and Result Analysis

This section demonstrates the efficiency of the introduced semi-decentralized multi-path energy routing algorithm using detailed simulations, encompassing varied networks and power transmission analysis scenarios. These scenarios include the presence of single and multiple simultaneous energy trading pairs. Before diving into the algorithm's results, as the major focus of this chapter is determining the least energy loss paths between energy trading pairs, the matching process has not been explicitly considered. Hence, it is assumed that the energy transactions comprising the source, destination, and power amount are created by the P2PET communication platform. Following that, each trading pair (consumer-associated ER) uses the proposed algorithm to determine the least energy loss path to use. The suggested algorithm is compared to the routing algorithms in [1–3, 120, 121] to show its superior performance.

5.4.1 Single predetermined source-load pair

EI networks described in Chapter 3 in Figures 3.2, 3.5 and 3.6 with their detailed parameters in Tables 3.1, 3.2, 3.5, 3.6, 3.7, and 3.8 are used for simulation. In each network, we assume the existence of a single source-load trading pair. The selected source-load trading pair in each network is located at its extremes to increase the number of possible power transmission paths between them. A power amount of 10 kW should be transmitted from ER_2 to ER_9, from ER_{14} to ER_{29}, and from ER_{30} to ER_{35}, in Figures 3.2, 3.5, and 3.6, respectively. Initially, it is assumed that the pre-existing power within the three networks is set to zero. Table 5.1 and Figures 5.5, 5.6, and 5.7 illustrate the simulation outcomes of the proposed semi-decentralized multi-path energy routing algorithm compared with the exhaustive search [1], Dijkstra [120, 121], DFS [2], and non-linear programming with DFS [3] algorithms.

Table 5.1: The total energy transmission loss of exhaustive search, Dijkstra, DFS, non-linear programming algorithms and the proposed algorithm in the single predetermined source-load pair case.

	Single-path energy routing			**Multi-path energy routing**	
EI Network	Exhaustive search (kW) [1]	Dijkstra (kW) [120, 121]	DFS (kW) [2]	non-linear programming with DFS(kW) [3]	Proposed Algorithm (kW)
Figure 3.2	1.706	1.706	1.706	1.415	1.294
Figure 3.5	1.691	1.691	1.691	1.655	1.516
Figure 3.6	2.431	2.431	2.431	2.250	1.999

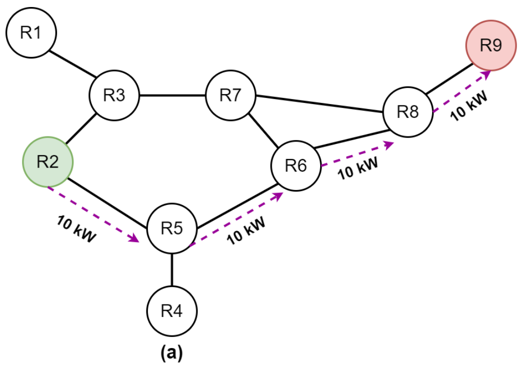

FIGURE 5.5: The least loss paths selected by (a) Exhaustive search, Dijkstra and DFS algorithms, (b) non-linear programming, and the proposed energy routing algorithm for the trading pair in Figure 3.2.

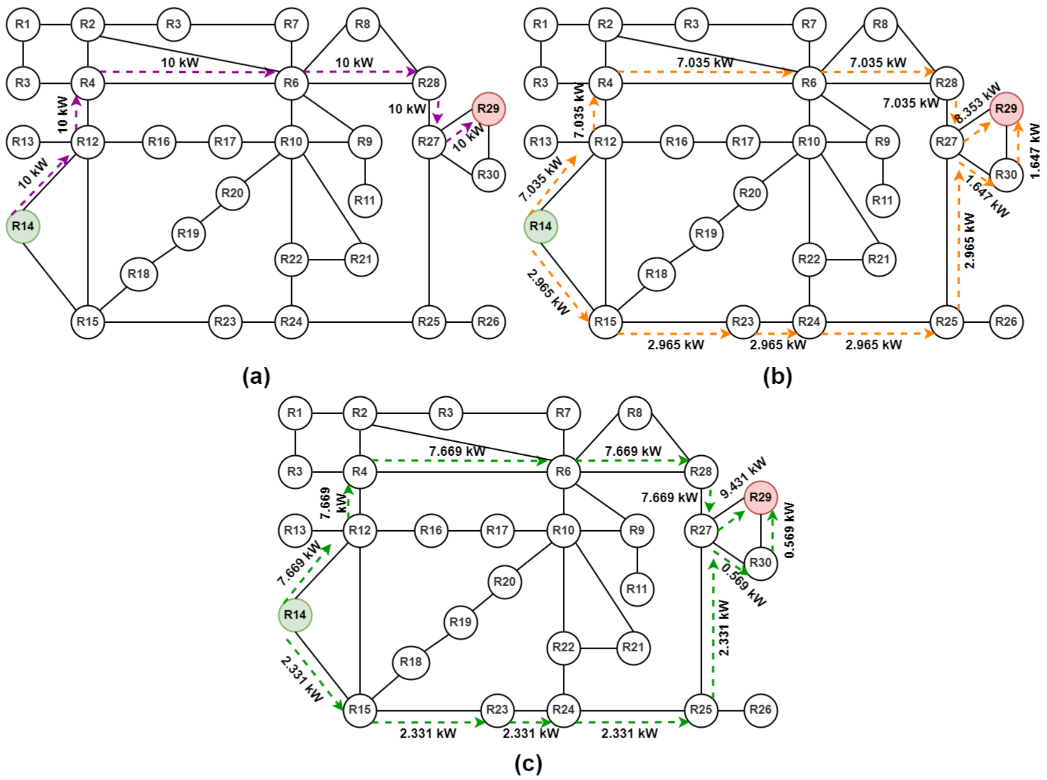

FIGURE 5.6: The least loss paths selected by (a) Exhaustive search, Dijkstra and DFS algorithms, (b) non-linear programming with DFS, and (c) the proposed energy routing algorithm for the trading pair in Figure 3.5.

As shown in Figures 5.5-5.7, the exhaustive search, Dijkstra, and DFS algorithms provide a single-path solution for transmitting power between the trading pairs in the different networks, while non-linear programming and the proposed semi-decentralized routing algorithms provide a multi-path solution where the power is split and sent through different paths. Evidently, from Table 5.1, the total energy transmission loss of multi-path routing is better than single-path routing. The same paths are chosen by both the non-linear programming and the suggested routing algorithms. However, calculating the power loss during the energy transmission using Algorithm 5.2 by the

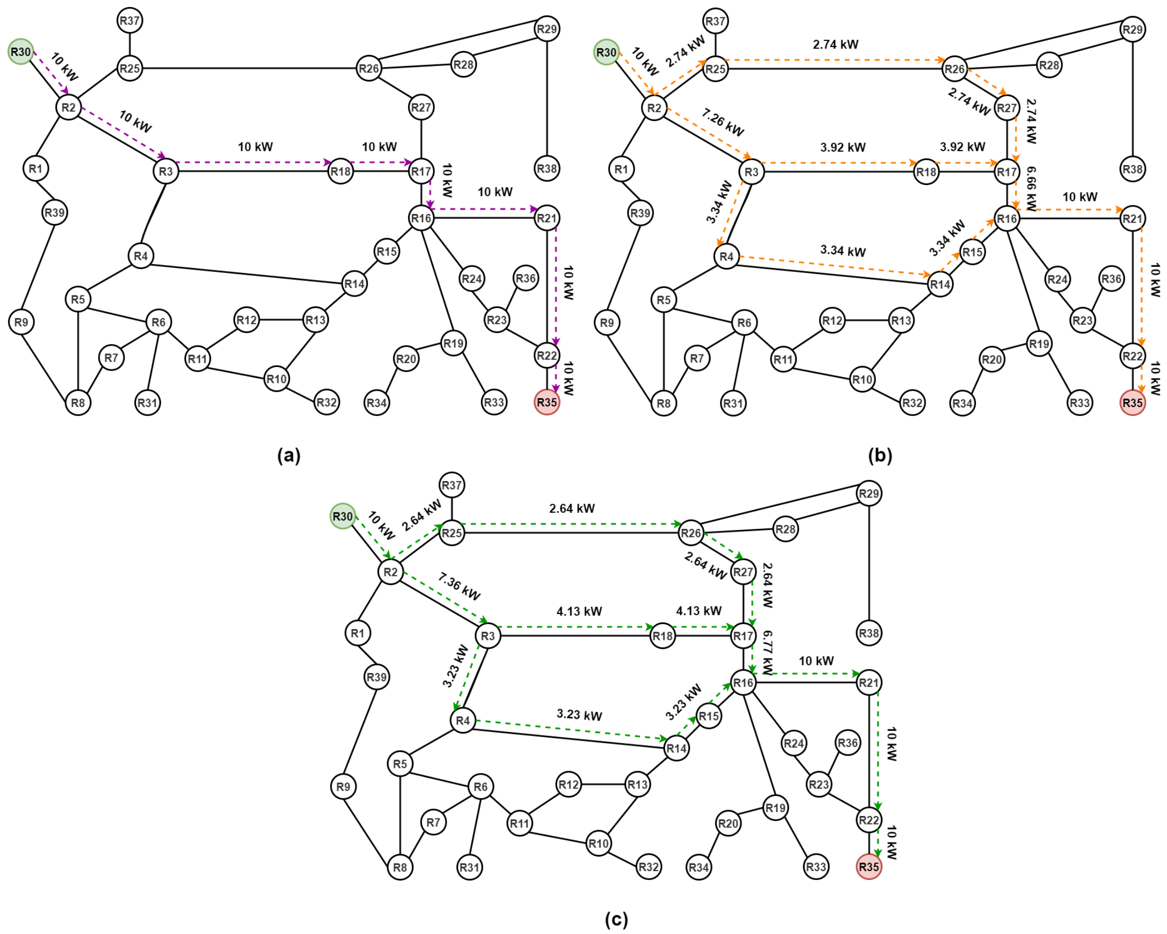

FIGURE 5.7: The least loss paths selected by (a) Exhaustive search, Dijkstra and DFS algorithms, (b) non-linear programming, and (c) the proposed energy routing algorithm for the trading pair in Figure 3.6.

proposed semi-decentralized multipath energy routing algorithm produces a different power distribution across these chosen paths (see Figures 5.6 and 5.7). This led to a reduction in the total transmission loss of the proposed algorithm by 24.15%, 10.34%, 17.77% in Figures 5.5, 5.6, and 5.7, respectively, when compared to the single-path solutions found by the exhaustive search, Dijkstra, and DFS algorithms. Additionally, it provides better energy transmission loss by 8.56%, 8.13%, and 11.15% in Figures 5.5, 5.6, and 5.7, respectively, when compared to the solution provided by non-linear programming in [3].

In the majority of the proposed P2PET systems, energy transmission loss is often compensated by the utility grid and paid by prosumers (energy trading pairs) [126, 142, 143]. Assuming that the utility grid charges each trading pair a 0.25 \$ for 1 kW power loss. The compensation fees for the trading pair ($ER_9 - ER_2$) depicted in Figure 3.2 is 0.43 \$ when using DFS, Dijkstra, or exhaustive search, drops to 0.36 \$ when nonlinear programming is used. However, applying the suggested energy routing algorithm with the accurate power loss for path generation further decreases

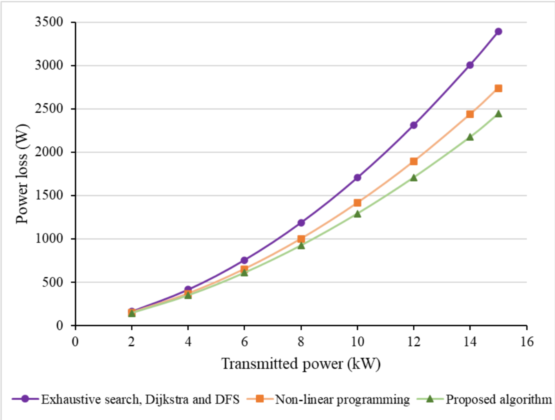

(A) Trading pair ($ER_2 - ER_9$) in Figure 3.2

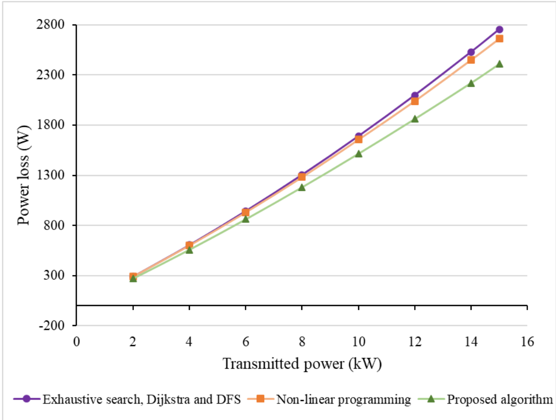

(B) Trading pair ($ER_{14} - ER_{29}$) in Figure 3.5

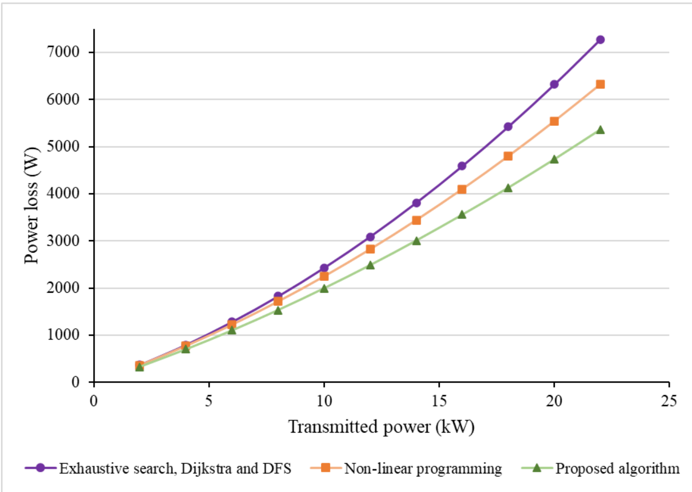

(C) Trading pair ($ER_{30} - ER_{35}$) in Figure 3.6

FIGURE 5.8: Energy transmission loss comparison of the proposed optimised algorithm with Exhaustive search, Dijkstra, DFS, and Non-linear programming concerning transmitted power in different EI networks.

the compensation fees to 0.32 \$, thereby offering the most cost-effective paths. This guarantees that prosumers are not saddled with costs that exceed their actual loss. Additionally, providing accurate energy transmission loss prevents the utility grid from injecting more energy into the grid than is necessary to compensate for losses. This reduces needless power circulation, relieving pressure on the grid infrastructure and lowering the possibility of increasing inefficiencies and costs for all parties concerned.

Figure 5.8 represents the total energy transmission losses resulting from transmitting different amounts of power between the trading pairs in the different networks. According to this figure, the suggested semi-decentralized multi-path energy routing algorithm clearly outperforms the previously mentioned algorithms in terms of power transmission loss minimization.

The trading power in P2PET systems is distributed through the grid's distribution lines; however, there is always some degree of demand on the grid, which is transferred over grid lines, implying that the pre-existing power on certain power lines is different from zero. Therefore to demonstrate the effectiveness of the proposed semi-decentralized multipath routing algorithm in such situations, we consider the following scenarios:

5.4.1.1 Network congestion case

In the first scenario, taking the same trading transactions in the previous simulation case $\{(ER_2, ER_9), 10kW\}$ in Figure 3.2, $\{(ER_{14}, ER_{29}), 10kW\}$ in Figure 3.5, and $\{(ER_{30}, ER_{35}), 10kW\}$ in Figure 3.6. Starting with the first trading pair, presuming the existence of a power flow of 12 kW transmitting through the path $4 \rightarrow 5 \rightarrow 6$ in the network in Figure 3.2. The selection of these power lines to transmit the 10 kW can create congestion in the grid. This power flow increases the power losses of the power lines L_{4-5} and L_{5-6} pushing Dijkstra and DFS algorithms to choose another single path to transmit the 10 kW between ER_2 and ER_9 as illustrated in Figure 5.9. It also decreases the capacity of the path $4 \rightarrow 5 \rightarrow 6$, as the new capacities of ER_5 (3 kW), ER_6(6 kW), and L_{5-6} (8 kW) can not carry the 10 kW, the exhaustive search algorithm prunes ER_5, ER_6, and L_{5-6} from the graph network which limits the number of possible paths to only one single-path ($2 \rightarrow 3 \rightarrow 7 \rightarrow 8 \rightarrow 9$) that is the same path found by Dijkstra and DFS algorithms. By contrast, as shown in Figure 5.9 and Table 5.2, the proposed multi-path energy routing algorithm proposes a better use of low-capacity paths. It splits the transmitted power into three power packets of 5.627 kW, 1.373 kW, and 3 kW. It distributes these packets through three different paths $2 \rightarrow 3 \rightarrow 7 \rightarrow 8 \rightarrow 9$, $2 \rightarrow 3 \rightarrow 7 \rightarrow 6 \rightarrow 8 \rightarrow 9$, and $2 \rightarrow 5 \rightarrow 6 \rightarrow 8 \rightarrow 9$ without violating the maximum capacities of the power lines and ERs in each selected path. This routing algorithm prevents efficiently congestion and produces a total transmission loss of 1.602 kW, which saves 23.49% more energy than single-path transmission by exhaustive search, Dijkstra and DFS algorithms and saves 10.25% more energy than non-linear programming with DFS in [3].

For the second trading pair $\{(ER_{14}, ER_{29}), 10kW\}$ in Figure 3.5, an existing power of 16 kW decreases the capacity of the power line L_{4-5} to 9 kW which will incur congestion if the 10 kW power is routed through this line. In this case, the exhaustive search algorithm pruned this power line from the graph and found a new optimal single path. Dijkstra and DFS are single-path algorithms, however, authors in [120, 121] and [2] suggest using a power packet mode when the capacity of the optimal single path selected by DFS or Dijkstra algorithms is insufficient to transmit the total power,

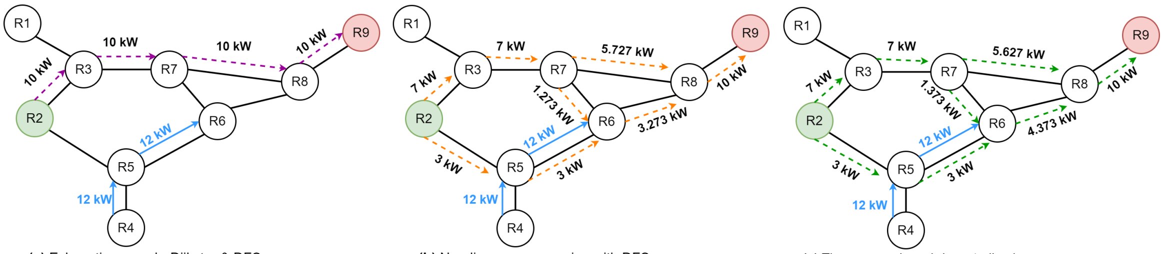

(a) Exhaustive search, Dijkstra & DFS **(b)** Non-linear programming with DFS **(c)** The proposed semi-decentralized multi-path algorithm

FIGURE 5.9: The selected least loss paths for trading pair (ER_2, ER_9) in network congestion case.

TABLE 5.2: The total energy transmission loss of exhaustive search, Dijkstra, DFS, non-linear programming algorithms and the proposed algorithm for the network congestion case.

		EI Network		
		Figure 3.2 with 12 kW in *4 → 5 → 6*	Figure 3.5 with 16 kW in *3 → 4 → 6*	Figure 3.6 with 4 kW in *3 → 18 → 17*
Single-path routing	Exhaustive search (kW) [1]	2.094	1.955	2.550
	Dijkstra (kW) [120, 121]	2.094	1.685	2.550
	DFS (kW) [2]	2.094	1.685	2.550
Multi-path routing	Non-linear programming with DFS(kW) [3]	1.785	1.672	2.322
	Proposed Algorithm (kW)	1.602	1.530	2.055

where the path available capacity is allocated to carry a portion of the power (in this case 9 kw) and new paths are allocated for the remaining power (for the 1 kW see Figure 5.10). In contrast, the proposed algorithm not only determines a set of paths to be used based on their capacities but also creates the best power dispatch through these paths so the total energy transmission loss is minimized, as demonstrated by the findings in Table 5.2 a 21.73% energy is saved compared to the single path solution by exhaustive search, while 9.2% and 8.5% energy saving compared to the energy packet mode used by Dijkstra, DFS, and non-linear programming, respectively.

To create a congestion case in Figure 3.6, first the capacity of the power line L_{3-18} is diminished to 10 kW, where 4 kW from it is used to transmit a 4 kW of power through the path *3 → 18 → 17*. This power flow increases the power loss of the power lines L_{17-18} and L_{3-18}, and as the remaining capacity of the later power line (6 kW) can not be used to transmit 10 kW, exhaustive search, Dijkstra and DFS routing algorithms selects a new single path to transmit the 10 kW from ER_{30} to ER_{31}. While the multipath solution provided by the proposed algorithm and the non-linear programming with DFS keep the same selected paths in the previous case (Figure 5.7) with a decrease in the power transmitted through the lines L_{17-18} and L_{3-18} with a better power distribution by the proposed semi-decentralized multipath algorithm which leads to lower total transmission loss by 19.5% and 11.5% compared to single path and non-linear solutions, respectively, as shown in Figure 5.11 and

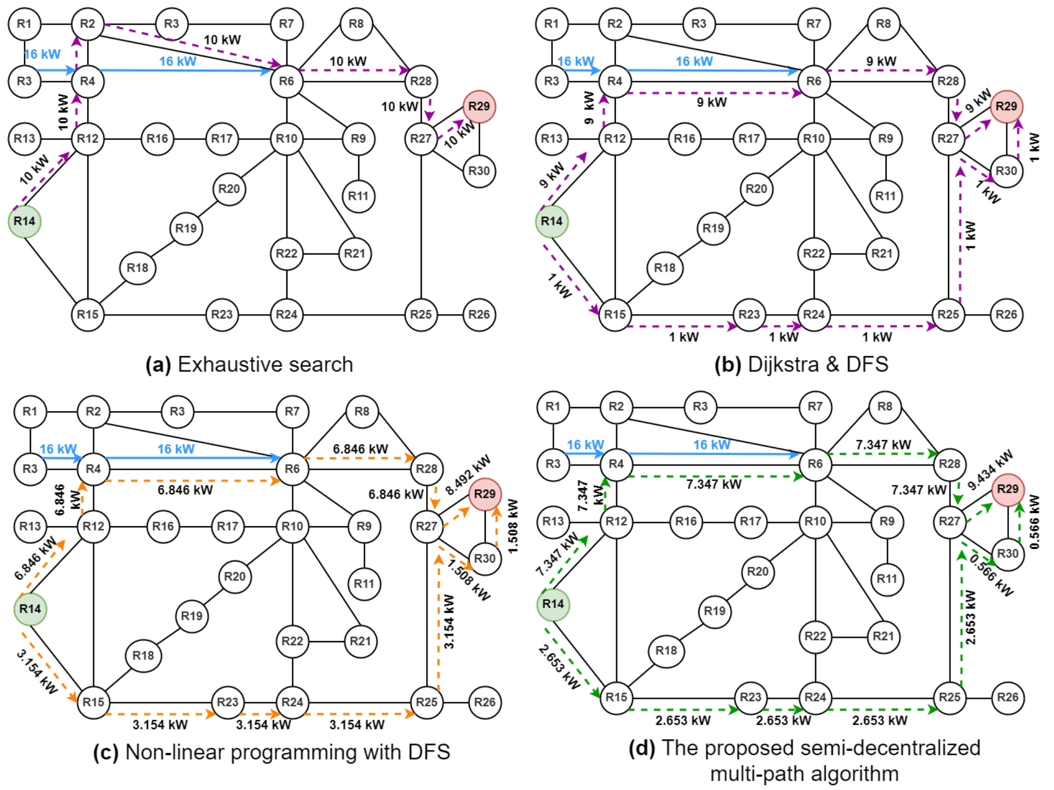

FIGURE 5.10: The selected least loss paths for trading pair (ER_{14}, ER_{19}) in network congestion case.

Table 5.2.

5.4.1.2 Power Flow Direction conflict case

To verify the efficiency of the proposed semi-decentralized multi-path energy routing algorithm in handling the PFD constraint, the same energy networks and trading pairs used in the previous scenarios are employed in this simulation case. However, the direction of the pre-existing power flow is reversed. Precisely, it is assumed that a 5 kW power flow is transmitted from ER_6 to ER_4 through the path $6 \rightarrow 5 \rightarrow 4$ in the network 3.2. Likewise, the same power amount is transmitted in the network 3.5 from ER_6 to ER_3 through the path $6 \rightarrow 4 \rightarrow 3$, while a 2 kW is transmitted in the network 3.6 from ER_{27} to ER_4 through the path $27 \rightarrow 17 \rightarrow 18 \rightarrow 3 \rightarrow 4$. The simulation results, provided in Table 5.3 and Figures 5.12, 5.13, and 5.14.
Exhaustive search, Dijkstra, DFS, and non-linear programming energy routing algorithms attempt to identify paths with the least energy transmission loss while adhering to ERs and power lines capacity constraints. Taking the networks in Figures 5.12, 5.13, and 5.14, as the power lines with pre-existing power flow still have a minimum energy loss and enough capacity to be used, they can be selected by the different algorithms. This resulted in PFD conflict on the power lines L_{5-6} in Figure 5.12,

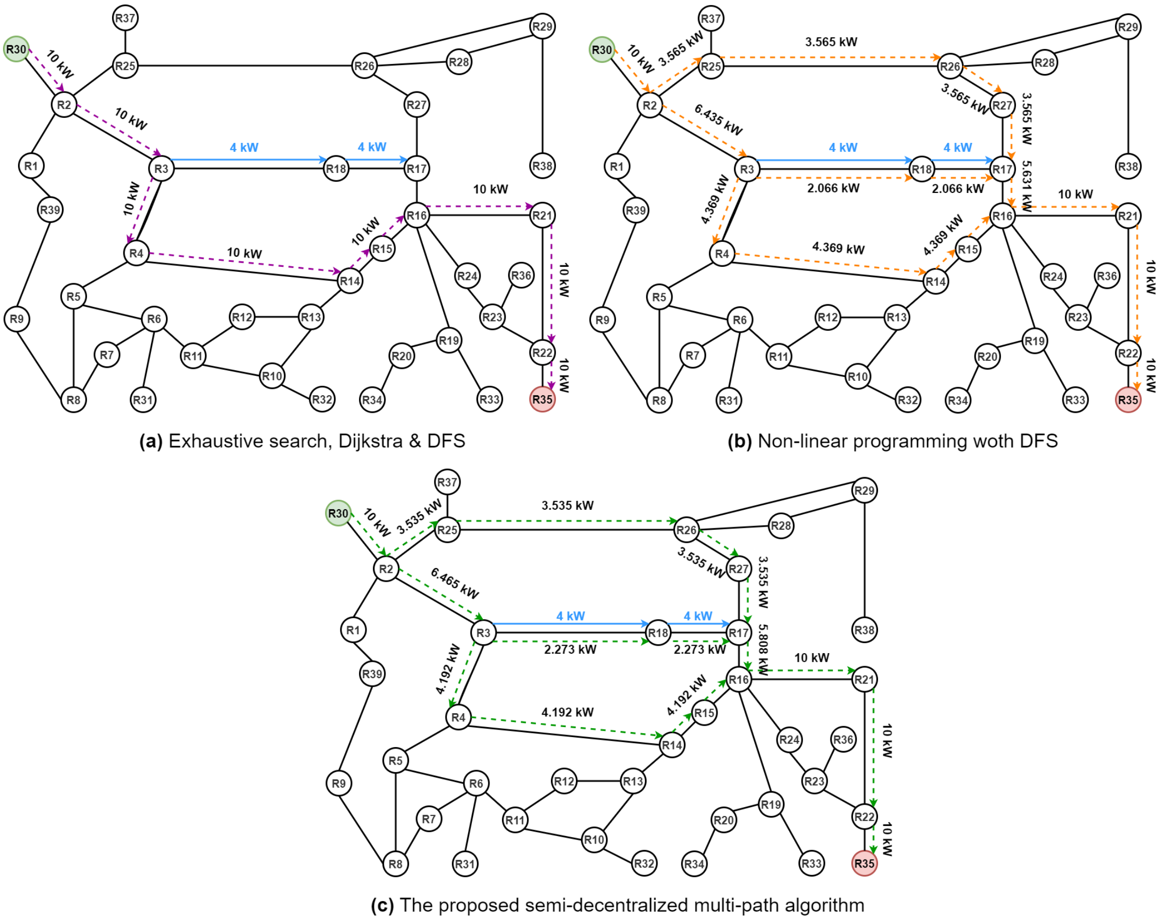

(a) Exhaustive search, Dijkstra & DFS

(b) Non-linear programming woth DFS

(c) The proposed semi-decentralized multi-path algorithm

FIGURE 5.11: The selected least loss paths for trading pair (ER_{30}, ER_{35}) in network congestion case.

TABLE 5.3: The total energy transmission loss of exhaustive search, Dijkstra, DFS, non-linear programming algorithms and the proposed algorithm for the PFD conflict case.

		EI Network		
		Figure 3.2 with 5 kW in *6 → 5 → 4*	Figure 3.5 with 5 kW in *6 → 4 → 3*	Figure 3.6 with 2 kW in *27 → 17 → 18 → 3 → 4*
Single-path routing	Exhaustive search (kW) [1]	PFDC	PFDC	PFDC
	Dijkstra (kW) [120, 121]	PFDC	PFDC	PFDC
	DFS (kW) [2]	PFDC	PFDC	PFDC
Multi-path routing	Non-linear programming with DFS(kW) [3]	PFDC	PFDC	PFDC
	Proposed Algorithm (kW)	1.807	1.642	2.094

L_{4-6} in Figure 5.13, L_{3-18} and L_{18-17} in Figure 5.14, as these power lines were selected by the different algorithms to transmit power in the reverse direction of their pre-existing power flow. The PFD conflict generates reverse power flow, which causes voltage fluctuations, overheating, and possible damage to these power lines resulting in an instability of the power grid. On the contrary, as shown in Figures 5.12, 5.13, and 5.14, the proposed semi-decentralized multi-path energy routing algorithm generates congestion-free energy least loss paths that avoid PFD constraint violation. The modified Dijkstra algorithm used in the path enumeration phase of the proposed

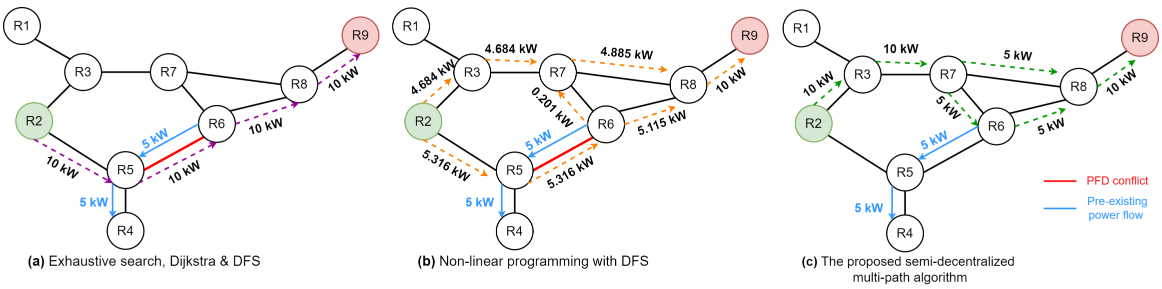

FIGURE 5.12: The selected least loss paths for trading pair (ER_2, ER_9) in PFD conflict case.

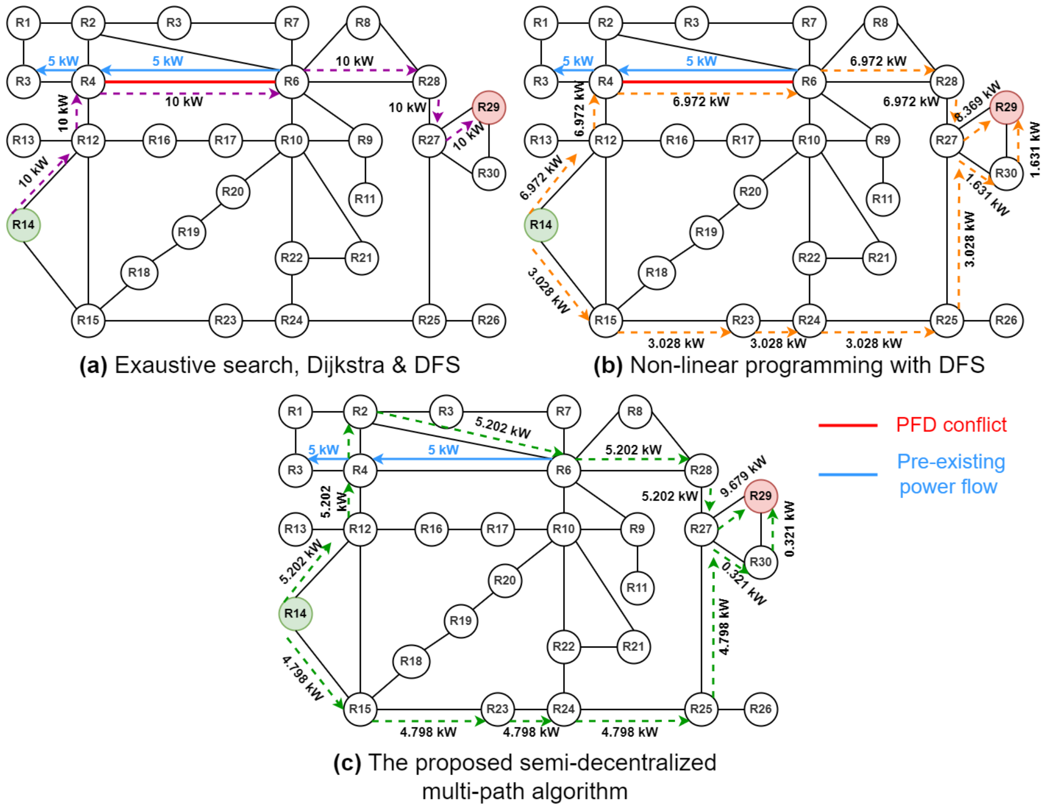

FIGURE 5.13: The selected least loss paths for trading pair (ER_{14}, ER_{29}) in PFD conflict case.

routing algorithm comprises a pruning mechanism. This mechanism entails abandoning the exploration of a power line if it transmits a reverse power flow to the search direction and considering it otherwise. Thus, taking Figure 5.13 as an illustration, when the search process starting from ER_{30} reaches ER_3, the power line L_{3-18} is pruned and ignored in path generation as it carries a pre-existing flow in the opposite direction to the search direction. On the other hand, as its pre-existing power flow aligns with the search direction, the power line L_{3-4} is taken into account for path generation. Furthermore, the consideration of the PFD constraint (Equation (5.1)) by the multi-start SQP prevents the PFD conflict when the self-path overlaps occur ensuring a more efficient and reliable energy routing.

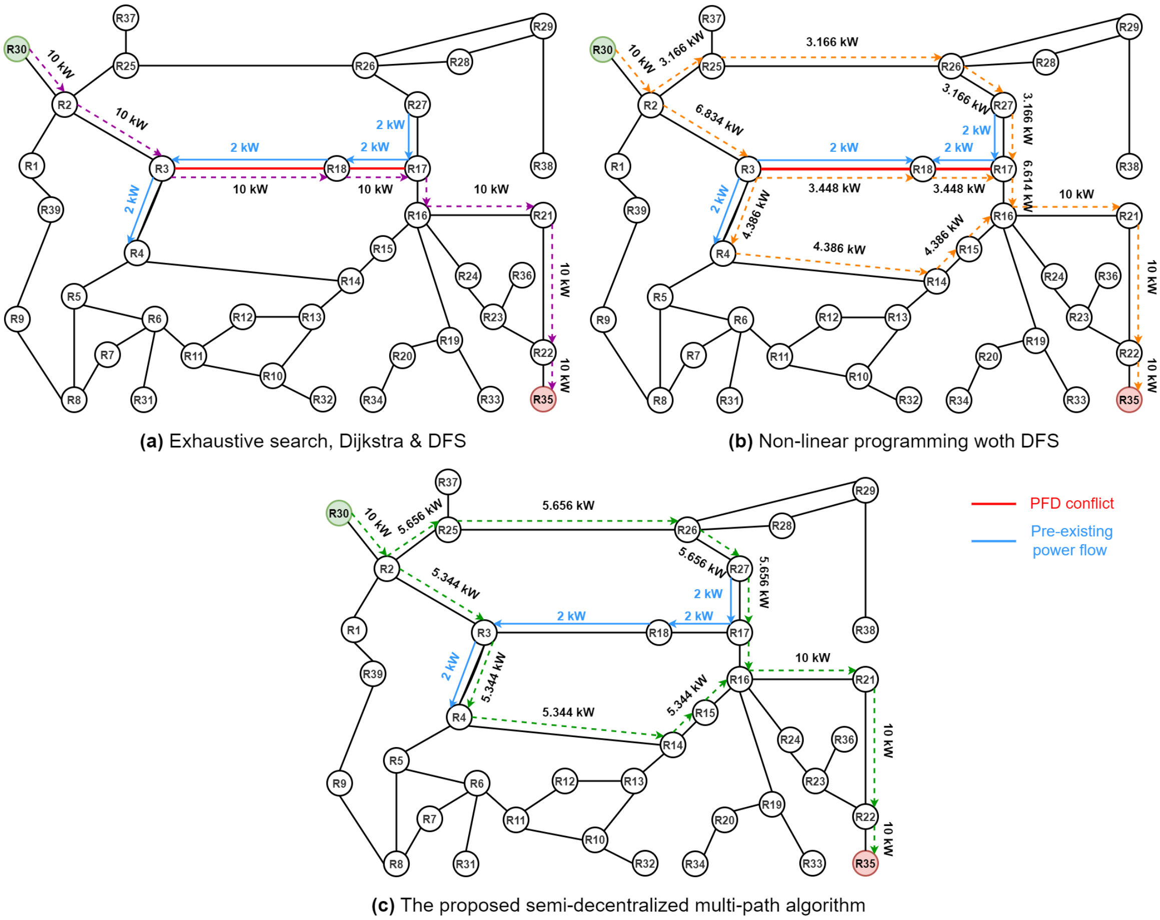

FIGURE 5.14: The selected least loss paths for trading pair (ER_{30}, ER_{35}) in PFD conflict case.

According to the provided results from the different networks and scenarios, the proposed semi-decentralized multi-path energy routing algorithm outperforms the cited routing algorithms by providing congestion-free least loss paths with accurate power loss while adhering to the grid physical constraints including the PFD constraint.

5.4.2 Multiple predetermined source-load pair

To demonstrate the efficiency of the proposed semi-decentralized multi-path energy routing algorithm in handling the PFD constraint and avoiding congestion problems in the existence of multiple source-load pairs, EI network in Figure 3.5 is used where the capacity of ER_{18} and power line L_{15-18} has increased to 25 kW. In this network, it is assumed that the following energy transactions are executed simultaneously $\{(ER_{12}, ER_3), 30kW\}$, $\{(ER_2, ER_{18}), 25kW\}$, $\{(ER_{13}, ER_6), 25kW\}$, $\{(ER_{30}, ER_{28}), 10kW\}$, and $\{(ER_{25}, ER_{23}), 10kW\}$. Figures 5.15, 5.16, and 5.17 depict the selected paths by each trading pair using the proposed energy routing algorithm, non-linear programming-based multi-path routing algorithm [3], exhaustive

search [1], Dijkstra algorithm [120, 121], and the DFS algorithm in [2].
The exhaustive search and Dijkstra-based energy routing algorithms are fully decentralized, where each trading pair selects a transmission path without considering the path selection of other pairs in the system. As shown in Figure 5.15, the selected paths of trading pairs (ER_{12}, ER_3), (ER_2, ER_{18}), and (ER_{13}, ER_6) overlaps at power line $L_{4,12}$.The total transmitted power over this line is 80 kW, which exceeds its maximum capacity of 65 kW, resulting in congestion. Furthermore, this line is utilized in two opposing ways from ER_{12} to ER_4 to send 55 kW, and in the other direction to transmit 25 kW, violating the PFD constraint. Consequently, these two energy routing algorithms were unable to produce practical solutions that avoided congestion and PFD conflicts in the present scenario.

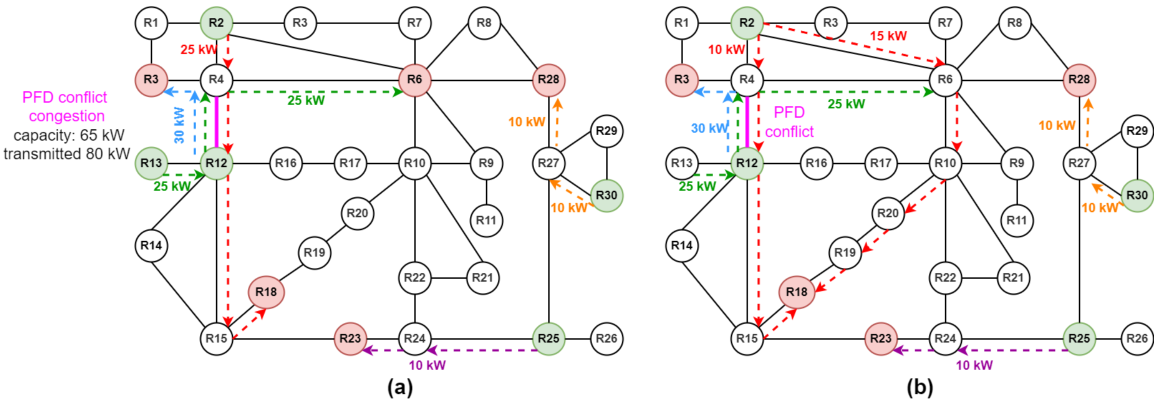

FIGURE 5.15: The selected least loss paths for the multiple source load trading pairs using (a) exhaustive search and Dijkstra, (b) DFS-based energy routing algorithms.

The proposed energy routing protocol in [2], is a centralized protocol where a central unit is responsible for determining the trading pairs and the transmission paths to use for all network prosumers. The protocol determines the best prosumers matching schedule with the minimum transmission loss. To compare its performance with the proposed algorithm, we presumed that the pairs already exist. The protocol is used to determine the path allocation schedule of the five trading pairs so the total power transmission loss is minimized. As depicted in Figure 5.15, this protocol avoids line congestion by relieving the overload on the line $L_{4,12}$ where transmitted power between the trading pair is split in two power packets of 10 kW and 15 kW and transmitted through the paths *2 → 4 → 12 → 16 → 18* and *2 → 6 → 10 → 20 → 19 → 18*, respectively. However, the power line $L_{4,12}$ is still used in opposite directions simultaneously leading to PFD conflict. It has a considerable execution time that highly increases with the increasing number of trading pairs.
Similarly, as shown in Figure 5.16, the proposed algorithm in [3] is divided into two parts, in the first part trading pairs use the non-linear programming routing to select their paths in a decentralized way which creates a PFD conflict and congestion on line

L_{4-12}. To resolve this congestion problem, a coalition cooperative game is executed at the network central unit between the pairs whose paths have overlapped (ER_{12}, ER_3), (ER_2, ER_{18}), and (ER_{13}, ER_6). The objective of the collision is the minimization of the total transmission loss. The new paths for the trading pairs avoid line congestion but create a PFD conflict in power lines L_{4-12} and L_{6-10}.

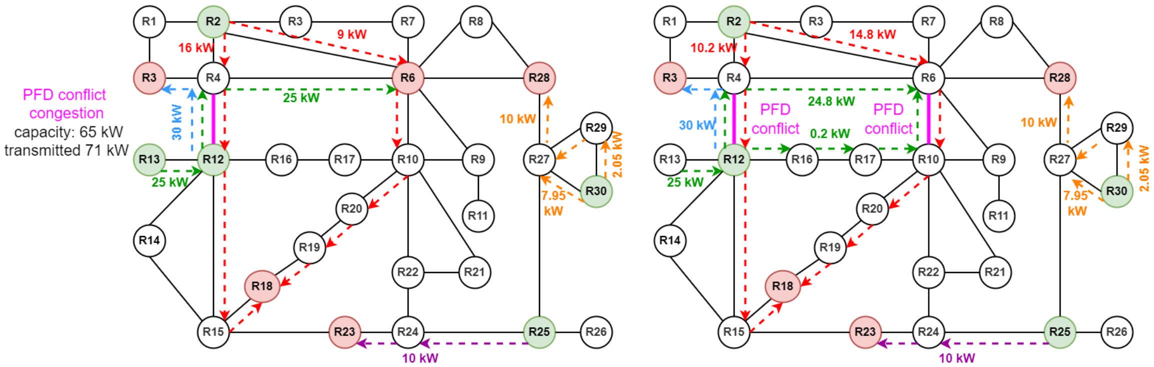

(a) Nonlinear programming & DFS routing **(b)** Cooperative routing

FIGURE 5.16: The selected least loss paths for the multiple source load trading pairs using non-linear programming.

On the contrary, as shown in Figure 5.17, in the proposed semi-decentralized multi-path energy routing protocol, each trading pair invokes the local path discovery phase independently where the modified Yen's k least loss paths and multi-start SQP algorithms are used to determine the energy least loss paths that adhere to the PFD constraint and avoid network congestion without considering the path selection of other pairs. The results of the local path discovery phase for each trading pair are submitted to the NSO for congestion and PFD conflict check. As the selected paths by (ER_{12}, ER_3), (ER_2, ER_{18}), and (ER_{13}, ER_6) overlap in power line L_{4-12}, the NSO invokes the global path conflict resolution phase. First, for the pairs with no overlapping paths (ER_{30}, ER_{28}) and (ER_{25}, ER_{23}), the NSO creates a path confirmation. Then for the trading pairs with overlapping paths (ER_{12}, ER_3), (ER_2, ER_{18}), and (ER_{13}, ER_6), as each trading pair has a priority, the NSO gives the overlapping path to the pair with the highest priority assuming that that is (ER_{13}, ER_6) and decreases its priority. It determines new transmission paths for the remaining pairs (ER_{12}, ER_3), (ER_2, ER_{18}) using the same algorithm where the objective is to minimize the total transmission loss while respecting the physical characteristics of the network including PFD constraint. The total power loss is shared between these trading pairs according to the Equation (5.13). According to Figure 5.17 (b), the transmitted power in line L_{4-12} decreased from 74.3 kW to 55 kW, and new paths are allocated for trading pair (ER_2, ER_{18}), which successfully eradicated the congestion and PFD conflict.

It is important to mention that re-planning new paths for all trading pairs with path conflicts and ignoring pair decisions as in [3], may reduce the willingness of some trading pairs to engage in energy trading. Conversely, using the priority principle (ranking) will give one of these pairs its path choice, and reducing this priority gives the remaining pairs that did not take their desired paths a high possibility of taking them in the next trading period.

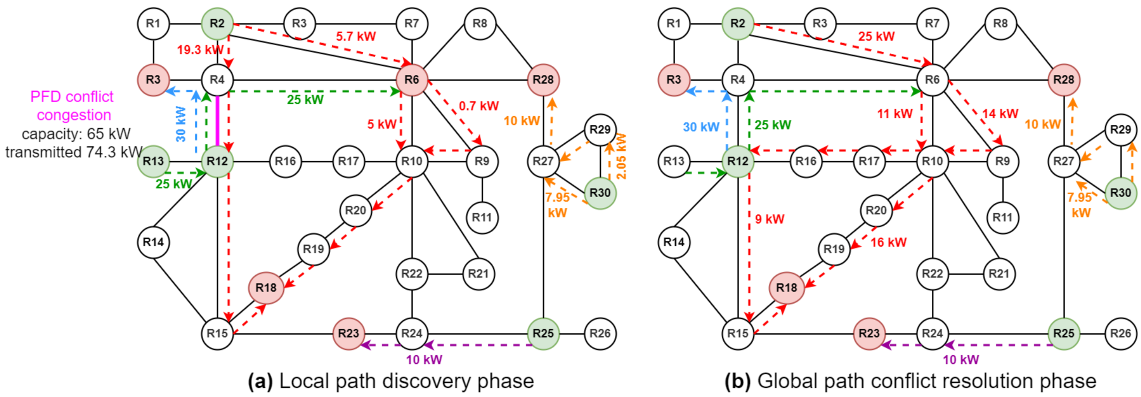

FIGURE 5.17: The selected least loss paths for the multiple source load trading pairs using the proposed semi-decentralized multi-path energy routing algorithm.

Table 5.4, displays the execution time of the different algorithms. The proposed energy routing algorithm and the non-linear programming algorithm in [3] have a decentralized part that is executed in parallel by the individual trading pairs. Thus, the maximum computational time of the five trading pairs—that is, the time provided by trading pair (ER_2, ER_{18})—determines the computing time of the decentralized routing part. The use of DFS in the path enumeration phase to determine all the possible paths between a trading pair in algorithm [3], increases the search space for the non-linear programming phase especially in complex and huge networks which reflects on the execution time. In contrast, determining the most promising paths instead of all paths using the suggested Yens least loss path algorithm decreases the search space for the multi-start SQP algorithm. According to the results in Table 5.4, the execution time taken by the local path discovery and global path conflict resolution phases of the proposed semi-decentralized multi-path algorithm is reduced by 45.61% and 82.23% compared to the algorithms in [3] and the centralized one in [2].

The proposed algorithm outperforms the previous algorithms and effectively avoids congestion and PFD conflict problems.

Table 5.4: A comparison of computational time between the proposed semi-decentralized algorithm, the semi-decentralized algorithm in [3] and the centralized algorithm in [2]

Algorithm	Decentralized part	Centralized part	Total computational time
Proposed semi-decentralized	9.52	43.94	53.46
Semi-decentralized in [3]	28.30	70	98.30
Centralized in [2]	-	-	301

5.5 Conclusion

The energy routing problem is formulated as a non-convex non-linear optimization problem. To solve this problem, a semi-decentralized multi-path energy routing protocol is proposed in this chapter, where a modified Yen's k least loss path and multi-start SQP algorithms are suggested for path enumeration and power dispatch. The proposed algorithm computes power losses accurately during path selection while respecting all the physical power system constraints, including the PFD constraint. Providing accurate power loss benefits both trading pairs and the utility grid. The semi-decentralized algorithm lies between the advantages of fully centralized energy routing algorithms and the fully decentralized one; it keeps some central coordination through the use of the NSO, however, most energy transmission path decisions are taken locally by the individual trading pairs. This relieves the computational burden on the NSO. The multi-path provided solutions, decreased the transmission losses, improved the utilisation of the grid power lines and contributed to the alleviation of line congestion. The deployment of the NSO keeps the P2PET under control and solves the path conflict issues during the simultaneous power transmission cases. It uses a ranking principle that allows some trading pairs to take the desired paths in path-conflict situations. Simulation findings from various scenarios using different EI networks confirmed the suggested energy routing algorithm's efficacy. These findings emphasize the proposed algorithm's multiple advantages, indicating that it is a potential option for routing energy in the developing P2PET in EI. Table 5.5 summarizes the key differences between the proposed semi-decentralized multi-path energy routing algorithm and other algorithms described in the literature.

TABLE 5.5: The key differences between the proposed semi-decentralized multi-path energy routing algorithm and other algorithms described in the literature.

Criteria	**Algorithm**				
	Exhaustive search [1]	**Dijkstra** [120, 121]	**DFS** [2]	**Non-linear programming** [3]	**The proposed**
Fully centralized			✓		
Fully decentralized	✓	✓			
Semi-decentralized				✓	✓
Grid physical constraints	✓	✓	✓	✓	✓
PFD constraint					✓
Accurate power losses					✓
Simultaneous energy transmission			✓	✓	✓

Chapter 6

Prosumers matching and energy routing through Yens and SOS algorithms in P2PET systems

This chapter focuses on solving the energy routing problem, including subscriber matching, energy-efficient paths, and transmission scheduling. The energy routing problem is formulated as a non-convex mixed-integer non-linear optimization problem that minimizes the consumer's energy cost. The energy cost comprises both the energy purchasing and transmission costs. The transmission cost incorporates the exogenous costs (power loss compensation fees and grid infrastructure utilisation fees) imposed by the utility grid. The objective function combines the matching process and the non-congestion energy-efficient path selection process. To solve this problem in polynomial time, a semi-decentralized energy routing approach that incorporates graph theory and metaheuristics is given. Firstly, Yen's k least loss paths algorithm (detailed in Chapter 5) is used to determine a set of possible paths to each possible producer in the network. Secondly, the Symbiotic Organisms Search algorithm (SOS) is employed to determine the best producers that minimize the energy cost for each consumer, the amount of power to get from each producer, and the least energy transmission cost paths between the energy trading pair while respecting the market and physical constraints of the grid, including the PFD constraint. The NSO is a fundamental component of the proposed approach for solving path and source conflicts in simultaneous energy transmission cases. The simulation results demonstrate the effectiveness of the suggested semi-decentralized energy routing approach in solving the energy routing issues.

6.1 Introduction

The effective transmission of power between trading peers in P2PET over the complicated EI is significantly dependent on the deployment of an efficient energy routing algorithm. Energy routing algorithms have three major challenges: subscriber matching, finding an efficient path, and transmission scheduling. As detailed in Chapter 2, most of the referenced literature split the subscriber matching from the energy routing problem. Very few articles included subscriber matching in the energy routing algorithms. Remarkably, subscriber matching was mostly investigated in articles suggesting market-clearing techniques, trading algorithms, and P2PET platforms, where energy trading peers are matched based on their monetary benefits; however, losses caused by the matched transactions are avoided without adequate technical justifications. Attempting to maximize the prosumers' profits at the expense of energy routing and power transmission losses might lead to network congestion and voltage fluctuations by providing power flows that violate grid physical constraints, jeopardizing the system's ability to operate safely. Therefore, recently, the newly proposed P2PET systems have included power losses in the prosumers matching process [126, 145–148]. However, the electrical transmission power losses are calculated using the electrical distance, which is estimated by Thevenin's impedance distance [146], power transfer distance [147], and a distance factor [126, 145]. Using electrical distance to estimate the transmission power losses between trading pairs is not appropriate and not applicable in EI, as the power transmission losses in EI have a direct relation to the power lines losses and ERs losses (detailed in Chapter 3).

Additionally, according to the most often proposed P2PET systems in the literature, P2PET is not completely independent of the grid. It is carried out via the utility grid's distribution infrastructure, which transfers power via grid distribution lines. In these P2PET systems, the utility grid charges the trading pairs network utilisation fees for the use of its power lines [126, 145, 147], and power loss compensation fees to compensate for transmission power losses between trading pairs [126, 127], ensuring the receiving of completely traded power. Furthermore, according to the works in [146, 149, 150] congestion costs are also imposed by the utility grid to the trading pairs to prevent congestion on the grid's power lines. The utility grid uses these exogenous costs to cover the operation and maintenance expenditures [150]. These exogenous costs increase the total energy cost for trading prosumers, which can push them to cancel their energy transactions to avoid paying high fees. As a result, it is critical to build a subscriber-matching process that considers these exogenous costs, allowing consumers to reduce these fees through careful supplier

On the other hand, the few energy-routing algorithms that incorporate subscriber matching perform the matching often by focusing on either price [135] or power loss [2, 133], which increases the transmission losses in the first case and trading prices in the second one. However, combining the transmission power losses and the power prices in the same objective function provides a better solution for energy routing that optimizes both, as demonstrated in Chapter 4. Furthermore, ignoring the P2P market factors (prosumers prices, power loss compensation fees, network utilisation fees, etc) in the matching process in the previously mentioned energy routing protocols [2, 133, 135] makes them unsuitable for real application. Additionally, determining the energy-efficient transmission paths based only on their energy losses is insufficient in the existence of the network utilisation and power compensation fees. These fees need to be considered during the path generation process and the paths should be selected based on their total transmission cost.

Drawing from the discussions presented earlier in this section and to overcome the shortcomings encountered in previous energy routing algorithms for P2PET in EI, the work in this chapter aims to solve the energy routing problem, including its three main issues, by providing a new energy routing approach that compromises the matching of prosumers with the selection of free-congestion energy least cost paths. The contributions of this chapter encompass:

- Introducing a novel P2PET framework in EI
- Formulating the energy routing problem as a constrained non-convex non-linear mixed integer optimization problem to optimize the total energy cost that combines the purchasing cost and energy transmission paths cost.
- Developing a novel semi-decentralized energy routing approach that uses graph theory and metaheuristic methods to match the prosumers and select the free-congestion least cost paths to solve the constrained non-convex mixed integer non-linear optimization problem.
- Introducing a novel Symbiotic Organism Search-based multi-path energy routing algorithm that determines for each consumer the best set of producers with the amount of power to get from each one, the least cost paths to transmit the traded power, and the amount of power to send in each path while considering the purchasing power prices of producer-prosumers, the accurate power losses of the network's power lines and ERs, the network utilisation fees, the power loss compensation fees, network capacity and PFD constraints.

6.2 The proposed P2PET framework and problem formulation

6.2.1 The proposed P2PET framework

As detailed in Chapter 3, the EI is a mesh network that connects prosumers (with excess or shortage energy), consumers (loads without RESs) and traditional generation units with the DESs (owned by utility grid) by power lines and ERs. Prosumers and consumers can engage in P2PET, where the utility grid acts as a backup market participant. To encourage prosumers and consumers to actively engage in the P2PET market and promote direct energy exchange while improving system efficiency, resilience, and safety, we present a novel P2PET framework. The suggested framework and its fundamental assumptions are described as follows:

- The proposed framework comprises a NSO, which acts as an impartial observer to ensure grid stability during P2PET without compromising the trading peers' autonomy. The NSO does not intervene in trading peers' matching decisions or energy transactions' establishment. In contrast, it provides in advance the network charges, including network utilisation fees and power loss compensation fees alongside the utility grid selling and buying prices, verifies source and path overlaps in situations of simultaneous power transmissions, and grants approval to trading pairs or implements network conflict management mechanisms as required. Before executing the P2P energy transactions, all the energy trading pairs must receive approval from the NSO. This proactive technique reduces the possibility of power line overloading congestion and supply-demand imbalances in the network.

- At a time slot T, a prosumer can act as a producer or a consumer based on its local energy generation but cannot do both at the same time. Therefore, the market participants in this model are divided into three categories: consumers, who are traditional loads without RESs or prosumers who have a shortage in their local energy generation; producers, who are prosumers with excess local power generation, and the utility grid.

- We presume the existence of a P2PET communication platform. Through their associated ERs, producers and consumers use this platform to make offers—offering extra energy—or demands—requesting energy—with information including the power amount, price, and preferred time slots. Additionally, the network ERs use this platform to submit their current state, including capacity, conversion efficiency, and information on linked ERs and power lines. This information exchange enables all ERs to get an overview of the network structure and current state, promoting effective energy trading operations and well-informed decision-making.

- In addition to their power losses, PFD and capacity constraints, each power line in the network has a utilisation cost UC_l, which is proportional to the amount of power being transported through it [126]. Equation 6.1 depicts the line utilisation cost of transmitting an amount of power P through a power line (L_{ij}) that connects ERs i and j, where $C_{L_{(i,j)}}$ is the unit price for using the line L_{ij}.

$$UC_{L_{(i,j)}} = P \times C_{L_{(i,j)}} \tag{6.1}$$

- The proposed P2PET framework requires energy trading pairs, whether producers or consumers, to pay network utilisation fees for using the utility grid's infrastructure to send and receive energy. Each energy trading pair can use single or multiple energy transmission paths to transmit the purchased energy and should pay their utilisation fees. The utilisation fees of a path are the summation of the utilisation costs of the lines that construct the path. Equation 6.2 represents the network utilisation fees for a trading pair.

$$NUF = \sum_{k=1}^{Np} \sum_{L_{(i,j)} \in p_k} UC_{L_{(i,j)}} \tag{6.2}$$

It is significant to highlight that these network utilisation fees are not paid twice by both trading parties (producer and consumer) at the same time, but they are shared equally between them.

- The power losses in the network lines and ERs are inevitable during the power transmission process in P2PET in EI. These losses need to be compensated to ensure the reception of the agreed amount of trading power by the consumer. We presume that the utility grid compensates for these losses by injecting extra power into the network to cover them, which incurs extra costs charged to the trading pairs. Energy trading pairs are required to pay power loss compensation fees to the utility grid, which are proportional to the power losses incurred by their energy trading transactions. Equation 6.3, depicts the power loss compensation fees charged to an energy trading pair $(s - l)$, where π_c^G is the compensation price of the utility grid and $TL_{Total}^{s \to l}$ is the total transmission loss of the selected paths.

$$PLCF = \pi_c^G \times TL_{Total}^{s \to l} \tag{6.3}$$

A prosumer with excess local energy generation at time slot T that behaves as a producer can encounter a shortfall in its local energy generation in the next time slot T+1 and transform into a consumer. Similarly, the consumer at time slot T may turn into a producer in the next time slot T+1. Based on this role transition, producers are considered beneficiaries of P2PET as they are selling their excess energy to other consumers in the P2PET market at their established pricing instead of selling it to the utility grid at cheaper rates specified by the utility grid (price negotiating mechanisms are not considered in this work). Consumers assume responsibility for the matching process by choosing the producers from which they will buy energy, the amount of power to get from each one, and the transmission paths to take. As a result, consumers are responsible for covering the power loss compensation fees.

- The proposed P2PET market is a forward market, in which energy transactions for the next time interval T+1 are determined in time slot T called the matching window. During the matching window, producers and consumers submit bids and make routing decisions under the supervision of an NSO. After the market window closes, the physical transfer of energy and financial transactions occurs in time slot T+1, detailed in the section 6.2.2.

- The utility grid is considered a participant in the proposed framework, where producers can trade the surplus energy with other consumers in the P2PET system or with the utility grid, and consumers can purchase the energy demand from the producers in the P2PET or from the utility grid. This provides an advantage in cases where the power loss compensation fees and network utilisation fees are high, however in the majority of the cases the selling price of the utility grid is higher than the price of producers in the P2PET while the buying price of the utility grid is lower than producers prices in P2PET. To create a fairness situation between the participants (producers and consumers) of the P2PET and give all of them a chance to benefit from the P2PET market, after the submission of the total demand and offers, the communication platform calculates the total demand and energy surplus for the next time slot, T+1. If the entire energy surplus available exceeds the total demand in the P2PET market, all consumers can meet their needs through the P2PET network. However, in this case, some of the network producers may be able to sell all of their available power in the P2PET market, while others may be unable to find consumers and must sell it to the utility grid at a lower price (FiT) which may disincentive their engagement in the P2PET market. To address this problem, the proposed P2PET framework's communication platform sets a threshold for each producer that specifies the maximum quantity of power that can be sold in the P2PET network; any remaining power should be sold to the utility grid. Equation 6.4 outlines the threshold of a producer i, where P_{l_j} represents the energy demand of consumer j (load), P_{s_i} represents the energy available of producer i (energy source), n and m are the number of producers and consumers in the network, respectively.

$$Threshold_i = \frac{\sum_{j=1}^{m} P_{l_j}}{\sum_{i=1}^{n} P_{s_i}} \times P_{s_i} \tag{6.4}$$

On the other hand, if the total energy demand exceeds the entire availability, consumers must complete their energy demand from the utility grid. This can lead to a situation in which certain consumers buy all of their demand from the P2PET market while others buy it from the grid, discouraging their participation in the P2PET. Thus, in the suggested model, the communication platform sets a threshold, but this time for consumers to restrict the amount of power they may purchase from the P2PET market. The remaining demand for each consumer should be supplied from the utility grid. Equation 6.5 illustrates the threshold of a consumer j.

$$Threshold_j = \frac{\sum_{i=1}^{n} P_{s_i}}{\sum_{j=1}^{m} P_{l_j}} \times P_{l_j} \tag{6.5}$$

The use of the threshold incentivizes producers and consumers to actively participate in the P2PET market.

- Unlike previous P2PET systems proposed in the literature where consumers can engage in P2PET only with producers that can provide its total demand and select one of them while ignoring producers with small power availability, consumers in the proposed P2PET framework can buy energy from one or multiple producers in the network, even those that can not provide the whole demand. According to the work in [1], a consumer's matching decision involving fewer energy producers is recommended to reduce the complexity of the decision-making process and boost the reliability, security, and robustness of the system. Using fewer elements in energy routing can lower the risk of errors or threats [2]. Thus, it is anticipated that during each trade period T, the NSO can limit the maximum number of producers a consumer can choose. This number is referred to as N in the following sections.

- As demonstrated in Chapter 5, multi-path energy routing provides better utilization of the network infrastructure and minimises the total transmission loss. The multi-path energy routing is adopted in the proposed energy routing approach in this chapter. It is assumed that, according to the state of the network, the NSO can limit the number of paths used by each trading pair. This will reduce the computational burden and execution time of the routing decisions, decrease network utilization fees, prevent a single trading pair from monopolizing multiple paths, potentially creating bottlenecks and unfair network utilization, and minimize overlapping path conflicts and congestion issues. This number is referred to as M in the following sections.

6.2.2 Problem formulation

The proposed P2PET framework is a consumer-centric system where consumers should make their own energy routing decisions. The consumer energy routing decision includes the selected producers to buy energy from, the power amount to get from each producer and the non-congested minimum energy cost transmission paths to use. This routing decision should consider the network's physical constraints, including capacity and PFD constraints, and P2PET market constraints (economic constraints), including network utilisation fees, power loss compensation fees, the limited number of producers and paths constraints. Building upon the energy routing problem formulation introduced in chapters 3 and 5, we introduce an enhanced mathematical formulation of the problem that incorporates the additional constraints of the P2PET market. The energy routing problem is formulated as an optimization problem that aims to minimize the energy cost for consumers (Equation (6.6)).

$$f = \min\left(\sum_{i=1}^{n}(\pi_{s_i} \times P_{s_i} + TC_{s_i \to l}) + \pi_s^G \times (P_l - \sum_{i=1}^{n} P_{s_i})\right) \tag{6.6}$$

s.t. (3.4)

(3.6) − (3.12)

(5.2) − (5.8)

$$TC_{s_i \to l} = \sum_{k=1}^{N_p} CW_{Total}^{P_k : s_i \to l} \tag{6.7}$$

$$CW_{Total}^{P:s_i \to l} = \sum_{R_i \in p} (w_i \times \pi_c^G) + \sum_{L_{i,j} \in p} (w_{i,j} \times \pi_c^G + \alpha \times P_{s_i - l} \times C_{L_{(i,j)}}) \tag{6.8}$$

$$\sum_{i=1}^{n} P_{s_i} \leq P_l \tag{6.9}$$

$$0 \leq P_{s_i} \leq P_{s_i}^{max} \quad \forall s_i \in S \tag{6.10}$$

$$\sum_{i=1}^{n} y_i \leq N \tag{6.11}$$

$$y_i = \begin{cases} 1, & \text{if } P_{s_i} > 0, \\ 0, & \text{otherwise.} \end{cases} \tag{6.12}$$

$$\sum_{k=1}^{N_p} z_k \leq M \tag{6.13}$$

$$z_k = \begin{cases} 1, & \text{if } P_{s_i - l}^{k} > 0, \\ 0, & \text{otherwise.} \end{cases} \tag{6.14}$$

Consumers in the proposed P2PET system can purchase energy from one or several producers, even if individual producers are unable to provide all of the demand, from the utility grid, or both producers and the utility grid at the same time, to meet their energy needs. Therefore, as indicated by Equation (6.6), the total energy cost of buying energy for consumer l is divided into two parts: the first reflects the cost of purchasing from different producers in the P2PET system, while the second represents the cost of purchasing from the utility grid. The first cost is the summation of the paid price of buying energy from the selected producers and the energy transmission cost of the paths chosen to transmit power. Consumers pay power loss compensation fees, and as each power line has a utilisation cost, choosing energy transmission paths based on transmission cost is preferable to selecting paths based on energy losses (Equation (6.8)). This allows consumers to reduce the network's excessive prices. Energy can be transmitted through multiple paths between a trading pair consumer-producer (Equation (6.7)), where constraints (3.4), (3.6)-(3.12), (5.2)-(5.8), represent the power losses of ERs and power lines, their capacity constraints, PFD constraint, etc, as detailed in Chapters 3 and 5. The constraint in Equation (6.9) guarantees that the consumers' energy demand is not surpassed. Equation (6.10) assures that

Table 6.1: Variables description

Symbol	Description
π_{s_i}	The selling price of producer i in the P2PET system
π_s^G	The selling price of the utility grid.
π_c^G	The power loss compensation fees for 1 kWh (Equation (6.8))
n	The number of the producers in the P2PET system
N_p	The number of k least energy cost paths selected by the modified Yensḱ algorithm in Chapter 5
N	The maximum number of producers that can be selected by a consumer i
M	The maximum number of paths that a trading pair can select to transmit an amount of power between them
S	The set of all the producers in the P2PET system at a time slot T
P_{s_i}	The amount of power to get from a producer s_i
$TC_{s_i \to l}$	The total energy transmission cost of the selected paths between the producer s_i and the consumer l
P_l	The energy demand of a consumer
$P_{s_i}^{max}$	The maximum energy available at producer s_i
$CW_{Total}^{P:s_i \to l}$	The energy transmission cost of a transmission path between a producer s_i and consumer l
$P_{s_i - l}^{k}$	The amount of power transmitted through the path k between the producer s_i and the consumer l
α	A factor that indicates the consumer's portion of network utilisation fees. In this work, α is set to 0.5, indicating that network utilisation fees are equally shared between the trading pair producer-consumer
w_i	The energy loss of an ER_i
w_{ij}	The energy loss of an L_{ij}
y_i	A binary variable that indicates if a producer i is selected or not to power a consumer
z_i	A binary variable that indicates if a path k is selected to transmit power between a trading pair

power bought from a producer does not exceed its power availability, which reflects the upper and lower bounds of the power that can be extracted from it. However, Equations (6.11) and (6.13) restrict the number of producers a consumer can allocate and the number of paths a trading pair can choose, respectively.

It is crucial to point out that, the path transmission cost is a quadratic function of the transmitted power amount (see Equations (6.7), (6.8) and (3.6)).As discussed in the previous chapter, the existence of the PFD constraint (Equation (5.7)) in the multi-path routing problem adds non-convexity to the non-linear optimization problem. Thus, the energy routing problem in Equation (6.6) is a non-convex, non-linear optimization problem. Furthermore, the restriction of the number of selected producers and paths for each consumer in Equations (6.11) and (6.13) introduces combinatorial aspects to the optimization problem making it a non-convex mixed-integer non-linear optimization problem. Non-convex mixed-integer non-linear optimization problems are difficult to solve, and there is no universally guaranteed approach for finding the global optimum [151]. To address the energy routing problem we opted for the use of metaheuristics specifically the Symbiotic Organisms Search [152] (SOS) algorithm and suggested a semi-decentralized energy routing approach that is discussed in the following section.

6.3 A semi-decentralized energy routing approach

This work aims to create an efficient energy-routing approach that solves the energy-routing problem. The routing approach should allow consumers in the P2PET network to select the best set of producers to buy energy from, to determine the power amount to get from each producer, and the non-congested minimum energy cost transmission paths to use to satisfy their demand. The energy routing decisions should consider the network physical constraints, including capacity and PFD constraints, and the market constraints, including network utilisation fees, power loss compensation fees, energy prices, availability and demand, and the limits on the number of paths and producers allowed. However, the problem in (6.6) is a non-convex mixed integer non-linear optimization problem with several local solutions, making it difficult to discover a global solution. Thus, a metaheuristic algorithm is employed to solve the energy routing problem as it produces near-optimal solutions by iteratively merging and improving candidate solutions while handling constraints in reasonable execution time, which is beneficial in complex networks (increasing network size and producer and consumer numbers). Equation 6.6 shows that energy prices and path costs are incorporated in the same objective function; the alteration in power allocation from each producer can have a direct impact on the path selection process. As multi-path energy routing shows promising results in minimizing the energy transmission loss in the previous chapter, we introduce a new multi-path energy routing algorithm that combines the modified Yen's k least loss paths algorithm (in the previous Chapter 5 section 5.3.1.1) with the SOS algorithm.

The suggested energy routing approach distributed computational load between individual ERs (consumers) and the NSO to eliminate congestion in the case of simultaneous power transmissions. It provides a local, autonomous decision under the control of the NSO. Figure 6.1 illustrates the proposed semi-decentralized energy routing approach that operates as follows:

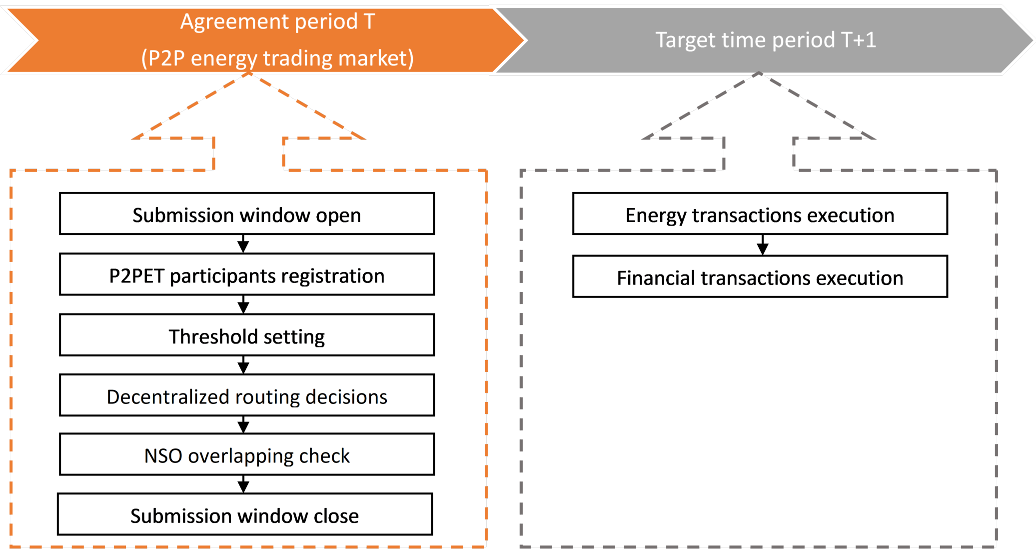

FIGURE 6.1: The timeline of the proposed P2PET framework and energy routing approach.

- **Daily market setup:** At the start of each day, the NSO uploads the utility grid's purchasing and selling prices for the following 24 hours, and updates grid infrastructure utilisation fees, which fluctuate during the day.

- **Network status setup:** All network ERs submit their status information dynamically on the platform. Therefore, each ER has an overview of the network structure.

- **Submission window:** The P2PET market starts by opening a matching window at the beginning of a time slot T (for instance, hourly).

- **P2PET participant registration:** Producers and consumers, through their associated ERs, submit their demands and offers to announce their intention to purchase or sell energy during time slot T+1. That covers the amount of power requested by each consumer and the power availability with the corresponding price of each producer. Producers and consumers who miss the submission window must wait until the next trading session begins.

- **Threshold setting:** According to the total demand and availability, the communication platform determines a threshold if there is an imbalance between demand and generation.

- **Decentralized routing decisions:** Each consumer-associated ER takes the necessary real-time information about the network from the platform and invokes the proposed SOS-based multipath energy routing algorithm with Yens k least cost paths discovery (SOS-Yen's ERA) to determine the producers to get energy from, the amount of power, and the selected paths to each one. The routing algorithm employs multi-path energy routing, where the modified yens k least loss paths algorithm (see Chapter 5 section 5.3.1.1) is used to determine k least cost energy transmission paths between a consumer and a set of possible producers, while the SOS algorithm is employed to determine the power amount to get from each producer and how much to send in each path so the total energy cost is minimized. To ensure fair and accurate network utilisation and power loss compensation fees for prosumers, Algorithm 5.2 from the previous chapter is utilized to accurately compute the power loss for each energy transaction.

- **Routing decision submission:** Each consumer-associated ER submits its decisions to the platform for path and source overlapping check by the NSO.
- **NSO overlapping check:** The NSO gets the routing decisions of the different consumer-associated ERs and checks for path and source conflicts. Path conflict occurs when multiple consumers select the same path or when portions of their chosen paths overlap, increasing the overall energy loss of this path and potentially surpassing its capacity limit, causing congestion and grid instability. Source conflict arises when multiple consumers choose the same prosumer, but the latter cannot meet all the desired demands. The NSO uses the energy transmission scheduling mechanism 6.2 to resolve the path and source conflict, sends an approval or revision request to consumers, and updates network information on the platform. Consumers who received a revision request recalculate the SOS-Yen's ERA and select a new solution; this process is repeated until all the consumers get approval or the matching window closes (the time slot T ends).
- **Finantial and energy transactions execution:** Once the matching window closes, consumers with approval complete transaction details (financial transactions) and start the physical transfer of energy within the specified time frame (transaction execution). Consumers who cannot get approval from the NSO before the matching window closes can get their entire demand from the utility grid or wait until the next trading session.

The suggested energy routing approach is divided into two parts: a decentralized part where the routing decisions are made independently based on local information and perspectives at the ER level, and a centralized part executed at the NSO level where approval or revision requests of the generated decentralized routing decisions are made, ensuring network stability and congestion-free power in simultaneous power transmissions. The semi-decentralized approach balances the benefits of both centralized and decentralized energy routing algorithms.

6.3.1 Symbiotic Organisms Search-based multipath energy routing algorithm with Yens k least cost paths discovery (SOS-Yen's ERA)

SOS is a population-based metaheuristic algorithm inspired by the different interactions between organisms in the natural ecosystem [152]. Each possible solution in the SOS algorithm is represented as an organism, where three distinct relationships—mutualism, commensalism, and parasitism— are employed between the preexisting organism solutions to explore the search space and produce new ones. Due to its simplicity (few parameters), stability, balanced exploration and exploitation [153], the SOS algorithm has attracted much attention from the optimization research community and has been successfully applied to different optimization problems such as engineering design problems [154], data mining and machine learning problems [155, 156], task scheduling in cloud computing [157], etc.
Therefore, a Symbiotic Organisms Search-based multipath energy routing algorithm with Yens k least cost paths discovery (SOS-Yen's based ERA) is executed by each consumer-associated ER to solve the non-convex mixed integer nonlinear optimization problem stated in Section 6.2.2. The SOS-Yen's based ERA determines from the set of possible producers including the utility grid, which producers select with the best power allocation and paths selection so consumer demand is satisfied while the total energy cost is minimized.
As illustrated in Algorithm 6.1, SOS-Yen's based ERA initially initiates the set of all possible producers $S = \{s_1, ..., s_n\}$. It first uses the modified Yen's k least loss paths algorithm proposed in the previous chapter (5.3.1.1) in paths discovery to create a set of k most feasible paths to each producer s_i within the set S. The most feasible paths are those with the least energy transmission cost (Equation (6.7)). Therefore, instead of getting these k paths based on their energy transmission loss, the energy transmission costs of each power line and ER in the network are calculated based on consumer demand using Equations (3.4), (3.6) and (6.7). Subsequently, the most promising paths (K paths with the lowest energy transmission cost) to each possible producer s_i in the set S are found using Yen's algorithm (Figure 5.3). These paths are denoted as $Paths$, which is a matrix of size (n, k), where n is the number of all possible producers in the set S and k is the number of promising paths to each producer. As illustrated in (6.15), each cell in this matrix reflects a potential path from producer s_i to consumer l. $Path_{i,j}$ represents the j^{th} path from producer s_i to the

consumer l.

$$Paths = \begin{Bmatrix} Path_{1,1} & Path_{1,2} & \cdots & Path_{1,k} \\ Path_{2,1} & Path_{2,2} & \cdots & Path_{2,k} \\ \vdots & \vdots & \ddots & \vdots \\ Path_{n,1} & Path_{n,2} & \cdots & Path_{n,k} \end{Bmatrix} \tag{6.15}$$

After, determining the set of k feasible paths to each producer ($Paths$), the algorithm randomly initiates the best organism X_{best} with a population of $PopSize$ organisms denoted as X. An organism $X_m \in X$, with $m = 1, 2 ... PopSize$, as indicated in Equation (6.16) is a candidate solution matrix of size (n, k), where each case x_{ij} in the matrix X_m represents the power amount to send in the j^{th} path between a producer s_i and the consumer l (P^k_{s-l} in Equations (3.4), (3.6) (6.14)). The sum of row i ($\sum_{j=1}^{k} x_{i,j}$) in X_m represents the total power amount to get from the producer s_i in the set S (P_{s_i} in Equation (6.6)). These variables with y and z in Equations (6.11),(6.12),(6.13), and (6.14) correspond to the decision variables of our optimization problem.

$$X_m = \begin{Bmatrix} x_{1,1} & x_{1,2} & \cdots & x_{1,k} \\ x_{2,1} & x_{2,2} & \cdots & x_{2,k} \\ \vdots & \vdots & \ddots & \vdots \\ x_{n,1} & x_{n,2} & \cdots & x_{n,k} \end{Bmatrix} \tag{6.16}$$

To create a feasible set of random solutions (organisms) that adhere to the constraints of limited number of selected producers (N) and paths (M) outlined in Equations (6.9), (6.11)-(6.14), as well as to the paths and producers capacity constraints defined in Equations (3.9) and (3.10), the Algorithm 6.2 is employed. It uses Equation (6.17) to create random values in the capacity bounds.

$$x = rand * (UB - LB) + LB \tag{6.17}$$

The while loop represents the iterative process of the SOS-Yens-based ERA, in which each organism $X_m \in X$ goes through three different phases mutualism, commensalism, and parasitism, to update the best organism X_{best}.In the mutualism phase, a random organism X_j is selected to intersect with an organism X_m, where the mutual vector and the benefits factors BF_1 and BF_2 are used to reflect the mutual benefit relationship between the two organisms. The resulting organisms from this mutual relationship are calculated according to Equations (6.18) and (6.19).

$$X_{mnew} \leftarrow X_m + rand(n, k) \times (X_{best} - BF_1 \times X_{mutual}), rand \in [0, 1] \tag{6.18}$$

$$X_{jnew} \leftarrow X_j + rand(n, k) \times (X_{best} - BF_2 \times X_{mutual}), rand \in [0, 1] \tag{6.19}$$

Algorithm 6.1: Symbiotic Organisms Search-based multipath energy routing algorithm with Yens k least cost paths discovery (Part 1)

Input: consumer l, energy demand P_l, set of producers $S = \{s_1, ..., s_n\}$, fitness function f, network & market parameters, N, M
Output: best identified feasible solution X_{best}

Calculate the energy transmission cost of ERs and power lines using P_l, Eqs (3.4), (3.6) and (6.7)
$Paths \leftarrow$ Apply Yens Algorithm to find k feasible paths to each producer in S
Set: $UB, LB, PopSize, MaxIter$

```
/* Initialize random X_best, population */
```

Generate random X_{best} using Algorithm 6.2
Evaluate the fitness function of X_{best} as $f(X_{best})$
Generate random initial population $X = \{X_m | m = 1, ...PopSize\}$ of $PopSize$ organisms using Algorithm 6.2
for *each* $X_m \in X$ **do**
  Evaluate the fitness function of X_m as $f(X_m)$
  if $f(X_m) < f(X_{best})$ **then**
    $X_{best} \leftarrow X_m$
    $f(X_{best}) \leftarrow f(X_m)$
while $t < maxIter$ **do**
  for *each* $X_m \in X$ **do**
```
      /* Mutualism Phase */
```
    Select a random organism $X_j \in X$, $j \in [1...PopSize]$, $j \neq m$
    Determine BF_1,BF_2 using Eqs (6.21) & (6.22)
    Create a mutual vector, $X_{mutual} \leftarrow (X_m + X_j)/2$
    $X_{mnew} \leftarrow X_m + rand(n, k) \times (X_{best} - BF_1 \times X_{mutual})$
    $X_{jnew} \leftarrow X_j + rand(n, k) \times (X_{best} - BF_2 \times X_{mutual})$
    $X_{mnew} \leftarrow Limiter(X_{mnew})$
    $X_{jnew} \leftarrow Limiter(X_{jnew})$
    Evaluate the fitness function of X_{mnew}, X_{jnew} as $f(X_{mnew})$,$f(X_{jnew})$
    if $f(X_{mnew}) < f(X_m)$ **then**
      $X_m \leftarrow X_{mnew}$
      $f(X_m) \leftarrow f(X_{mnew})$
      if $f(X_m) < f(X_{best})$ **then**
        $X_{best} \leftarrow X_m$
        $f(X_{best}) \leftarrow f(X_m)$
    if $f(X_{jnew}) < f(X_j)$ **then**
      $X_j \leftarrow X_{jnew}$
      $f(X_j) \leftarrow f(X_{jnew})$
      if $f(X_j) < f(X_{best})$ **then**
        $X_{best} \leftarrow X_j$
        $f(X_{best}) \leftarrow f(X_j)$
    ...
  ...

Algorithm 6.1: Symbiotic Organisms Search-based multipath energy routing algorithm with Yens k least cost paths discovery (part 2)

```
while t < maxIter do
    for each X_m ∈ X do
                                                    /* Commensalism Phase */
        Select a random organism X_j ∈ X, j ∈ [1...PopSize], j ≠ m
        X_mnew ← X_m + (2 × rand(n,k) − 1) × (X_best − X_j)
        X_mnew ← Limiter(X_mnew)
        Evaluate the fitness function of X_mnew as f(X_mnew)
        if f(X_mnew) < f(X_m) then
            X_m ← X_mnew
            f(X_m) ← f(X_mnew)
            if f(X_m) < f(X_best) then
                X_best ← X_m
                f(X_best) ← f(X_m)
                                                    /* Parasitism Phase */
        Select a random organism X_j ∈ X, j ∈ [1...PopSize], j ≠ m
        X_parasite ← X_m
        Select random indices between [1, n ∗ k] from X_parasite and set their values
          using Eq (6.17).
        X_parasite ← Limiter(X_parasite)
        Evaluate the fitness function of X_parasite as f(X_parasite)
        if f(X_parasite) < f(X_j) then
            X_j ← X_parasite
            f(X_j) ← f(X_parasite)
            if f(X_j) < f(X_best) then
                X_best ← X_j
                f(X_best) ← f(X_j)
    t ← t + 1
```

$$X_{mutual} \leftarrow (X_m + X_j)/2 \tag{6.20}$$

$$BF_1 = (1 + round(rand)), rand \in [0, 1] \tag{6.21}$$

$$BF_2 = (1 + round(rand)), rand \in [0, 1] \tag{6.22}$$

The commensalism phase depicts a relationship between two organisms in which one benefits from the other without affecting it. In this phase, a random organism X_j is selected from the population X to interact with the organism (X_m). The organism X_m exploits the search space by taking the information from the organism X_j using Equation (6.23).

$$X_{mnew} \leftarrow X_m + rand(n, k) \times (X_{best} - X_j), rand \in [-1, 1] \tag{6.23}$$

Algorithm 6.2: Initialize SOS algorithm population

Input: consumer l, energy demand P_l, set of producers $S = \{s_1, ..., s_n\}$
$PopSize, N, M, k, n, UB_s, LB_s, UB_{Paths}, LB_{Paths}$

Output: initial population X

for $m = 1$ *to* $PopSize$ **do**
    Initialize a zeros matrix x
    Set the power to get from each producer in the set S to zero ($Power$)
    `/* Check constraint (6.11) */`
    Select N random producers from the set S to get energy from (Eq (6.11))
    for *each producer* s_i *in the selected set* **do**
        $Power_{s_i} \leftarrow rand \times (UB_{s_i} - LB_{s_i}) + LB_{s_i}$
    `/* check constraints (6.9) & (6.10) */`
    if $\sum_{i=1}^{n} Power_{s_i} > P_l$ **then**
        for *each producer* s_i *in the selected set* **do**
            $Power_{s_i} \leftarrow Power_{s_i} \times \frac{P_l}{\sum_{i=1}^{n} Power_{s_i}}$
            $Power_{s_i} \leftarrow \max(\min(Power_{s_i}, UB_{s_i}), LB_{s_i})$
    Initialize a zeros matrix z
    `/* check constraint (6.13) */`
    Select random paths from $Paths$ to use for each producer s_i in the selected set while $\sum_{i=1}^{n} \sum_{j=1}^{k} z_{i,j} <= M$
    for *each producer* s_i *in the selected set* **do**
        for *each selected path* j *in* $Paths_{i,j}$ *where* $z_{i,j} > 0$ **do**
            $x_{i,j} \leftarrow rand \times (UB_{Paths_{i,j}} - LB_{Paths_{i,j}}) + LB_{Paths_{i,j}}$
        if $\sum_{j=1}^{k} x_{i,j} \neq Power_{s_i}$ **then**
            $x_{i,j} \leftarrow x_{i,j} \times \frac{Power_{s_i}}{\sum_{j=1}^{k} x_{i,j}}$
            $x_{i,j} \leftarrow \max(\min(x_{ij}, UB_{Paths_{i,j}}), LB_{Paths_{i,j}})$
    $X_m \leftarrow x$

For the parasitism phase, it describes an interaction in which a parasite organism benefits from a host organism. Similarly to the previous phases, a random organism X_j is selected as a host for a parasite organism $X_{parasite}$. $X_{parasite}$ initially is created as a copy of X_i. Subsequently, certain random elements within the $X_{parasite}$ matrix are selected and randomly regenerated using equation (6.17).

To ensure the feasibility of the generated organisms during the optimization problem, we employ a feasibility check mechanism called Limiter detailed in Algorithm 6.3. This algorithm is applied to the newly created organisms (solutions) throughout each SOS phase (mutualism, commensalism and parasitism) to ensure that these new solutions comply with the optimization problem constraints in Section 6.2.2. In case of optimization problem constraints violation, the limiter adjusts the solutions to make sure they are feasible before evaluating their fitness function. Specifically, the constraints of the limited number of producers and paths to allocate by each consumer (Equations (6.11)-(6.14)), the capacity limit of producers (Equation (6.10)), the maximum amount of power to get from the producers (Equation (6.9)), and the paths capacity constraints (Equation 3.9) are all considered in this limiter. While, the multipath routing constraints including PFD, power loss constraints, etc detailed in the previous chapter in section 5.2 are added through a penalty method in the objective function (fitness function). The fitness function (optimization objective function in Equation (6.6)) denoted by $f(.)$, assesses the energy cost within each newly generated solution X_{mnew}. If the cost of the newly generated solution stated by $(f(X_{mnew}))$ is more beneficial (lower than) than the energy cost of the existing solution X_m stated by f(X_m), X_{mnew} replaces X_m in the population X of the candidate solutions. At each phase, the algorithm updates the best organism X_{best} whenever a new solution with superior performance emerges.

Algorithm 6.3: SOS-Yens ERA Limiter

Input: X, energy demand $P_l, N, M, k, n, UB_s, LB_s, UB_{Paths}, LB_{Paths}$
Output: The feasible solution X

```
/* Handling constraint violations */
```

for $i = 1$ *to* n **do**
  if $\sum_{j=1}^{k} X_{i,j} > 0$ **then**
    $y_i \leftarrow 1$ **otherwise** $y_i \leftarrow 0$

if $\sum_{i=1}^{n} y_i > N$ **then**
  Select N random producers where $y_i > 0$
  Set the power to get from the rest of the producers in X to 0

for $i = 1$ *to* n **do**
  for $j = 1$ *to* k **do**
    if $X_{i,j} > 0$ **then**
      $z_{i,j} \leftarrow 1$ **otherwise** $z_{i,j} \leftarrow 0$

if $\sum_{i=1}^{n} \sum_{j=1}^{k} z_{i,j} > M$ **then**
  Select M random paths where $z_{i,j} > 0$
  Set the power to send in the rest of the paths in X to 0

while $(\sum_{i=1}^{n} \sum_{j=1}^{k} X_{i,j} > P_l)$ *or* $(\forall i \sum_{j=1}^{k} X_{i,j} > UB_{s_i})$ **do**
  if $\sum_{i=1}^{n} \sum_{j=1}^{k} X_{i,j} > P_l$ **then**
    $X \leftarrow X \times \frac{P_l}{\sum_{i=1}^{n} \sum_{j=1}^{k} X_{i,j}}$
  if $\forall i \sum_{j=1}^{k} X_{i,j} > UB_{s_i})$ **then**
    $X_{i,j} \leftarrow \frac{UB_{s_i}}{\sum_{j=1}^{k} X_{i,j}}$
  max(min(X, UB_{Paths}), LB_{Paths})

6.3.2 Energy transmission scheduling mechanism

By receiving the energy routing decisions of the various consumers, the NSO triggers an energy transmission scheduling mechanism to coordinate the energy flow and prevent congestion. It aims to provide efficient energy transmission while accommodating consumer preferences within grid constraints. The suggested mechanism is priority-based, where the conflicting source or path is assigned to the consumer with the highest priority. As illustrated in Equation (6.24), consumer priority is determined based on four factors:

$$Priority_{l_i} = \alpha \times WF + \beta \times CF + \gamma \times PLR + \lambda \times DSR \tag{6.24}$$

- **Wins Factor (WF):** This factor promotes fairness between conflicted consumers by giving consumers who have recently won conflicts in previous trading slots less priority and consumers who have had less success in the previous conflicts more priority. NW_{l_i} in Equation (6.25) represents how many conflicts a consumer has won in recent conflict situations in previous trading markets (previous window). $\mathcal{L}$ is the set of conflicted consumers.

$$WF = 1 - \frac{NW_{l_i}}{\sum_{k=1}^{\mathcal{L}} NW_{l_k}} \tag{6.25}$$

- **Conflict Factor (CF):** A consumer's energy routing decision may involve various prosumers and paths, possibly resulting in multiple conflicts. Thus, this factor is used to give consumers with fewer conflicts a higher priority. NC_{l_i} in Equation (6.26) represents the number of consumer l_i conflicts in this round.

$$CF = 1 - \frac{NC_{l_i}}{\sum_{k=1}^{\mathcal{L}} NC_{l_k}} \tag{6.26}$$

- **Power Loss Ratio (PLR):** reflects the benefit of allocating the path by a consumer l_i, where the fraction in Equation (6.27) denotes the ratio of the consumer power loss to consumer transmitted power through the conflicted path.

$$PLR = 1 - \frac{W_{Total}^{P_{k:s \to l_i}}}{P_{s \to l_i}^{k}} \tag{6.27}$$

- **Demand Satisfaction Ratio (DSR):** indicates the demand satisfaction ratio when assigning the source to the consumer. It is estimated in Equation (6.28) as the percentage of consumer demand from the prosumer (P_{s-l_i}) to overall consumer demand (P_{l_i})

$$DSR = \frac{P_{s-l_i}}{P_{l_i}} \tag{6.28}$$

α, β, γ, and λ are weights in the range $[0, 1]$, with $\alpha + \beta + \gamma + \lambda = 1$. The NSO can modify these weights based on the relative relevance of each factor. Conflicted paths and prosumers are assigned where they are most efficient and valuable through the use of PLR and DSR. CF and WF set dynamic priorities that prevent an individual consumer from dominating resources and conflicts, increasing consumer fairness.
As shown in Figure 6.2, the NSO generates a transaction approval for consumers who did not create conflicts and for consumers who won them, while also generating a revision request for consumers who lost the conflicts to retake new energy trading decisions based on the new state of the grid.

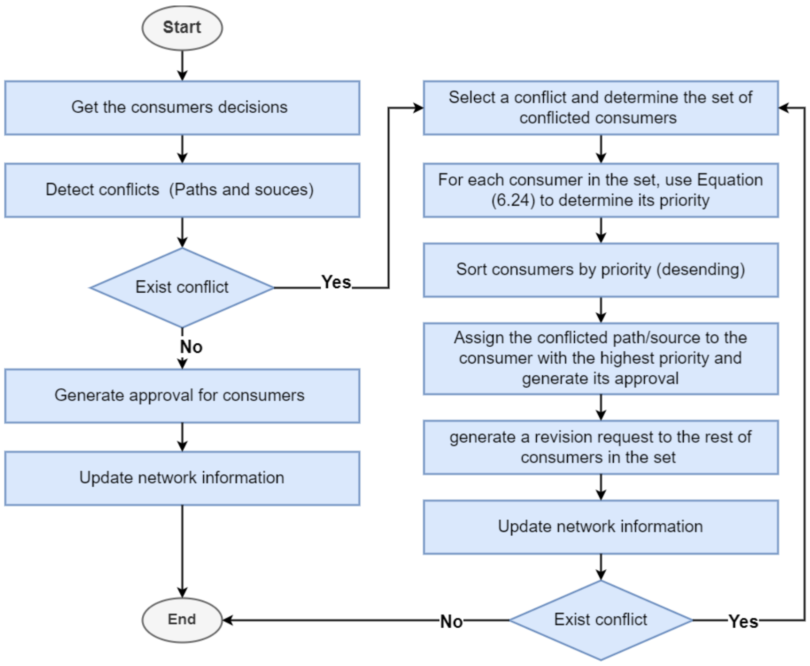

FIGURE 6.2: The proposed energy transmission scheduling mechanism.

6.4 Numerical Simulation and Result Analysis

This section includes simulations that show how the suggested energy routing approach solves the energy routing problem while minimizing energy costs for consumers and power transmission losses, avoiding physical constraint violations, and resolving path and source conflicts in simultaneous power transmission cases.
As the majority of the literature aforementioned energy routing algorithms in the previous chapters focus on addressing energy efficient path problem [1, 3, 120, 122], while

few of them integrate the matching process [2, 121, 133, 134, 136, 137], we employ a two-phase simulation evaluation strategy to assess the performance of our proposed approach. In the first phase, we evaluate the non-congestion paths created by our approach and compare them to other energy routing algorithms that prioritize path efficiency. Subsequently, in the second phase, we extend the evaluation by including the matching process and compare it to algorithms that incorporate matching and path selection.

6.4.1 Paths selection evaluation

This subsection assesses the performance of the proposed Yens-SOS-ERA in solving the energy-efficient path problem while avoiding the physical constraints violation. The following energy routing algorithms are selected for comparison.

- ES: Exhaustive Search -based energy routing algorithm proposed in [1].
- Dijkstra: The modified Dijkstra-based energy routing algorithm proposed in [120, 121].
- DFS: Depth First Search-based energy routing algorithm proposed in [2].
- ACO: ACO-based energy routing algorithm proposed in [137].
- DFS-NLP: The multipath energy routing algorithm proposed in [3], combines the non-linear programming with the DFS algorithm.
- Yens-SQP: The multipath energy routing algorithm proposed in the previous chapter, combines the Yens algorithm with the SQP.

The simulations performed using EI networks described in Chapter 3 in Figures 3.4, 3.5, 3.6, 3.7 and 3.8 with their detailed parameters in Tables 3.3-3.13. We assume the existence of a single source-load trading pair in each network. The selected source-load trading pair in each network is located at its extremes to increase the number of possible power transmission paths between them as follows:

- Figure 3.4: Transmit 20 kW of power from ER_1 to ER_{14}.
- Figure 3.5: Transmit 16 kW of power from ER_{14} to ER_{30}.
- Figure 3.6: Transmit 45 kW of power from ER_{11} to ER_{38}.

- Figure 3.7: Transmit 16 kW of power from ER_{201} to ER_{69}.
- Figure 3.8: Transmit 22 kW of power from ER_{118} to ER_{36}.

Table 6.2 represents the number of possible transmission paths between each trading pair in each network.

TABLE 6.2: The number of all possible paths between the energy trading pairs in each EI network.

	(ER_1, ER_{14}) Figure 3.4	(ER_{14}, ER_{30}) Figure 3.5	(ER_{11}, ER_{38}) Figure 3.6	(ER_{201}, ER_{69}) Figure 3.7
Paths number	48	286	68	5962

Initially, it is assumed that the pre-existing power in the different networks is set to zero (all power lines are initially empty). Moreover, power loss is the common metric used by the existing energy routing algorithms in the path selection process; thus, to guarantee a fair comparison, the suggested Yens-SOS ERA employs power loss as the key metric in path selection instead of energy transmission cost. Figures 6.3-6.8 and Tables 6.3, 6.4 illustrate the selected paths, the power amount to send in each path, power loss and the execution time of each algorithm in each network.
According to these results, the different algorithms adhere to the ERs and power lines capacity constraints and provide congestion-free energy transmission paths in the various networks. However, Multipath energy routing employed by DFS-NLP, Yens-SQP and Yens-SOS-ERA outperforms the single-path energy routing employed by Exhaustive Search, Dijkstra, DFS, and ACO by providing better power distribution and path allocation that leads to reduced energy transmission loss.
As shown in Figures 6.3 and Figure 6.4, the DFS-NLP, Yens-SQP, and Yens-SOS-ERA select the same power transmission paths with a small difference in the power distribution through these paths, as Yens-SQP, and Yens-SOS-ERA calculate the accurate power transmission loss of the different paths rather than assuming that the power is constant during the path generation process. This results in a lower energy transmission loss by 16.61% (518 W) and 15.23% (479 W) compared to single-path routing (Exhaustive Search, Dijkstra, DFS, and ACO), and by 6.54% (182W) and 9.6% (283 W) compared to DFS-NLP in Figures 6.3 and Figure 6.4, respectively. Furthermore, the use of Yens k least loss path algorithm to determine the set of most feasible paths ($k = 10$) instead of using all possible paths (Table 6.2) in the power dispatch reduces the search space and consequently decreases the execution time of Yens-SOS-ERA by 15 (2.91 s) and 142 times (39.72 s) compared to DFS-NLP energy routing algorithm. Furthermore, when compared to the execution times of Exhaustive Search, DFS, ACO, and Yens-SQP algorithms in Figures 6.3 and Figure 6.4, the proposed

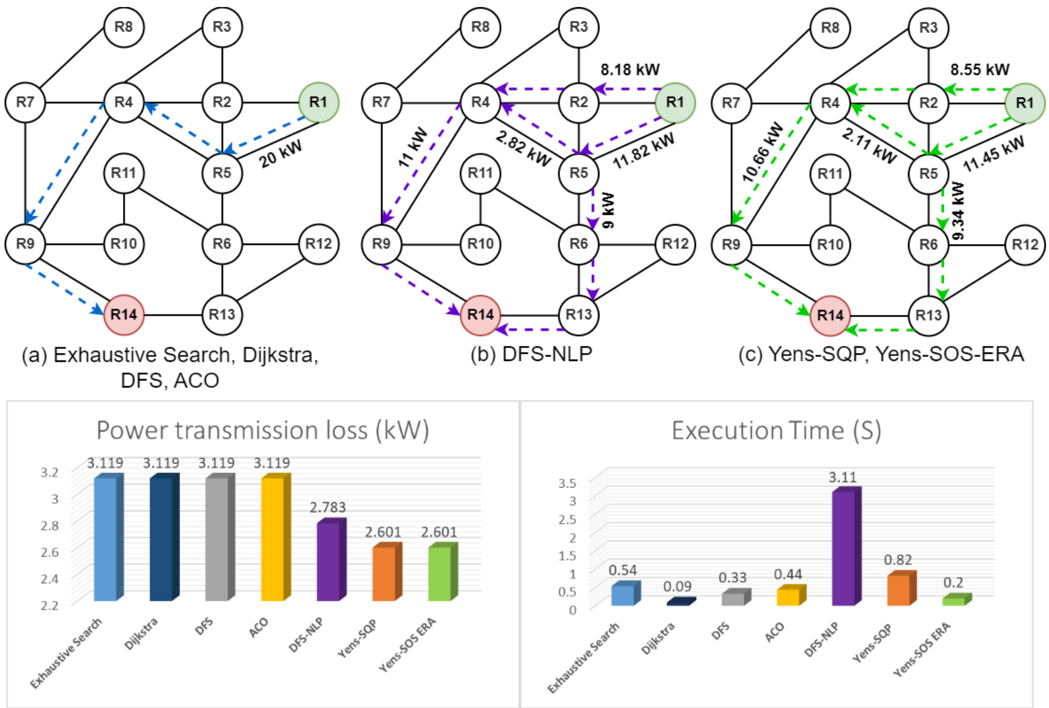

FIGURE 6.3: The selected least loss paths, power loss and execution time of each algorithm for the trading pair (ER_1, ER_{14}) in Figure 3.4.

Yens-SOS-ERA constantly surpasses them, demonstrating improved performance.
As illustrated in Figure 6.5, the Yens-SOS-ERA algorithm demonstrates superior performance by offering energy transmission paths for the trading pair (ER_{11}, ER_{38}) with a significantly lower energy transmission loss of 46.2% (11.52 kW) when compared to Exhaustive Search, Dijkstra DFS, and ACO, and of 22.29% (3.85 kW) when compared to DFS-NLP. Interestingly, the figure shows that Yens-SQP and Yens-SOS-ERA accomplish the same energy transmission loss with distinct path selection . Yens-SQP selects more paths (ERs and power lines) than Yens-SOS-ERA. In addition to network security and management concerns, selecting a large number of paths by one trading pair could indirectly influence the other trading pairs. As it will increase energy loss in the selected paths for other trading pairs sharing the same network, potentially limiting their choices and pushing them onto less efficient paths. Furthermore, allowing trading pairs to select a large number of paths, even if it decreases their power transmission loss, could increase conflicts on the power lines and result in increased congestion and PFD issues. Thus, to create a balance between the advantages and disadvantages of multi-path energy routing, we assume that the NSO can impose a limit on the number of paths that can be selected by each trading pair.
It is important to note that, according to Figure 6.6, the performance of Yens-SQP decreases (stuck in local optimum) with the increasing number of feasible paths (k) between the trading pair in Figure 6.5, unlike Yens-SOS-ERA, that stays stable and provides efficient energy routing paths with the least energy transmission loss.

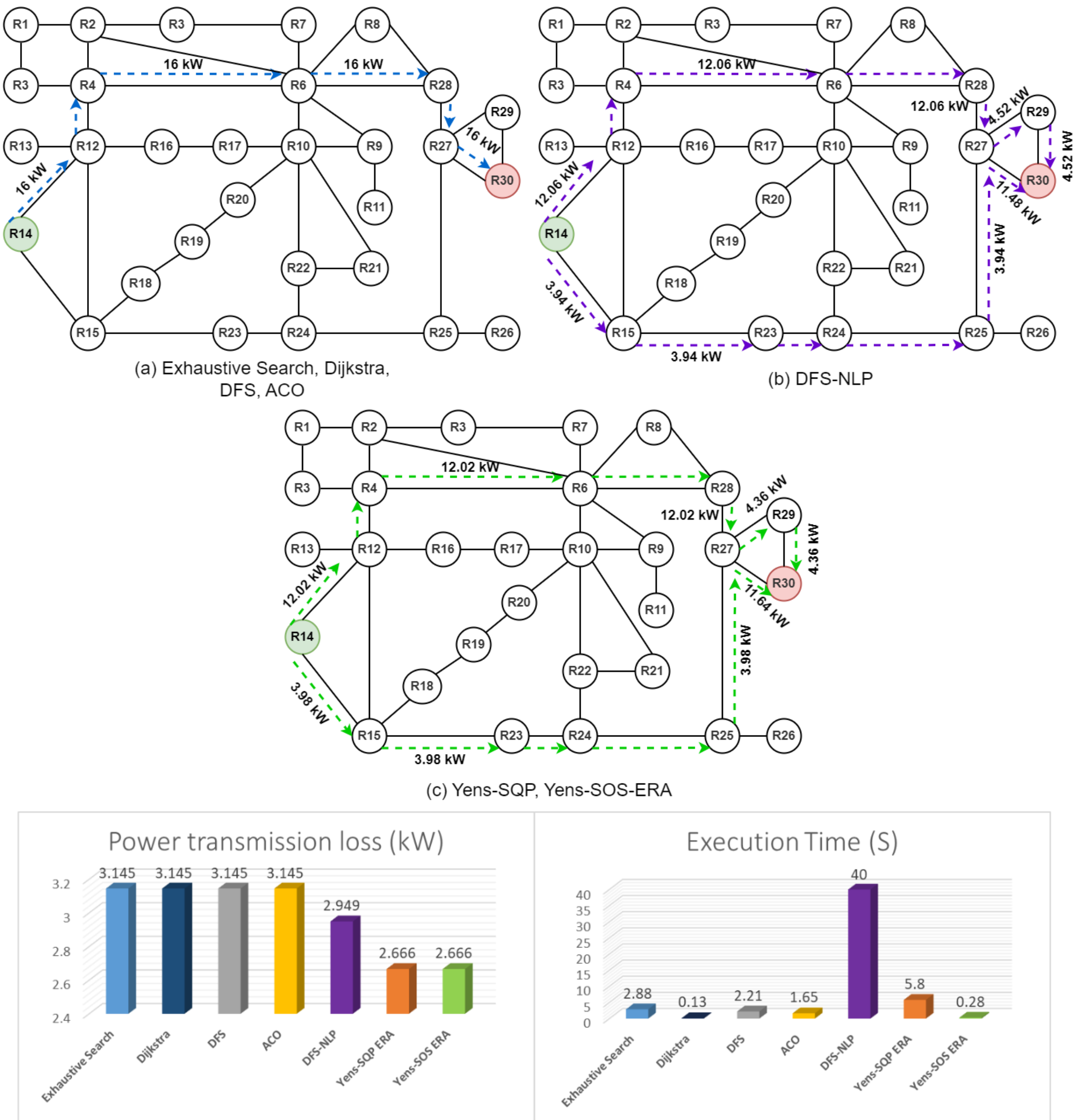

FIGURE 6.4: The selected least loss paths, power loss and execution time of each algorithm for the trading pair (ER_{14}, ER_{30}) in Figure 3.5.

To assess the scalability of Yens-SOS-ERA algorithm, we applied it to the large-scale networks illustrated in Figures 3.7 and 3.8. These networks comprise a large number of potential paths between the trading pairs (5962 paths in Figure 3.7). Yens-SOS-ERA calculates first the k most promising paths between the ER_{201}, ER_{69}, and ER_7, ER_{88} in Figures 3.7 and 3.8, respectively, where k is set to 20. Then it uses the SOS algorithm to determine which paths to select and the amount of power to send in each path while minimizing the energy transmission loss.

As shown in Figures 6.7, 6.8 and Tables 6.3, 6.4, Yens-SOS-ERA can effectively scale to manage these complex networks. It outperforms both the single-path routing algorithms (Exhaustive Search, Dijkstra, DFS, and ACO) and multi-path routing algorithms (DFS-NLP and Yens-SQP). Starting with the network in 3.7, Yens-SOS-ERA

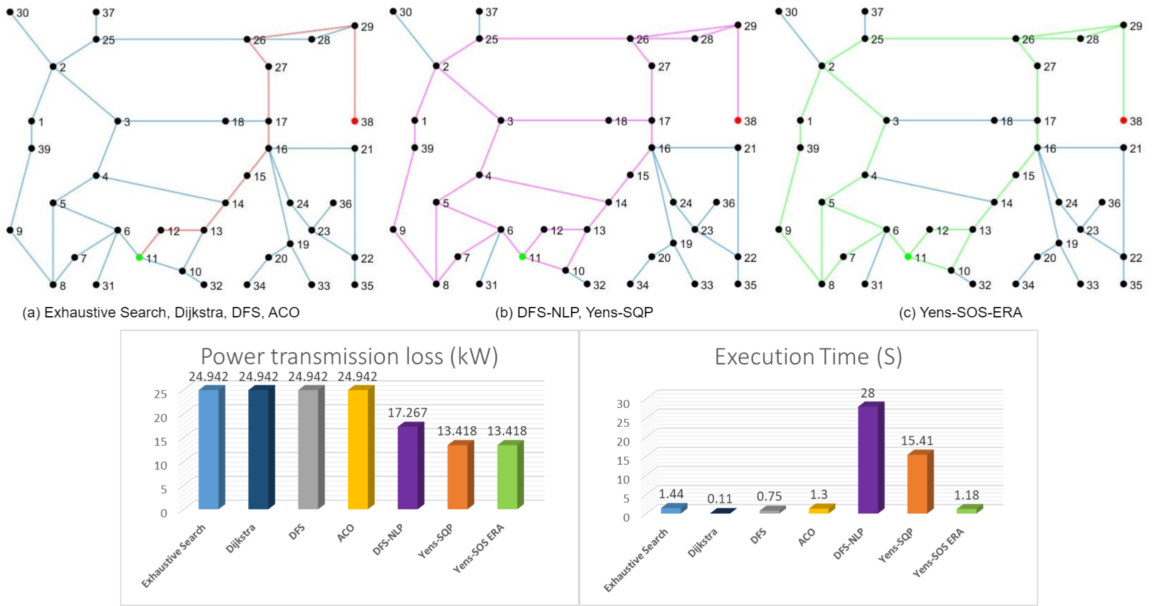

FIGURE 6.5: The selected least loss paths, power loss and execution time of each algorithm for the trading pair (ER_{11}, ER_{38}) in Figure 3.6.

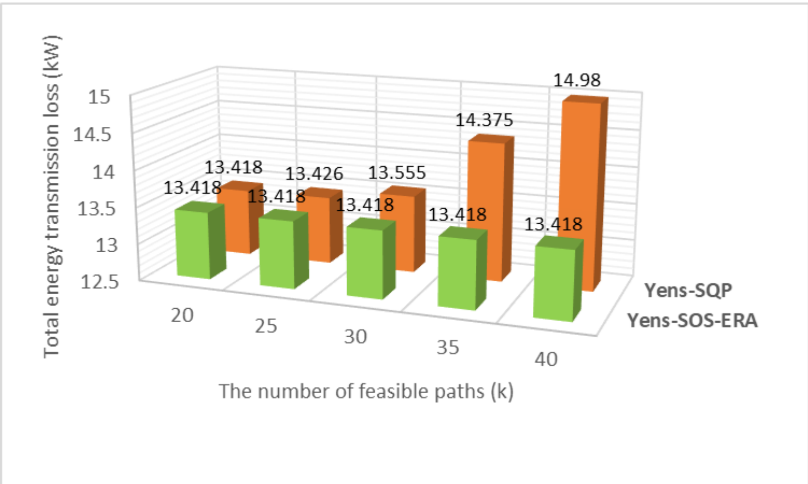

FIGURE 6.6: The total energy transmission loss calculated by Yens-SQP and Yens-SOS-ERA according to k variation for the trading pair in Figure 3.6.

reduces power loss by 21% compared to single path energy routing, and by 3% compared to Yens-SQP, while DFS-NLP failed to solve the problem with 5962 possible paths (NAN). In contrast, to DFS, Exhaustive Search, and DFS-NLP that are trapped in infinite loops (NAN) and failed to find efficient transmission paths for the trading pair within the highly connected EI network in Figure 3.8, Yens-SOS-ERA successfully identifies a multi-path solution with energy save of 24.55% compared to Dijkstra and ACO, and an energy transmission loss saving of 3.28% compared to Yens-SQP with a considerable execution time.

P2PET is not completely independent of the grid. Power lines in real-world grids are rarely empty. Thus, to evaluate the performance of the proposed Yens-SOS-ERA

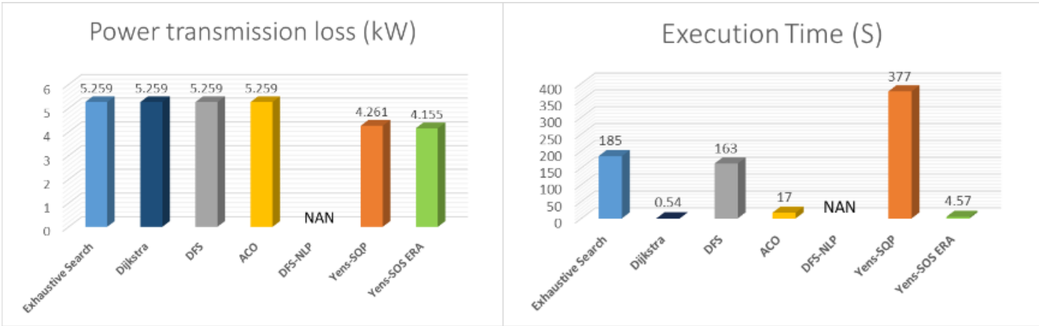

FIGURE 6.7: The total energy transmission loss and execution time of each algorithm for the trading pair (ER_{201}, ER_{69}) in Figure 3.7.

TABLE 6.3: The selected least loss paths of each algorithm for the trading pair (ER_{201}, ER_{69}) in Figure 3.7

Algorithm	Power (kW)	Selected Paths
Exhaustive Search	16	*201 → 91 → 1 → 12 → 3 → 11 → 14 → 10 → 9 → 87 → 88 → 66 → 67 → 65 → 69*
Dijkstra	16	*201 → 91 → 1 → 12 → 3 → 11 → 14 → 10 → 9 → 87 → 88 → 66 → 67 → 65 → 69*
DFS	16	*201 → 91 → 1 → 12 → 3 → 11 → 14 → 10 → 9 → 87 → 88 → 66 → 67 → 65 → 69*
ACO	16	*201 → 91 → 1 → 12 → 3 → 11 → 14 → 10 → 9 → 87 → 88 → 66 → 67 → 65 → 69*
DFS-NLP	NAN	NAN
Yens-SQP	7,92	*201 → 91 → 1 → 12 → 3 → 11 → 14 → 10 → 9 → 87 → 88 → 66 → 67 → 65 → 69*
	7,1	*201 → 91 → 1 → 13 → 15 → 18 → 7 → 8 → 29 → 87 → 88 → 66 → 67 → 65 → 69*
	0,36	*201 → 91 → 1 → 16 → 17 → 4 → 5 → 6 → 219 → 57 → 61 → 63 → 66 → 67 → 65 → 69*
	0,62	*201 → 189 → 158 → 181 → 185 → 165 → 169 → 173 → 179 → 159 → 128 → 153 → 155 → 136 → 143 → 147 → 56 → 20 → 71 → 72 → 76 → 58 → 69*
Yens-SOS-ERA	6,61	*201 → 91 → 1 → 12 → 3 → 11 → 14 → 10 → 9 → 87 → 88 → 66 → 67 → 65 → 69*
	5,64	*201 → 91 → 1 → 13 → 15 → 18 → 7 → 8 → 29 → 87 → 88 → 66 → 67 → 65 → 69*
	3,32	*201 → 122 → 119 → 93 → 118 → 121 → 117 → 83 → 32 → 19 → 57 → 61 → 63 → 66 → 67 → 65 → 69*
	0,43	*201 → 122 → 119 → 93 → 118 → 121 → 117 → 83 → 32 → 19 → 57 → 59 → 60 → 62 → 70 → 64 → 68 → 58 → 69*

TABLE 6.4: The selected least loss paths of each algorithm for the trading pair (ER_{118}, ER_{36}) in Figure 3.8

Algorithm	Power (kW)	Selected Paths
Exhaustive Search	NAN	NAN
Dijkstra	22	*118 → 75 → 69 → 49 → 45 → 44 → 43 → 34 → 36*
DFS	NAN	NAN
ACO	22	*118 → 75 → 69 → 49 → 45 → 44 → 43 → 34 → 36*
DFS-NLP	NAN	NAN
Yens-SQP	7,79	*118 → 75 → 69 → 68 → 65 → 38 → 37 → 35 → 36*
	0,82	*118 → 75 → 70 → 69 → 49 → 45 → 44 → 43 → 34 → 36*
	4,99	*118 → 75 → 69 → 49 → 42 → 40 → 37 → 35 → 36*
	7,62	*118 → 75 → 77 → 69 → 49 → 45 → 44 → 43 → 34 → 36*
	0,53	*118 → 75 → 69 → 49 → 66 → 65 → 38 → 37 → 35 → 36*
	0,25	*118 → 76 → 77 → 69 → 49 → 45 → 44 → 43 → 34 → 36*
Yens-SOS-ERA	8,57	*118 → 75 → 69 → 49 → 45 → 44 → 43 → 34 → 36*
	5,55	*118 → 75 → 69 → 68 → 65 → 38 → 37 → 35 → 36*
	3,38	*118 → 75 → 69 → 68 → 65 → 38 → 37 → 34 → 36*
	4,5	*118 → 75 → 69 → 49 → 42 → 40 → 37 → 35 → 36*

in more realistic scenarios, we integrate per-existing power flows in the network by assuming the existence of other energy transactions in the different networks.

As depicted in the figures 6.9 and 6.10, Dijkstra, Exhaustive Search, DFS, ACO, and DFS-NLP, selected paths with power lines experiencing opposing power flow ($L_{4,5}$ in Figure 6.9 and $L_{6,4}$ in Figure 6.10) creating PFD conflict leading to transaction

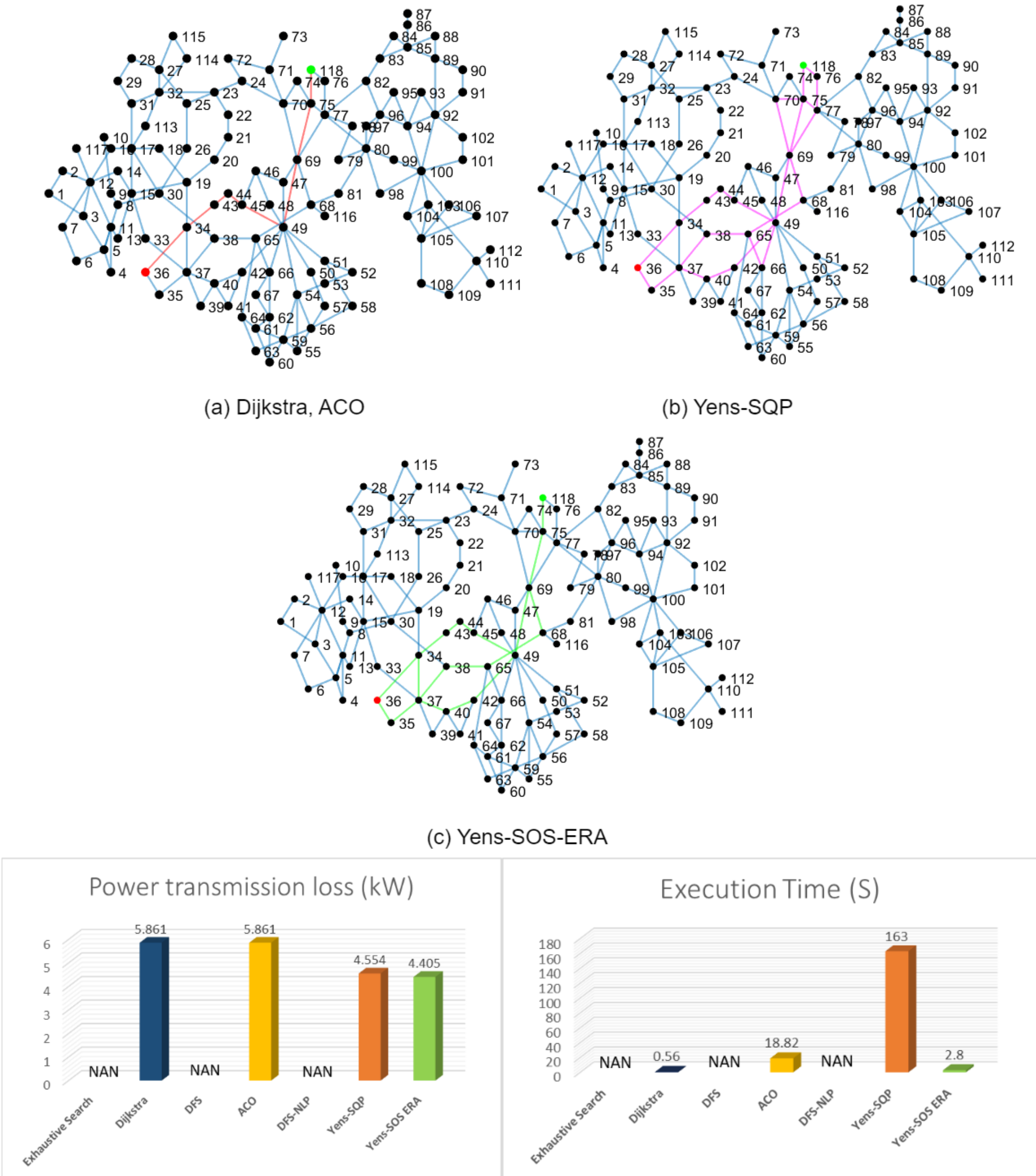

FIGURE 6.8: The total energy transmission loss and execution time of each algorithm for the trading pair (ER_{118}, ER_{36}) in Figure 3.8.

failures, grid instability and inefficiencies. In contrast, the Yens-SOS-ERA algorithm successfully addresses these issues. It determines alternative efficient energy transmission paths by considering the PFD constraint during the path generation. It replaces $L_{6,4}$ in Figure 6.10 by sub-path $4 \rightarrow 2 \rightarrow 6$ with a small increase in the power loss while adhering to the capacity and PFD constraints ensuring efficient and compliant power transmission. Correspondingly, Yens-SOS-ERA abandoned the $L_{4,5}$ in Figure 6.9 and distributed the power through the two paths $1 \rightarrow 2 \rightarrow 4 \rightarrow 9 \rightarrow 14$ and $1 \rightarrow 5 \rightarrow 6 \rightarrow 13 \rightarrow 14$ as they are the most efficient alternative given the network's physical constraints.

As with many newly suggested P2PET systems, prosumers are often charged with power loss compensation and network utilisation fees by the utility grid. To properly

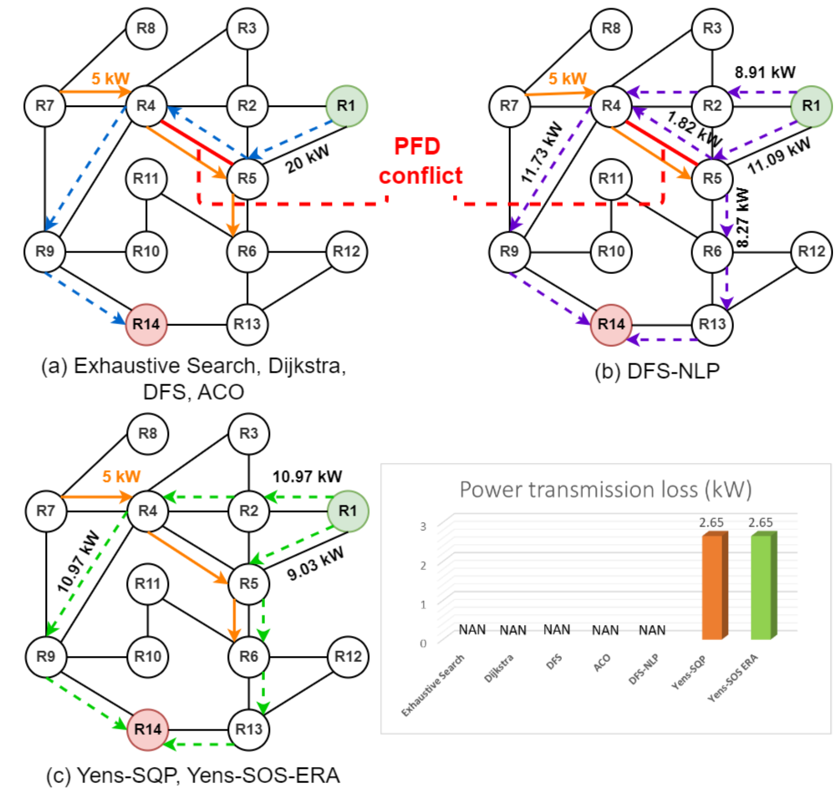

FIGURE 6.9: Transmission power loss and energy paths obtained by the different algorithms with the pre-existing power flow case for the trading pair (ER_1, ER_{14})

analyze the applicability of our suggested Yens-SOS-ERA in such real-world settings, we take into account certain economic aspects. To illustrate, we use a compensation cost of 0.01 per kWh to account for transmission loss. Line utilization costs are randomly assigned to each power line in the range [0.001,0.005]. In this scenario, Yens-SOS-ERA uses the energy transmission cost (see Equations (6.7) and (6.8)) to determine the selected paths between the trading pairs. Figures 6.11 and 6.12 compare the selected energy transmission paths and energy transmission cost of trading pairs resulting from the six energy routing algorithms.

In contrast to Dijkstra, Exhaustive Search, DFS, ACO, and DFS-NLP based energy routing algorithms that only examine power loss for path selection, the Yens-SOS-ERA incorporates accurate power loss calculation, power loss compensation and network utilisation fees. This holistic technique decreases energy transmission costs for prosumers by 28.58% and 25.74%, respectively, when compared to Dijkstra, Exhaustive Search, DFS, ACO based algorithms (Figures 6.11 and 6.12), as well as by 12.10% and 22.18% when compared to the DFS-NLP method. The accurate power loss calculation prevents prosumers from paying unfair costs for estimated power losses that may not reflect reality; rather, it provides the actual power loss that gives the actual power transmitted through each power line, ensuring fair prosumer pricing.

It is vital to highlight that the suggested Yens-SOS-ERA permits choosing one or more

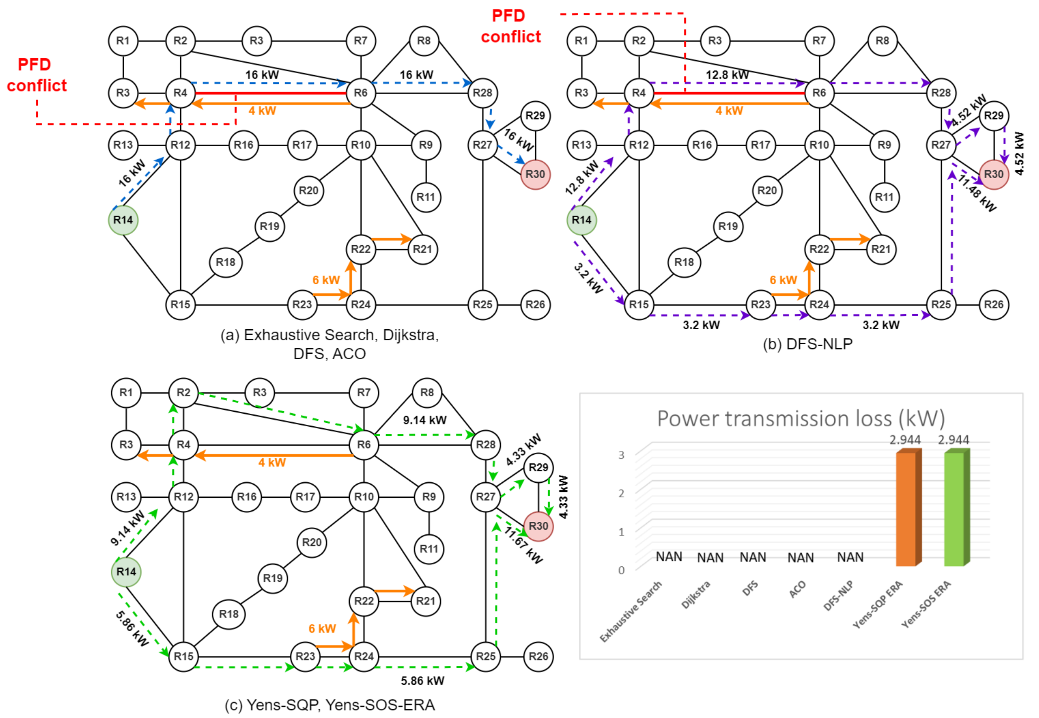

FIGURE 6.10: Transmission power loss and energy paths obtained by the different algorithms with the pre-existing power flow case for the trading pair $\{ER_{14}, ER_{30}\}$

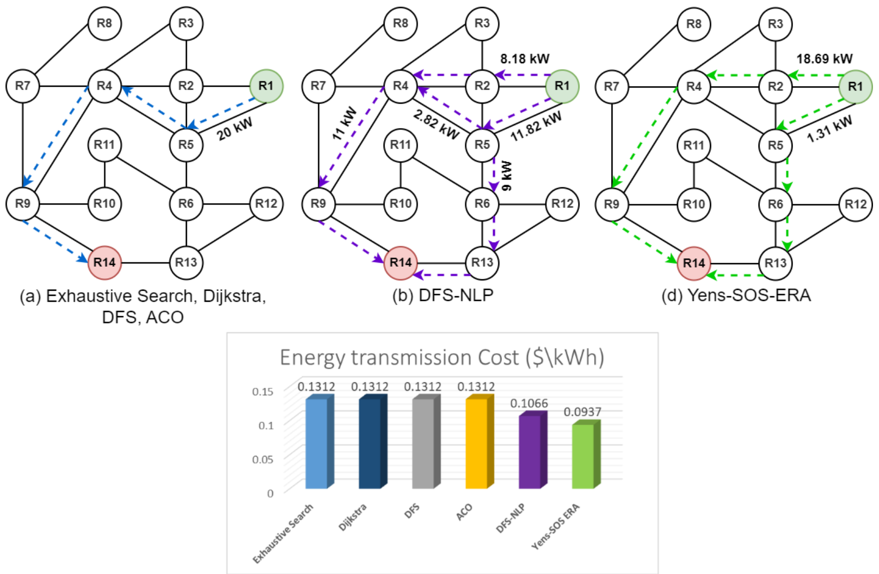

FIGURE 6.11: Energy transmission loss and transmission paths obtained by the different algorithms for the trading pair $\{ER_1, ER_{14}\}$

paths for energy trading pairs. It delivers the solution with the lowest energy transmission cost while adhering to the network's physical constraints (PFD and capacity constraints), whether it is a single or multipath solution, as seen in Figure 6.12.

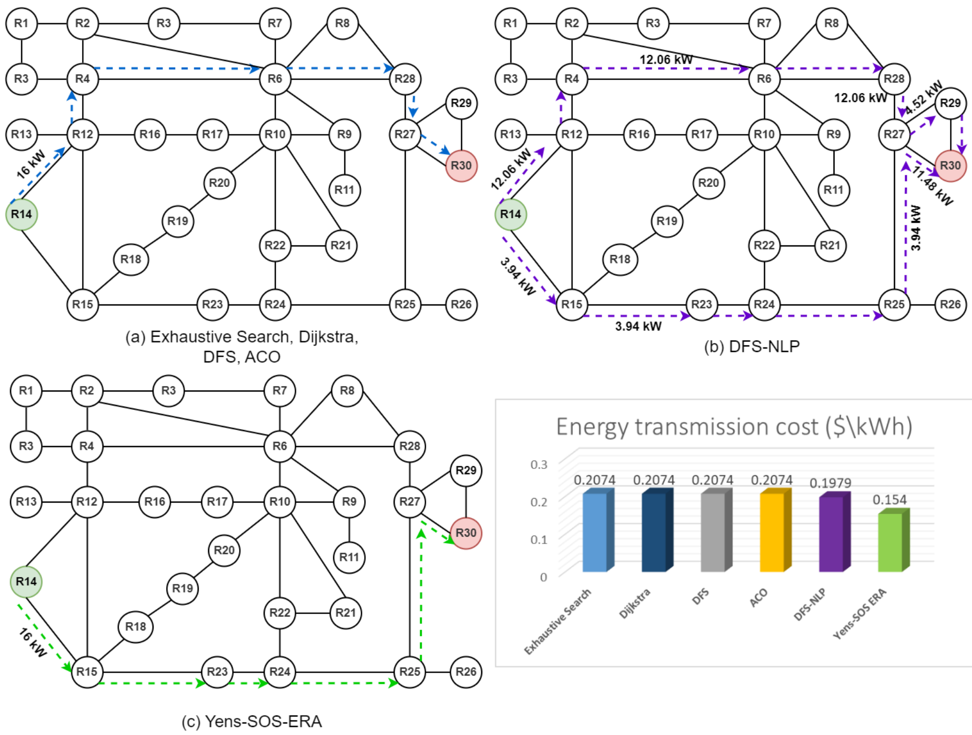

FIGURE 6.12: Energy transmission loss and transmission paths obtained by the different algorithms for the trading pair $\{ER_{14}, ER_{30}\}$

6.4.2 Integrated Matching and path selection evaluation

This sub-section assesses the proposed Yens-SOS-ERA's performance in solving the subscriber matching problem while adhering to the network's physical and market constraints. The network in Figure 3.4 is used for simulation, where we assume the existence of four producer-prosumers: ER_8, ER_{11}, ER_{13}, and ER_{14}, with distinct power availabilities of 12 kW, 20 kW, 25 kW, and 30 kW, respectively. These producers are associated with different prices of 0.085 \$/kWh, 0.12 \$/kWh, 0.11 \$/kWh, and 0.095 \$/kWh, respectively, and must supply 20 kW of power to meet consumer ER_1 demand. The utility grid is considered a possible producer; the selling price of the utility grid π_s^G is set to 0.18 \$/kWh, while the buying price of the utility grid π_b^G is set to 0.05\$/kWh. The power loss compensation fee is set to 0.01\$kWh, and line utilization costs are randomly assigned to each power line in the network in the range [0.001,0.005]. As there is only a single consumer, we did not restrict the number of producers or transmission paths to be selected by the consumer in this scenario. It is worth mentioning that, as there are only a few energy routing protocols that integrate the matching process into the routing decisions, we selected the following energy routing algorithms for comparative simulation with Yens-SOS-ERA:

- Algorithm 1: Decentralized algorithm that matches prosumers based on their prices and then uses Dijkstra algorithm for path selection [121].
- Algorithm 2: Centralized, uses the DFS algorithm to find the energy minimum loss path to each possible producer, and select the producer with the minimum energy transmission loss [2].
- Algorithm 3: The proposed decentralized algorithm in Chapter 4 [137].

As depicted in Figure 6.13, Algorithms 1 and 3 eliminate producer ER_8 from the list of possible producers as its available energy capacity cannot fulfil ER_1's demand. Although the ultimate objective of this strategy is to reduce the number of selected producers, it prevents producers with limited energy availability from participating in the trading. This might reduce interest in future participation in P2PET markets. Algorithm 1 chooses ER_{14} as it is the producer with the minimum energy price that can fulfil ER_1 demand. Based on the minimum energy transmission loss to each producer, Algorithm 2 selects the ER_{11}. Algorithm 3 tries to create a balance between optimizing both price and energy transmission loss and selects producer ER_{13}. In contrast, Yens-SOS-ERA keeps ER_8 as a trading option even if it can not provide the whole demand and based on the energy cost that includes producers' prices, power loss compensation fees, and network utilisation fees (see Equation (6.6)), Yens-SOS-ERA purchases 12 kW from ER_8 through the path $8 \rightarrow 7 \rightarrow 4 \rightarrow 5 \rightarrow 1$ and an additional 8 kW from ER_{14} through the path $14 \rightarrow 9 \rightarrow 4 \rightarrow 2 \rightarrow 1$. It significantly decreases the cost of energy when compared to Algorithms 1, 2, and 3. Specifically, it reduces costs by 7.73%, 24.81%, and 17.58%.
To further complicate the network, we presume the existence of two producer-consumer trading pairs $\{4, 10\}$ and $\{5, 12\}$ in the network, transmitting 4 kW and 3 kW power through the paths $4 \rightarrow 9 \rightarrow 10$ and $5 \rightarrow 6 \rightarrow 12$, respectively. As illustrated in Figure 6.14, Algorithms 1, 2, and 3 retain the selected sources and paths from the prior scenario, leading to the violation of the PFD constraint in power lines $L_{4,9}$ and $L_{5,6}$, thus cancelling the energy transmission. In contrast, as the power line $L_{4,9}$ has a power flow in the direction from ER_4 to ER_9, it can not be used in the opposite direction, thus the proposed Yens-SOS-ERA replaces this line with the line $L_{9,7}$.

6.4.3 Source and paths conflict management evaluation

Taking the previous network in Figure 3.4 with the same characteristics, we presume the existence of three prosumers and two consumers with simultaneous transmission

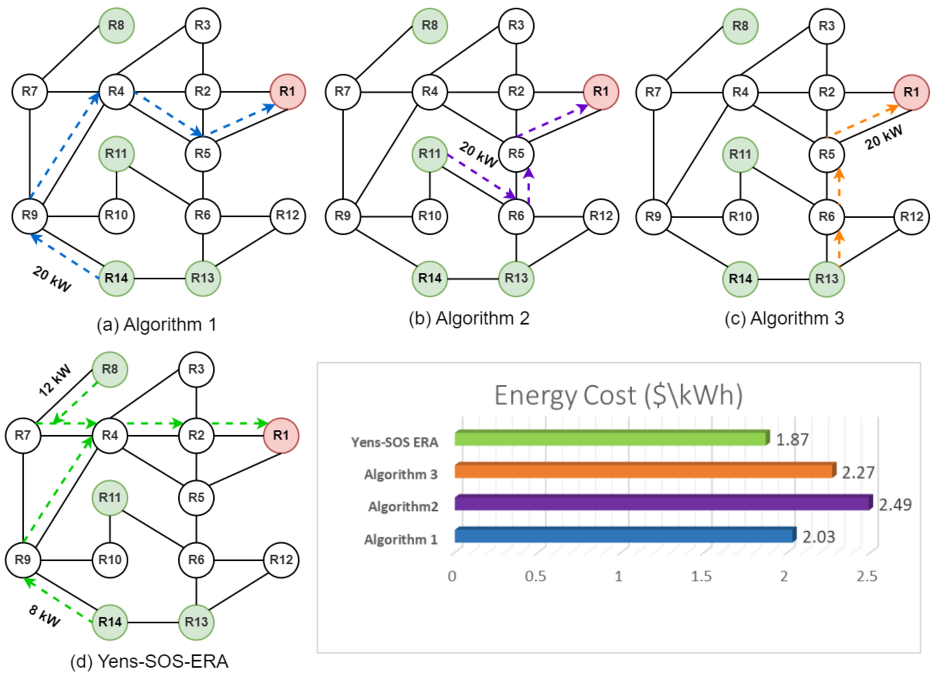

FIGURE 6.13: Energy routing decisions obtained by the different algorithms for the consumer ER_1

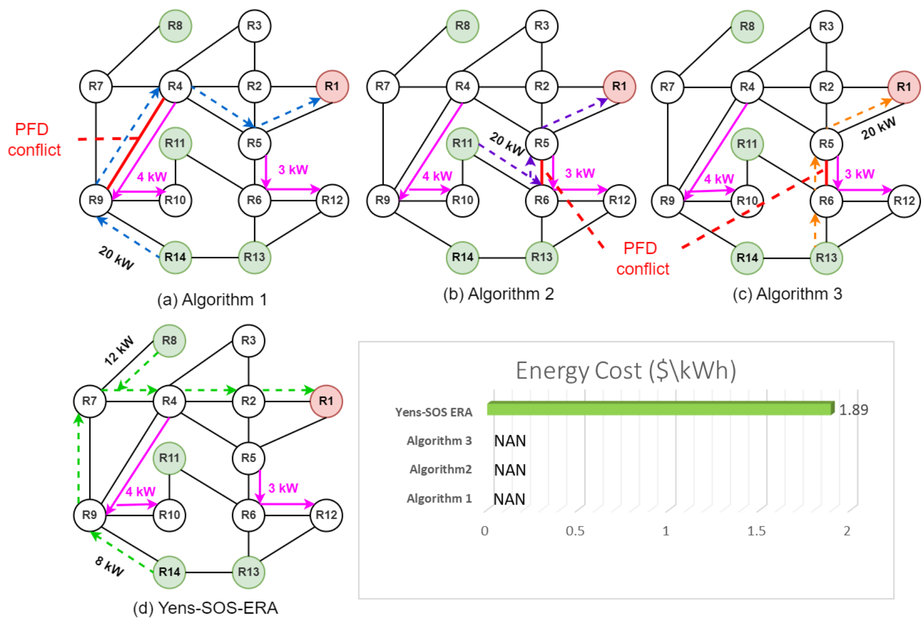

FIGURE 6.14: Energy routing decisions obtained by the different algorithms for the consumer ER_1 with the pre-existing power flow case

time and varying power demand, availabilities, and selling prices as listed in Table 6.5. Each consumer can choose up to two producers and three energy transmission paths within the proposed system.

TABLE 6.5: Producers and consumers parameters.

Algorithm	Energy Availability (kW)	Selling Price ($/kWh)	Consumer	Energy Demand (kW)
ER_{11}	20	0.12	$ER1$	20
ER_{13}	30	0.11	$ER9$	28
ER_{14}	25	0.095		

Figure 6.15 illustrates energy routing decisions taken by Algorithm 1, Algorithm 2 and the proposed semi-decentralized energy routing approach. Starting with the results of Algorithm 1, a path conflict occurs on power line L_{14-9} that is selected by consumers ER_1 to bring 20 kW through the path $14 \rightarrow 9 \rightarrow 4 \rightarrow 5 \rightarrow 1$ and by ER_9 to bring 25 kW through the path $13 \rightarrow 14 \rightarrow 9$ exceeding its maximum capacity (25 kW) creating a congested power line. In Algorithm 2, all consumers' energy routing decisions are taken by a central unit to avoid line congestion. The power line L_{14-9} is allocated to transmit 25 kW from ER_{14} to the consumer ER_9. However, PFD conflict occurs in the transmission line L_{6-5} as the PFD constraint is ignored by Algorithm 2. The proposed semi-decentralized energy routing approach allows each consumer to use the Yens-SOS-ERA in the first step and make energy routing decisions independently based on their preferences in a decentralized way. The consumer ER_1 selects the prosumer ER_{14} to satisfy its demand (20 kW) through the path $14 \rightarrow 9 \rightarrow 4 \rightarrow 5 \rightarrow 1$, while the consumer ER_9 selects the prosumers ER_{14} and ER_{13} to satisfy its demand (28 kW) through the paths $14 \rightarrow 9$ and $13 \rightarrow 6 \rightarrow 11 \rightarrow 10 \rightarrow 9$, respectively, and submit their routing decisions in the communication platform. The NSO triggers the proposed energy transmission scheduling mechanism to check for path or source conflicts in the collected routing decisions. As shown in Figure 6.15 (c), a source and path conflict occurs on ER_{14} and power line L_{14-9}. Thus, the NSO uses Equation (6.24) to calculate the priority of each consumer. As ER_1 has a higher priority (1.85) compared to ER_9 (1.83), the NSO allocates the conflicted path and source to ER_1, sends its approval, updates network information, and generates a revision request for ER_9. By receiving the revision request ER_9 execute the Yens-SOS ERA and select new energy sources and paths eliminating the path and source conflict as shown in Figure 6.15 (d). The proposed semi-decentralized multi-path energy routing approach ensures that energy trading exchange during period T+1 will not violate the network's physical constraints (capacity and PFD constraints).

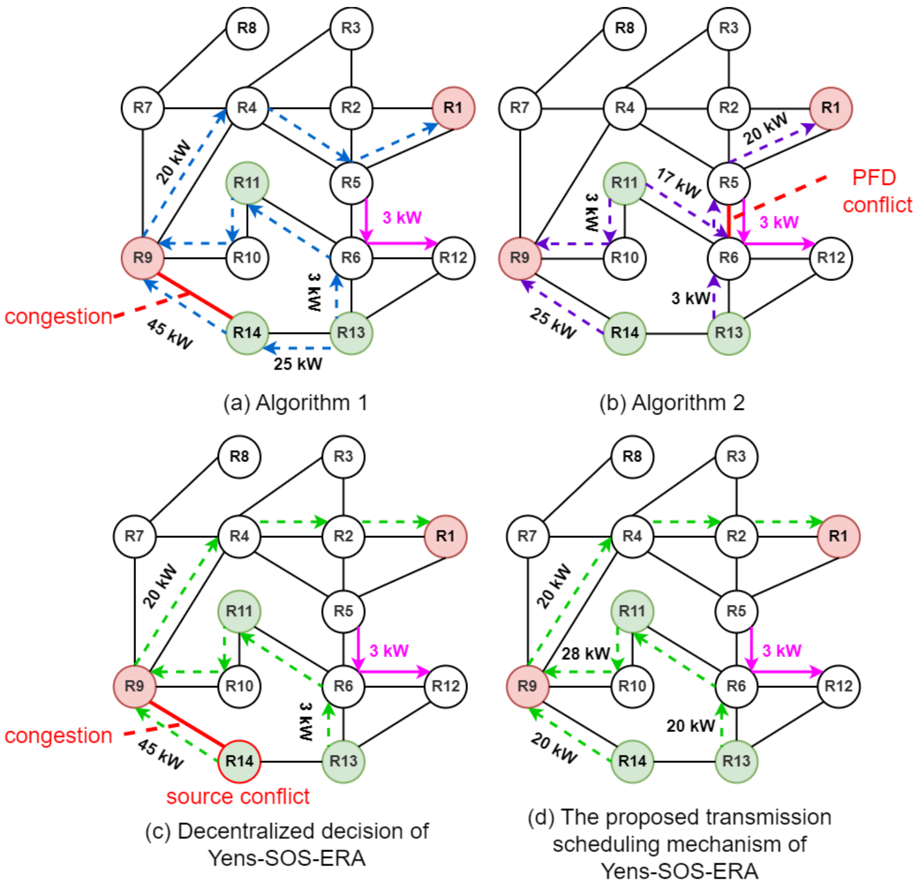

FIGURE 6.15: Energy routing decisions planned by the different algorithms for simultaneous energy transmissions.

6.5 Conclusion

Routing energy from producers to consumers in the EI, as indicated in Chapter 1, entails matching consumers to producers and selecting non-congestion paths with minimum energy loss between the matched peers. Trading pairs in the P2PET system are charged network utilisation fees and power loss compensation fees by the utility grid. These exogenous costs need to be included in the matching mechanism besides the network's physical constraints. Thus, the energy routing problem in this chapter is formulated as a non-convex mixed-integer non-linear optimization problem that minimizes the consumer's energy cost. The objective function combines the matching process and the non-congestion energy-efficient path selection process. To solve this problem, a new semi-decentralized energy routing approach has been proposed. It allows consumers to make energy-routing decisions independently according to their preferences through the use of a Symbiotic Organisms Search-based multipath energy routing algorithm with Yens k least cost paths discovery. The algorithm determines the appropriate energy sources, the energy amount to get from each source, and the least energy cost paths that optimize the energy cost while considering accurate power

Table 6.6: The key differences between the proposed semi-decentralized energy routing approach and other algorithms described in the literature.

		Algorithm							
		[1]	[120]	[121]	[2]	[3]	[137]	Yens-SQP	Proposed approach
Solved Problem	**Subscriber Matching**			✓	✓		✓		✓
	Energy efficient path	✓	✓	✓	✓	✓	✓	✓	✓
	transmission scheduling	✓	✓	✓	✓	✓	✓	✓	✓
Criteria	**Fully centralized**				✓				
	Fully decentralized	✓	✓	✓			✓		
	Semi-decentralized					✓		✓	✓
	Energy prices			✓			✓		✓
	Power loss compensation fees								✓
	Network utilisation fees								✓
	Energy availability and demand			✓	✓		✓		✓
	Grid physical constraints	✓	✓	✓	✓	✓	✓	✓	✓
	PFD constraint							✓	✓
	Accurate power losses							✓	✓
	Simultaneous energy transmission				✓			✓	✓
	Path and source overlap							✓	✓

loss, network utilisation fees, power loss compensation fees, power availability and demand, prosumers prices, and the network's physical constraints, including capacity and PFD constraints. To solve path and source conflicts and avoid congestion problems in simultaneous energy transmissions, a transmission scheduling method based on a priority mechanism is proposed. This mechanism represents the centralized part and it is executed by the NSO. This allows consumers to make the routing decision under the supervision of an NSO. The simulation results demonstrate the effectiveness of the suggested semi-decentralized energy routing approach in solving the three energy routing issues. Table 6.6 summarizes the key differences between the proposed semi-decentralized multi-path energy routing approach and other algorithms described in the literature.

Conclusion and Future Perspectives

Conclusions

The objective of this thesis is to design a proper and realistic energy routing approach for P2PET in EI. The designed energy routing approach should incorporate an appropriate subscriber-matching mechanism that allows consumers to select the best producers to satisfy their demand, an efficient energy path selection algorithm to determine the least loss energy transmission path and a transmission scheduling method to avoid network congestion issues for a normal operation of EI. The subscriber matching mechanism needs to consider other network factors than price or power loss alone. To achieve the study objectives, this thesis investigates how to combine the matching process and energy-efficient path selection into a single objective function and extends the work by improving the routing decision by adding new parameters and constraints.

Initially, a decentralized hybrid energy routing protocol is proposed to solve the energy routing problem in EI. The matching method integrates energy transmission losses and pricing into a single optimization problem, providing a good solution that minimizes both power loss and price compared with other literature algorithms that perform matching based either on price or power loss. The ACO-based energy routing algorithm used to determine the least loss paths has less computational time compared to other literature algorithms, which is extremely desirable in large-scale networks. The algorithm uses a pruning process before path selection, which ensures free-congestion paths.

To create a more realistic energy routing algorithm, Chapter 5 proposes a multi-path-based formulation of the energy routing problem with the integration of PFD constraint. This constraint adds a non-convexity aspect to the non-linear optimization problem. To solve the problem, a semi-decentralized multi-path energy routing algorithm was proposed. The simulation findings indicate that multi-path energy routing decreased transmission losses, improved the utilisation of grid power lines and contributed to the alleviation of line congestion compared to frequently used single-path-based energy routing algorithms. Furthermore, using accurate power loss during path selection benefits both trading pairs and the utility grid. The use of NSO prevents congestion and solves path conflict in the presence of multiple simultaneous trading pairs through a new ranking method. Taking the routing decisions by ERs and using the NSO to control the network decreases the execution time compared to centralized algorithms and decreases congestion and path conflict issues compared to fully decentralized algorithms.

As in the most proposed P2PET systems, the utility grid charges the trading pairs network utilisation fees for the use of its power lines in energy transfer and power loss compensation fees to compensate for transmission power losses between them. For more realistic matching and appropriate energy routing protocols for real P2PET systems, the work in Chapter 6 incorporates power loss compensation fees and network utilisation fees into the multi-path energy routing problem formulation in Chapter 5. The chapter introduces a new P2PET system that limits the number of paths and consumers to be selected. Adding this constraint to the routing problem makes it a non-convex mixed-integer non-linear optimization problem. A semi-decentralized energy routing approach is proposed to solve the problem. The approach allows consumers to select the appropriate energy sources, the energy amount to get from each source, and the least energy-cost paths that optimize the energy cost using a Symbiotic Organisms Search-based multipath energy routing algorithm with Yens k least cost paths discovery. During the routing decision-making process, the algorithm considers accurate power loss, network utilisation fees, power loss compensation fees, power availability and demand, prosumers prices, and the network's physical constraints, including capacity and PFD constraints. To ensure grid stability, all the decentralized energy routing decisions must be approved by the NSO. This later uses a priority-based transmission scheduling method to solve path and source conflicts during simultaneous energy transmissions which ensures congestion-free transactions. The simulation results indicate that the integration of power loss compensation and network utilization fees decreases the energy cost for prosumers compared to other routing algorithms. Additionally, selecting energy transmission paths based on their energy transmission cost and using the accurate power loss ensures fair prosumer pricing and allows the consumer to adjust their selected paths according to the change in grid utility fees. The selection of the k feasible paths using Yens decreases the search space for the power dispatch algorithm. The use of NSO and priority-based transmission scheduling ensures congestion-free P2P energy transactions in EI.

Major Contributions

Our main contributions can be stated as follows:

- A hybrid energy routing protocol based on the use of metaheuristic methods is proposed to address the three energy routing issues: subscriber matching, energy-efficient paths, and transmission scheduling.
- A semi-decentralized multi-path energy routing algorithm is proposed where a combination of a modified Yens' k least loss path with a multi-start SQP method is proposed to determine multi-path routing solutions for power transmission between each trading pair with the objective of minimizing transmission loss.
- A new semi-decentralized energy routing approach that incorporates graph theory and meta-heuristics is introduced to allow each consumer to select the best producers that minimize the energy cost, the amount of power to get from each one, and the least energy transmission cost paths between the energy trading pair while respecting the market and network physical constraints. The approach uses a priority-based transmission scheduling method to ensure congestion-free simultaneous energy transactions.

Suggestions for Future Work

While this thesis has made significant progress in developing an efficient energy routing system, future research offers the possibility for additional improvement. One possible route of exploration

- Investigate the incorporation of real-time data from smart homes and meters, renewable energy generation prediction, and energy storage systems into the suggested energy routing algorithms.

- Establish and evaluate more advanced energy transmission scheduling algorithms capable of successfully reducing path and source conflicts while considering grid stability, consumers' perspectives, and fairness.
- Investigate the use of machine learning approaches to improve energy routing decisions.

List of Publications[1]

Journal Articles

- **Hebal, S.**, Harous, S., and Mechta, D. (2021), "Energy routing challenges and protocols in energy internet: a survey", *Journal of Electrical Engineering & Technology*, 16(6), 3197-3212.
- **Hebal, S.**, Mechta, D., Harous, S., and Dhriyyef, M., (2021). "Hybrid energy routing approach for energy internet", *Energies*, 14(9), 2579.
- **Hebal, S.**, Mechta, D., Harous, S., and Louail, L.,(2024), "A comparative study of energy routing algorithms to optimize energy transmission in Energy Internet", *The Journal of Supercomputing*, pages 1–57, 2024.
- **[Submitted] Hebal, S.**, Harous, S., and Mechta, D., "Prosumers matching and energy routing through Yens and SOS algorithms in P2PET systems".

Conference Proceedings

- **Hebal, S.**, Mechta, D., and Harous, S.,(2019, October) "Aco-based distributed energy routing protocol in smart grid," in *2019 IEEE 10th Annual Ubiquitous Computing, Electronics Mobile Communication Conference (UEMCON) (pp. 0568-0571). IEEE.*
- **Hebal, S.**, Harous, S., and Mechta, D. (2020, June). "Latency and energy transmission cost optimization using bco-aware energy routing for smart grid", in *2020 International Wireless Communications and Mobile Computing (IWCMC) (pp. 1170-1175). IEEE.*

[1]The superscript * indicates joint first authors

- **Hebal, S.**, Harous, S., and Mechta, D. (2022, May), "Solving energy routing problem in energy internet using a discrete artificial bee colony algorithm", in *2022 International Wireless Communications and Mobile Computing (IWCMC) (pp. 641-646). IEEE.*

- [**Submitted**] **Hebal, S.**, Harous, S., Mechta, D., and Louail, L.,(2024), "A semi-decentralized congestion-free multi-path energy routing for P2P energy trading systems".

Bibliography

[1] Ruichi Wang, Jiande Wu, Zhongnan Qian, Zhengyu Lin, and Xiangning He. A graph theory based energy routing algorithm in energy local area network. *IEEE Transactions on Industrial Informatics*, 13(6):3275–3285, 2017.

[2] Reza Razi, Minh-Cong Pham, Ahmad Hably, Seddik Bacha, Quoc-Tuan Tran, and Hossein Iman-Eini. A novel graph-based routing algorithm in residential multimicrogrid systems. *IEEE Transactions on Industrial Informatics*, 17(3):1774–1784, 2020.

[3] Xingyue Jiang, Chuan Sun, Lingling Cao, Ngai Fong Law, and K. H. Loo. Semi-decentralized energy routing algorithm for minimum-loss transmission in community energy internet. *International Journal of Electrical Power and Energy Systems*, 135(September 2021), 2022.

[4] Sara Hebal, Djamila Mechta, Saad Harous, and Lemia Louail. A comparative study of energy routing algorithms to optimize energy transmission in energy internet. *The Journal of Supercomputing*, pages 1–57, 2024.

[5] Neil Strachan and Alexander Farrell. Emissions from distributed vs. centralized generation: The importance of system performance. *Energy Policy*, 34(17):2677–2689, 2006.

[6] Cathy Xin Cui. The uk electricity markets: its evolution, wholesale prices and challenge of wind energy. 2010.

[7] J Lelieveld, K Klingmüller, A Pozzer, RT Burnett, A Haines, and V Ramanathan. Effects of fossil fuel and total anthropogenic emission removal on public health and climate. *Proceedings of the National Academy of Sciences*, 116(15):7192–7197, 2019.

[8] David Infield and Leon Freris. *Renewable energy in power systems*. John Wiley & Sons, 2020.

[9] Kari Alanne and Arto Saari. Distributed energy generation and sustainable development. *Renewable and sustainable energy reviews*, 10(6):539–558, 2006.

[10] Hui Guo, Fei Wang, Jian Luo, and Lijun Zhang. Review of energy routers applied for the energy internet integrating renewable energy. In *2016 IEEE 8th International Power Electronics and Motion Control Conference (IPEMC-ECCE Asia)*, pages 1997–2003. IEEE, 2016.

[11] Wencong Su and Jianhui Wang. Energy management systems in microgrid operations. *The Electricity Journal*, 25(8):45–60, 2012.

[12] Simon R Sinsel, Rhea L Riemke, and Volker H Hoffmann. Challenges and solution technologies for the integration of variable renewable energy sources—a review. *renewable energy*, 145:2271–2285, 2020.

[13] H Husin, M Zaki, et al. A critical review of the integration of renewable energy sources with various technologies. *Protection and Control of Modern Power Systems*, 6(1):1–18, 2021.

[14] Ahmed Sharique Anees. Grid integration of renewable energy sources: Challenges, issues and possible solutions. In *2012 IEEE 5th India International Conference on Power Electronics (IICPE)*, pages 1–6. IEEE, 2012.

[15] Vinayagam Arangarajan, A Maung Than Oo, Jaideep Chandran, GM Shafiullah, and Alex Stojcevski. Role of energy storage in the power system network. *Renewable energy and sustainable development*, pages 201–225, 2015.

[16] Mohammed Yekini Suberu, Mohd Wazir Mustafa, and Nouruddeen Bashir. Energy storage systems for renewable energy power sector integration and mitigation of intermittency. *Renewable and Sustainable Energy Reviews*, 35:499–514, 2014.

[17] R Al-Foraih, KJ Sreekanth, and A Al-Mulla. A techno-economic analysis of the integration of energy storage technologies in electric power systems. *Journal of Renewable and Sustainable Energy*, 10(5):054102, 2018.

[18] Wayes Tushar, Bo Chai, Chau Yuen, David B Smith, Kristin L Wood, Zaiyue Yang, and H Vincent Poor. Three-party energy management with distributed energy resources in smart grid. *IEEE Transactions on Industrial Electronics*, 62(4):2487–2498, 2014.

[19] Xi Fang, Satyajayant Misra, Guoliang Xue, and Dejun Yang. Smart grid—the new and improved power grid: A survey. *IEEE communications surveys & tutorials*, 14(4):944–980, 2011.

[20] Imane Worighi, Abdelilah Maach, Abdelhakim Hafid, Omar Hegazy, and Joeri Van Mierlo. Integrating renewable energy in smart grid system: Architecture, virtualization and analysis. *Sustainable Energy, Grids and Networks*, 18:100226, 2019.

[21] Sandhya Armoogum and Vandana Bassoo. Privacy of energy consumption data of a household in a smart grid. In *Smart Power Distribution Systems*, pages 163–177. Elsevier, 2019.

[22] Mohammed Dhriyyef, Abdelmalek El Mehdi, Mohammed Elhitmy, and Mohammed Elhafyani. Management strategy of power exchange in a building between grid, photovoltaic and batteries. In *International Conference on Electronic Engineering and Renewable Energy*, pages 831–841. Springer, 2020.

[23] Liang-Cheng Ye, João FD Rodrigues, and Hai Xiang Lin. Analysis of feed-in tariff policies for solar photovoltaic in china 2011–2016. *Applied energy*, 203:496–505, 2017.

[24] Thomas Morstyn and Malcolm D McCulloch. Peer-to-peer energy trading. In *Analytics for the Sharing Economy: Mathematics, Engineering and Business Perspectives*, pages 279–300. Springer, 2020.

[25] Yusuke Manabe. Application of ders in electricity market. In *Integration of Distributed Energy Resources in Power Systems*, pages 295–302. Elsevier, 2016.

[26] Andri Pyrgou, Angeliki Kylili, and Paris A Fokaides. The future of the feed-in tariff (fit) scheme in europe: The case of photovoltaics. *Energy Policy*, 95:94–102, 2016.

[27] Sandro Schopfer, Verena Tiefenbeck, and Thorsten Staake. Economic assessment of photovoltaic battery systems based on household load profiles. *Applied energy*, 223:229–248, 2018.

[28] Esteban A Soto, Lisa B Bosman, Ebisa Wollega, and Walter D Leon-Salas. Peer-to-peer energy trading: A review of the literature. *Applied Energy*, 283:116268, 2021.

[29] Liliane Ableitner, Verena Tiefenbeck, Arne Meeuw, Anselma Wörner, Elgar Fleisch, and Felix Wortmann. User behavior in a real-world peer-to-peer electricity market. *Applied Energy*, 270:115061, 2020.

[30] Wayes Tushar, Tapan Kumar Saha, Chau Yuen, Thomas Morstyn, Malcolm D McCulloch, H Vincent Poor, and Kristin L Wood. A motivational game-theoretic approach for peer-to-peer energy trading in the smart grid. *Applied energy*, 243:10–20, 2019.

[31] Jongbaek An, Minhyun Lee, Seungkeun Yeom, and Taehoon Hong. Determining the peer-to-peer electricity trading price and strategy for energy prosumers and consumers within a microgrid. *Applied Energy*, 261:114335, 2020.

[32] Wayes Tushar, Chau Yuen, Hamed Mohsenian-Rad, Tapan Saha, H Vincent Poor, and Kristin L Wood. Transforming energy networks via peer-to-peer energy trading: The potential of game-theoretic approaches. *IEEE Signal Processing Magazine*, 35(4):90–111, 2018.

[33] M Imran Azim, SA Pourmousavi, Wayes Tushar, and Tapan K Saha. Feasibility study of financial p2p energy trading in a grid-tied power network. In *2019 IEEE Power & Energy Society General Meeting (PESGM)*, pages 1–5. IEEE, 2019.

[34] Wayes Tushar, Tapan Kumar Saha, Chau Yuen, Thomas Morstyn, H Vincent Poor, Richard Bean, et al. Grid influenced peer-to-peer energy trading. *IEEE Transactions on Smart Grid*, 11(2):1407–1418, 2019.

[35] Sonnen website. `https://sonnengroup.com/`. Last access: September 2024.

[36] Piclo website. `https://www.piclo.energy/`. Last access: September 2024.

[37] Vendebron website. `https://vandebron.nl/`. Last access: September 2024.

[38] Yeloha website. `https://www.yeloha.com/`. Last access: September 2024.

[39] Esther Mengelkamp, Johannes Gärttner, Kerstin Rock, Scott Kessler, Lawrence Orsini, and Christof Weinhardt. Designing microgrid energy markets: A case study: The brooklyn microgrid. *Applied Energy*, 210:870–880, 2018.

[40] Je Hong Park, Minkyu Kim, and Daesung Kwon. Security weakness in the smart grid key distribution scheme proposed by xia and wang. *IEEE Transactions on Smart Grid*, 4(3):1613–1614, 2013.

[41] Muhammad Faheem, Syed Bilal Hussain Shah, Rizwan Aslam Butt, Basit Raza, Muhammad Anwar, Muhammad Waqar Ashraf, Md A Ngadi, and Vehbi C Gungor. Smart grid communication and information technologies in the perspective of industry 4.0: Opportunities and challenges. *Computer Science Review*, 30:1–30, 2018.

[42] Jeremy Rifkin. *The third industrial revolution: how lateral power is transforming energy, the economy, and the world*. Macmillan, 2011.

[43] Lefteri H Tsoukalas and Rong Gao. Inventing energy internet the role of anticipation in human-centered energy distribution and utilization. In *2008 SICE Annual Conference*, pages 399–403. IEEE, 2008.

[44] LH Tsoukalas and R Gao. From smart grids to an energy internet: Assumptions, architectures and requirements. In *2008 Third international conference on electric utility deregulation and restructuring and power technologies*, pages 94–98. IEEE, 2008.

[45] Rozina R Surani. From smart grids to an energy internet: A review paper on key features of an energy internet. *Int. J. Eng. Res. Technol*, 8(4):228–231, 2019.

[46] Yijia Cao, Qiang Li, Yi Tan, Yong Li, Yuanyang Chen, Xia Shao, and Yao Zou. A comprehensive review of energy internet: basic concept, operation and planning methods, and research prospects. *Journal of modern power systems and clean energy*, 6(3):399–411, 2018.

[47] Yijia Cao, Qiang Li, Yi Tan, Yong Li, Yuanyang Chen, Xia Shao, and Yao Zou. A comprehensive review of energy internet: basic concept, operation and planning methods, and research prospects. *Journal of modern power systems and clean energy*, 6(3):399–411, 2018.

[48] Kaile Zhou, Shanlin Yang, and Zhen Shao. Energy internet: the business perspective. *Applied energy*, 178:212–222, 2016.

[49] Zhenxiao Chen, Qianjin Liu, Yiqing Li, and Shiping Liu. Discussion on energy internet and its key technology. *Journal of Power and Energy Engineering*, 5(12):1–9, 2017.

[50] Mohd Asim Aftab. Software defined networks for smart substations in an active distribution system. *Journal of Engineering Research*, 7(1), 2019.

[51] YR Kafle, Khizir Mahmud, Sayidul Morsalin, and GE Town. Towards an internet of energy. In *2016 IEEE International Conference on Power System Technology (POWERCON)*, pages 1–6. IEEE, 2016.

[52] Gerald T Heydt. Future renewable electrical energy delivery and management systems: Energy reliability assessment of freedm systems. In *IEEE PES General Meeting*, pages 1–4. IEEE, 2010.

[53] Akhil Joseph and Patil Balachandra. Energy internet, the future electricity system: Overview, concept, model structure, and mechanism. *Energies*, 13(16):4242, 2020.

[54] Alex Q Huang, Mariesa L Crow, Gerald Thomas Heydt, Jim P Zheng, and Steiner J Dale. The future renewable electric energy delivery and management (freedm) system: the energy internet. *Proceedings of the IEEE*, 99(1):133–148, 2010.

[55] BDI Initiative et al. Internet of energy. *Federation of German Industries: Berlin, Germany*, 2008.

[56] John Boyd. An internet-inspired electricity grid. *IEEE Spectrum*, 50(1):12–14, 2012.

[57] Juhar Abdella, Khaled Shuaib, and Saad Harous. Energy routing algorithms for the energy internet. In *2018 International Conference on Intelligent Systems (IS)*, pages 80–86. IEEE, 2018.

[58] Ying Wu, Yanpeng Wu, Josep M Guerrero, and Juan C Vasquez. Digitalization and decentralization driving transactive energy internet: Key technologies and infrastructures. *International Journal of Electrical Power & Energy Systems*, 126:106593, 2021.

[59] Min Gao, Kun Wang, and Lei He. Probabilistic model checking and scheduling implementation of an energy router system in energy internet for green cities. *IEEE Transactions on Industrial Informatics*, 14(4):1501–1510, 2018.

[60] Xingyue Jiang, Chuan Sun, Lingling Cao, Ngai-Fong Law, and KH Loo. Review and comparative study of energy routing algorithms for energy internet. In *2021 IEEE 5th Conference on Energy Internet and Energy System Integration (EI2)*, pages 567–572. IEEE, 2021.

[61] Yingshu Liu, Jun Li, Yao Wu, and Feng Zhou. Coordinated control of the energy router-based smart home energy management system. *Applied Sciences*, 7(9):943, 2017.

[62] Yingshu Liu, Yao Wu, Ke Yang, Chunping Bi, Xi Chen, and Yao Zhao. Novel energy router with multiple operation modes. *Energy Procedia*, 158:2586–2591, 2019.

[63] Ayman I Sabbah, Amr El-Mougy, and Mohamed Ibnkahla. A survey of networking challenges and routing protocols in smart grids. *IEEE Transactions on Industrial Informatics*, 10(1):210–221, 2013.

[64] Akhil Joseph and Patil Balachandra. Smart grid to energy internet: A systematic review of transitioning electricity systems. *IEEE Access*, 8:215787–215805, 2020.

[65] Danielly B Avancini, Joel JPC Rodrigues, Simion GB Martins, Ricardo AL Rabêlo, Jalal Al-Muhtadi, and Petar Solic. Energy meters evolution in smart grids: A review. *Journal of cleaner production*, 217:702–715, 2019.

[66] Haochen Hua, Yuchao Qin, Hanxuan Xu, Chuantong Hao, and Junwei Cao. Robust control method for dc microgrids and energy routers to improve voltage stability in energy internet. *Energies*, 12(9):1622, 2019.

[67] Yi Xu, Jianhua Zhang, Wenye Wang, Avik Juneja, and Subhashish Bhattacharya. Energy router: Architectures and functionalities toward energy internet. In *2011 IEEE International Conference on Smart Grid Communications (SmartGridComm)*, pages 31–36. IEEE, 2011.

[68] Minh-Cong Pham, Reza Razi, Ahmad Hably, Seddik Bacha, Quoc-Tuan Tran, and Hossein Iman-Eini. Power management in multi-microgrid system based on energy routers. In *2020 IEEE International Conference on Industrial Technology (ICIT)*, pages 1178–1183. IEEE, 2020.

[69] Bin Liu, Bingzhao Zhu, Ziyou Guan, Chengxiong Mao, and Dan Wang. Energy router interconnection system: A solution for new distribution network architecture toward future carbon neutrality. *Energy Conversion and Economics*, 2022.

[70] Jianhua Zhang, Wenye Wang, and Subhashish Bhattacharya. Architecture of solid state transformer-based energy router and models of energy traffic. In *2012 IEEE PES Innovative Smart Grid Technologies (ISGT)*, pages 1–8. IEEE, 2012.

[71] Youiie Ma, Hongqin Liu, Xuesong Zhou, and Zhiqiang Gao. An overview on energy router toward energy internet. In *2018 IEEE International Conference on Mechatronics and Automation (ICMA)*, pages 259–263. IEEE, 2018.

[72] Samuele Granata, Marco Di Benedetto, Cristina Terlizzi, Riccardo Leuzzi, Stefano Bifaretti, and Pericle Zanchetta. Power electronics converters for the internet of energy: A review. *Energies*, 15(7):2604, 2022.

[73] SM Suhail Hussain, Furquan Nadeem, Mohd Asim Aftab, Ikbal Ali, and Taha Selim Ustun. The emerging energy internet: Architecture, benefits, challenges, and future prospects. *Electronics*, 8(9):1037, 2019.

[74] Bin Liu, Yuwei Peng, Jiachao Xu, Chengxiong Mao, Dan Wang, and Qing Duan. Design and implementation of multiport energy routers toward future energy internet. *IEEE Transactions on Industry Applications*, 57(3):1945–1957, 2021.

[75] Jingdou Liu, Fen Tang, Mian Wang, Pengfei Chen, Zefu Xu, Liangliang Wu, and Wei Wang. A home energy router and energy management strategy for ac/dc hybrid sources and consumers. In *2018 13th IEEE Conference on Industrial Electronics and Applications (ICIEA)*, pages 1498–1503. IEEE, 2018.

[76] Bin Liu, Weihan Wu, Chunxiao Zhou, Chengxiong Mao, Dan Wang, Qing Duan, and Guanglin Sha. An ac–dc hybrid multi-port energy router with coordinated control and energy management strategies. *IEEE Access*, 7:109069–109082, 2019.

[77] Yan Hao, Chunliang Zhou, Xudong Zhang, Dongyan Zhao, Fei Li, and Hongxi Wang. Power line communication challenges in the energy internet. In *IOP Conference Series: Earth and Environmental Science*, volume 645, page 012079. IOP Publishing, 2021.

[78] Takashi Hikihara, Keiji Tashiro, Yutaro Kitamori, and Ryo Takahashi. Power packetization and routing for smart management of electricity. In *10th International Energy Conversion Engineering Conference*, page 3732, 2012.

[79] Haobo Zhang, Hongliang Zhang, Lingyang Song, Yonghui Li, Zhu Han, and H Vincent Poor. Peer-to-peer energy trading in dc packetized power microgrids. *IEEE Journal on Selected Areas in Communications*, 38(1):17–30, 2019.

[80] Jinghuan Ma, Lingyang Song, and Yonghui Li. Optimal power dispatching for local area packetized power network. *IEEE Transactions on Smart Grid*, 9(5):4765–4776, 2017.

[81] Naoaki Fujii, Ryo Takahashi, and Takashi Hikihara. Networked power packet dispatching system for multi-path routing. In *2014 IEEE/SICE International Symposium on System Integration*, pages 357–362. IEEE, 2014.

[82] Yingshu Liu, Yao Wu, Ke Yang, Chunping Bi, Xi Chen, and Yao Zhao. Novel energy router with multiple operation modes. *Energy Procedia*, 158:2586–2591, 2019.

[83] Yingshu Liu, Chunping Bi, Yao Zhao, Yao Wu, and Xi Chen. Energy router with load switching functionality. *Energy Procedia*, 158:2561–2566, 2019.

[84] Chuantong Hao, Haochen Hua, Yuchao Qin, and Junwei Cao. A class of optimal and robust controller design for energy routers in energy internet. In *2018 IEEE International Conference on Smart Energy Grid Engineering (SEGE)*, pages 14–19. IEEE, 2018.

[85] Tong Wu, Changhong Zhao, and Ying-Jun Angela Zhang. Distributed ac-dc optimal power dispatch of vsc-based energy routers in smart microgrids. *IEEE Transactions on Power Systems*, 36(5):4457–4470, 2021.

[86] Yingshu Liu, Xi Chen, Yao Wu, Ke Yang, Jiebei Zhu, and Bin Li. Enabling the smart and flexible management of energy prosumers via the energy router with parallel operation mode. *IEEE Access*, 8:35038–35047, 2020.

[87] Junwei Cao and Mingbo Yang. Energy internet–towards smart grid 2.0. In *2013 Fourth international conference on networking and distributed computing*, pages 105–110. IEEE, 2013.

[88] Hafiz Majid Hussain, Arun Narayanan, Pedro HJ Nardelli, and Yongheng Yang. What is energy internet? concepts, technologies, and future directions. *Ieee Access*, 8:183127–183145, 2020.

[89] Chu Donatus Iweh, Samuel Gyamfi, Emmanuel Tanyi, and Eric Effah-Donyina. Distributed generation and renewable energy integration into the grid: Prerequisites, push factors, practical options, issues and merits. *Energies*, 14(17):5375, 2021.

[90] Khizir Mahmud, Behram Khan, Jayashri Ravishankar, Abdollah Ahmadi, and Pierluigi Siano. An internet of energy framework with distributed energy resources, prosumers and small-scale virtual power plants: An overview. *Renewable and Sustainable Energy Reviews*, 127:109840, 2020.

[91] J Mitali, S Dhinakaran, and AA Mohamad. Energy storage systems: A review. *Energy Storage and Saving*, 2022.

[92] Xiao-Ping Zhang. Development of european energy internet and the role of energy union. In *The energy internet*, pages 347–367. Elsevier, 2019.

[93] Guanwei Liu, Lu Qu, Rong Zeng, and Feng Gao. Energy internet in china. In *The energy internet*, pages 265–282. Elsevier, 2019.

[94] Mahammad A Hannan, Mohammad Faisal, Pin Jern Ker, Looe Hui Mun, Khadija Parvin, Teuku Meurah Indra Mahlia, and Frede Blaabjerg. A review of internet of energy based building energy management systems: Issues and recommendations. *Ieee Access*, 6:38997–39014, 2018.

[95] Pablo Ralon, Michael Taylor, Andrei Ilas, Harald Diaz-Bone, and K Kairies. Electricity storage and renewables: Costs and markets to 2030. *International Renewable Energy Agency: Abu Dhabi, United Arab Emirates*, 164, 2017.

[96] Jijiang He, Yu Wang, and Wenying Chen. Energy transition driven by the energy internet. In *Annual report on China's response to climate change (2017)*, pages 77–89. Springer, 2020.

[97] Himadry Shekhar Das, Mohammad Mominur Rahman, S Li, and CW Tan. Electric vehicles standards, charging infrastructure, and impact on grid integration: A technological review. *Renewable and Sustainable Energy Reviews*, 120:109618, 2020.

[98] Shengyang Li, Ping Yi, Zhichuan Huang, Tiantian Xie, and Ting Zhu. Energy scheduling and allocation in electric vehicles energy internet. In *2016 IEEE Power & Energy Society Innovative Smart Grid Technologies Conference (ISGT)*, pages 1–5. IEEE, 2016.

[99] William Infante, Jin Ma, Xiaoqing Han, Wei Li, and Albert Y Zomaya. Two-stage optimization strategies for integrating electric vehicles in the energy internet. In *Energy Internet*, pages 209–238. Springer, 2020.

[100] Evgeny Nefedov, Seppo Sierla, and Valeriy Vyatkin. Internet of energy approach for sustainable use of electric vehicles as energy storage of prosumer buildings. *Energies*, 11(8):2165, 2018.

[101] Thanh Luan Vu, Nam Tuan Le, Yeong Min Jang, et al. An overview of internet of energy (ioe) based building energy management system. In *2018 International Conference on Information and Communication Technology Convergence (ICTC)*, pages 852–855. IEEE, 2018.

[102] Khizir Mahmud, Graham E Town, Sayidul Morsalin, and MJ Hossain. Integration of electric vehicles and management in the internet of energy. *Renewable and Sustainable Energy Reviews*, 82:4179–4203, 2018.

[103] Wayes Tushar, Chau Yuen, Tapan K Saha, Thomas Morstyn, Archie C Chapman, M Jan E Alam, Sarmad Hanif, and H Vincent Poor. Peer-to-peer energy systems for connected communities: A review of recent advances and emerging challenges. *Applied Energy*, 282:116131, 2021.

[104] Siripha Junlakarn, Phimsupha Kokchang, and Kulyos Audomvongseree. Drivers and challenges of peer-to-peer energy trading development in thailand. *Energies*, 15(3):1229, 2022.

[105] Alejandro Navarro-Espinosa and Luis F Ochoa. Probabilistic impact assessment of low carbon technologies in lv distribution systems. *IEEE Transactions on Power Systems*, 31(3):2192–2203, 2015.

[106] Wayes Tushar, Tapan Kumar Saha, Chau Yuen, David Smith, and H Vincent Poor. Peer-to-peer trading in electricity networks: An overview. *IEEE Transactions on Smart Grid*, 11(4):3185–3200, 2020.

[107] Jaysson Guerrero, Archie C Chapman, and Gregor Verbič. Decentralized p2p energy trading under network constraints in a low-voltage network. *IEEE Transactions on Smart Grid*, 10(5):5163–5173, 2018.

[108] M Imran Azim, Wayes Tushar, and Tapan K Saha. Investigating the impact of p2p trading on power losses in grid-connected networks with prosumers. *Applied Energy*, 263:114687, 2020.

[109] Sara Hebal, Saad Harous, and Djamila Mechta. Energy routing challenges and protocols in energy internet: a survey. *Journal of Electrical Engineering & Technology*, 16(6):3197–3212, 2021.

[110] Yangyang Liu, Hongbo Lian, Xiaowei Tang, Zhongqi Shen, Jiarui Li, and Lian Liu. Tcm considering eizs' integration. *The Journal of Engineering*, 2019(16):850–855, 2019.

[111] Nurul Idayu Yusoff, Abdullah Asuhaimi Mohd Zin, and Azhar Bin Khairuddin. Congestion management in power system: A review. In *2017 3rd international conference on power generation systems and renewable energy technologies (PGSRET)*, pages 22–27. IEEE, 2017.

[112] Muhammad Bachtiar Nappu and Ardiaty Arief. Network losses-based economic redispatch for optimal energy pricing in a congested power system. *Energy Procedia*, 100:311–314, 2016.

[113] Xiaoyu Wang, Tao Xu, Yunfei Mu, Zibo Wang, Youjun Deng, Tao Zhang, Qian Jiang, Yaqing Zhang, and Hongjie Jia. Congestion management under peer-to-peer energy trading scheme among microgrids through cooperative game. *Energy Reports*, 8:59–66, 2022.

[114] Erol Gelenbe and Elif Tugce Ceran. Energy packet networks with energy harvesting. *IEEE access*, 4:1321–1331, 2016.

[115] Fadi El Awar, Amani Fawaz, Imad Mougharbel, and Hadi Y Kanaan. Simulation platform for power packet distribution. In *2022 3rd International Conference on Smart Grid and Renewable Energy (SGRE)*, pages 1–7. IEEE, 2022.

[116] Yunfei Du, Xianggen Yin, Jinmu Lai, Guanqun Sun, Zhiwei Zhao, and Zia Ullah. Energy router based minimum loss cost routing strategy in energy internet. In *2020 IEEE 1st China International Youth Conference on Electrical Engineering (CIYCEE)*, pages 1–6. IEEE, 2020.

[117] Ping Yi, Ting Zhu, Bo Jiang, Ruofan Jin, and Bing Wang. Deploying energy routers in an energy internet based on electric vehicles. *IEEE Transactions on Vehicular Technology*, 65(6):4714–4725, 2016.

[118] Yu Sui, Ping Yi, Xin Liu, and Ting Zhu. Energy transport station deployment in electric vehicles energy internet. *IEEE Access*, 7:97986–97995, 2019.

[119] Xiaoying Tang, Suzhi Bi, and Ying-Jun Angela Zhang. Distributed routing and charging scheduling optimization for internet of electric vehicles. *IEEE Internet of Things Journal*, 6(1):136–148, 2018.

[120] Hui Guo, Fei Wang, Geoff James, Lijun Zhang, and Jian Luo. Graph theory based topology design and energy routing control of the energy internet. *IET Generation, Transmission & Distribution*, 12(20):4507–4514, 2018.

[121] Hui Guo, Fei Wang, Li Li, Lijun Zhang, and Jian Luo. A minimum loss routing algorithm based on real-time transaction in energy internet. *IEEE Transactions on Industrial Informatics*, 15(12):6446–6456, 2019.

[122] S Hemalatha and P Valsalal. Identification of optimal path in power system network using bellman ford algorithm. *Modelling and Simulation in Engineering*, 2012:28–28, 2012.

[123] Tamer Başar and Geert Jan Olsder. *Dynamic noncooperative game theory*. SIAM, 1998.

[124] Wayes Tushar, Tapan Kumar Saha, Chau Yuen, Paul Liddell, Richard Bean, and H Vincent Poor. Peer-to-peer energy trading with sustainable user participation: A game theoretic approach. *IEEE Access*, 6:62932–62943, 2018.

[125] Jema Sharin PankiRaj, Abdulsalam Yassine, and Salimur Choudhury. An auction mechanism for profit maximization of peer-to-peer energy trading in smart grids. *Procedia Computer Science*, 151:361–368, 2019.

[126] Jema Sharin Pankiraj, Abdulsalam Yassine, and Salimur Choudhury. Double-sided auction mechanism for peer-to-peer energy trading markets. In *2021 IEEE International Conference on Progress in Informatics and Computing (PIC)*, pages 443–452. IEEE, 2021.

[127] Mohsen Khorasany, Amrit Paudel, Reza Razzaghi, and Pierluigi Siano. A new method for peer matching and negotiation of prosumers in peer-to-peer energy markets. *IEEE Transactions on Smart Grid*, 12(3):2472–2483, 2020.

[128] Luis Arturo Soriano, Manuel Avila, Pedro Ponce, José de Jesús Rubio, and Arturo Molina. Peer-to-peer energy trades based on multi-objective optimization. *International Journal of Electrical Power & Energy Systems*, 131:107017, 2021.

[129] Yinliang Xu, Hongbin Sun, and Wei Gu. A novel discounted min-consensus algorithm for optimal electrical power trading in grid-connected dc microgrids. *IEEE Transactions on Industrial Electronics*, 66(11):8474–8484, 2019.

[130] Christopher M Colson and M Hashem Nehrir. Algorithms for distributed decision-making for multi-agent microgrid power management. In *2011 IEEE Power and Energy Society General Meeting*, pages 1–8. IEEE, 2011.

[131] Xiaoying Shi, Yinliang Xu, and Hongbin Sun. A biased min-consensus-based approach for optimal power transaction in multi-energy-router systems. *IEEE Transactions on Sustainable Energy*, 11(1):217–228, 2018.

[132] Sara Hebal, Saad Harous, and Djamila Mechta. Solving energy routing problem in energy internet using a discrete artificial bee colony algorithm. In *2022 International Wireless Communications and Mobile Computing (IWCMC)*, pages 641–646. IEEE, 2022.

[133] Olamide Jogunola, Weizhuo Wang, and Bamidele Adebisi. Prosumers matching and least-cost energy path optimisation for peer-to-peer energy trading. *IEEE Access*, 8:95266–95277, 2020.

[134] Amani Fawaz, Imad Mougharbel, and Hadi Y Kanaan. New routing application using bees colony for energy internet. In *2022 3rd International Conference on Smart Grid and Renewable Energy (SGRE)*, pages 1–8. IEEE, 2022.

[135] Hui Guo, Fei Wang, Li Li, Lijun Zhang, and Jian Luo. A minimum loss routing algorithm based on real-time transaction in energy internet. *IEEE Transactions on Industrial Informatics*, 15(12):6446–6456, 2019.

[136] Zhengqi Jiang, Vinit Sahasrabudhe, Ahmed Mohamed, Haim Grebel, and Roberto Rojas-Cessa. Greedy algorithm for minimizing the cost of routing power on a digital microgrid. *Energies*, 12(16):3076, 2019.

[137] Sara Hebal, Djamila Mechta, Saad Harous, and Mohammed Dhriyyef. Hybrid energy routing approach for energy internet. *Energies*, 14(9):2579, 2021.

[138] Sara Hebal, Djamila Mechta, and Saad Harous. Aco-based distributed energy routing protocol in smart grid. In *2019 IEEE 10th Annual Ubiquitous Computing, Electronics & Mobile Communication Conference (UEMCON)*, pages 0568–0571. IEEE, 2019.

[139] Afsah Sharmin, F Anwar, and SMA Motakabber. A novel bio-inspired routing algorithm based on aco for wsns. *Bulletin of Electrical Engineering and Informatics*, 8(2):718–726, 2019.

[140] Xinyu Wang, Tsan-Ming Choi, Haikuo Liu, and Xiaohang Yue. Novel ant colony optimization methods for simplifying solution construction in vehicle routing problems. *IEEE Transactions on Intelligent Transportation Systems*, 17(11):3132–3141, 2016.

[141] Sabrina Oliveira, Mohamed Saifullah Hussin, Andrea Roli, Marco Dorigo, and Thomas Stützle. Analysis of the population-based ant colony optimization algorithm for the tsp and the qap. In *2017 IEEE congress on evolutionary computation (CEC)*, pages 1734–1741. IEEE, 2017.

[142] Alexandros I Nikolaidis, Charalambos A Charalambous, and Pierluigi Mancarella. A graph-based loss allocation framework for transactive energy markets in unbalanced radial distribution networks. *IEEE Transactions on Power Systems*, 34(5):4109–4118, 2018.

[143] Jaysson Guerrero, Archie C Chapman, and Gregor Verbic. Trading arrangements and cost allocation in p2p energy markets on low-voltage networks. In *2019 IEEE Power & Energy Society General Meeting (PESGM)*, pages 1–5. IEEE, 2019.

[144] Jin Y Yen. Finding the k shortest loopless paths in a network. *management Science*, 17(11):712–716, 1971.

[145] Natnaree Tubteang and Paramet Wirasanti. Peer-to-peer electrical energy trading considering matching distance and available capacity of distribution line. *Energies*, 16(6):2520, 2023.

[146] Amrit Paudel, Lahanda Purage Mohasha Isuru Sampath, Jiawei Yang, and Hoay Beng Gooi. A peer-to-peer electricity marketplace for simultaneous congestion management and power loss reduction. *IEEE Transactions on Smart Grid*, 11(6):4727–4737, 2020.

[147] Amrit Paudel, Lahanda Purage Mohasha Isuru Sampath, Jiawei Yang, and Hoay Beng Gooi. Peer-to-peer energy trading in smart grid considering power losses and network fees. *IEEE Transactions on Smart Grid*, 11(6):4727–4737, 2020.

[148] Ashutosh Timilsina and Simone Silvestri. P2p energy trading through prospect theory, differential evolution, and reinforcement learning. *ACM Transactions on Evolutionary Learning*, 3(3):1–22, 2023.

[149] Wei Zhou, Yuying Wang, Feixiang Peng, Ying Liu, Hui Sun, and Yu Cong. Distribution network congestion management considering time sequence of peer-to-peer energy trading. *International Journal of Electrical Power & Energy Systems*, 136:107646, 2022.

[150] Thomas Baroche, Pierre Pinson, Roman Le Goff Latimier, and Hamid Ben Ahmed. Exogenous cost allocation in peer-to-peer electricity markets. *IEEE Transactions on Power Systems*, 34(4):2553–2564, 2019.

[151] Pietro Belotti, Christian Kirches, Sven Leyffer, Jeff Linderoth, James Luedtke, and Ashutosh Mahajan. Mixed-integer nonlinear optimization. *Acta Numerica*, 22:1–131, 2013.

[152] Min-Yuan Cheng and Doddy Prayogo. Symbiotic organisms search: a new metaheuristic optimization algorithm. *Computers & Structures*, 139:98–112, 2014.

[153] Absalom E Ezugwu and Doddy Prayogo. Symbiotic organisms search algorithm: theory, recent advances and applications. *Expert Systems with Applications*, 119:184–209, 2019.

[154] M Kenan Dosoglu, Ugur Guvenc, Serhat Duman, Yusuf Sonmez, and H Tolga Kahraman. Symbiotic organisms search optimization algorithm for economic/emission dispatch problem in power systems. *Neural Computing and Applications*, 29:721–737, 2018.

[155] Samia Noureddine, Baarir Zineeddine, Abida Toumi, Abir Betka, and Aïcha-Nabila Benharkat. A new predictive medical approach based on data mining and symbiotic organisms search algorithm. *International Journal of Computers and Applications*, 44(5):465–479, 2022.

[156] Fahui Miao, Li Yao, and Xiaojie Zhao. Evolving convolutional neural networks by symbiotic organisms search algorithm for image classification. *Applied Soft Computing*, 109:107537, 2021.

[157] Ajoze Abdulraheem Zubair, Shukor Abd Razak, Md Asri Ngadi, Arafat Al-Dhaqm, Wael MS Yafooz, Abdel-Hamid M Emara, Aldosary Saad, and Hussain Al-Aqrabi. A cloud computing-based modified symbiotic organisms search algorithm (ai) for optimal task scheduling. *Sensors*, 22(4):1674, 2022.